



THE UNIVERSITY OF
WAIKATO
Te Whare Wānanga o Waikato

Research Commons

<http://researchcommons.waikato.ac.nz/>

Research Commons at the University of Waikato

Copyright Statement:

The digital copy of this thesis is protected by the Copyright Act 1994 (New Zealand).

The thesis may be consulted by you, provided you comply with the provisions of the Act and the following conditions of use:

- Any use you make of these documents or images must be for research or private study purposes only, and you may not make them available to any other person.
- Authors control the copyright of their thesis. You will recognise the author's right to be identified as the author of the thesis, and due acknowledgement will be made to the author where appropriate.
- You will obtain the author's permission before publishing any material from the thesis.

•

NONEQUILIBRIUM TRANSITIONS
IN
QUANTUM OPTICAL SYSTEMS

A thesis presented to the
University of Waikato
in fulfilment of the requirements
for the Degree of
Doctor of Philosophy in Physics
by
PETER DAVID DRUMMOND

January 1979

To

Jean, Alexi and Tessa

NONEQUILIBRIUM TRANSITIONS IN QUANTUM OPTICAL SYSTEMS

P. D. Drummond 1979

October 22, 2025

Corrections

- Page 17:

$$\hat{H} = \sum_{\lambda} \hbar\omega_{\lambda} \hat{a}_{\lambda}^{\dagger} \hat{a}_{\lambda}$$

- Page 55:

$$\langle z | \hat{J}^+ \hat{J}^- | z \rangle = \frac{2J}{1 + |z|^2} + 2J(2J - 1) \frac{|z|^2}{(1 + |z|^2)^2}$$

- Page 56: $\langle \hat{J}^2 \rangle = \frac{1}{4}N(N + 2)$ in the collective ground state
- Page 65: they are both equal to each other at $t = t'$.
- Page 88: for bistability it is necessary to have both:

$$\begin{aligned} \chi'^2 \kappa'^2 + \chi''^2 \kappa''^2 + 8\chi' \chi'' \kappa' \kappa'' - 3\chi'^2 \kappa''^2 - 3\chi''^2 \kappa'^2 &> 0 \\ \chi' \kappa' + \chi'' \kappa'' &< 0 \end{aligned}$$

- Page 165:

$$\begin{aligned} I_n = \sum_{m=0}^{\infty} \oint_{\Phi} z_1^{j_1-1} (1 - z_1)^{j_2-j_1-1} [(1 - 2z_1)(1 - 2z_2)]^{m+n} z_2^{j_1^*-1} \\ \times (1 - z_2)^{j_2^*-j_1^*-1} dz_1 dz_2 \times \left[\frac{2^{m+2}}{m!} \left(\frac{|c|^2}{\eta^2} \right)^{m+n+1} (2c)^{j_2-2} (2c^*)^{j_2^*-2} \right] \end{aligned}$$

- Page 166:

$$\begin{aligned} I_n = \sum_{m=0}^{\infty} \frac{2^{m+2}}{m!} \left(\frac{|c|^2}{\eta^2} \right)^{m+n+1} |{}_2F_1(-m-n, j_1, j_2, 2) B(j_1, j_2 - j_1)|^2 \\ \times (2c)^{j_2-2} (2c^*)^{j_2^*-2} \left| (1 - e^{2\pi i j_1}) (1 - e^{2\pi i (j_2 - j_1)}) \right|^2 \end{aligned}$$

- Page 278: $c^{n/2}, c^{m/2} \rightarrow c^n, c^m$, throughout
- Page 298: $\sin(it/T), \cos(it/T) \rightarrow \sin(t/T), \cos(t/T)$
- Page 308: Insert $1/2$ in front of second term

ACKNOWLEDGEMENTS

Throughout the writing of this thesis great help has been given in suggesting topics of interest, and in discussing mathematical techniques and physical results, by my supervisor Dr. D.F. Walls and his colleague Dr. C.W. Gardiner.

I would like to acknowledge very stimulating discussions and cooperation with the following past and present researchers at Waikato University: Dr. H.J. Carmichael, Dr. S. Chaturvedi, Dr. S.S. Hassan, Dr. K.J. McNeil and Mrs. M. Steyn-Ross.

Thanks are also due to Mrs. W. Moore for typing the thesis manuscript in a very careful way.

ABSTRACT

The topic of this thesis is a theoretical study of nonequilibrium transitions and quantum statistical properties of nonlinear quantum optical systems driven by an external radiation source. In certain limiting cases, a comparison is made between these transitions and the phase transitions found in equilibrium physical systems.

In chapters one and two, the mathematical tools are introduced. In operator terms, the time development is described by a Markovian master equation in the interaction picture. This is equivalent to a corresponding time-development equation or Fokker-Planck equation in a vector space of c-numbers. In order to deal with the type of Fokker-Planck equation that results, we introduce a quantum-classical correspondence resulting in a distribution function over a complex phase-space, which is a generalisation of the Glauber-Sudarshan P-function.

In chapter three this is applied to a model of a coherently driven mode with nonlinear dispersion and absorption. We find in the limit of zero temperature, that the spectrum is symmetric relative to the input frequency, and an exact solution is obtained for the distribution function. For a detuned driving field and nonlinear dispersion, optical bistability can occur.

In chapter four a model of sub/second harmonic generation is introduced. This has several non-equilibrium transitions, including dispersive optical bistability, and bistable behaviour with coherent phase-locked input to both

modes. Exact solutions occur in the limit of zero temperature and adiabatic elimination of one mode. In both chapters three and four, steady-state photon antibunching occurs with an absorptive nonlinearity.

In chapter five we include interactions between the radiation mode and a fluorescent atomic system. In this case different behaviour occurs depending on the relative decay rates of the individual atoms and of the radiation mode. In the case of a high-Q interferometer, the atomic variables can be adiabatically eliminated. Both dispersive and absorptive bistability can occur. We show by analytic and numerical calculations (in the case of inhomogeneous broadening) that dispersive operation has advantages in requiring a lower atomic density and input field to observe bistability. When the input field has Gaussian (rather than coherent) photon statistics, there is no bistability, but enhanced photon bunching occurs.

Finally, there is a different type of behaviour when the field mode decays rapidly and can be adiabatically eliminated. Within the cooperation lifetime the system can be described by a J^2 -invariant Hamiltonian, giving the special case of only collective damping. The result is a new type of critical point transition in the thermodynamic limit, with the appearance of a family of solutions like Lotka-Volterra cycles for a coherent driving field above threshold.

NONEQUILIBRIUM TRANSITIONSINQUANTUM OPTICAL SYSTEMSCONTENTS

	Page
Notation	(viii)
List of Figures	(x)
<u>CHAPTER I: INTRODUCTION</u>	1
1.1 Summary of Results	2
1.2 Theory of Open Quantum Systems	17
<u>CHAPTER 2: COMPLEX P-REPRESENTATIONS</u>	25
2.1 Coherent State Representations	28
2.2 Atomic Coherent State Representations	46
2.3 General Operator Representations	59
<u>CHAPTER 3: SINGLE MODE TRANSITIONS</u>	71
3.1 Unified Theory for Nonlinear Dispersion and Absorption	73
3.2 Moment Calculations and Potential Solutions	98
3.3 The Laser with Injected Signal	110
3.4 The Nonlinear Absorber: Photon Antibunching	123
3.5 Purely Dispersive Optical Bistability	131
<u>CHAPTER 4: COUPLED MODE TRANSITIONS</u>	143
4.1 Theory of Sub/Second Harmonic Generation	145
4.2 Moment Calculations and Potentials in the Adiabatic Limit	162
4.3 Subharmonic Generation	167
4.4 Secondharmonic Generation	172
4.5 Bistability and Photon Antibunching	176

	Page
<u>CHAPTER 5: COOPERATIVE FLUORESCENCE</u>	182
5.1 Introduction: Cooperative Fluorescence and Optical Bistability	184
5.2 Atomic Operators and Bloch Equations	190
5.3 Dispersive Bistability in a High-Q Interferometer	198
5.4 Inhomogeneous Broadening in a High-Q Interferometer	216
5.5 Quantum Fluctuations in a High-Q Interferometer	231
5.6 Photon Bunching with a Gaussian Input	247
5.7 Volterra Cycles and the Cooperative Fluorescence Critical Point	256
5.8 Multiple Sidebands in Cooperative Fluorescence	267
5.9 Quantum Distribution in the Cooperative Thermodynamic Limit	285
<u>APPENDIX A: FOKKER-PLANCK AND STOCHASTIC DIFFERENTIAL EQUATIONS</u>	308
<u>APPENDIX B: CORRELATIONS AND SPECTRUM OF A LINEAR DIFFUSING SYSTEM</u>	314
<u>APPENDIX C: NUMERICAL METHODS</u>	318
<u>APPENDIX D: QUANTUM FLUCTUATIONS OF THE HIGH-Q CAVITY IN THE LARGE INTENSITY LIMIT</u>	323
<u>REFERENCES:</u>	327

NOTATION

$\hat{a}_\lambda, \hat{a}_\lambda^\dagger$	- boson annihilation and creation operators (mode λ)
$A_M(\)$	- Fokker-Planck drift function
$\hat{A}(\hat{a}^\dagger, \hat{a})$	- normal ordered operator functional
\underline{A}	- vector potential
$B_{\mu\nu}(\)$	- stochastic coefficient function
\underline{B}	- magnetic field
c	- velocity of light
\mathcal{C}	- integration contour
$D_{\mu\nu}(\)$	- Fokker-Planck diffusion function
\mathcal{D}	- integration domain
\underline{e}_λ	- vector of polarisation (mode λ)
\underline{E}	- electric field vector
$g, g_{\lambda\mu}$	- coupling between field and atom
H, \hat{H}	- Hamiltonian (operator)
j^+, j^-, d	- atomic transition variables
J^+, J^-, D	- collective atomic transition variables
$k = K'(1+i\lambda)$	- interferometer decay rate and detuning
\underline{k}_λ	- wave-vector (of mode λ)

\bar{n}, \hat{n}	- number of photons (operator)
N	- number of interacting atoms
\underline{P}	- polarisation (atomic)
$P(\alpha)$	- (complex) P-function
t	- time
T	- absolute temperature
u_λ	- scalar mode function
\underline{u}_λ	- vector mode function
V_r, V_o	- volume of cavity (active volume)
$\alpha_\lambda, \alpha_\lambda^+$	- variables corresponding to $\hat{a}_\lambda, \hat{a}_\lambda^+$
$\gamma_M = \gamma_\perp(1 + i\delta_M)$	- atomic decay rate and detuning
$\gamma_{ }$	- inversion decay rate
$\delta(x)$	- delta function
$\partial_M = \partial_{x_M} = \frac{\partial}{\partial x_M}$	- derivative with respect to x_M
ϵ_o	- dielectric permittivity (S.I. units)
χ	- cubic nonlinearity parameter
η	- quadratic nonlinearity parameter
μ_o	- magnetic permeability (S.I. units)
$\xi(t)$	- delta-correlated Gaussian random function

LIST OF FIGURES

<u>Figure</u>	Page
Fig (3.3.1) Laser with an injected signal; state equation of photon number <u>vs</u> input power ($\kappa' = -10, \chi = 1$): (a) $\kappa'' = 0$ (b) $\kappa'' = 5/\sqrt{3}$ (c) $\kappa'' = 10/\sqrt{3}$ (d) $\kappa'' = 15/\sqrt{3}$ (e) $\kappa'' = 20/\sqrt{3}$	114
Fig (3.3.2) Laser with an injected signal; limit cycles of amplitude <u>vs</u> time for a low level input ($\kappa = -10 + i5, \chi = 1, E = 5$)	116
Fig (3.3.3) Laser with an injected signal; limit cycles of amplitude <u>vs</u> time close to threshold ($\kappa = -10 + i5, \chi = 1, E = 10$)	
Fig (3.3.4) Laser with an injected signal; limit cycle frequency <u>vs</u> input amplitude for different detuning ($\kappa' = -10, \chi = 1.0$)	118
Fig (3.4.1) Nonlinear absorber; correlation and photon number <u>vs</u> input power ($\kappa' = 0.1, \chi = 1, \Gamma = 0$): (a) $g^2(0)$ - exact (b) \bar{n} - exact (c) \bar{n} - semiclassical	130
Fig (3.5.1) Dispersive bistability; correlation and photon number <u>vs</u> input power ($\kappa = 2.5 - i10, \chi'' = 1.0, \Gamma = 0$): (a) $g^2(0)$ - exact (b) \bar{n} - exact (c) \bar{n} - semiclassical	135
Fig (3.5.2) Dispersive bistability; correlation and photon number <u>vs</u> input power (close to critical point): (a) $g^2(0)$ - exact (b) \bar{n} - exact (c) \bar{n} - semiclassical	136

- Fig (3.5.3) Dispersive bistability spectrum; 139
 quasilinear region (arbitrary units).
 (a) zero temperature ($\Gamma = 0$)
 (b) finite temperature ($\Gamma > 0$)
- Fig (3.5.4) Dispersive bistability spectrum; 140
 subthreshold region (arbitrary units).
 (a) zero temperature ($\Gamma = 0$)
 (b) finite temperature ($\Gamma > 0$)
- Fig (3.5.5) Dispersive bistability spectrum; upper 141
 branch region (arbitrary units).
 (a) zero temperature ($\Gamma = 0$)
 (b) finite temperature ($\Gamma > 0$)
- Fig (4.1.1) Sub/Second harmonic generation; state 152
 equation of interferometer amplitude vs
 input amplitude.
 (a) $E_2 < E_2^c$ (b) $E_2 = E_2^c$ (c) $E_2 > E_2^c$
- Fig (4.3.1) Second harmonic generation; limit 170
 cycles of intensity vs time above the
 hard mode threshold.
 (a) primary intensity
 (b) second harmonic intensity
- Fig (5.3.1) Absorptive bistability; state equation 208
 of interferometer amplitude vs input
 amplitude ($c = 40$).
- Fig (5.3.2) Detuned atoms bistability; state 209
 equation of interferometer amplitude
vs input amplitude ($c = 40$).
 (a) $\delta = 0$ (b) $\delta = 4$ (c) $\delta = 8$
 (d) $\delta = 12$ (e) $\delta = 16$ (critical point)
- Fig (5.3.3) Detuned atoms and interferometer 210
 bistability; state equation of inter-
 ferometer amplitude vs input
 amplitude ($c = 40$).
 (a) $\delta = \lambda = 0$ (b) $\delta = 10, \lambda = 2.5$
 (c) $\delta = \lambda = 7$ (critical point)

Fig 5.3.4	Schematic diagram of the bistability region as a function of δ, λ for $c \gg 4$	211
Fig 5.4.1	Bistability with inhomogeneous broadening; state equation of interferometer amplitude <u>vs</u> input amplitude ($c = 500$).	221
	(a) $\delta = \lambda = \sigma = 0$ (resonant, homogeneous case)	
	(b) $\delta = \lambda = 0, \sigma = 31$ (resonant, critical point)	
	(c) $\delta = \sigma = 31, \lambda = 10$ (nonresonant, bistable region)	
Fig 5.4.2	Bistability with inhomogeneous broadening; state equation of interferometer amplitude <u>vs</u> input amplitude for different values of c ($\sigma = 31$).	222
	(a) $c = 500, \delta = \lambda = 0$	
	(b) $c = 500, \lambda = 10, \delta = 31$	
	(c) $c = 400, \lambda = 10, \delta = 31$	
	(d) $c = 340, \lambda = 10, \delta = 31$	
	(e) $c = 300, \lambda = 10, \delta = 31$	
Fig 5.8.1	J^2 -invariant cooperative fluorescence; relative semiclassical peak areas (for multiple sidebands) <u>vs</u> input amplitude ($J \rightarrow \infty$).	282
Fig 5.8.2	J^2 -invariant cooperative fluorescence; polarisation (a) and inversion (b) <u>vs</u> input amplitude ($J \rightarrow \infty$).	304
Fig 5.9.2	J^2 -invariant cooperative fluorescence: interferometer amplitude <u>vs</u> input amplitude.	305
	(a) exact ($J \rightarrow \infty$)	
	(b) uncorrelated atom factorisation ($J = 40$).	

CHAPTER 1: INTRODUCTION

Research into open systems and nonequilibrium transitions is a growing part of modern physical science. One of the earliest works to recognise how fluctuations can arise from the interaction of a physical system with its environment was that of A. Einstein (1905). In fact these ideas are really the foundation of modern treatments of nonequilibrium physical systems.

The essential character of a nonequilibrium system is that a balance exists between the energy input externally and the energy dissipated via interaction with the thermal reservoirs. In this situation a stationary state can occur that has a lower entropy than a similar equilibrium state (where we interpret entropy in a probabilistic sense). This observation was the starting point for the research of I. Prigogine (1945) and the Brussels school (Nicolis & Prigogine 1978). By changing the external driving fields (or energy inputs) it is possible to cause transitions in which one stationary state becomes unstable, and a new stationary state occurs which may have completely different properties.

The nonequilibrium transitions that can occur are found in many diverse fields, and similar techniques of theoretical analyses have been applied in different situations. Examples of nonequilibrium transitions are found in hydrodynamics, chemical systems, quantum optics, biochemical and ecological systems (Haken, 1974, 1975).

One of the best known nonequilibrium transitions is that of the single mode laser, which is caused by an increase in the energy input to the laser via optical pumping of the atoms.

This has been treated by many researchers, and results are reviewed in the books by Haken (1970), Louisell (1973), Sargent, Scully & Lamb (1974).

In the present thesis, the topic of research is nonequilibrium transitions in quantum optical systems. We will be interested in transitions between nonequilibrium steady states caused by an external source of radiation directly driving the "order parameters" or field modes. The results are summarised in the next section: we do not give a comprehensive survey, but instead have studied straightforward cases where a relatively exact theory is possible.

1.1 SUMMARY OF RESULTS

The motivation for this research was in recent advances in experiments on optical bistability and on atomic fluorescence. These are experiments in which a stabilised single-mode laser is used to drive a fluorescent atomic system (or other nonlinear medium) with measurements being made on the transmitted or fluorescent radiation.

The first observation of differential gain and bistability in a fluorescent atomic system was made by Gibbs, McCall & Venkatesan (1976) as was earlier predicted theoretically (see McCall (1974) and references in the paper by Gibbs et al). This is a nonequilibrium transition in a driven quantum optical system. Of some interest are the uses of these types of transition in communications and logic, which gives a possible practical application (Venkatesan, 1977).

The observation of the basic quantum statistical property of photon antibunching in atomic resonance fluorescence was made by Kimble, Dagenais and Mandel (1977, 1978) as originally predicted by Carmichael & Walls (1976). This occurs in the fluorescent radiation of one atom, and is a completely non-classical property of the radiation field. For this reason it is of great interest as an intrinsically quantal description of the interaction is necessary.

Clearly the physics of other nonlinear optical processes involves more than the classical description, which is presumably accurate only in the limit of large photon numbers. The objective of this thesis was therefore to attempt to unify the theory of nonequilibrium transitions like optical bistability with the theory of quantum fluctuations in the radiation field. The quantum fluctuations are of especial interest in nonequilibrium transitions, in that they provide a basic theoretical limitation to the stability and output coherence of a nonlinear device. We remark here that in the semiclassical description there is no limitation of this type: a bistable device at zero temperature would be indefinitely stable and have a completely coherent output.

In addition to optical bistability in atomic systems, other types of nonequilibrium steady states and transitions can potentially occur: some of these are investigated in the present thesis. Of special interest are the existence of photon antibunching in the steady-state (Chapter 3); the bistability and antibunching occurring in sub/second harmonic generation (Chapter 4); and the existence of solutions like

Volterra cycles above a critical-point for cooperative fluorescence on time-scales less than the cooperation lifetime (Chapter 5). The thesis is organised by starting in Chapters 1 and 2, with the mathematical tools involved, and moving on to specific calculations on physical systems in Chapters 3, 4 and 5.

In Chapter 1.2 we introduce the theory of an open quantum system interacting with an environment of thermal reservoirs, following the standard treatments of Louisell (1973) and other authors. The purpose of this theory is to eliminate the large numbers of dynamical variables involved in energy dissipation from the nonequilibrium system. With the use of projection operators it is possible to eliminate these "reservoir" operators and to obtain an exact time-development equation in terms of system operators only. This can be further simplified by use of the Markovian approximation, to give a time development equation in terms of operators at the same time, called the master equation.

In Chapter 2, we introduce various classical-quantum correspondences used to solve master equations, including the Glauber-Sudarshan coherent state P-representation. This representation is in terms of a distribution function defined on a real phase-space with variables (p, q) or (α, α^*) . This has the advantage of following relatively simple time development equations, and having moments of the phase-space distribution that are equal to normal-ordered correlations of physical observables. However in some cases the representation does not exist except in terms of generalised functions. This is reflected by a time-development equation

having the form of a Fokker-Planck equation, but with non positive-definite diffusion, giving a singular distribution in the steady-state.

In order to deal with this situation, we prove the existence of a "complex P-representation", that is defined on a complex phase-space of $4n$ dimensions for n field modes. This can either be defined as a generalised line-integral within the complex phase-space, or as a probability distribution without singularities on the full complex phase-space. The representation is closely related to the R-representation of Glauber (1963b), but is defined with a different normalisation and has time-development equations similar to those of the Glauber-Sudarshan P-representation. The advantage of this representation is that it exists for any quantum optical system without singularities. We show that in special cases potential solutions exist for Fokker-Planck equations with non positive-definite diffusion, that are defined as line-integrals in a complex phase-space. In addition, any Fokker-Planck equation may be transformed to a positive-(semi)definite Fokker-Planck equation on the full complex phase-space. This proves to have practical advantages when obtaining physical observables that include quantum fluctuations. We also show how complex P-representations can be defined for atomic coherent states and for other operator algebras, and derive the results for correlations in these representations.

In Chapter 3, we turn to the specific problem of a single field mode interacting with a medium with nonlinear (cubic) polarisability. Both dispersive and absorptive nonlinearities are included, corresponding to an intensity-dependent

refractive index and to two-photon absorption processes respectively. The mode is driven externally by a coherent driving field, and is damped by single-photon losses as well as by nonlinear absorption. A Fokker-Planck equation is obtained with a complex parameter describing both dispersive and absorptive nonlinearities, in a unified way. In the deterministic limit, we derive the state equation and obtain the boundaries of bistability as a function of the damping and detuning. Small fluctuations can be treated by linearising the Fokker-Planck equation close to the deterministic stable branches. As the Fokker-Planck equation in the Glauber-Sudarshan P-representation has a non-positive definite diffusion, the complex P-representation is used to obtain a positive-definite Fokker-Planck equation in a 4-dimensional phase-space, and hence a linearised stochastic differential equation.

The results regarding fluctuations depend on the relative sizes of thermal and quantum fluctuations. In the limit of a large thermal background, the driven nonlinear system behaves like a classical anharmonic oscillator with nonlinear damping. The spectrum is essentially asymmetric relative to the input frequency, with symmetrically displaced sidebands of different peak heights, as well as a coherent line at the input frequency. The transmitted fluctuation spectrum has the greatest intensity at the effective interferometer tuning. This varies with the input intensity, so that the spectral line-shape is a function of the intensity of the driving field.

Far below the bistable threshold, the fluctuation line-shape is identical to that of a linear interferometer, with a single Lorentzian at the linear interferometer tuning point. With increasing input intensity an extra symmetrically displaced Lorentzian line appears. The lines merge below threshold, and one of the eigenvalues vanishes at the bistable threshold with characteristic critical fluctuations. Above the threshold the reverse situation occurs. There are symmetrically displaced sidebands that merge, this time with decreasing input intensity. However a crossover occurs above the bistable threshold, and the largest intensity sideband is on the other side of the input frequency, relative to the linear case.

In the case of dominant quantum fluctuations, the spectrum is different. While the eigenvalues (peak frequencies) are unchanged, the relative weights of the sidebands are equal, giving a symmetric spectrum. As far as we know, the existence of a symmetric spectrum in lossless dispersive optical bistability in the quantum limit, has not been calculated previously. However this behaviour has a remarkable similarity to that of the spectrum for atomic fluorescence (Mollow, 1969) in that this is also symmetric for a coherent driving field. In addition, just as in atomic fluorescence there can be photon antibunching, there can also be photon antibunching in the transmitted field of the nonlinear interferometer. This last result also depends on the type of nonlinearity, and is most noticeable for a purely absorptive nonlinearity.

In order to deal with the quantum limiting case more

precisely, the Fokker-Planck equation is solved exactly for the steady-state, in this limit. The result is singular on the real phase-space domain of the Glauber-Sudarshan P-representation. However when the complex P-representation is utilised, an integrable solution is found as a generalised line-integral on a complex phase-space. This solution holds for an arbitrary dispersive or absorptive nonlinearity, and for arbitrary detuning of the coherent driving field. The exact solution has a different character from the Landau-Ginsberg solutions of equilibrium Fokker-Planck equations and of the laser Fokker-Planck equation; it includes (under certain circumstances) correlation functions giving photon antibunching. We show that photon antibunching is most readily observed for an absorptive nonlinearity with minimal thermal background and low one-photon (linear) damping. For a dispersive nonlinearity with a bistable region, there is enhanced photon bunching throughout the bistable region, showing increased steady-state fluctuations.

In sections 3.3 - 3.5 of Chapter 3, the general results for a nonlinear polarisability are applied to different physical systems. In 3.3 we show that the laser with an injected signal can be treated with the present theory, and has different types of entrainment (phase-locking) transitions that depend on the detuning. These results are largely of a standard nature, as laser entrainment has been observed in experiment. In 3.4 we treat the case of a purely absorptive nonlinearity in detail. For a coherent input, photon antibunching occurs,

and this can be treated exactly in the zero-temperature limit. In the case of a fluctuating input, a reduction in the fluctuations occurs, as has been observed by Krasinski & Dinev (1977). In section 3.5 we treat the case of purely dispersive optical bistability. While a classical treatment has been previously obtained by Marburger & Felber (1978), this is the first treatment to include quantum fluctuations, with the calculation of the distribution function in the zero-temperature limit, as well as the linearised spectrum and intensity correlations close to a stable branch.

In Chapter 4, we treat an interferometer with a non-linear (quadratic) polarisability and wave-vector matching, so that the mode-mode coupling problem occurs. The theoretical treatment is similar to that in Chapter 3, with the inclusion of the extra mode operator. A Fokker-Planck equation is derived to describe quantum fluctuations in the coupled-mode system, with the inclusion of coherent driving fields at either frequency. The deterministic analysis of the full coupled system involves a real four-dimensional phase-space for the classical fields, so we restrict the analysis to the case of zero-detuning for the full coupled equations. However we are able to show that in addition to the subharmonic generation critical point (Graham, 1973), and the second harmonic generation hard-mode transition (McNeil, Drummond & Walls, 1978), there is also a region of bistable behaviour with coupled, phase-locked driving fields.

To calculate fluctuations in this case, we use the adiabatic limit of a rapid decay of the second-harmonic field. In this situation the deterministic analysis can be extended to arbitrary detuning. We show that the resulting equations are completely equivalent to the nonlinear single-mode problem of Chapter 3, provided only the lower-frequency mode is driven. This leads to a prediction of dispersive optical bistability in second-harmonic generation (in addition to the transitions mentioned previously).

In the case of subharmonic generation, we derive results for the spectrum, correlation function, and distribution function in the adiabatic, zero temperature limit that have not been obtained previously. Finally some interesting behaviour can occur with coupled (phase-locked) driving fields. In this case bistability and antibunching statistics on inputting a driving field at both frequencies will occur, depending on the relative phase and amplitude of the driving fields. With in-phase fields one obtains bistability for a large second-harmonic input. On the other hand a low intensity second-harmonic, input 180° out of phase, will cause induced emission out of the lower frequency, resulting in photon antibunching. This is a similar phenomenon to that predicted by Stoler (1974) in the transient case, although it seems more likely as a practical experiment to be observed in the present situation.

In Chapter 5, interactions with an atomic transition are included, giving a specific model of the nonlinear

medium. In sections 5.1 and 5.2 we give a general discussion of atomic fluorescence in one atom and in cooperative atomic systems, leading to the coupled Maxwell-Bloch equations. We include both inhomogeneous broadening and a general mode function to give a realistic model of experiments (Gibbs et al (1976), Sandle (1978)). A single-mode treatment, as given here, has the advantage of giving more tractable equations than those of McCall (1974) so that the bistable region and critical points can be readily obtained in most cases.

In section 5.2 we treat atoms within a high-Q Fabry-Perot interferometer, with adiabatic elimination of the atomic variables. In the simplest case (homogeneous line, travelling wave mode, resonant interactions) this leads to the semiclassical theory of absorptive optical bistability advanced by Bonifacio & Lugiato (1976). Of more practical interest in experiments, is the problem of dispersive optical bistability. We give a complete treatment of the region of bistability in this case, as a function of the detuning of the atoms and the interferometer. In addition a discussion is given of the effects of standing-waves in the mode function. In the large detuning limit, the deterministic stability theory reduces to that for a medium with intensity-dependent refractive index, as obtained in Chapter 3.

In section 5.4 the effects of inhomogeneous broadening are included to give a more realistic situation. The theoretical result in absorptive bistability, is that a large increase in the cooperativity parameter (or effective number of

interacting atoms) is required to observe any bistability. The critical point is obtained for Gaussian broadening as a function of the inhomogeneously broadened atomic linewidth. We find by exact numerical study, that bistability can be obtained both at lower driving fields and with lower atomic densities with the input laser detuned relative to both the Fabry-Perot interferometer and the atomic transition frequency. In the dispersive limit, once again a relatively simple theory can be obtained similar to the treatment of Chapter 3.

In section 5.5 a treatment of quantum fluctuations in dispersive optical bistability is obtained. A generalised Fokker-Planck equation results, that includes both field and atomic fluctuations, based on the treatment of quantum fluctuations in a single-mode laser (Haken, 1970). We make the approximations of neglecting higher order derivatives, and adiabatic elimination of the atomic variables, to obtain a Fokker-Planck equation in field variables alone. While this type of approximation is not always valid for a high-intensity laser, we expect it to be valid certainly in the dispersive limit. The off diagonal terms of the diffusion array are found to approach a constant at high intensity, similar to the result of Willis (1978). We also find diagonal terms in the diffusion array. These results agree exactly with the quantum fluctuation terms found in Chapter 3, in the dispersive limit.

In section 5.6 a treatment is given of the results when Gaussian fluctuations in the input field are significant. For a completely Gaussian input, a potential solution is

obtained to the resulting Fokker-Planck equation (neglecting quantum fluctuations). While no bistability occurs, there is enhanced photon bunching over a certain range of input intensity. This may be of value as the enhanced higher order correlations obtained in this way would give increased multiphoton interactions in the device output, relative to single photon interactions. That is, the nonlinear device can be regarded as a correlation filter, which alters the statistical composition of the transmitted field.

In section 5.7 a rather different problem is discussed, where the decay rate of the field is fast enough to adiabatically eliminate the field modes. This gives a model for an "angular momentum oscillator" as proposed by Senitzky (1972), with a collective decay similar to that of superfluorescence. By the use of the variables of the atomic coherent state representation, it is possible to exactly solve the semiclassical equations. The result is an extremely fast response below a threshold point (similar to the superfluorescent behaviour of a group of atoms with a population inversion). Above the threshold (which is shown to be a critical point in the thermodynamic limit), the higher driving field results in a family of Lotka-Volterra cycle type responses. We emphasise that this model is a J^2 -invariant model, with a collective decay mode: it is therefore applicable within the cooperation lifetime, but cannot describe J^2 -breaking behaviour.

In section 5.8 the semiclassical method is used to derive an exact result for the semiclassical fluorescent

spectrum, showing multiple sidebands occurring above threshold. This calculation neglects quantum fluctuation and line-width effects, which are of order $(1/N)$ in the thermodynamic limit of $N \rightarrow \infty$. The full quantum spectrum is therefore still an open question. The new result obtained here is the semiclassical calculation for a finite driving field in the region above threshold. We show that this is the optimal region for a physical experiment to detect extra sidebands.

Finally, in section 5.9, we treat quantum fluctuations in the model for cooperative fluorescence with a collective decay. We use the complex representation derived in 2.2 to obtain a stochastic differential equation in a four-dimensional phase-space. This is used to obtain an exact result for the distribution function, in the thermodynamic limit. Below the threshold, the distribution has the form of a generalised function in the (θ, ϕ) variables of the atomic coherent state-representation. Above the threshold, the distribution is spread over the entire sphere of (θ, ϕ) variables. We find that critical slowing down occurs in the cycle period, and that spontaneous emission breaks the invariance of the cycle parameter. This gives an interesting analogy between this case and the spontaneous symmetry breaking characteristic of equilibrium critical point phase transitions.

Some of the results obtained in this thesis have been published, and the reader is referred to the following papers:

1. "Two photon absorption with coherent and partially coherent driving fields", S. Chaturvedi, P.D. Drummond & D.F. Walls.
J. Phys. A10, L187 (1977).
2. "Intensity correlations in resonance fluorescence with atomic number fluctuations", H.J. Carmichael, P.D. Drummond, P. Meystre & D.F. Walls.
J. Phys. A11, L121 (1978).
3. "Volterra cycles and the cooperative fluorescence critical point", P.D. Drummond & H.J. Carmichael.
Optics Communications, 27, 160 (1978).
4. "Dispersive optical bistability in a ring cavity", S.S. Hassan, P.D. Drummond & D.F. Walls.
Optics Communications, in press.
5. "Non equilibrium phase transitions in cooperative atomic systems", D.F. Walls, P.D. Drummond, S.S. Hassan & H.J. Carmichael.
Progress in Theoretical Physics, in press.
6. "Self pulsing in second harmonic generation", K.J. McNeil, P.D. Drummond & D.F. Walls.
Optics Communications, in press.
7. "Optical bistability in cooperative atomic systems", H.J. Carmichael, P.D. Drummond, S.S. Hassan & D.F. Walls.
I.E.E.E. J. Quant. Electronics, in press.

8. "Bistability and photon antibunching in sub/second harmonic generation", P.D. Drummond, K.J. McNeil & D.F. Walls.
Optics Communications, in press.
9. "Multiple sidebands in cooperative resonance fluorescence: Exact semiclassical results", P.D. Drummond & S.S. Hassan.
(Submitted for publication.)

1.2 THEORY OF OPEN QUANTUM SYSTEMS

(a) Quantum Electrodynamics

In the standard treatment of quantum electrodynamics, the free field operators are expanded in terms of transverse mode functions in the radiation gauge where:

$$\underline{A}_4 = \nabla \cdot \underline{A} = 0$$

In terms of the radiation gauge mode operators, we can write (Bjorken & Drell (1965), Louisell (1973)):

$$\underline{A} = \sum_{\lambda} \left[\frac{\hbar}{2\omega_{\lambda}\epsilon_0} \right]^{1/2} \left[\underline{e}_{\lambda} u_{\lambda}(\underline{r}) \hat{a}_{\lambda} + \underline{e}_{\lambda}^* u_{\lambda}^*(\underline{r}) \hat{a}_{\lambda}^{\dagger} \right]$$

$$\underline{E} = i \sum_{\lambda} \left[\frac{\hbar\omega_{\lambda}}{2\epsilon_0} \right]^{1/2} \left[\underline{e}_{\lambda} u_{\lambda}(\underline{r}) \hat{a}_{\lambda} - \underline{e}_{\lambda}^* u_{\lambda}^*(\underline{r}) \hat{a}_{\lambda}^{\dagger} \right]$$

Here \underline{e}_{λ} are polarisations defined so that $\underline{e}_{\lambda} \cdot \underline{e}_{\lambda}^* = 1$ while the u_{λ} are mode functions defined so that:

$$\int |u_{\lambda}(\underline{r})|^2 d^3\underline{r} = 1$$

In the simplest case of a plane wave we would define:

$$u_{\lambda}(\underline{r}) = \exp(i\underline{k} \cdot \underline{r}) / \sqrt{V_r}$$

By means of the mode expansion, the quantum mechanical operators are all in the form of harmonic oscillator operators \hat{a}_{λ} which obey the usual relations:

$$\begin{aligned} [\hat{a}_{\lambda}, \hat{a}_{\lambda'}^{\dagger}] &= \delta_{\lambda\lambda'} \\ \hat{H} &= \sum_{\lambda} \omega_{\lambda} \hat{a}_{\lambda}^{\dagger} \hat{a}_{\lambda} \\ \hat{x}_{\lambda} &= (\hbar/2m\omega_{\lambda})^{1/2} (\hat{a}_{\lambda}^{\dagger} + \hat{a}_{\lambda}) \\ \hat{p}_{\lambda} &= i(\hbar m\omega_{\lambda}/2)^{1/2} (\hat{a}_{\lambda}^{\dagger} - \hat{a}_{\lambda}) \end{aligned}$$

The operators \hat{x}, \hat{p} are introduced here as they are the momentum and position operators of the corresponding harmonic oscillator of mass (m).

At this point, it is worth noting some facts about coherence properties. We shall define coherence in terms of mode operators: that is, the n-th correlation function of a mode function is: (Glauber 1963a) -

$$G_{(t)}^{(n)} = \text{Tr} \{ \hat{\rho} \hat{a}^\dagger(t_1) \dots \hat{a}^\dagger(t_n) \hat{a}(t_{n+1}) \dots \hat{a}(t_{2n}) \}$$

Normalised functions can be defined as:

$$g_{(t)}^{(n)} = (G_{(t)}^{(n)}) / \left(\prod_{j=1}^{2n} G^{(1)}(t_j, t_j) \right)^{1/2}$$

Of particular interest to the physicist are the spectrum and photon correlation functions:

$$S(\omega) \equiv \frac{1}{2\pi} \int_{-\infty}^{\infty} G^{(1)}(t, 0) e^{-i\omega t} dt$$

$$g_{(t)}^{(2)} \equiv (G^{(2)}(0, t, t, 0)) / (G^{(1)}(0, 0) \cdot G^{(1)}(t, t))$$

Here the order of time-variables has been specified to correspond to a photo-count correlation experiment. Now the value of $g_{(0)}^{(2)}$ has some interest in quantum physics, because the corresponding classical correlation is always greater or equal to 1. For a fully coherent (quantum) system we also have $g_{(0)}^{(2)} = 1$. However for a quantum system it is possible to obtain $g_{(0)}^{(2)}$ less than 1. The following relation holds for any quantum state:

$$g_{(0)}^{(2)} \geq \left(1 - \frac{1}{n}\right)$$

where: $\bar{n} = g^{(1)}(0,0) = \langle \hat{a}^+ \hat{a} \rangle$

This can be proved simply by expanding in number states:

$$\begin{aligned} g^2(0) &= \frac{1}{\bar{n}^2} \sum_n \langle n | \hat{a}^{+2} \hat{a}^2 | n \rangle \langle n | \hat{\rho} | n \rangle \\ &= \frac{1}{\bar{n}^2} \sum_n \langle n | (\hat{a}^+ \hat{a})^2 - (\hat{a}^+ \hat{a}) | n \rangle \rho_{nn} \\ &= \frac{1}{\bar{n}^2} \langle \hat{n}(\hat{n}-1) \rangle_\rho \\ &\geq 1 - \frac{1}{\bar{n}} \quad (\bar{n} \geq 1) \end{aligned}$$

In any experiment for which $g^2(0) < 1$, the photons are "antibunched" at time $t = 0$; since for $t \neq 0$, even a classical process could have an anticorrelation with $g^2(t) < 1$. In the limit of $\bar{n} < 1$, we still have the relation $g^2(0) \geq 0$:- it is in this limit that non-classical properties due to quantum mechanics become significant. (The fact that classically one can have $g^2(t) < 1$ is mentioned by Jakeman et al (1977)).

Finally it is worth emphasising that antibunching photon statistics have recently been observed in experiment. The possibility of antibunching was predicted in atomic resonance fluorescence by Carmichael & Walls (1975, 1976). This was recently observed in experiments by Kimble et al (1977, 1978) although there were problems initially in the interpretation of Kimble's data, relating to atomic number fluctuations, as pointed out by Jakeman et al (1977), Carmichael et al (1978). However, after correcting the data for the atomic number fluctuations it seems that photon antibunching with $g^2(0) < 1$ can be inferred from these experiments.

(b) Open classical systems

The foundation for the theory of open systems was in the work of A. Einstein (1905) on a classical system of diffusing particles. This was later generalised to include specific models for fluctuating forces due to interaction with thermal reservoirs, and external forces. An isolated system has the following equations of motion for the position and momentum:

$$\begin{aligned}\dot{p}_\alpha &= -\partial H / \partial x_\alpha \\ \dot{x}_\alpha &= \partial H / \partial p_\alpha\end{aligned}$$

In an open system the Hamiltonian includes extra terms describing an interaction with the environment and any external energy sources. This can be described by adding external time dependent forces. An equilibrium system with linear damping dissipates energy at a rate proportional to $|\dot{x}_\alpha|^2$, and is described as follows:

$$\dot{p}_\alpha = -(\partial H / \partial x_\alpha) - \Gamma_\alpha (\partial H / \partial p_\alpha) + \sqrt{2D_\alpha} f_\alpha(t)$$

It is normally supposed that the thermal fluctuation term, $f_\alpha(t)$, has rapid fluctuations relative to the system response time, and can be approximated by a delta-correlated Gaussian random function:

$$\langle f_\alpha(t) f_\beta(t') \rangle = \delta_{\alpha\beta} \delta(t-t')$$

Non-Markovian theories have also been developed which include a "memory functional" (Y. Pomeau & P. Resibois, 1975); although in practice provided the set of dynamical variables $(\underline{p}, \underline{x})$ is large enough, the Markovian equations will be sufficient. Equations of the above sort can be used to describe equilibrium critical point phenomena (Ma, 1976).

It can be readily shown that the phase-space distribution function approaches a Maxwell-Boltzmann distribution, provided the Einstein relation holds:

$$D_{\alpha} = kT \Gamma_{\alpha}$$

Now the same equations that hold for the equilibrium are also able to be extended to non-equilibrium systems when external driving forces are included. In general one would obtain in this way an equation of the following form; where ϕ_{α} are dynamical variables:

$$\dot{\phi}_{\alpha} = -A_{\alpha}(\underline{\phi}) + B_{\alpha\beta} \xi_{\beta}(t)$$

This is equivalent to a Fokker-Planck equation, as pointed out in Appendix (A).

In the case of open quantum systems we will obtain similar types of Fokker-Planck equation via the use of a normal-ordered classical-quantum correspondence. The differences are that the diffusion array can now be a function of the system variables, and in addition may be non-positive definite. In order to deal with this problem we will find it useful to define a normal ordered

P-representation on a complex phase-space, which has a Fokker-Planck equation with positive semi-definite diffusion. In this case, the corresponding stochastic equations have complex fluctuating terms, so that the variables corresponding to the classical $(\underline{p}, \underline{x})$ variables will be complex in general. We will find that nonclassical correlations like photon anti-bunching directly correspond to the multinomial moments of a complex phase-space probability distribution, which enables them to be evaluated in a straightforward way.

(c) Open quantum systems

The theory of open quantum systems involves, just as before, the addition of Hamiltonian terms to describe an interaction with an environment of thermal reservoirs. This is thoroughly discussed by Louisell (1973), Picard & Willis (1977).* We therefore give a brief account of the method of Louisell, involving tracing over the reservoir variables. We suppose the system is described by the following Hamiltonian:

$$\hat{H} = \hat{H}_0 + \hat{H}_r + \sum_i \hat{P}_i \hat{A}_i$$

Here \hat{H}_0 is the system Hamiltonian, \hat{H}_r the reservoir Hamiltonian, \hat{P}_i are the reservoir operators and \hat{A}_i are system operators. We let $\hat{W}(t)$ be the total density operator in the interaction picture, with a coupling perturbation between the reservoir and system:

* Other work on master equations include Nakajima (1958), Prigogine & Resibois (1961), Zwanzig (1964), Haake (1973), Lugiato (1976).

$$i\hbar \frac{\partial}{\partial t} \hat{W} = [\hat{H}_c, \hat{W}] = [\sum_i \hat{\Gamma}_i \hat{A}_i, \hat{W}]$$

We also define a reduced density operator for the system, by tracing over the reservoir variables:

$$\hat{\rho} \equiv \text{Tr}_R[\hat{W}]$$

The next step is to integrate the equations of motion for \hat{W} to give:

$$\begin{aligned} \partial_t \hat{W}(t) = & \left(\frac{1}{i\hbar}\right) [\hat{H}_c(t), \hat{W}(0)] \\ & + \left(\frac{1}{i\hbar}\right)^2 \int_0^t [\hat{H}_c(t), [\hat{H}_c(t'), \hat{W}(t')]] dt' \end{aligned}$$

We assume that the interaction has no diagonal terms in the representation that diagonalises \hat{H}_r , that the density operator factorises initially, and that the coupling is a small perturbation. We then obtain:

$$\partial_t \hat{\rho}(t) = \text{Tr}_R \left(\frac{-1}{\hbar^2} \int_0^t [\hat{H}_c(t), [\hat{H}_c(t'), \hat{\rho}(t') \hat{f}_R]] dt' \right)$$

Here \hat{f}_R is the initial reservoir density operator, assumed to remain in equilibrium at all times. Next, we make the Markovian approximation that $\hat{\rho}$ only depends on $\hat{\rho}(t)$ at the same time. Hence we finally obtain:

$$\begin{aligned} \partial_t \hat{\rho} = & - \sum_{ij} \delta(\omega_i, -\omega_j) \left\{ [\hat{A}_i \hat{A}_j \hat{\rho} - \hat{A}_j \hat{\rho} \hat{A}_i] \omega_{ij}^+ \right. \\ & \left. - [\hat{A}_i \hat{\rho} \hat{A}_j - \hat{\rho} \hat{A}_j \hat{A}_i] \omega_{ji}^- \right\} \end{aligned}$$

Here the ω_{ij} terms are correlation functions of reservoir operators; (ω_i is the frequency of \hat{A}_i):

$$\begin{aligned} \omega_{ij}^+ &= \int_0^\infty \exp(+i\omega_i t) \text{Tr}_R [\hat{f}_R \hat{\Gamma}_i(t) \hat{\Gamma}_j(0)] dt / \hbar^2 \\ \omega_{ji}^- &= \int_0^\infty \exp(+i\omega_j t) \text{Tr}_R [\hat{f}_R \hat{\Gamma}_j(0) \hat{\Gamma}_i(t)] dt / \hbar^2 \end{aligned}$$

In particular, we will be interested in the cases where $\hat{\Gamma}_i$ are a set of field operators with very closely spaced modes, as in radiative damping. Hence (neglecting light shift terms) one obtains:

$$\partial_t \hat{\rho} = \sum_j \kappa'_j \left[(1+n_j^{th}) ([\hat{A}_j \hat{\rho}, \hat{A}_j^\dagger] + [\hat{A}_j, \hat{\rho} \hat{A}_j^\dagger]) \right. \\ \left. + n_j^{th} ([\hat{A}_j^\dagger \hat{\rho}, \hat{A}_j] + [\hat{A}_j^\dagger, \hat{\rho} \hat{A}_j]) \right]$$

Where:

$$i \sum \hat{\Gamma}_i \hat{A}_i = i \sum \left\{ \hat{A}_i^\dagger \sum_\lambda g_\lambda \hat{a}_\lambda + \hat{A}_i \sum_\lambda g_\lambda^* \hat{a}_\lambda^\dagger \right\}$$

$$n_j^{th} = [\exp(\hbar \omega_j / kT) - 1]^{-1}$$

Thus κ'_j is the decay rate due to the reservoir coupling, ω_j is the (laboratory frame) frequency of the operator \hat{A}_j , n_j^{th} is the thermal occupation number of the reservoir photons at this frequency.

CHAPTER 2: COMPLEX P-REPRESENTATIONS

In general it is a nontrivial problem to solve a master equation of the type derived in Chapter 1 using either operator techniques or representations in an orthogonal basis for the density matrix. In some cases where the master equation is in terms of diagonal number-state matrix elements, the equations become soluble utilising generating function techniques. A survey of some of these methods is given by McNeil & Walls (1974), McNeil (1976).

However in most of the cases we wish to study here, the nondiagonal number-state matrix elements are significant. Elegant techniques have been evolved by several researchers to study quantum time-development equations as represented by a distribution function over a real vector space, in these cases. For the harmonic oscillator (obeying boson algebra) a representation was developed called the P-representation, by Sudarshan (1963) and Glauber (1963b). In this representation, the distribution domain is a two-dimensional real space with coordinates (x,p) being the analogs of the non-commutating operators \hat{x}, \hat{p} (alternatively a single variable with a complex domain is used).

Similar techniques for atomic collective transition operators were developed by Arecchi et al (1972), Narducci (1974), Glauber and Haake (1974): in this case the distribution domain could either be the surface of a sphere (the "Bloch sphere") or its map, the complex domain. Just as with the Glauber-Sudarshan P-representation, the density operator representation is an expansion in terms of

hermitian projection operators on a set of minimum uncertainty states.

For general operator algebras, similar phase-space descriptions were developed by Agarwal & Wolf (1968), Lax (1968), Louisell & Marburger (1969), Haken (1970). However perhaps the earliest phase-space description was that of Wigner (1932) who used the method to describe an N-particle quantum system. The advantage of the phase-space descriptions developed in recent years, is that by choosing an appropriate operator ordering, it is possible to obtain very simple time-development equations (as generalised Fokker-Planck equations), and equations for observables similar to classical phase-space means or correlations. In particular, normal orderings (and the generalised normal ordering of atomic operators of Haken, Risken & Weidlich (1967)) have proved useful in practical problems.

It was recognised by these authors that the distributions on a real phase-space need not always exist except as generalised functions. In fact, while the antinormal representation of the harmonic oscillator exists, the normal ordering representation (or P-representation) is not always positive-definite and does not exist except as a generalised function in some cases (Cahill & Glauber (1969), Glauber (1970)). Yet the P-representation is appealing because it transforms away the quantum fluctuations of a coherent state, while still having a classical limit as a probability distribution in phase-space. In addition the normal-ordering (P-representation) has an advantage relative

to the antinormal-ordering (Q-representation), in that physical observables like the spectrum directly result from a correlation function calculation in phase-space.

Problems arise with the P-representation when the diffusion terms in the Fokker-Planck equation become non-positive-definite. Similar Fokker-Planck equations in the theory of nonequilibrium chemical processes are mentioned by Chaturvedi, Gardiner & Walls (1976) and Chaturvedi & Gardiner (1977). These authors handle this situation in some cases by allowing the representation variable to have complex values.

For this reason we introduce a generalisation of the Glauber-Sudarshan P-representation called the "complex P-representation". This is a representation in nonhermitian projection operators, defined on a manifold in a complex phase space. Different representations can be obtained by choosing different integration domains. In the case of a complex contour integration, exact solutions to the Fokker-Planck equation are obtained when potential equations apply. In the case of integration over the whole complex phase-space, we prove rigorously that at least one real positive P-function exists for an arbitrary density operator. In this case, we show that provided a Fokker-Planck equation for the diagonal (Glauber-Sudarshan) P-representation exists, there is an equivalent equation with positive-(semi)definite diffusion terms for the complex P-representation. This means that the propagation of the P-function is equivalent to a stochastic process on a complex phase-space. The advantage of this generalised P-representation is that it

allows the calculation of physical observables in a straightforward way, for normal-ordered operators, even when the Glauber-Sudarshan P-function is singular.

The same technique of representation on a complex phase space can be generalised to other operator algebras. This is treated in 2.2, 2.3 for the cases of the atomic coherent state representation, and the general phase-space descriptions of ordered operators.

2.1 COHERENT STATE REPRESENTATIONS

(a) The diagonal P-representation

A coherent state is defined to be an eigenstate of the \hat{a} -operator: An explicit representation is -

$$|\alpha\rangle = e^{-\frac{1}{2}|\alpha|^2} \sum_{n=0}^{\infty} \frac{\alpha^n}{\sqrt{n!}} |n\rangle = e^{-\frac{1}{2}|\alpha|^2 + \alpha \hat{a}^\dagger} |0\rangle$$

It is possible to prove that these states form a complete non-orthogonal basis of the Hilbert space (Glauber 1963b, Sudarshan 1963):

$$|\langle \beta | \alpha \rangle|^2 = \exp(-|\alpha - \beta|^2)$$

$$\int |\alpha\rangle \langle \alpha| d^2\alpha = \pi$$

The states are also minimum uncertainty states, in the sense of Heisenberg's uncertainty principle:

$$\left. \begin{aligned} (\Delta p)^2 &= \langle \hat{p}^2 \rangle_\alpha - \langle \hat{p} \rangle_\alpha^2 \\ (\Delta x)^2 &= \langle \hat{x}^2 \rangle_\alpha - \langle \hat{x} \rangle_\alpha^2 \end{aligned} \right\} \Delta p \Delta x = \frac{\hbar}{2}$$

These states form an extremely useful basis for an expansion of the density matrix, called the P-representation:

$$\hat{\rho} = \int |\{\alpha_\lambda\}\rangle \langle \{\alpha_\lambda\}| P(\{\alpha_\lambda\}) \prod_\lambda d^2\alpha_\lambda$$

Here the set $\{\alpha_\lambda\}$ represents a complete set of modes. In the case that $P(\{\alpha_\lambda\})$ is a delta function, the quantum system has some interesting properties. In fact this density matrix is the one produced by the radiation into a vacuum of a classical current distribution. The n-th order correlation function in this case factorises completely, so the quantum field is coherent to all orders.

We frequently wish to expand operator products of form $\hat{A} \hat{\rho} \hat{B}$ in the P-representation, so the following identities will be useful:

$$\hat{a} |\alpha\rangle \langle \alpha| = \alpha |\alpha\rangle \langle \alpha| \quad ; \quad |\alpha\rangle \langle \alpha| \hat{a}^\dagger = \alpha^* |\alpha\rangle \langle \alpha|$$

$$\hat{a}^\dagger |\alpha\rangle \langle \alpha| = [\partial_\alpha + \alpha^*] |\alpha\rangle \langle \alpha| \quad ; \quad |\alpha\rangle \langle \alpha| \hat{a} = [\partial_{\alpha^*} + \alpha] |\alpha\rangle \langle \alpha|$$

Given a time development equation of the form:

$$\partial_t \hat{\rho} = \hat{\mathcal{L}}[\hat{\rho}]$$

it is possible to define an equivalent time development equation for the P-representation of form:

$$\partial_t P(\alpha) = \mathcal{L}[\partial_\alpha, \alpha^*] P(\alpha)$$

In the case of a normally ordered operator function $\hat{A}(\hat{a}^+, \hat{a})$ the one time operator averages are:

$$\begin{aligned} \langle \hat{A} \rangle_\rho &\equiv \text{Tr}(\hat{A}\hat{\rho}) / \text{Tr}(\hat{\rho}) \\ &= \int P(\alpha) A(\alpha^*, \alpha) d^2\alpha \end{aligned}$$

where we suppose that $P(\alpha)$ is normalised to give -

$$\int P(\alpha) d^2\alpha = 1$$

For two-time averages, it is necessary to know the propagator function $P(\alpha' t' | \alpha t)$. In this case we can show that (Agarwal & Wolf, 1968): ($t' > t$) -

$$\langle \hat{A}'(t') \hat{A}(t) \rangle = \iint P(\alpha' t' | \alpha t) A'(\alpha'^*, \alpha') A(\alpha^* - \partial\alpha, \alpha) P(\alpha, t) d^2\alpha' d^2\alpha$$

$$\langle \hat{A}_1(t) \hat{A}'_1(t') \hat{A}'_2(t') \hat{A}_2(t) \rangle$$

$$\begin{aligned} &= \iint P(\alpha' t' | \alpha t) A'_1(\alpha'^*, \alpha') A'_2(\alpha'^*, \alpha') \times \\ &\times A_1(\alpha^*, \alpha - \partial\alpha^*) A_2(\alpha^* - \partial\alpha, \alpha) P(\alpha, t) d^2\alpha' d^2\alpha \end{aligned}$$

In particular, this gives very simple results analogous to a classical correlation function for normally ordered, time-ordered correlation functions: the proof is a special case of a more general result given in 2.3.

We note that the propagator function is defined to be the solution to the c-number time development equation, relative to an initial delta function:

$$\partial_{t'} P(\underline{\alpha}' t' | \underline{\alpha} t) = \mathcal{L}[\partial \underline{\alpha}', \underline{\alpha}'] P(\underline{\alpha}' t' | \underline{\alpha} t)$$

$$P(\underline{\alpha}' t | \underline{\alpha} t) = \delta^n(\underline{\alpha}' - \underline{\alpha})$$

(b) The complex P-representation

While the diagonal P-representation has many useful applications, as mentioned earlier it is not well-defined for an arbitrary quantum system (except as a generalised function). In many cases, the use of this representation leads to a simple Fokker-Planck equation. However the steady-state solution to the Fokker-Planck equation is singular in some cases, due to a non positive-definite diffusion operator: this can be the case when there is photon antibunching.

In order to overcome the problem, we extend the domain of definition of the P-function to a complex phase-space. Now in the Glauber-Sudarshan P-representation, the density operator is expanded in hermitian projection operators. The complex P-representation is therefore defined as an expansion in terms of nonhermitian projection operators:

$$\hat{\Lambda}(\alpha, \beta) = |\alpha\rangle\langle\beta^*| / (\langle\beta^* | \alpha\rangle) = e^{-\alpha\beta + \alpha\hat{a}^+} |0\rangle\langle 0| e^{\beta\hat{a}}$$

$$\hat{\rho} = \int_{\mathcal{D}} P(\alpha, \beta) \hat{\Lambda}(\alpha, \beta) d\mu(\alpha, \beta)$$

In the case of an n-mode problem, define:

$$\hat{\Lambda}(\underline{\alpha}) = \hat{\Lambda}(\alpha_1, \beta_1, \dots, \alpha_n, \beta_n) = \frac{|\{\alpha_1, \dots, \alpha_n\}\rangle \langle \{\beta_1^*, \dots, \beta_n^*\}|}{\langle \{\beta_1^*, \dots, \beta_n^*\} | \{\alpha_1, \dots, \alpha_n\} \rangle}$$

$$\hat{\rho} = \int_{\mathcal{D}} P(\underline{\alpha}) \hat{\Lambda}(\underline{\alpha}) \prod_{i=1}^n d\mu^{(i)}(\alpha_i, \beta_i)$$

In either case, the following normalisation holds:

$$1 = \text{Tr}(\hat{\rho}) = \int_{\mathcal{D}} P(\underline{\alpha}) \prod_{i=1}^n d\mu^{(i)}(\alpha_i, \beta_i)$$

This follows trivially as the trace of the projection operator is one.

Here (α_i, β_i) are non complex-conjugate variables, and it is readily verified that $\hat{\Lambda}(\underline{\alpha})$ is a projection operator that reduces to $|\{\alpha_i\}\rangle \langle \{\alpha_i\}|$ in the case of $\beta_i = \alpha_i^*$. The integration measure $d\mu^{(i)}(\alpha_i, \beta_i)$ and integration domain \mathcal{D} are undefined at present: we leave these free to be adapted to individual problems. It is readily shown that one choice possible is just the usual diagonal choice, although \mathcal{D} can be a general manifold in \mathbf{C}^{2n}

Other possibilities are:

- | | | |
|------|---|-------------------------------------|
| I- | $\iint d^2\alpha d^2\beta \delta^2(\alpha - \beta^*)$ | (Diagonal case) |
| II- | $\int_B^A d\alpha \int_{B'}^{A'} d\beta$ | (Open integral) |
| III- | $\int_B^A d\alpha \oint d\beta$ | (Closed β -integral) |
| IV- | $\oint d\alpha \oint d\beta$ | (Closed α, β -integrals) |
| V- | $\iint d^2\alpha d^2\beta$ | (Complete complex phase-space) |

In general the choice depends on the properties of the Fokker-Planck equation, which has to have a bounded integrable solution that can be integrated by parts. This can be attained by using measure (V), but in many cases a simpler result will be defined in one of the lower dimensional manifolds: the prime example of this is measure (I) which is the measure for a Glauber-Sudarshan diagonal P-representation.

It is useful to note that the density operator is uniquely defined by its characteristic function (Glauber, 1970):

$$\chi(\lambda) \equiv \text{Tr} [\hat{\rho} e^{\lambda \hat{a}^\dagger} e^{-\lambda^* \hat{a}}]$$

Hence the complex P-representation is also a representation for the characteristic function: in section 2.3 the characteristic function will be used as a common denominator to define general representations. This approach is also used by Cahill & Glauber (1969).

We can now compare the present representation with the R-representation of Glauber (1963b, Equⁿ 9.5):

$$\hat{\rho} = \int |\alpha_i\rangle \langle \beta_i| R(\alpha_i^*, \beta_i) \prod_i \left[e^{-\frac{1}{2}(|\alpha_i|^2 + |\beta_i|^2)} \cdot \frac{d^2\alpha_i d^2\beta_i}{\pi^2} \right]$$

R is an analytic function of (α_i^*, β_i) and exists for an arbitrary quantum system. It is uniquely defined by:

$$R(\alpha_i^*, \beta_i) = \langle \alpha_i | \hat{\rho} | \beta_i \rangle \prod_i \left[e^{-\frac{1}{2}(|\alpha_i|^2 + |\beta_i|^2)} \right]$$

Now the R-representation is also a representation for the characteristic function, and we can prove the following identity:

$$\chi(\underline{\lambda}) = \int R(\underline{\alpha}^*, \underline{\lambda} + \underline{\alpha}) \prod_i \left[e^{-\lambda_i^* \alpha_i - |\alpha_i|^2} \cdot \frac{d^2 \alpha_i}{\pi} \right]$$

We can now prove some useful theorems relating to the existence of the complex P-representation. All the following results hold for a single mode, but can be readily extended to n-modes. In proving the theorems, extensive use is made of the fact that $R, \hat{\Lambda}$ are analytic functions in both variables.

Theorem: At least one complex P-representation exists relative to the line-integral measure, for a density operator expanded in a finite set of number states.

Proof: We expand the density operator as a finite series as follows, using Cauchy's theorem:

$$\begin{aligned} \hat{\rho} &= \sum_{n,m} \rho_{nm} (\hat{a}^+)^n |0\rangle\langle 0| (\hat{a})^m \\ &= \sum_{n,m} \rho_{nm} \left[\frac{-n!m!}{4\pi^2} \right] \oint \oint \hat{\Lambda}(\alpha, \beta) e^{\alpha\beta} \cdot \frac{d\alpha}{\alpha^{n+1}} \cdot \frac{d\beta}{\beta^{m+1}} \end{aligned}$$

Hence a P-function exists with the following definition:

$$P(\alpha, \beta) = \left(\frac{-1}{4\pi^2} \right) e^{\alpha\beta} \sum_{n,m} \rho_{nm} \frac{n!}{\alpha^{n+1}} \frac{m!}{\beta^{m+1}}$$

The path of integration is for any line integrals enclosing the origins in both α and β .

The above theorem shows that this type of complex P-representation is useful in representing operators expanded in a finite number of number states, which would have a

singular representation in the diagonal (Glauber-Sudarshan) P-representation. We will show in Chapters 3 and 4, that the representation also is useful in obtaining exact solutions for nonlinear quantum systems with photon anti-bunching. In fact, the restriction to a finite number of number states, can be relaxed as follows:

Theorem: At least one complex P-representation exists relative to the line integral measure, for a density operator expanded in coherent states with bounded support.

Proof: By bounded support we mean a domain \mathcal{D} exists in the (\mathbb{C}^2) space within a finite radius from the origin, so that the density operator can be expanded as:

$$\begin{aligned}\hat{\rho} &\equiv \int_{\mathcal{D}} \rho(\alpha, \beta) |\alpha\rangle \langle \beta^*| d^2\alpha d^2\beta \\ &= \left(\frac{1}{4\pi^2}\right) \int_{\mathcal{D}} \rho(\alpha, \beta) \langle \beta^* | \alpha \rangle \left[\oint \frac{\hat{\Lambda}(\alpha', \beta') d\alpha' d\beta'}{(\alpha - \alpha')(\beta - \beta')} \right] d^2\alpha d^2\beta\end{aligned}$$

Here the integration paths must be defined so that any $(\alpha, \beta) \in \mathcal{D}$ are enclosed within both line integrals. The corresponding P-function is then:

$$P(\alpha, \beta) = \left(\frac{1}{4\pi^2}\right) \int_{\mathcal{D}} \rho(\alpha', \beta') \langle \beta'^* | \alpha' \rangle \frac{d^2\alpha'}{(\alpha - \alpha')} \frac{d^2\beta'}{(\beta - \beta')}$$

We next are interested in the complex P-representation defined as an integral over the full complex space (\mathbb{C}^2). It is trivial that one complex P-representation exists in this case, for arbitrary $\hat{\rho}$. This follows by noting that the Glauber R-representation exists in all cases, and we can define P as follows:

$$\begin{aligned}
 P(\alpha, \beta) &= R(\alpha^*, \beta^*) \left[e^{\alpha\beta - |\alpha|^2 - |\beta|^2} \right] \pi^{-2} \\
 &= \langle \alpha | \hat{\rho} | \beta^* \rangle \left[e^{\alpha\beta - \frac{1}{2} [|\alpha|^2 + |\beta|^2]} \right] \pi^{-2}
 \end{aligned}$$

Of much more interest, is the possibility of obtaining a real, positive probability distribution in the (\mathbb{C}^2) space. This leads to the following result:

Theorem: A real positive P-function on the complete (\mathbb{C}^2) space can be defined whenever a diagonal (Glauber-Sudarshan) P-function exists.

Proof: The density operator has positive eigenvalues and is hermitian. Hence the following function is real and positive:

$$P(\alpha, \beta) = \left[\frac{1}{4\pi^2} \right] \exp \left[-\frac{|\alpha|^2 - |\beta|^2}{2} \right] \langle f(\alpha, \beta) | \hat{\rho} | f(\alpha, \beta) \rangle$$

where:

$$\begin{aligned}
 |f(\alpha, \beta)\rangle &= \left[\frac{1}{\pi} \right] \int |\alpha'\rangle \exp \left[(\alpha + \beta^*) \alpha'^* / 2 - |\alpha'|^2 / 2 \right] \cdot d^2 \alpha' \\
 &= \exp \left[|\alpha + \beta^*|^2 / 8 \right] |[\alpha + \beta^*] / 2\rangle
 \end{aligned}$$

It is necessary to show that $P(\alpha, \beta)$ as defined above, gives a representation for the density operator. Let $P'(\alpha)$ be the diagonal P-function, then:

$$P(\alpha, \beta) = \left[\frac{1}{4\pi^2} \right] \int P'(\alpha') \cdot \exp \left[-\frac{|\alpha - \alpha'|^2}{2} - \frac{|\beta^* - \alpha'|^2}{2} \right] \cdot d^2 \alpha'$$

Next, we note the following identity for an analytic function:

$$f(\alpha') = \left(\frac{1}{2\pi} \right) \int f(\alpha) \exp \left[-\frac{|\alpha - \alpha'|^2}{2} \right] d^2 \alpha$$

Hence on integrating over (α, β) we obtain:

$$\begin{aligned}\hat{\rho} &= \int \hat{\Lambda}(\alpha', \alpha'^*) P'(\alpha') d^2\alpha' \\ &= \iint \hat{\Lambda}(\alpha, \beta) P(\alpha, \beta) d^2\alpha d^2\beta\end{aligned}$$

The above theorem holds whenever a Glauber-Sudarshan P-function exists. In view of the work of Sudarshan (1963) on generalised function P-representations, this is sufficient for all density operators. As the theorem is of some interest, it is worth proving it directly as follows, without using generalised functions.

Theorem: A real positive P-function on the complete (\mathbf{C}^2) space exists for any quantum density operator.

Proof: We can define a real, positive P-function as previously. To show that this represents an arbitrary density operator, it is sufficient to demonstrate equality of the characteristic functions. The characteristic function defined relative to $P(\alpha, \beta)$ is:

$$\begin{aligned}\chi_p(\lambda) &= \iint e^{\lambda\beta - \lambda^*\alpha} P(\alpha, \beta) d^2\alpha d^2\beta \\ &= \left(\frac{1}{4\pi^2}\right) \iiint \exp\left[\lambda\beta - \lambda^*\alpha - \frac{|\alpha|^2}{2} - \frac{|\beta|^2}{2} - |\alpha'|^2 - |\beta'|^2 + \right. \\ &\quad \left. + \beta'^*(\frac{\alpha + \beta^*}{2}) + \alpha'(\frac{\alpha^* + \beta}{2})\right] R(\alpha', \beta') d^2\alpha d^2\beta d^2\alpha' d^2\beta'\end{aligned}$$

We now make a variable change by defining:

$$\begin{aligned}\gamma &= (\alpha + \beta^*)/2 \\ \delta &= (\alpha - \beta^*)/2 \\ \alpha &= (\gamma + \delta) \\ \beta^* &= (\gamma - \delta) \\ d^2\alpha d^2\beta &= 4 d^2\gamma d^2\delta\end{aligned}$$

Noting that R is an analytic function, the following identity is useful:

$$R(\alpha^*, \gamma) = \frac{1}{\pi} \int e^{\gamma \beta^* - |\beta|^2} R(\alpha^*, \beta) d^2\beta$$

Hence the above expression for the characteristic function can be simplified to give:

$$\begin{aligned} \chi_\rho(\lambda) &= \frac{1}{\pi^3} \iiint \exp[\lambda(\gamma-\delta)^* - \lambda^*(\gamma+\delta) - |\gamma|^2 - |\delta|^2 - |\alpha'|^2 + \alpha'\gamma^*] R(\alpha', \gamma) d^2\gamma d^2\delta d^2\alpha' \\ &= \frac{1}{\pi^2} \iint \exp[|\lambda|^2 + \lambda\gamma^* - \lambda^*\gamma - |\gamma|^2 - |\alpha'|^2 + \alpha'\gamma^*] R(\alpha', \gamma) d^2\gamma d^2\alpha' \\ &= \frac{1}{\pi} \int \exp[-\lambda^*\alpha - |\alpha|^2] R(\alpha^*, \lambda+\alpha) d^2\alpha \\ &= \text{Tr} [\hat{\rho} e^{\lambda \hat{q}^\dagger} e^{-\lambda^* \hat{q}}] \end{aligned}$$

The last step follows from the identity for the characteristic function defined relative to the Glauber R-representation, as given previously.

In summary, the above results define the existence properties of the complex P-representation. The most useful result is the last theorem, which states that a real positive probability distribution exists over the complex phase-space of (\mathbf{C}^2), for an arbitrary density operator. This can also be used to prove the following result:

Theorem: An arbitrary density operator can be generated from its diagonal coherent state matrix elements.

Proof: From the previous theorem, it is possible to write:

$$\begin{aligned} P(\alpha, \beta) &= \left(\frac{1}{4\pi^2}\right) \exp\left(-\frac{|\alpha|^2 - |\beta|^2}{2}\right) \langle f(\alpha, \beta) | \hat{\rho} | f(\alpha, \beta) \rangle \\ &= \left(\frac{1}{4\pi^2}\right) \exp\left(-\left|\frac{\alpha - \beta^*}{2}\right|^2\right) \langle \frac{\alpha + \beta^*}{2} | \hat{\rho} | \frac{\alpha + \beta^*}{2} \rangle \end{aligned}$$

Hence we can immediately obtain the following identity:

$$\begin{aligned}\hat{\rho} &= \iint \hat{\Lambda}(\alpha, \beta) P(\alpha, \beta) d^2\alpha d^2\beta \\ &= \left(\frac{1}{\pi^2}\right) \iint \left[\frac{|\delta+\delta\rangle\langle\delta-\delta|}{\langle\delta-\delta|\delta+\delta\rangle} \right] e^{-|\delta|^2} \langle\delta|\hat{\rho}|\delta\rangle d^2\delta d^2\delta\end{aligned}$$

This theorem has also been obtained in a different way by Lonke (1978) whose result for $\hat{\rho}$ is slightly different from the expression above. The above theorem is more elegant as it can be obtained from analyticity properties only, without the use of special functions.

Having established the existence of various complex P-representations, we note that the representations of this type are not necessarily unique. However a set of operator identities can be obtained for defining time-evolution equations; and given a complex P-representation at any time the resulting operator expectation values are uniquely defined as multinomial moments of the distribution over the complex phase-space. It is worthwhile to obtain the relevant operator identities using the coherent states of Bargmann (1961). These are defined as:

$$|\alpha\rangle = e^{\alpha\hat{a}^+} |0\rangle = e^{\frac{1}{2}|\alpha|^2} |\alpha\rangle$$

For simplicity, the following results are obtained for a single mode, with (α, β) written as $(\underline{\alpha})$ when necessary.

It is straightforward to develop the following identities (where $\alpha = \alpha_x + i\alpha_y$; $\beta = \beta_x + i\beta_y$):

$$\langle\alpha|\beta\rangle = \exp(\alpha^*\beta)$$

$$\hat{a}^\dagger |\alpha\rangle = \partial_\alpha |\alpha\rangle = \frac{\partial}{\partial \alpha_x} |\alpha\rangle = -i \frac{\partial}{\partial \alpha_y} |\alpha\rangle$$

$$\langle \alpha | \hat{a} = \partial_{\alpha^*} \langle \alpha | = \frac{\partial}{\partial \alpha_x} \langle \alpha | = i \frac{\partial}{\partial \alpha_y} \langle \alpha |$$

$$\hat{a} |\alpha\rangle = \alpha |\alpha\rangle$$

$$\langle \alpha | \hat{a}^\dagger = \alpha^* \langle \alpha |$$

Hence in terms of these coherent states, the projection operator and elementary operator products are:

$$\hat{\Lambda}(\underline{\alpha}) = |\alpha\rangle \langle \beta^*| e^{-\alpha\beta}$$

$$\hat{a} \hat{\Lambda}(\underline{\alpha}) = \alpha \hat{\Lambda}(\underline{\alpha})$$

$$\hat{a}^\dagger \hat{\Lambda}(\underline{\alpha}) = (\partial_\alpha + \beta) \hat{\Lambda}(\underline{\alpha}) = (\partial_{\alpha_x} + \beta) \hat{\Lambda}(\underline{\alpha}) = (-i \partial_{\alpha_y} + \beta) \hat{\Lambda}(\underline{\alpha})$$

$$\hat{\Lambda}(\underline{\alpha}) \hat{a} = (\alpha + \partial_\beta) \hat{\Lambda}(\underline{\alpha}) = (\alpha + \partial_{\beta_x}) \hat{\Lambda}(\underline{\alpha}) = (\alpha - i \partial_{\beta_y}) \hat{\Lambda}(\underline{\alpha})$$

$$\hat{\Lambda}(\underline{\alpha}) \hat{a}^\dagger = \beta \hat{\Lambda}(\underline{\alpha})$$

These operator product identities are useful in obtaining c-number time-development equations for the complex P-representation. It is instructive to compare the identities with those for the diagonal P-representation. Clearly the chief difference is the replacement of α^* by β in each equation: and we note that (α, β) are not complex conjugates. In addition it is clear that several different time-development equations can be obtained by replacing ∂_α by ∂_{α_x} or $-i \partial_{\alpha_y}$ (and similarly for ∂_β). Any equation obtained in this way has a different time-development, but

is equivalent in terms of physical observables: this is due to the nonuniqueness of the complex P-representation.

We finally give an explicit formula for the expectation value of a normally ordered product:

$$\langle \hat{A}(\hat{a}^\dagger, \hat{a}) \rangle_\rho = \int_{\mathfrak{D}} P(\alpha, \beta) A(\beta, \alpha) d\mu(\alpha, \beta)$$

This result follows trivially from the operator identities obtained above. Similarly one can obtain results for multi-time correlations analogous to those obtained previously: ($t' > t$) -

$$\begin{aligned} \langle \hat{A}'(t') \hat{A}(t) \rangle_\rho &= \iint_{\mathfrak{D}} P(\underline{\alpha}'t' | \underline{\alpha}t) A'(\beta', \alpha') A(\beta - \partial\alpha, \alpha) \times \\ &\times P(\underline{\alpha}, t) d\mu(\underline{\alpha}) d\mu(\underline{\alpha}') \end{aligned}$$

$$\begin{aligned} \langle \hat{A}_1(t) \hat{A}'_1(t') \hat{A}'_2(t') \hat{A}_2(t) \rangle &= \iint_{\mathfrak{D}} P(\underline{\alpha}'t' | \underline{\alpha}t) A'_1(\beta', \alpha') A'_2(\beta', \alpha') \times \\ &\times A_1(\beta, \alpha - \partial\beta) A_2(\beta - \partial\alpha, \alpha) P(\underline{\alpha}, t) d\mu(\underline{\alpha}) d\mu(\underline{\alpha}') \end{aligned}$$

These results will be proved in 2.3, for a general operator ordering.

(c) Time development equations

In the usual master equation treatment, the time development of $\hat{\rho}$ in the Schroedinger or the interaction picture will be described by:

$$\partial_t \hat{\rho} = \hat{\mathcal{L}}[\hat{\rho}]$$

Where $\hat{\mathcal{L}}$ is an operator functional that can be represented by left and right multiplications of $\hat{\rho}$ in power series of $(\hat{a}^\dagger, \hat{a})$. In either case the identities of operator products are used to obtain a differential functional acting on $\hat{\mathcal{L}}$:

$$\partial_t \hat{\rho} = \int_{\mathcal{D}} P(\underline{\alpha}) \{ \mathcal{L}'[\partial \underline{\alpha}, \underline{\alpha}] \hat{\mathcal{L}}(\underline{\alpha}) \} d\mu(\underline{\alpha})$$

Now provided \mathcal{D} is chosen appropriately, and it is possible to integrate with $(P, \partial \underline{\alpha} \cdot P)$ vanishing at the boundary of integration this can be written:

$$\int_{\mathcal{D}} \dot{P}(\underline{\alpha}) \hat{\mathcal{L}}(\underline{\alpha}) d\mu(\underline{\alpha}) = \int_{\mathcal{D}} \{ \mathcal{L}[\partial \underline{\alpha}, \underline{\alpha}] P(\underline{\alpha}) \} \hat{\mathcal{L}}(\underline{\alpha}) d\mu(\underline{\alpha})$$

This equation is still an operator equation: at least one solution of the operator equation can be obtained by equating the c-number parts of both integrals to give -

$$\partial_t P(\underline{\alpha}) = \mathcal{L}[\partial \underline{\alpha}, \underline{\alpha}] P(\underline{\alpha})$$

In particular, in many cases the derivatives of third or higher order do not occur or are negligible, and this equation reduces to a Fokker-Planck of form:

$$\partial_t P(\underline{\alpha}) = \left[\frac{\partial}{\partial \alpha_M} \cdot A_M(\underline{\alpha}) + \frac{1}{2} \frac{\partial}{\partial \alpha_M} \frac{\partial}{\partial \alpha_N} D_{MN}(\underline{\alpha}) \right] P(\underline{\alpha})$$

Here we note that the vector of coordinates $\underline{\alpha}$ can in general include $(\alpha_1, \beta_1, \alpha_2, \beta_2, \dots, \alpha_n, \beta_n)$ for an n-mode problem, so that there is no loss of generality.

In practice an overall factor of $(\frac{\partial}{\partial \alpha_{\mu}} \equiv \partial_{\mu})$ is obtained: this is equivalent to the conservation of the trace of $\hat{\rho}$ which follows from the form of the original operator equations for $\hat{\rho}$. In the case of one of the domains of integration I-IV it is useful to leave the differential operators in the present form, as complex differentials. It is easily demonstrated that the same time development equations for any observables expressed as power series in (α, β) are obtained regardless of the integration domain, provided integration by parts is permitted.

In many cases an exact solution for the steady-state P-function will be obtained on utilizing potential equations: that is provided -

$$\partial_{\nu} v_{\mu} = \partial_{\mu} v_{\nu}$$

where:

$$v_{\mu} \equiv D_{\mu\rho}^{-1}(\underline{\alpha}) \left[2A_{\rho}(\underline{\alpha}) + \partial_{\nu} D_{\nu\rho}(\underline{\alpha}) \right]$$

In the case of a potential solution, the following result is obtained:

$$P(\underline{\alpha}) = \mathcal{N} \cdot e^{\chi\rho} \left[- \int^{\underline{\alpha}} v_{\mu}(\underline{\alpha}) d\alpha_{\mu} \right]$$

Here \mathcal{N} is a normalisation factor; and it is in evaluating the overall normalisation that the alternate integration domains become useful. For some quantum systems \mathcal{N} is undefined (infinite) on the usual diagonal domain of integration with $\beta \equiv \alpha^*$. However it is possible to adapt the integration domain to the quantum system, and by

choosing an appropriate manifold an integrable normalisation will be obtained. The above remarks can also be generalised to include cases of terms of different time-reversal symmetry and singular diffusion arrays.

(d) Stochastic equations

The time development properties of $P(\alpha)$ can also be described by a stochastic differential equation for α . In this case the probability of the stochastic process developing in time from (α, t) to (α', t') equals the propagator $P(\alpha', t' | \alpha, t)$, provided a stochastic process exists. In the simplest case (for $\beta \equiv \alpha^*$), one obtains an Ito stochastic differential equation provided $D_{\mu\nu}(\alpha)$ is positive-semidefinite (Arnold, 1974):

$$\partial_t \alpha_\mu = -A_\mu(\alpha) + B_{\mu\nu}(\alpha) \cdot \xi_\nu(t)$$

Where:

$$D_{\mu\nu}(\alpha) = B_{\mu\sigma}(\alpha) \cdot B_{\nu\sigma}(\alpha)$$

The stochastic process realises a path in a real phase-space (p, x) , and (α, β) remain complex conjugate. Thus there always exists a diagonal representation of the density operator relative to the coherent state basis, provided there is a diagonal representation initially.

However when $D_{\mu\nu}(\alpha)$ is not positive-semidefinite, a stochastic differential equation cannot be directly obtained from the Fokker-Planck equation defined in (2.1c). Instead

it is necessary to develop a Fokker-Planck equation and a stochastic differential equation defined on a complex phase-space. We show in (2.3) that this is possible because of the equivalence among differential operators:

$$\frac{\partial}{\partial \alpha_M} \leftrightarrow \frac{\partial}{\partial \alpha_M^x} \leftrightarrow \frac{-i \partial}{\partial \alpha_M^y}$$

Therefore one can define $P(\underline{\alpha})$ on a $4n$ -dimensional space for n -modes; of $\{\alpha_M^x, \alpha_M^y, \beta_M^x, \beta_M^y \mid (M=1, n)\}$. This gives a complex phase-space in (p, X) where:

$$p = \frac{1}{2i}(\alpha - \beta) \quad ; \quad x = \frac{1}{2}(\alpha + \beta)$$

Because the $4n$ -dimensional Fokker-Planck equation has positive-semidefinite diffusion, there is an equivalent stochastic differential equation defined on the complex phase-space:

$$\frac{\partial}{\partial t} \begin{bmatrix} \alpha_M^x \\ \alpha_M^y \end{bmatrix} = - \begin{bmatrix} A_M^x(\underline{\alpha}) \\ A_M^y(\underline{\alpha}) \end{bmatrix} + \begin{bmatrix} B_{M\nu}^x(\underline{\alpha}) \xi_\nu(t) \\ B_{M\nu}^y(\underline{\alpha}) \xi_\nu(t) \end{bmatrix} \quad (M=1, 2n)$$

Where the coefficients are real functions:

$$A_M = A_M^x + i A_M^y \quad (M=1, 2n)$$

$$D_{M\nu} = [B_{M\sigma}^x + i B_{M\sigma}^y][B_{\nu\sigma}^x + i B_{\nu\sigma}^y]$$

The significant point arising here is that we have explicitly derived equations for the real and imaginary parts of both α and β . The equations show that for an arbitrary diffusion array $D_{M\nu}$, the variables (α, β) have different (possibly independent) stochastic behaviour. They do not in general remain complex conjugate, even if they are complex

conjugate initially. This therefore gives a direct reason for the development of nondiagonal terms in the coherent state representation of $\hat{\rho}$.

In addition, the occurrence of complex phase-space paths with a finite probability provides a way of obtaining nonclassical photon statistics within a normally ordered operator representation (Chaturvedi, Drummond & Walls, 1977). The advantage of this method is that all observable mean values and correlations are obtained using the moments and propagator functions of a real, positive probability distribution (or stochastic process) in a straightforward way.

2.2 ATOMIC COHERENT STATE REPRESENTATIONS

(a) The diagonal A.C.S. representation

We earlier defined a representation for bosons in terms of "minimum uncertainty" linear combinations of states. A similar representation is possible for collective atomic states. However there are several differences which are worth mentioning. Firstly the most direct analog of the boson coherent states is obtained by selecting states that have a fixed "angular momentum".* This gives the atomic

* By "angular momentum" is meant the observable corresponding to $[\hat{x}_i, \hat{p}_i]^2$

coherent state representation, which only represents a subset of all possible atomic states. The next difference between the ACS representation and the boson coherent state representation, is that there are only a finite number of energy levels in the collective atomic system. This is reflected in the different algebra obeyed by the raising and lowering operators \hat{J}_{\pm} , relative to their analogs \hat{a}^+ , \hat{a} in the boson system. Because of this the algebraic details of the representation are different. The factorisation of correlation functions which is very useful for boson coherent states, no longer holds in the case of the atomic coherent states, and in particular observable correlations of order greater than $2J$ all are zero. This is the reason for the well-known antibunching in the fluorescent radiation from an individual atom, which has $J = \frac{1}{2}$ (Carmichael & Walls 1976). A similar result of a vanishing correlation function of order n for $n > 2J$ holds for any collective atomic system of "angular momentum" J . Noting that the maximum value of J is $N/2$ for N atoms, we see that this simply means that at most N photons are emitted simultaneously from N 2-level atoms in the dipole approximation.

The analog of the number states for a boson system are the Dicke states for an atomic system. These are a basis of eigenvectors of the collective operators \hat{J}^2 , \hat{J}_z . For eigenvectors with $J \leq N/2$ it is necessary to define additional indices λ to distinguish states of different permutation symmetry: the basis is then -

$$(\text{Dicke states}) \quad |J, m, \lambda\rangle$$

In the following treatment, we suppose that $J = N/2$ provided N is a positive integer. Our derivation follows that of Arecchi et al (1972).

Corresponding to the coherent states of the boson system are the atomic coherent states (sometimes called Bloch states) of the atomic system. Like the boson coherent states, these can be generated from the ground state by a symmetry operator. In geometric terms the symmetry operation is a rotation on the Bloch sphere (which semiclassically is a sphere whose coordinate points are J_x, J_y, J_z for an atomic state). We define:

$$\begin{aligned}\hat{R}(\theta, \phi) &= \exp[-i\theta(\hat{J}_x \sin\phi - \hat{J}_y \cos\phi)] \\ &= \exp[\xi \hat{J}^+ - \xi^* \hat{J}^-] \\ &= \exp[\tau \hat{J}^+] \exp[\ln(1+|\tau|^2) \cdot \hat{J}^z] \exp[-\tau^* \hat{J}^-]\end{aligned}$$

Where:

$$\xi = \left(\frac{\theta}{2}\right) e^{-i\phi} \quad ; \quad \tau = \left(\tan \frac{\theta}{2}\right) e^{-i\phi}$$

The equivalence of these forms is shown in Arecchi (1974), Arecchi et al (1972).

The atomic coherent state is then defined to be:

$$\begin{aligned}|\theta, \phi\rangle &= \hat{R}(\theta, \phi) |J, -J\rangle \\ &= (1+|\tau|^2)^{-J} \exp(\tau \hat{J}^+) |J, -J\rangle\end{aligned}$$

These states form a nonorthogonal basis for the subspace of atomic states of fixed J :-

$$\langle \theta, \phi | \theta', \phi' \rangle = \left\{ [1 + \tau^* \tau']^2 [1 + |\tau|^2]^{-1} [1 + |\tau'|^2]^{-1} \right\}^J$$

It can also be shown that these Bloch states form minimum uncertainty states, in the sense of rotated operators

$\hat{J}' \equiv \hat{R} \hat{J} \hat{R}^{-1}$. These operators obey a commutation relation of the type:

$$[\hat{J}'_x, \hat{J}'_y] = i\hat{J}'_z$$

Hence : $\langle \hat{J}'_x{}^2 \rangle \langle \hat{J}'_y{}^2 \rangle \geq \frac{1}{4} \langle \hat{J}'_z{}^2 \rangle$

The equality sign holds for the Bloch states, which have the minimum uncertainty property.

The $|0, \phi\rangle$ states can be written in terms of the $|J, m\rangle$ states as follows:-

$$|0, \phi\rangle = (1 + |\tau|^2)^{-J} \sum_{m=-J}^J \tau^{m+J} \begin{bmatrix} 2J \\ m+J \end{bmatrix}^{\frac{1}{2}} |J, m\rangle$$

A similar definition of atomic coherent states can be obtained by rotating the fully inverted state $|J, J\rangle$, as follows (Glauber & Haake, 1974):

$$\begin{aligned} |z\rangle &= (1 + |z|^2)^{-J} \exp[z \hat{J}^-] |J, J\rangle \\ &= (1 + |z|^2)^{-J} \sum_{m=-J}^J z^{J-m} \begin{bmatrix} 2J \\ J+m \end{bmatrix}^{\frac{1}{2}} |J, m\rangle \end{aligned}$$

If we set $z = 1/\tau$ we find:

$$\begin{aligned} |z\rangle &= (\tau\tau^*)^J (1 + |\tau|^2)^{-J} \sum_{m=-J}^J \tau^{-J+m} \begin{bmatrix} 2J \\ J+m \end{bmatrix} |J, m\rangle \\ &= e^{i\phi 2J} |0, \phi\rangle \end{aligned}$$

Hence we see that with $z = e^{i\phi} \alpha g(\frac{\theta}{2})$, the two definitions of an atomic coherent state are identical apart from a phase factor. However this phase factor disappears on defining the diagonal atomic coherent state representation, so that the two types of atomic coherent state can be used interchangeably on making a variable change.

At this point it is worth pointing out that the distribution of m -values in an atomic coherent state is a binomial:

$$|\langle \tau | m \rangle|^2 = (1 + |\tau|^2)^{-2J} (|\tau|^2)^{J+m} \binom{2J}{m+J}$$

This distribution is the analog of the Glauber coherent state photon number distribution, which is well known to be Poissonian.

In order to use the ACS representation, it is necessary to obtain operator identities and represent the density matrix as a distribution. We first introduce the ACS distribution for the density matrix:

$$\hat{\rho} = \int P(z) \hat{\Lambda}(z, z^*) d^2z$$

$$\hat{\Lambda}(z, z^*) \equiv |z\rangle\langle z|$$

An alternative to this representation, is the use of a distribution over (θ, ϕ) variables (Narducci, 1974):

$$\hat{\rho} = \int D(\theta, \phi) |\theta, \phi\rangle\langle \theta, \phi| \cdot d\theta d\phi$$

However this representation is equivalent to the one for z -variables, and can always be obtained by a straightforward variable-change. For this reason we shall utilise

the z -variables which give simple operator identities as follows:

$$\begin{aligned}\hat{\Lambda}(z, z^*) &= (1+|z|^2)^{-2J} \exp(z^{-1} \hat{J}^+) |J, -J\rangle \langle J, -J| \exp(z^{-1} \hat{J}^-) \\ &= (1+|z|^2)^{-2J} \exp(z \hat{J}^-) |J, J\rangle \langle J, J| \exp(z^* \hat{J}^+) \\ \partial_z \hat{\Lambda}(z, z^*) &= \left(\frac{2J}{z(1+|z|^2)} - \hat{J}^+/z^2 \right) \hat{\Lambda}(z, z^*) \\ &= \left(\frac{-2Jz^*}{(1+|z|^2)} + \hat{J}^- \right) \hat{\Lambda}(z, z^*)\end{aligned}$$

Hence we obtain directly the following results; in terms of a differential operator $\mathcal{D}_J [z, \frac{\partial}{\partial z}]$:

$$\begin{aligned}\hat{J}^+ \hat{\Lambda}(z, z^*) &= \mathcal{D}_{J^+} \hat{\Lambda}(z, z^*) = \left[\frac{2Jz}{1+|z|^2} - z^2 \frac{\partial}{\partial z} \right] \hat{\Lambda}(z, z^*) \\ \hat{J}^- \hat{\Lambda}(z, z^*) &= \mathcal{D}_{J^-} \hat{\Lambda}(z, z^*) = \left[\frac{\partial}{\partial z} + \frac{2Jz^*}{(1+|z|^2)} \right] \hat{\Lambda}(z, z^*) \\ \hat{\Lambda}(z, z^*) \hat{J}^+ &= \mathcal{D}_{J^+}^* \hat{\Lambda}(z, z^*) \\ \hat{\Lambda}(z, z^*) \hat{J}^- &= \mathcal{D}_{J^-}^* \hat{\Lambda}(z, z^*)\end{aligned}$$

The equivalent formulae for (θ, ϕ) variables are rather cumbersome, and can be referred to in Narducci (1974). We similarly define operator products using the standard methods of calculus of phase-space:

$$\begin{aligned}\hat{B}_2 \hat{B}_1 \hat{\Lambda} &= \mathcal{D}_{B_1} \mathcal{D}_{B_2} \hat{\Lambda} \\ \hat{\Lambda} \hat{A}_1 \hat{A}_2 &= \mathcal{D}_{A_1}^* \mathcal{D}_{A_2}^* \hat{\Lambda} \\ \hat{B} \hat{\Lambda} \hat{A} &= \mathcal{D}_B \mathcal{D}_{A^+}^* \hat{\Lambda} \\ &= \mathcal{D}_{A^+}^* \mathcal{D}_B \hat{\Lambda}\end{aligned}$$

Finally the expression for \hat{J}^3 is readily deduced as follows:

$$\begin{aligned}\hat{J}^3 \hat{\Lambda}(z, z^*) &= \frac{1}{2} [\hat{J}^+, \hat{J}^-] \hat{\Lambda}(z, z^*) \\ &= \frac{1}{2} [D_{J^-} D_{J^+} - D_{J^+} D_{J^-}] \hat{\Lambda}(z, z^*) \\ &= \left(J \frac{1 - |z|^2}{1 + |z|^2} - z \frac{\partial}{\partial z} \right) \hat{\Lambda}(z, z^*) \\ \hat{\Lambda}(z, z^*) \hat{J}^3 &= D_{J^3}^* \hat{\Lambda}(z, z^*)\end{aligned}$$

Using these expressions for operators, it is possible to translate an equation of motion for the density matrix (master equation) to a Fokker-Planck equation for the distribution function $P(z)$, or (with a variable change) for the distribution function $D(\theta, \phi)$.

(b) The complex A.C.S. representation

In the previous section, the diagonal ACS representation has been obtained following the work of Arrechi et al (1972), Glauber & Haake (1974). In the work of Glauber & Haake, a master equation and Fokker-Planck equation are obtained for super-radiance, giving a non-positive definite diffusion term. However these authors make the approximation of neglecting the non-positive definite terms (Glauber & Haake (1974) Equation 5.9). While this approximation is probably acceptable in super-radiance (because the relevant terms are small close to complete inversion), it cannot be

made in general for a driven quantum system.

We therefore turn to the definition of a complex ACS representation, similar to the complex P-representation of 2.1, in order to obtain a positive definite Fokker-Planck equation. We first define a non-hermitian projection operator:

$$\begin{aligned}\hat{\Lambda}(z_1, z_2) &= |z_1\rangle\langle z_2^*| / \langle z_2^*|z_1\rangle \\ &= [1+z_1 z_2]^{-2J} \exp[z_1 \hat{J}^-] |J, J\rangle \langle J, J| \exp[z_2 \hat{J}^+]\end{aligned}$$

The definition of the complex ACS representation is as follows:

$$\hat{\rho} = \int_{\mathcal{D}} P(z_1, z_2) \hat{\Lambda}(z_1, z_2) d\mu(z_1, z_2)$$

In exactly the same way as previously, operator identities can be obtained, which transform to the diagonal representation identities in the case of $(z=z_1)$; $(z^*=z_2)$.

In particular one obtains:

$$\hat{J}^+ \hat{\Lambda}(z_1, z_2) = \left[\frac{2J z_1}{1+z_1 z_2} - z_1^2 \frac{\partial}{\partial z_1} \right] \hat{\Lambda}(z_1, z_2) = \mathcal{D}_{J^+} \hat{\Lambda}(z_1, z_2)$$

$$\hat{\Lambda}(z_1, z_2) \hat{J}^- = \left[\frac{2J z_2}{1+z_1 z_2} - z_2^2 \frac{\partial}{\partial z_2} \right] \hat{\Lambda}(z_1, z_2) = \mathcal{D}'_{J^-} \hat{\Lambda}(z_1, z_2)$$

$$\hat{J}^- \hat{\Lambda}(z_1, z_2) = \left[\frac{\partial}{\partial z_1} + \frac{2J z_2}{1+z_1 z_2} \right] \hat{\Lambda}(z_1, z_2) = \mathcal{D}_{J^-} \hat{\Lambda}(z_1, z_2)$$

$$\hat{\Lambda}(z_1, z_2) \hat{J}^+ = \left[\frac{\partial}{\partial z_2} + \frac{2J z_1}{1+z_1 z_2} \right] \hat{\Lambda}(z_1, z_2) = \mathcal{D}'_{J^+} \hat{\Lambda}(z_1, z_2)$$

$$\hat{J}^2 \hat{\Lambda}(z_1, z_2) = \left[J \left[\frac{1-z_1 z_2}{1+z_1 z_2} \right] - z_1 \frac{\partial}{\partial z_1} \right] \hat{\Lambda}(z_1, z_2) = \mathcal{D}_{J^2} \hat{\Lambda}(z_1, z_2)$$

Using the above identities it is possible to write down either 2-dimensional (line-integral) or 4-dimensional Fokker-Planck equations. The 4-dimensional equations are obtained just as in 2.1, by utilising the equivalence:

$$\frac{\partial}{\partial z} \leftrightarrow \frac{\partial}{\partial z^*} \leftrightarrow \frac{-i\partial}{\partial z^{\prime}}$$

Therefore these equations will have positive semi-definition diffusion and we can develop a stochastic differential equation in a four dimensional phase-space.

In order to obtain physical observables, we will be interested in the weight functions for normally ordered products. These are well known in the case of the diagonal representation (Arrechi et al 1972, Glauber & Haake 1974):

$$\langle (\hat{J}^+)^{\ell} (\hat{J}^-)^{\ell'} \rangle = \int [P(z) (1+|z|^2)^{-2J} \frac{\partial^{\ell+\ell'}}{\partial z^{\ell} \partial z^{\prime \ell'}} (1+|z|^2)^{2J}] d^2z$$

We now proceed to demonstrate that exactly the same forms can be utilised for a nondiagonal representation with the replacement ($z \rightarrow z_1, z^* \rightarrow z_2$):

$$\langle (\hat{J}^+)^{\ell} (\hat{J}^-)^{\ell'} \rangle_{\rho} = \text{Tr} \left\{ \int P(z_1, z_2) \hat{\Lambda}(z_1, z_2) d\mu(z_1, z_2) \hat{J}^{\ell} \hat{J}^{-\ell'} \right\}$$

$$\text{Tr} [\hat{J}^{\ell} \hat{J}^{-\ell'} \hat{\Lambda}] = \text{Tr} \left\{ \hat{J}^{-\ell'} (1+z_1, z_2)^{-2J} \exp(z_1 \hat{J}^-) |J, J\rangle \langle J, J| \exp(z_2 \hat{J}^+) \hat{J}^{\ell} \right\}$$

$$= \text{Tr} \left\{ (1+z_1, z_2)^{-2J} \frac{\partial^{\ell+\ell'}}{\partial z_2^{\ell} \partial z_1^{\ell'}} \exp(z_1 \hat{J}^-) |J, J\rangle \langle J, J| \exp(z_2 \hat{J}^+) \right\}$$

$$= \text{Tr} \left\{ (1+z_1, z_2)^{-2J} \frac{\partial^{\ell+\ell'}}{\partial z_2^{\ell} \partial z_1^{\ell'}} (1+z_1, z_2)^{2J} \hat{\Lambda}(z_1, z_2) \right\}$$

Using the identity:

$$\text{Tr}(\hat{\Lambda}(z_1, z_2)) = 1$$

We then obtain -

$$\langle \hat{J}^+{}^{\ell} \hat{J}^-{}^{\ell'} \rangle_{\rho} = \int_{\mathcal{D}} [P(z_1, z_2) (1+z_1 z_2)^{-2J} \frac{z_1^{\ell+\ell'}}{z_2^{\ell} z_1^{\ell'}} (1+z_1 z_2)^{2J}] d\mu(z_1, z_2)$$

For future use, some of the common weight functions are listed below:

$$\hat{J}^+ \sim 2J z_1 / (1+z_1 z_2)$$

$$\hat{J}^- \sim 2J z_2 / (1+z_1 z_2)$$

$$\hat{J}^+ \hat{J}^- \sim (2J / (1+z_1 z_2)) + 2J(2J-1) z_1 z_2 / (1+z_1 z_2)^2$$

$$\hat{J}^+{}^2 \hat{J}^-{}^2 \sim \frac{4J(2J-1)}{(1+z_1 z_2)^2} \left[1 + \frac{2z_1 z_2 (2J-2)}{(1+z_1 z_2)} + \frac{(2J-2)(2J-3)(z_1 z_2)^2}{2(1+z_1 z_2)^2} \right]$$

$$\hat{J}^2 \sim J(1-z_1 z_2) / (1+z_1 z_2)$$

Earlier in this section the fact that correlation functions do not factorise exactly in a coherent state was mentioned. These can now be calculated explicitly as follows:

$$\langle z | \hat{J}^+ \hat{J}^- | z \rangle = \frac{2J}{1+|z|^2} + 2J(2J-1) |z|^2 / (1+|z|^2)$$

$$\langle \rho | \hat{J}^2 | \rho \rangle = (J + \langle J_y \rangle) + (1 - \frac{1}{2J}) \langle J^+ \rangle \langle J^- \rangle$$

We note at this point that this expression is identical to that obtained in the case of atoms in an uncorrelated state; provided $2J = N$;

$$\begin{aligned} \langle \hat{J}^+ \hat{J}^- \rangle_u &= \left\langle \sum_{j=1}^N (\hat{\sigma}_j^+ \hat{\sigma}_j^-) \right\rangle + \sum_{i \neq j} \langle \hat{\sigma}_i^+ \rangle \langle \hat{\sigma}_j^- \rangle \\ &= \left(\frac{N}{2} + \langle \hat{J}_z \rangle_u \right) + (1 - \frac{1}{N}) \langle \hat{J}^+ \rangle_u \langle \hat{J}^- \rangle_u \end{aligned}$$

However this correspondence is not a general one: in particular \hat{J}^2 is invariant in a coherent state, but it varies with the mean polarisation and inversion in an uncorrelated state:

$$\begin{aligned} \langle \hat{J}^2 \rangle_u &= \langle \hat{J}_z^2 + \hat{J}^+ \hat{J}^- - \hat{J}_z \rangle_u \\ &= \frac{3}{4} N + (1 - \frac{1}{N}) \left[\langle \hat{J}^+ \rangle_u \langle \hat{J}^- \rangle_u + \langle \hat{J}_z \rangle_u^2 \right] \end{aligned}$$

In the uncorrelated state it is possible to show that we obtain $\langle \hat{J}^2 \rangle = J(J+1)$ in the collective ground state, but not in general.

The next correlation function of interest is the one corresponding to correlations of fluorescent photons:

$$\langle \hat{J}_z \hat{J}^2 \hat{J}^2 \hat{J}_z \rangle = \frac{4J(2J-1)}{(1+|z|^2)^2} \left[1 + \frac{2|z|^2(2J-2)}{(1+|z|^2)} + \frac{(J-1)(2J-3)|z|^4}{(1+|z|^2)^2} \right]$$

Clearly as mentioned earlier this vanishes at $J = \frac{1}{2}$ (in general all correlation functions of order greater than $2J$ vanish). However the behaviour at large J values is also of interest, as this corresponds to correlations of photons emitted from an atomic system in an atomic coherent state.

We therefore proceed to calculate the normalised correlation function $g^{(2)}(\theta)$ in the case of $J > \frac{1}{2}$:

$$g^{(2)}(\theta) = \frac{4J(2J-1)}{(1+|z|^2)^2} \left[\frac{J-1}{2J-1} + \frac{|z|^2(2J-4)}{1+|z|^2} + \frac{(3-4J)|z|^4}{(1+|z|^2)^2} \right]$$

$$\therefore g^{(2)}(\theta) = 1 + \frac{\left[\frac{(2J-2)}{(2J-1)} + \frac{4J-8}{2J-1} \cos^2 \frac{\theta}{2} + \frac{(6-8J)}{2J-1} \cos^4 \frac{\theta}{2} \right]}{\left[2J/(2J-1) + 4J \cos^2 \frac{\theta}{2} + 2J(2J-1) \cos^4 \frac{\theta}{2} \right]}$$

Thus we see the following limits occur; depending on the degree of atomic inversion ($\theta = 0$ corresponds to the ground state, $\theta = \pi$ to the completely inverted state):

(a) $\theta = 0$: $g^{(2)}(\theta) = 1 - 1/J + O(1/J^2)$

(b) $\theta = \pi/2$: $g^{(2)}(\theta) = 1 - \frac{3}{2J^2} + O(1/J^3)$

(c) $\theta = \pi - \frac{2}{J}$: $g^{(2)}(\theta) = 1 + \frac{5}{9} + O(1/J)$

(d) $\theta = \pi$: $g^{(2)}(\theta) = 2 - 1/J + O(1/J^2)$

It is interesting to see that over most of the range of θ the system remains approximately coherent: for $0 \leq \theta \leq \pi/2$ there is a degree of antibunching of order at most $(1/J)$. For atomic systems that are inverted, we have a degree of photon bunching for $\pi/2 < \theta \leq \pi$. Then finally, close to complete inversion there is a rapid change with nearly chaotic photon statistics in the completely inverted state. The behaviour of the atomic coherent states is completely different here from the boson coherent states, which of course have completely factorised

correlation functions with $g_2(0) = 1$ for all values of α .

(c) Correlation functions in the A.C.S. representation

The expression for correlation functions in the diagonal ACS representation has been obtained for time-ordered multitime correlation functions by Narducci (1974). In fact as we will show in 2.3, these results also hold for the complex ACS representation: ($t' > t$) -

$$\langle \hat{A}'(t') \hat{A}(t) \rangle = \iint_{\mathcal{D}} P(\underline{z}, t) \mathcal{D}_{A'}(\underline{z}) P(\underline{z}', t' | \underline{z}, t) \langle \hat{A}' \rangle_{\underline{z}'} \cdot d\mu(\underline{z}) \cdot d\mu(\underline{z}')$$

$$\begin{aligned} \langle \hat{A}_1(t) \hat{A}'_1(t') \hat{A}'_2(t') \hat{A}_2(t) \rangle = \\ = \iint P(\underline{z}, t) \mathcal{D}_{A_2}(\underline{z}) \mathcal{D}'_{A_1}(\underline{z}) \times \\ \times P(\underline{z}', t' | \underline{z}, t) \times \langle \hat{A}'_1 \hat{A}'_2 \rangle_{\underline{z}'} \cdot d\mu(\underline{z}) \cdot d\mu(\underline{z}') \end{aligned}$$

While these results can be used to obtain the time-correlation functions, they do not simplify in the same way as the corresponding expressions for normal ordered, time-ordered correlations in the P-representation: it is necessary to include derivative terms to obtain the full quantum fluctuation spectrum.

2.3 GENERAL OPERATOR REPRESENTATIONS

(a) Operator representations in a general phase-space

We now wish to extend the operator representations of sections 2.1 and 2.2 to a general set of noncommuting operators $\hat{a}_1, \dots, \hat{a}_n$. The derivation is similar to that of previous authors, except that the generalised P-function is defined relative to a complex phase-space. Special cases include the ACS representation, the Glauber-Sudarshan P-representation, and the associated classical descriptions of Agarwal & Wolf (1968), Lax (1968), Louisell & Marburger (1969), Haken (1970).

The general P-representation is defined by specifying an operator valued function $\hat{\chi}(\underline{\lambda})$ and a complex function $\chi(\underline{\lambda}, \underline{\alpha})$. The function $\hat{\chi}(\underline{\lambda})$ in turn defines the quantum characteristic function $\chi(\underline{\lambda})$ of the density matrix relative to a particular operator ordering:

$$\chi(\underline{\lambda}) \equiv \text{Tr}[\hat{\rho} \hat{\chi}(\underline{\lambda})]$$

The (complex) P-representation relative to a given measure $dM(\underline{\alpha})$, is then obtained by defining a corresponding P-function $P(\underline{\alpha})$ that must satisfy:

$$\chi(\underline{\lambda}) = \int_{\mathcal{D}} P(\underline{\alpha}) \chi(\underline{\lambda}, \underline{\alpha}) dM(\underline{\alpha})$$

We suppose that $[\hat{\chi}, \chi, dM]$ are defined (for the coherent state case see section 2.1) so that $P(\underline{\alpha})$ exists; and these functions are normally selected so that:

$$\hat{\chi}(\underline{\alpha}) = \hat{1} \quad ; \quad \chi(\underline{\alpha}, \underline{\alpha}) = 1$$

This leads to the normalisation equation:

$$\text{Tr}(\hat{\rho}) = 1 = \int_{\mathcal{D}} P(\underline{\alpha}) d\mu(\underline{\alpha})$$

In most cases X is obtained from $\hat{\chi}$ by substituting a variable c-number for the corresponding operator: but this is not necessary in general.

In order for the representation to be well-defined, it is necessary that $\hat{\chi}(\underline{\lambda})$ is a complete basis for the system operators; i.e. for any system operator \hat{A} , there is an expansion as a linear functional of $\hat{\chi}(\underline{\lambda})$:

$$\hat{A} = \int_{\mathcal{D}} \bar{A}(\underline{\lambda}) \hat{\chi}(\underline{\lambda}) d\bar{\mu}(\underline{\lambda})$$

Here $d\bar{\mu}(\underline{\lambda})$ is an integration measure (which could be a discrete summation) in the space of $\underline{\lambda}$ variables. In many cases $\bar{A}(\underline{\lambda})$ is a generalised function that corresponds to a linear differential operator.

We now list some representations that can be written in the form defined above.

$\hat{\chi}(\underline{\lambda})$	$X(\underline{\lambda}, \underline{\alpha})$	
(a) $\exp(\lambda \hat{a}^+) \exp(-\lambda^* \hat{a})$	$\exp(\lambda \alpha^* - \lambda^* \alpha)$	(P-representation)
(b) $\exp(-\lambda^* \hat{a}) \exp(\lambda \hat{a}^+)$	$\exp(\lambda \alpha^* - \lambda^* \alpha)$	(Q-representation)
(c) $\hat{Y}_z^m(\hat{\underline{j}})$	$\gamma_z^m(\theta, \phi)$	(ACS-representation) (Arecchi et al 1972)
(d) $\exp(\lambda \hat{a}^+) \exp(-\lambda^* \hat{a})$	$\exp(\lambda \beta - \lambda^* \alpha)$	(Complex P-representation)
(e) $\exp(i\lambda_1 \hat{a}_1) \dots \exp(i\lambda_n \hat{a}_n)$	$\exp(i\lambda \cdot \underline{\alpha})$	(General representation)

The last representation (e) is the general associated classical description of Agarwal & Wolf, Lax, Louisell & Marburger and Haken. However, while these authors have a real variable corresponding to an hermitian operator, we will define a general representation without this restriction, so that a complex variable corresponds to an hermitian operator. This gives a natural generalisation of the complex P-representation defined in section 2.1. As pointed out in 2.1, the integration domain for \underline{z} can be a line integral or the whole complex plane, provided integration by parts is possible.

In order to find the expectation value of the operator \hat{A} , we write:

$$\begin{aligned} \langle \hat{A} \rangle_p &= \iint P(\underline{z}) \bar{A}(\underline{\lambda}) X(\underline{\lambda}, \underline{z}) d\mu(\underline{z}) d\bar{\mu}(\underline{\lambda}) \\ &= \int P(\underline{z}) \hat{A}(\underline{z}) d\mu(\underline{z}) \end{aligned}$$

Where:

$$\hat{A}(\underline{z}) = \int \bar{A}(\underline{\lambda}) X(\underline{\lambda}, \underline{z}) d\bar{\mu}(\underline{\lambda})$$

In many cases of interest (normal ordered operators in a normal ordering representation) the associated classical function \hat{A} is simply obtained by replacing \hat{a}_i by a_i in the normal ordered operator power series expansion.

We also often wish to represent expectation values using differential operators:

$$\text{Tr}(\hat{A} \hat{\rho} \hat{\chi}(\underline{\lambda})) = \int \bar{\mathcal{D}}_A(\underline{\lambda}, \underline{\lambda}') \text{Tr}[\hat{\rho} \hat{\chi}(\underline{\lambda}')] d\bar{\mu}(\underline{\lambda}')$$

$$\text{Tr}(\hat{\rho} \hat{A} \hat{\chi}(\underline{\lambda})) = \int \bar{\mathcal{D}}'_A(\underline{\lambda}, \underline{\lambda}') \text{Tr}[\hat{\rho} \hat{\chi}(\underline{\lambda}')] d\bar{\mu}(\underline{\lambda}')$$

In the usual representations, the expectation values in the above form can always be transformed to a differential operator acting on $X(\underline{\lambda}, \underline{\alpha})$, so that:

$$\text{Tr}(\hat{A} \hat{\rho} \hat{X}(\underline{\lambda})) = \int P(\underline{\alpha}) \mathcal{D}_A(\partial_{\underline{\alpha}}, \underline{\alpha}) X(\underline{\lambda}, \underline{\alpha}) d\mu(\underline{\alpha})$$

$$\text{Tr}(\hat{A} \hat{X}(\underline{\lambda}) \hat{\rho}) = \int P(\underline{\alpha}) \mathcal{D}'_A(\partial_{\underline{\alpha}}, \underline{\alpha}) X(\underline{\lambda}, \underline{\alpha}) d\mu(\underline{\alpha})$$

It is now possible to use the operator identities to evaluate the time-development equations. We have given the relevant identities for the complex P-representation and complex ACS-representation in 2.1, 2.2: further useful identities for atomic operators are given in Haken (1970), Louisell (1973). We note the following product rule:

$$\begin{aligned} \text{Tr}[\hat{A} \hat{B} \hat{\rho} \hat{X}(\underline{\lambda})] &= \int \bar{\mathcal{D}}_A(\underline{\lambda}, \underline{\lambda}') \text{Tr}[\hat{B} \hat{\rho} \hat{X}(\underline{\lambda}')] d\bar{\mu}(\underline{\lambda}') \\ &= \int P(\underline{\alpha}) \mathcal{D}_B(\partial_{\underline{\alpha}}, \underline{\alpha}) \mathcal{D}_A(\partial_{\underline{\alpha}}, \underline{\alpha}) X(\underline{\lambda}, \underline{\alpha}) d\mu(\underline{\alpha}) \end{aligned}$$

In general the time-development equations can be written with the use of the operator identities in the following form:

$$\begin{aligned} \text{Tr}[\hat{\mathcal{L}}[\hat{\rho}] \hat{X}(\underline{\lambda})] &= \int \bar{\mathcal{L}}(\underline{\lambda}, \underline{\lambda}') X(\underline{\lambda}') d\bar{\mu}(\underline{\lambda}') \\ &= \int P(\underline{\alpha}) \mathcal{L}'(\partial_{\underline{\alpha}}, \underline{\alpha}) X(\underline{\lambda}, \underline{\alpha}) d\mu(\underline{\alpha}) \end{aligned}$$

Hence on integrating by parts and equating the coefficients of X , one obtains a time-development differential equation in $P(\underline{\alpha})$:

$$\partial_t P(\underline{\alpha}) = \mathcal{L}[\partial_{\underline{\alpha}}, \underline{\alpha}] P(\underline{\alpha})$$

It is useful to define a propagator function in \underline{q} space by setting:

$$\partial_{t'} P(\underline{q}', t' | \underline{q}, t) = \mathcal{L}[\partial_{\underline{q}'}, \underline{q}'] P(\underline{q}', t' | \underline{q}, t)$$

$$P(\underline{q}', t' | \underline{q}, t) = \delta^n(\underline{q}' - \underline{q})$$

Where the delta-function is defined in the usual way relative to the measure $d\mu(\underline{q})$. For later use, we define a hybrid propagator:

$$\chi^H(\underline{\lambda}', t' | \underline{q}, t) \equiv \int P(\underline{q}', t' | \underline{q}, t) X(\underline{\lambda}', \underline{q}') d\mu(\underline{q}')$$

We note that at $t' = t$ the propagator is given by:

$$\chi^H(\underline{\lambda}', t | \underline{q}, t) = X(\underline{\lambda}', \underline{q})$$

While for $t' > t$ it is necessary that the hybrid propagator follows the time-development of the characteristic function:

$$\partial_{t'} \chi^H(\underline{\lambda}', t' | \underline{q}, t) = \int \bar{\mathcal{L}}(\underline{\lambda}', \underline{\lambda}'') \chi^H(\underline{\lambda}'', t' | \underline{q}, t) d\bar{\mu}(\underline{\lambda}'')$$

As pointed out previously (in 2.1, 2.2) the time-development is not unique: that is, there can be several different (\mathcal{L}) functions with corresponding propagators.

In order to determine correlation properties we define a time-development operator \hat{U} (Louisell & Marburger, 1968):

$$\hat{A}(t') = \hat{U}(t, t') \hat{A}(t) \hat{U}(t', t)$$

Any time-correlation function can be written, for $t' \succ t$, as:

$$\langle \hat{A}(t') \hat{B}(t) \rangle_\rho = \text{Tr} \left[\hat{B}(t) \hat{\rho}(t) \{ \hat{U}(t, t') \hat{A}(t) \hat{U}(t', t) \} \right]$$

This equation is exact in the absence of reservoirs. We also suppose that on a long enough time scale (relative to the reservoir correlation function) it also holds after tracing over the reservoirs, and that the operator \hat{U} is a function of system operators only. (These assumptions can be regarded as the definition of a quantum Markovian system, and they imply the quantum regression theorem of Lax (1968)).

In particular, we can apply the time-development operator to the kernel $\hat{\chi}(\underline{\lambda})$, and the result must be a linear functional of $\hat{\chi}(\underline{\lambda}')$; owing to the completeness of $\hat{\chi}(\underline{\lambda}')$ as a basis:

$$\{\hat{U}(t, t') \hat{\chi}(\underline{\lambda}', t) \hat{U}(t', t)\} \equiv \int \chi^c[\underline{\lambda}', t' | \underline{\lambda}, t] \hat{\chi}(\underline{\lambda}, t) d\bar{\mu}(\underline{\lambda})$$

This defines the characteristic propagator function, for $t' > t$. The propagator functions for $\hat{\chi}$, P have similar properties:

$$\hat{\chi}(\underline{\lambda}', t) = \int \chi^c[\underline{\lambda}, t' | \underline{\lambda}, t] \hat{\chi}(\underline{\lambda}, t) d\bar{\mu}(\underline{\lambda})$$

$$P(\underline{\alpha}', t') = \int P(\underline{\alpha}', t' | \underline{\alpha}, t) P(\underline{\alpha}, t) d\bar{\mu}(\underline{\alpha})$$

We can also redefine the hybrid propagator as follows:

$$\begin{aligned} \chi^H(\underline{\lambda}', t' | \underline{\alpha}, t) &= \int \chi^c(\underline{\lambda}', t' | \underline{\lambda}, t) X(\underline{\lambda}, \underline{\alpha}) d\bar{\mu}(\underline{\lambda}) \\ &= \int P(\underline{\alpha}', t' | \underline{\alpha}, t) X(\underline{\lambda}', \underline{\alpha}') d\mu(\underline{\alpha}') \end{aligned}$$

Clearly: (in each case) -

$$\chi^H(\underline{\lambda}', t' | \underline{\alpha}, t) = X(\underline{\lambda}', \underline{\alpha})$$

We note that this is well-defined for $t' > t$ since both definitions have the same time-development as a function of $(\underline{\lambda}')$, and they are equal to each other at $(t = t')$.

Next, it is helpful to evaluate a specific correlation function:

$$\langle \hat{A}(t') \hat{B}(t) \rangle = \text{Tr}[\hat{B}(t) \hat{\rho}(t)] \int \bar{A}(\underline{\lambda}') \chi(\underline{\lambda}', t' | \underline{\lambda}, t) \hat{\chi}(\underline{\lambda}, t) d\bar{\mu}(\underline{\lambda}') d\mu(\underline{\lambda})$$

$$\text{Tr}[\hat{B}(t) \hat{\rho}(t) \hat{\chi}(\underline{\lambda}, t)] = \int P(\underline{\alpha}, t) [\mathcal{D}_B(\underline{\alpha}) X(\underline{\lambda}, \underline{\alpha})] d\mu(\underline{\alpha})$$

Combining the above equations we obtain, with the use of the hybrid propagator:

$$\begin{aligned} \langle \hat{A}(t') \hat{B}(t) \rangle &= \iiint \bar{A}(\underline{\lambda}') \chi(\underline{\lambda}', t' | \underline{\lambda}, t) P(\underline{\alpha}, t) [\mathcal{D}_B(\underline{\alpha}) X(\underline{\lambda}, \underline{\alpha})] d\mu(\underline{\alpha}) d\bar{\mu}(\underline{\lambda}) d\bar{\mu}(\underline{\lambda}') \\ &= \iint \bar{A}(\underline{\lambda}') P(\underline{\alpha}, t) \mathcal{D}_B(\underline{\alpha}) \chi^H(\underline{\lambda}', t' | \underline{\alpha}, t) d\mu(\underline{\alpha}) d\bar{\mu}(\underline{\lambda}') \\ &= \int A^c(\underline{\alpha}') P(\underline{\alpha}, t) \mathcal{D}_B(\underline{\alpha}) P(\underline{\alpha}', t' | \underline{\alpha}, t) d\mu(\underline{\alpha}) d\mu(\underline{\alpha}') \end{aligned}$$

A similar expression is also found by Agarwal & Wolf (1968), Lax (1968), Louisell & Marburger (1969), Haken (1970) for the usual operator representations. The above expression extends these results to complex representations, where it is not possible to express the P-function uniquely in terms of the density operator: similar results hold for n-fold correlation functions.

We finally point out that for normally ordered, time ordered functions in the general ordered representation (e), these expressions reduce to the correlations of multinomial

products similar to a true classical phase-space description. The one difference is that in this case, it is a complex phase-space. For n dynamical variables (operators) this is a manifold embedded in \mathbb{C}^n ; instead of the classical phase-space of \mathbb{R}^n .

(b) Fokker-Planck and stochastic equations

In general the procedure outlined above, leads to a differential equation with derivatives of all orders. In practical applications, derivations of third or higher order are often not present or very small. In these cases the P-function obeys a Fokker-Planck equation of the following form:

$$\partial_t P(\underline{\alpha}) = \left\{ \partial_\mu A_\mu(\underline{\alpha}) + \frac{1}{2} \partial_\mu \partial_\nu D_{\mu\nu}(\underline{\alpha}) \right\} P(\underline{\alpha})$$

The discussion of 2.1 holds for this type of Fokker-Planck equation; and just as previously, different equations occur on different integration domains. When potential equations hold, it is sometimes possible to obtain exact solutions by integrating in a real phase-space of (n) dimensions for an (n) operator representation. In cases where these solutions are not normalisable*, it may be necessary to use a line integral in a complex phase-space. However it should be verified that complex potential

* We assume that this is not because of a global instability in the deterministic equations; but is due to a non positive-definite diffusion array.

solutions obtained in this way have physical moments, resulting from physically accessible initial distributions.

When potential equations are not applicable, and the array $(D_{\mu\nu})$ is in general not positive-definite, it is useful to transform the Fokker-Planck equation to a form that has positive semi-definite diffusion. The following equivalence relation holds whenever $X(\underline{\lambda}, \underline{q})$ is an analytic function of \underline{q} :

$$\frac{\partial}{\partial q_M} \leftrightarrow \frac{\partial}{\partial x_M} \leftrightarrow \frac{-i\partial}{\partial y_M}$$

Where:

$$q_M \equiv x_M + iy_M \quad ; \quad \partial_M^x \equiv \frac{\partial}{\partial x_M} \quad ; \quad \partial_M^y \equiv \frac{\partial}{\partial y_M}$$

Define:

$$A_M = A_M^x + iA_M^y$$

$$D_{\mu\nu} = B_{\mu\sigma} B_{\nu\sigma}$$

$$B_{M\sigma} = B_{M\sigma}^x + iB_{M\sigma}^y$$

Then the following time-development equation holds for $P(\underline{q})$ defined on a complex phase-space:

$$\partial_t P(\underline{x}, \underline{y}) = \left[\partial_M^x A_M^x + \partial_M^y A_M^y + \frac{1}{2} (\partial_M^x \partial_N^x (B_{\mu\sigma}^x B_{\nu\sigma}^x) + \partial_M^x \partial_N^y (B_{\mu\sigma}^x B_{\nu\sigma}^y) + \partial_M^y \partial_N^x (B_{\mu\sigma}^y B_{\nu\sigma}^x) + \partial_M^y \partial_N^y (B_{\mu\sigma}^y B_{\nu\sigma}^y)) \right] P(\underline{x}, \underline{y})$$

Thus we see that it is possible to define a time-development equation in the complex phase-space that is positive semi-definite and therefore allows the distribution to have the characteristics of a complex phase-space probability.

Utilising the theorems of Ito stochastic calculus, we see that the overall diffusion array of the new Fokker-Planck equation is:

$$\underline{D}' = \begin{bmatrix} \underline{B}^x \underline{B}^{xT} & \underline{B}^x \underline{B}^{yT} \\ \underline{B}^y \underline{B}^{xT} & \underline{B}^y \underline{B}^{yT} \end{bmatrix} = \begin{bmatrix} \underline{B}^x & 0 \\ \underline{B}^y & 0 \end{bmatrix} \begin{bmatrix} \underline{B}^{xT} & \underline{B}^{yT} \\ 0 & 0 \end{bmatrix}$$

Hence we obtain the following Ito stochastic differential equation (provided the coefficients obey the usual existence restrictions):

$$\frac{\partial}{\partial t} \begin{bmatrix} X_M \\ Y_M \end{bmatrix} = - \begin{bmatrix} A_M^x(\underline{q}) \\ A_M^y(\underline{q}) \end{bmatrix} + \begin{bmatrix} B_{Mv}^x(\underline{q}) \xi_v(t) \\ B_{Mv}^y(\underline{q}) \xi_v(t) \end{bmatrix}$$

This equation is equivalent to the Fokker-Planck equation in the sense that the probability of an initial value (\underline{q}, t) propagating to (\underline{q}', t') is equal to the propagator of the Fokker-Planck equation, $P(\underline{q}', t' | \underline{q}, t)$. (Arnold, 1974.)

Methods of solving the stochastic equations generally rely on an asymptotic expansion in the diffusion variance (Appendix A). In the present thesis, we shall use the first order (linearised) terms in this expansion, as outlined in Appendix B. An alternative is the direct numerical simulation of the equations using a computer-generated discrete time random function. In this technique problems arise occasionally due to the nonlinear deterministic equations which have "spiking" trajectories in the complex phase-space. However a very careful use of numerical integration routines can overcome this problem and good agreement is obtained with the complex potential method and with the asymptotic expansion in the relevant limits (Steyn-Ross, 1979).

We emphasise that the positive-definite Fokker-Planck equation and the stochastic differential equation defined here, are defined on a space of larger dimension than usual (for non-classical operator statistics). In the case of a single radiation mode, the space is \mathbb{C}^2 which is isomorphic to a four-dimensional real space. By comparison, a classical process would be defined on \mathbb{R}^2 - a real space of lower dimension. The positive-definite Fokker-Planck equation on the four-dimensional space has four different differentials ($\partial\alpha^x, \partial\alpha^y, \partial\beta^x, \partial\beta^y$). Normally this would generate a stochastic differential equation with four random functions. However by choosing a nonsymmetric matrix square root, only one random function is needed for each operator. Now the random functions are uncorrelated, so that the variables representing (\hat{a}, \hat{a}^\dagger) are non complex-conjugate. It is often useful to write them as (α, α^\dagger) to distinguish them from (α, α^*) as normally used. Because the (α, α^\dagger) variables are non complex-conjugate, they require to be defined on a space (\mathbb{C}^2) which is of larger dimension than the space (\mathbb{C}) or (\mathbb{R}^2) that would be sufficient for a classical process. However we will see later, that calculations in the space (\mathbb{C}^2) are straightforward, especially in the physically relevant case of normally ordered correlations.

In summary we have defined several different types of complex P-representations. When the measure (V) (see 2.1) is utilised, the complex P-function has many of the characteristics of a probability distribution defined on a complex phase-space. In particular the normally ordered representations are useful, as they give the physically observable quantities of interest, in terms of straightforward complex phase-space moments or correlations in most cases. Overall, the representation has an advantage over the usual real phase-space representations, in that when a Fokker-Planck equation exists, it will have a positive semi-definite diffusion array.

Non-classical statistical properties (like photon anti-bunching) can arise when the distribution develops finite values for $\alpha^+ \neq \alpha^*$ in the radiation field representation; however no singularity occurs in the distribution. In terms of the position and momentum variables, this corresponds to a complex equivalent position and momentum occurring with a certain weight. If the initial distribution was complex valued, then the stochastic process only describes propagation effects, and the probabilistic interpretation is no longer valid (except possibly in the steady state).

However we have proved rigorously in the case of the radiation field, that a real positive probability distribution on the complex phase-space exists for all initial density operators.

CHAPTER 3: SINGLE MODE TRANSITIONS

In this chapter, the theory of a coherently driven boson mode with nonlinear dispersion and absorption is presented, with emphasis on quantum statistical properties. The principal application is to an externally driven quantum optical system where a single mode is selected by an interferometer. For this reason the discussion is in terms of quantum optics, although the Hamiltonian and Fokker-Planck equation would equally apply to other driven quantum systems described by boson algebra.

The classical theory of nonlinear optical phenomena results in a linear, quadratic or cubic polarisation relative to the input field. Naturally it is possible for higher order nonlinearities to occur, but these will be assumed to be small in this chapter. It is well known that a linear polarisation results in an alteration in the refractive index and a linear absorption: but the linear response does not change the quantum coherence properties of the field (Shen, 1967).

The nonlinearities will couple different field modes, and quantum statistical properties are altered by the medium. However mode-mode coupling only occurs when wave-number matching requirements are met (in practice, with the use of birefringent crystals or other means). The simplest case is therefore a single mode with a quadratic or cubic polarisability and that is the situation we treat here. In general there is both nonlinear dispersion and absorption, so we treat both these situations in a unified way.

In 3.1 the general Hamiltonian is obtained and this is used to develop a master equation and Fokker-Planck equation for the complex P-function following Chapters 1, 2. General expressions for correlations are obtained, in the case of small fluctuations close to a stable branch of the deterministic state equation. In 3.2, exact steady state results are obtained in the cases where potential solutions exist. In particular the usual Landau-Ginzberg result is obtained for a resonant excitation and thermal fluctuations. However a new type of exact solution occurs in the limit of zero-temperature, which has a nonclassical behaviour and gives antibunching: this also holds for a detuned driving field.

In 3.3 - 3.5 the general results are used in specific problems. We first turn to the laser with an injected signal, where some well known results for the driven van der Pol oscillator can be used to describe phase entrainment. In 3.4, the driven nonlinear absorber is studied, giving fluctuation reduction and photon antibunching. Finally in 3.5, the problem of an interferometer with nonlinear dispersion leads to optical bistability. This can be described by the linearised results of 3.1; while in the limit of zero thermal fluctuations there is an exact non Landau-Ginzberg potential solution for the complex P-function, giving the steady state moments.

3.1 UNIFIED NONLINEAR THEORY FOR A SINGLE MODE OPERATOR

(a) Nonlinear dispersion

We start with the Hamiltonian for a nonlinear optical system, with the polarisability expanded to third order in the mean electric field amplitude. As a single mode treatment is intended, it is possible to omit the frequency dependence of the susceptibility. The expression for the Hamiltonian is (Bloembergen, 1965):

$$\hat{H} = \int d^3r \left[\frac{1}{2\mu_0} |\hat{B}|^2 + \epsilon_0 \hat{E} \left\{ (1 + \chi^{(1)}) \hat{E} / 2 + \chi^{(2)} \hat{E} \hat{E} / 3 + \chi^{(3)} \hat{E} \hat{E} \hat{E} / 4 \right\} \right]:$$

Here $\chi^{(n)}$ is an (n+1)th rank tensor. Now subtracting the zero point energy and transforming to the \hat{a}, \hat{a}^\dagger representation with boson operators leads to:

$$\hat{H} = \hbar\omega \hat{a}^\dagger \hat{a} + \int d^3r \left[\epsilon_0 \hat{E} \left\{ \chi^{(2)} \hat{E} \hat{E} / 3 + \chi^{(3)} \hat{E} \hat{E} \hat{E} / 4 \right\} \right]:$$

$$\hat{E} = i \left[\frac{\hbar\omega}{2\epsilon_0} \right]^{1/2} \left[\hat{a} u(\underline{r}) - \hat{a}^\dagger u^*(\underline{r}) \right]$$

The mode function $u(\underline{r})$ is defined to satisfy the orthogonality relation:

$$\int u^*(\underline{r}) \cdot [1 + \chi^{(1)}(\underline{r})] u(\underline{r}) \cdot d^3r = 1$$

Now we have only included a single mode term in the expansion, so that there is just a single frequency involved. This is appropriate provided the modes have a large frequency spacing, relative to the detuning of the input field and the nonlinear frequency shifts. In addition, all harmonic generation is neglected which is valid when there is no phase matching (harmonic generation will be

treated in Chapter 4). It can readily be seen that for mode functions with spatial oscillations (like $\cos \underline{k} \cdot \underline{r}$) any product of three mode functions averages to zero. For this reason the quadratic nonlinearity can be neglected: this term is only significant when second harmonic generation is possible due to phase matching.

For simplicity we now suppose \underline{u} is plane polarised and the medium is isotropic, although an analogous effective Hamiltonian would occur in more general cases:

$$\hat{H} = \hbar\omega \hat{a}^\dagger \hat{a} + \frac{(\hbar\omega)^2}{16\epsilon_0} \int_V \chi^{(3)}(\underline{r}) [\hat{a} u(\underline{r}) - \hat{a}^\dagger u^*(\underline{r})]^4 d^3r$$

We can also simplify the normalisation equation by defining a refractive index of $n^2 = 1 + \chi^{(1)}$. We now make the rotating wave approximation, of only including terms of the form $(\hat{a}^\dagger \hat{a})$. Noting that the Hamiltonian is defined to be normal ordered, we obtain:

$$\hat{H} = \hbar\omega \hat{a}^\dagger \hat{a} + \hbar\chi'' \hat{a}^{\dagger 2} \hat{a}^2$$

Where the anharmonicity parameter is defined as follows:

$$\begin{aligned} \chi'' &\equiv \left[\frac{3\hbar\omega^2}{8\epsilon_0} \right] \int_V \chi^{(3)}(\underline{r}) |u(\underline{r})|^4 d^3r \\ &= \left[\frac{3\hbar\omega^2}{8\epsilon_0} \right] \chi^{(3)} I^4_x \left(\frac{V_0}{V_r^2} \right) \end{aligned}$$

and V_0 is the active volume in which $\chi^{(3)}$ is non-zero.

Here I^4 is a constant depending on the mode function. For a plane wave, we would have $I^4 = 1$. However, this is unrealistic: in general I^4 will depend closely on the resonator geometry. A somewhat more realistic case is obtained for a mode function of the form $\sin k_1 x \cdot \sin k_2 y \cdot \sin k_3 z$. In this case one has:

$$u(\underline{r}) = 2\sqrt{2} \sin K_1 x \cdot \sin K_2 y \cdot \sin K_3 z \cdot \sqrt{V_r}$$

$$I^u = \left(\frac{27}{8}\right)$$

Similarly, one can obtain different values for I^u depending on the spot size in a Gaussian beam with spherical mirrors. The above treatment is only valid for a high-Q cavity where the beam loss on traversal of the interferometer is small. We have also supposed that no self-focussing occurs: i.e. the relative anharmonicity must be small enough not to cause a large change in the refractive index, in order for the single mode theory to be applicable. In Marburger & Felber (1978) it is shown that there is a critical power for self-focussing, and these results are only valid for transmitted power densities much less than this critical limit. A point of interest in the above result, is the dependence on the system volume: clearly quantum effects (due to large χ'') will increase with a decreasing quantisation volume.

We point out here that the Hamiltonian we have derived is the anharmonic oscillator Hamiltonian in the rotating wave approximation. This can have broader applications than just to optical systems, and in fact the relationship of the anharmonic oscillator to optical bistability is not extensively discussed in the literature. The nonlinear polarisability model is used to discuss optical bistability by Marburger & Felber (1978) without mention of its relation to the anharmonic oscillator, although bistable behaviour in the classical anharmonic oscillator is well known.

Another application of the quantum anharmonic oscillator Hamiltonian is to the problem of molecular multiphoton ionisation. Here the Hamiltonian is used to simulate the vibrational level spacing in the infra-red spectrum of a small molecule. This problem is of interest in determining laser stimulated dissociation rates and is discussed by Bloembergen (1975), Narducci et al (1977), Steyn-Ross (1979). However, we shall be chiefly interested in the application to optical problems here.

(b) Nonlinear absorption

In the classical theory of nonlinear polarisability, both nonlinear dispersion and nonlinear absorption can arise: therefore one would expect that it should be possible to have a quantum theory of nonlinear absorption that corresponds to a multiphoton process. This can be achieved by following the treatment of McNeil & Walls (1974), Shen (1967) for the nonlinear absorption. The general quadratic Hamiltonian would be:

$$\hat{H}_A = \hat{a} \hat{\Gamma}_1^+ + \hat{a}^+ \hat{\Gamma}_1 + \hat{a}^2 \hat{\Gamma}_2^+ + \hat{a}^{+2} \hat{\Gamma}_2 + \hat{a}^+ \hat{a} \hat{\Gamma}_0$$

Here $\hat{\Gamma}_1$ gives a one photon absorption, $\hat{\Gamma}_2$ a two photon absorption, and $\hat{\Gamma}_0$ gives an absorption-emission which results in phase damping. By the use of the two-photon absorption term, it is possible to obtain a model for nonlinear absorption from a field inside a cavity (Chaturvedi, Drummond & Walls, 1977). Investigation of the nonlinear

absorber leads to a prediction of antibunching photon statistics for the radiation field in a single-mode interferometer, provided thermal and driving field fluctuations are small.

When the Fokker-Planck equation for the nonlinear absorber is obtained, there is a great similarity to the equations for a laser operating near threshold. For the laser above threshold, the one photon reservoir acts as an amplifier. This can be formally regarded as a negative temperature reservoir, and is developed more fully when the atoms are included in Chapter 5. In the meantime however, the analysis of the Fokker-Planck equation for the nonlinear absorber can be readily adapted to the problem of a laser with an injected external signal, in order to give a unified approach to both these problems. The main change necessary is that in the laser above threshold, a linear gain coefficient occurs instead of a linear loss coefficient. An increased fluctuation term also occurs due to optical pumping. However the nonlinearity is similar to that occurring in the case of a straightforward nonlinear absorber. Thus the overall Fokker-Planck equations have a very close similarity for both a nonlinear absorber and a laser above threshold. This can be justified by a detailed treatment of the laser including atomic operators (Louisell, 1973), as shown in Chapter 5.

(c) Hamiltonian and master equation

We now wish to study the behaviour of the system with both nonlinear dispersion and absorption as well as an external driving field. The total Hamiltonian is therefore as follows:

$$\hat{H} = \hat{H}_1 + \hat{H}_2 + \hat{H}_3 + \hat{H}_4 + \hat{H}_5$$

$$\hat{H}_1 = \hbar\omega_c \hat{a}^\dagger \hat{a}$$

$$\hat{H}_2 = \hbar\chi'' (\hat{a}^\dagger)^2 (\hat{a})^2$$

$$\hat{H}_3 = i\hbar [E(t) e^{-i\omega_d t} \hat{a}^\dagger - E^*(t) e^{i\omega_d t} \hat{a}]$$

$$\hat{H}_4 = \hat{a}^\dagger \hat{\Gamma}_1 + \hat{a} \hat{\Gamma}_1^\dagger$$

$$\hat{H}_5 = \hat{a}^\dagger \hat{a} \hat{\Gamma}_0 + \hat{a}^{\dagger 2} \hat{\Gamma}_2 + \hat{a}^2 \hat{\Gamma}_2^\dagger$$

Here ω_c is the fundamental cavity resonance, χ'' is the anharmonicity, $E(t)$ is the driving field amplitude and ω_d the driving frequency: while $\hat{\Gamma}_j$ are the reservoir operators. This Hamiltonian is exact within the single mode and rotating wave approximations. We expect the rotating wave approximation to be a good one provided the level shift caused by the anharmonicity is much less than ω_c ; i.e. provided $(\bar{n}\chi'' \ll \omega_c)$ where \bar{n} is the mean excitation. It should be noted also that χ'' can be negative in some situations which would lead to a non-positive definite Hamiltonian. However, this is not a fundamental problem, as it is due to neglecting higher order terms in the

polarisability. Provided ($\bar{n}|\chi''| \ll \omega_j$) the level spacing remains positive, and no instabilities will occur from this cause in the present treatment. In the following work we shall neglect the phase damping ($\hat{\Gamma}_0$) which is expected to be small in an optical medium. (The effects of this in molecular systems are discussed by Bloembergen 1975, Narducci et al 1977, Steyn-Ross 1979.)

In a reference system rotating at a frequency ω_j , the total master equation for the density matrix is, on utilising the techniques of Louisell (1973):

$$\begin{aligned} \dot{\rho} &= \sum_{j=1}^5 \hat{\mathcal{L}}_j[\hat{\rho}] \\ \hat{\mathcal{L}}_1[\hat{\rho}] &= -i(\omega_1 - \omega_j) [\hat{a} + \hat{a}^\dagger, \hat{\rho}] \\ \hat{\mathcal{L}}_2[\hat{\rho}] &= -i\chi'' [\hat{a}^{\dagger 2} \hat{a}^2, \hat{\rho}] \\ \hat{\mathcal{L}}_3[\hat{\rho}] &= [E(t) \hat{a}^\dagger - E^*(t) \hat{a}, \hat{\rho}] \\ \hat{\mathcal{L}}_4[\hat{\rho}] &= \kappa' \{ 2\hat{a} \hat{\rho} \hat{a}^\dagger - \hat{\rho} \hat{a}^\dagger \hat{a} - \hat{a}^\dagger \hat{a} \hat{\rho} + 2n^{\text{th}} [[\hat{a}, \hat{\rho}], \hat{a}^\dagger] \} \\ \hat{\mathcal{L}}_5[\hat{\rho}] &= \chi' \{ 2\hat{a}^2 \hat{\rho} \hat{a}^{\dagger 2} - \hat{\rho} \hat{a}^{\dagger 2} \hat{a}^2 - \hat{a}^{\dagger 2} \hat{a}^2 \hat{\rho} \} \end{aligned}$$

Here κ' is the energy relaxation rate (from the one photon loss term $\hat{\Gamma}_1$), and n^{th} is the thermal occupation number due to Gaussian fluctuations in the thermal reservoir $\hat{\Gamma}_1$. Similarly, χ' is the two photon relaxation rate due to the two photon loss term $\hat{\Gamma}_2$, which is assumed to be a zero temperature reservoir.

The above master equation is a general model for a single mode, driven boson system with both nonlinear dispersion and absorption. In the absence of phase damping,

the model has minimal quantum fluctuations, which is of theoretical interest as well as having possible practical applications. The model also includes Gaussian fluctuations of a thermal type, due to the term $\hat{\Gamma}_1$ that determines the thermal occupation number in equilibrium. As we shall later include thermal type noise of a general type, we define the c-number Γ_1 to be the coefficient of the thermal fluctuations:

$$\Gamma_1 = 2\kappa' n^h$$

(d) Fokker-Planck equation and stochastic equations

The Fokker-Planck equation corresponding to the master equation can now be obtained on using the standard methods of the Glauber P-representation (Glauber 1963b, Louisell 1973). However the resulting Fokker-Planck equation does not always have solutions except as generalised functions: that is, the diagonal P-representation does not always exist (Glauber 1969). For this reason, we prefer to use the nondiagonal "complex P-function" representation outlined in Chapter 2, as this always has solutions on an appropriate domain. The Fokker-Planck equation is as follows:

$$\begin{aligned} \partial_t P(\underline{\alpha}) = & \left\{ \partial_{\alpha} (\kappa \alpha + 2\chi \alpha^2 \alpha^{\dagger} - E(t)) - \chi \partial_{\alpha}^2 \alpha^2 \right. \\ & + \partial_{\alpha^{\dagger}} (\kappa^* \alpha^{\dagger} + 2\chi^* \alpha^{\dagger 2} \alpha - E^*(t)) - \chi^* \partial_{\alpha^{\dagger}}^2 \alpha^{\dagger 2} \\ & \left. + \Gamma_1 \partial_{\alpha} \partial_{\alpha^{\dagger}} \right\} P(\underline{\alpha}) \end{aligned}$$

Here $\underline{\alpha} = (\alpha, \alpha^\dagger)$ is the vector in C^2 giving the argument of the complex P-function $P(\underline{\alpha})$. We also have defined complex parameters $\kappa = \kappa' + i\kappa''$ giving the linear dispersion and absorption; and $\chi = \chi' + i\chi''$ giving the non-linear dispersion and absorption. A table of the Fokker-Planck equation parameters is summarised below:

κ'	Energy relaxation rate
$\kappa'' \equiv \omega_1 - \omega_2$	Detuning parameter
χ'	Nonlinear relaxation rate
χ''	Anharmonicity parameter
$E(t)$	Driving amplitude
$\Gamma_1 \equiv 2\kappa'\eta^2$	Coefficient of thermal fluctuations

We note here that all the parameters except Γ_1, χ' can have either sign: however we must have $\Gamma_1 \geq 0, \chi' \geq 0$. The coefficient of the thermal fluctuations is positive, as this always has a positive variance. Also, we must have $\chi' \geq 0$ to have overall stability. However the dispersive components can have either sign (if $\chi'' < 0$, then the Hamiltonian is non positive-definite; when higher order terms are included in the Hamiltonian, positivity is restored.)

In the case of a finite temperature (absorbing) reservoir, κ' is positive. Nevertheless the Fokker-Planck equation with $\kappa' < 0, \chi' > 0$ also corresponds to a physical situation. This is just the Fokker-Planck equation for a

laser in an external field, up to the lowest order non-linear terms significant in the threshold region (Louisell (1973), Haken (1970)). This will be discussed together with absorptive optical bistability in Chapter 5: for the mean time the case of $\kappa' < 0$ can be regarded as due to an amplifying (negative temperature) reservoir.

We now turn to the derivation of stochastic differential equations from the Fokker-Planck equation. When the normal (diagonal) P-function representation is used, with $\alpha^* = \alpha^\dagger$ it is readily shown that the presence of nonlinear terms means that the Fokker-Planck diffusion is nonpositive definite. This means that the usual Ito theorems for stochastic differential equations are not applicable (Arnold, 1975). However, as we show in Chapter 2, the Fokker-Planck equation in (α, α^\dagger) can be transformed to a four-dimensional equation with positive-definite diffusion.

The exact stochastic differential equations in the Ito calculus are obtained on transforming the Fokker-Planck equation into the Ito form:

$$\frac{d}{dt} \begin{bmatrix} \alpha \\ \alpha^\dagger \end{bmatrix} = \begin{bmatrix} E(t) - \kappa\alpha - 2\chi\alpha^2\alpha^\dagger \\ E^*(t) - \kappa^*\alpha^\dagger - 2\chi^*\alpha^\dagger\alpha \end{bmatrix} + \begin{bmatrix} -2\chi\alpha^2, \Gamma_1 \\ \Gamma_1, -2\chi^*\alpha^\dagger\alpha \end{bmatrix}^{1/2} \begin{bmatrix} \xi_1(t) \\ \xi_2(t) \end{bmatrix}$$

Here $\xi_1(t)$, $\xi_2(t)$ are delta correlated random Gaussian functions so that α, α^\dagger are complex conjugate in the mean. The above equations cannot be integrated analytically for arbitrary $E(t)$ due to the nonlinearities. However a computer simulation with a Gaussian random noise generator is a possible approach and this has been implemented for the case of fixed $E(t)$ by M. Steyn-Ross (1979). In the

present treatment, we will utilise these equations in the case of small fluctuations to obtain the deterministic state equations and the linearised response to fluctuations.

At this point, we turn to the time dependence of the driving field. In the simplest treatment, we may suppose the driving field is completely coherent:

$$E(t) = E_0$$

However any physical radiation source will have fluctuations associated with it. One model for the fluctuations is:

$$E(t) = E_0 + \delta E(t)$$

$$\langle \delta E^*(t) \delta E(t') \rangle = \int_{\xi} \delta(t-t')$$

This can be treated very simply within the framework of the above equations, by including this additional fluctuation term with the fluctuations already present, to give a total nondiagonal term of:

$$\Gamma = \Gamma_1 + \int_{\xi}$$

Thus the overall stochastic equation would be:

$$\frac{\partial}{\partial t} \begin{bmatrix} \alpha \\ \alpha^+ \end{bmatrix} = \begin{bmatrix} E_0 - \kappa \alpha - 2\chi \alpha^2 \alpha^+ \\ E_0^* - \kappa^* \alpha^+ - 2\chi^* \alpha \alpha^{+2} \end{bmatrix} + \begin{bmatrix} -2\chi \alpha^2, \Gamma \\ \Gamma, -2\chi^* \alpha^{+2} \end{bmatrix} \begin{bmatrix} \xi_1(t) \\ \xi_2(t) \end{bmatrix}^{1/2}$$

In a more complete treatment, a single mode laser has phase and amplitude fluctuations: in this case the driving field would be (Haken, 1970):

$$E(t) = [E_0 + E_1(t)] e^{i\phi(t)}$$

$$\langle E_1(t) E_1(t') \rangle = a(E_0) e^{i\phi} [-|t-t'| b(E_0)]$$

$$\langle \dot{\phi}(t) \dot{\phi}(t') \rangle = c(E_0) \delta(t-t')$$

This type of fluctuation in the input can also be treated within the framework of linearised theory, as shown by Chaturvedi, Drummond & Walls (1977). In a situation where this type of fluctuation is significant, it can be included by adding an extra stochastic term with the following properties: $\dot{\alpha}_\mu \rightarrow \dot{\alpha}_\mu + \Gamma'_\mu(t)$; $[\Gamma'_\mu = (\Gamma', \Gamma'^+)] -$

$$\langle \Gamma'(t') \Gamma'(t) \rangle = a(E_0) e^{i\phi} [-|t-t'| b(E_0)] - c(E_0) \alpha^2 \delta(t-t')$$

$$\langle \Gamma'^+(t') \Gamma'(t) \rangle = a(E_0) e^{i\phi} [-|t-t'| b(E_0)] + c(E_0) \alpha \alpha^\dagger \delta(t-t') \quad (\text{etc.})$$

In the remainder of section 3.1 we suppose that the input laser is sufficiently well stabilised for these phase and amplitude terms to be negligible.

(e) Stability properties of the deterministic solutions

Deterministic behaviour can be obtained in the limit of small Γ, χ , where the noise (random fluctuation) terms are negligible. In this limit, if we choose $\alpha^+ = \alpha^*$ initially this relation will be time invariant. Therefore the system can be described by a deterministic differential equation of the following form:

$$\frac{d}{dt} \begin{bmatrix} \alpha \\ \alpha^+ \end{bmatrix} = \begin{bmatrix} E(t) - \alpha f(\alpha \alpha^+) \\ E^*(t) - \alpha^+ f^*(\alpha \alpha^+) \end{bmatrix}$$

Here: $f(\alpha \alpha^+) = \kappa + 2\chi \alpha \alpha^+$; provided $\alpha^+ = \alpha^*$ initially, they remain complex conjugate, so that $\alpha \alpha^+ = |\alpha|^2$. If we define $\alpha \alpha^+ = n$ (the mean excitation or photon number), one readily obtains the equations for the steady-state:

$$\begin{aligned} |E|^2 &= n |f(n)|^2 \\ &= n [(\kappa' + 2\chi' n)^2 + (\kappa'' + 2\chi'' n)^2] \end{aligned}$$

However not all values of n that satisfy the state equation defined above give rise to stable behaviour. One must include the stability of the differential equation to small perturbations in order to determine the physically relevant steady-states. In fact the problem defined above for a function $f(n)$ has a general significance: differential equations of this type turn up in the steady-state stability problem for nonlinearities of a general type, as well as for the simple case of cubic polarisability.

It is therefore of most interest to determine the regions of stability of the differential equation relative to an arbitrary "state function" $f(n)$; where n is an arbitrary solution of the state equation. Since noncomplex conjugate fluctuations are possible in the stochastic equation, we include these in general by defining:

$$\begin{bmatrix} \alpha(t) \\ \alpha^+(t) \end{bmatrix} = \begin{bmatrix} \alpha_0 \\ \alpha_0^* \end{bmatrix} + \begin{bmatrix} \alpha_0(t) \\ \alpha_0^+(t) \end{bmatrix}$$

In this case the fluctuation term $\alpha_0(t)$ obeys the following linearised equation:

$$\frac{\partial}{\partial t} \begin{bmatrix} \alpha_0(t) \\ \alpha_0^+(t) \end{bmatrix} = -\underline{\underline{A}} \begin{bmatrix} \alpha_0(t) \\ \alpha_0^+(t) \end{bmatrix}$$

$$\underline{\underline{A}} = \begin{bmatrix} n \frac{\partial f}{\partial n} + f(n) & \alpha_0^2 \frac{\partial f}{\partial n} \\ \alpha_0^{*2} \frac{\partial f}{\partial n} & n \frac{\partial f^*}{\partial n} + f^*(n) \end{bmatrix} = \begin{bmatrix} a & b \\ b^* & a^* \end{bmatrix}$$

Using the Hurwitz criterion for stability, one finds that to obtain stable eigenvalues it is necessary to have:

$$\text{Tr}(\underline{\underline{A}}) = 2 \text{Re} \left[f(n) + n \frac{\partial f}{\partial n} \right] > 0$$

$$\text{Det}(\underline{\underline{A}}) = |f(n)|^2 + n \left[f^*(n) \frac{\partial f}{\partial n} + f(n) \frac{\partial f^*}{\partial n} \right] > 0$$

A change in the stability properties can only occur if either $\text{Tr}(\underline{\underline{A}})$ or $\text{det}(\underline{\underline{A}})$ changes sign. The points where $\text{det}(\underline{\underline{A}})$ vanishes are soft-mode instabilities (since one of the eigenvalues is zero): while if $\text{det}(\underline{\underline{A}})$ is nonvanishing but $\text{Tr}(\underline{\underline{A}})$ is zero, there is a hard-mode instability with the

onset of oscillations. In fact $\det(\underline{\underline{A}}) = 0$ is equivalent to finding a turning point in the state equation, because:

$$\frac{\partial |E|^2}{\partial n} = \det(\underline{\underline{A}})$$

Thus to determine stability, it is first necessary to find the turning points ($\det(\underline{\underline{A}}) = 0$) and the hard-mode instabilities ($\text{Tr}(\underline{\underline{A}}) = 0$). Any intermediate value of n has a fixed stability, which can be found by evaluating $\det(\underline{\underline{A}}), \text{Tr}(\underline{\underline{A}})$ at any point on the branch to give the overall stability of the branch.

In the present situation, of a cubic polarisability, one obtains:

$$\text{Tr}(\underline{\underline{A}}) = 2[\kappa' + 4x'n] \quad ; \quad \underline{\underline{A}} \equiv \begin{bmatrix} \kappa + 4x'n & 2x\alpha_0^2 \\ 2x^* \alpha_0^{*2} & \kappa^* + 4x^*n \end{bmatrix}$$

$$\det(\underline{\underline{A}}) = 12|x|^2 n^2 + 4n[x\kappa^* + x^*\kappa] + |\kappa|^2$$

First of all, it is necessary to have $x' > 0$ for overall stability. In addition to this, in the usual cases one has $\kappa' > 0$ (for a linear loss mechanism) so that $\text{Tr}(\underline{\underline{A}}) > 0$ always. However in some cases one can have linear amplification (as in the laser with an external field). As we shall see later the linear amplifier can have $\text{Tr}(\underline{\underline{A}}) < 0$ resulting in instability for low photon numbers.

Of greatest interest are the points that correspond to $\det(\underline{\underline{A}}) = 0$, which are the threshold points for dispersive optical bistability. Solving for n one obtains the following threshold values:

$$n^{\pm} = \frac{-2(\kappa' \chi' + \kappa'' \chi'') \pm \sqrt{\chi'^2 \kappa'^2 + \chi''^2 \kappa''^2 + 8\chi' \chi'' \kappa' \kappa'' - 3\kappa'^2 \chi''^2 - 3\kappa''^2 \chi'^2}}{6(\chi'^2 + \chi''^2)}$$

$$|E^{\pm}|^2 = n^{\pm} |f(n^{\pm})|^2$$

Clearly these coordinate points are the turning points of the state equations. Of interest in later work will be the value of the critical point parameters. These are the parameters that determine the existence of a bistable region. That is, for bistability it is necessary to have:

$$\chi'^2 \kappa'^2 + \chi''^2 \kappa''^2 + 8\chi' \chi'' \kappa' \kappa'' - 3\kappa'^2 \chi''^2 - 3\kappa''^2 \chi'^2 > 0$$

However in addition to this, as stated earlier one must have $\text{Tr}(A) > 0$ on both upper and lower branches to prevent hard-mode oscillations that would preclude bistability.

(f) One time correlations close to a stable branch

We now proceed to analyse the behaviour of the stochastic differential equations close to a stable branch. This is an asymptotic expansion valid for small fluctuations (in Appendix A this is treated formally as an expansion in σ , where σ^2 is the fluctuation variance).

In the case of a multiple valued state equation, the exact steady-state moments can only be obtained by solving the Fokker-Planck equation. However the asymptotic expansion is useful in giving behaviour close to a stable branch, that would be observed in a transient experiment. In addition, the asymptotic expansion can be obtained where potential equations are not satisfied.

We suppose that the deterministic solution is α_0 , and the fluctuating variable $\alpha(t)$ is given as before by:

$$\begin{bmatrix} \alpha(t) \\ \alpha^+(t) \end{bmatrix} = \begin{bmatrix} \alpha_0 \\ \alpha_0^* \end{bmatrix} + \begin{bmatrix} \alpha_{(1)}(t) \\ \alpha_{(1)}^+(t) \end{bmatrix}$$

Then to first order $\alpha_{(1)}(t)$ obeys the following equation:

$$\dot{\alpha}_{(1)}(t) = -\underline{\underline{A}} \alpha_{(1)}(t) + \underline{\underline{D}}^{1/2}[\alpha_0] \cdot \underline{\underline{f}}(t)$$

Here $\underline{\underline{A}}$ is the linearised drift and $\underline{\underline{D}}$ is the diffusion array evaluated at $\alpha = \alpha_0$: these have the general form:

$$\underline{\underline{A}} = \begin{bmatrix} a & , & b \\ b^* & , & a^* \end{bmatrix}$$

$$\underline{\underline{D}} = \begin{bmatrix} -d & , & \Gamma \\ \Gamma & , & -d^* \end{bmatrix}$$

The correlation matrix $\underline{\underline{C}}$ can be evaluated using the method of Chaturvedi et al (1977a):

$$\underline{\underline{C}} \equiv \begin{bmatrix} \langle \alpha_{(1)}^2 \rangle & , & \langle \alpha_{(1)} \alpha_{(1)}^+ \rangle \\ \langle \alpha_{(1)}^+ \alpha_{(1)} \rangle & , & \langle \alpha_{(1)}^{+2} \rangle \end{bmatrix}$$

$$\underline{\underline{C}} = \frac{\underline{\underline{D}} \cdot \det(\underline{\underline{A}}) + (\underline{\underline{A}} - \underline{\underline{I}} + \Gamma(\underline{\underline{A}})) \underline{\underline{D}} (\underline{\underline{A}} - \underline{\underline{I}} + \Gamma(\underline{\underline{A}}))^T}{2 \cdot \text{tr}(\underline{\underline{A}}) \cdot \det(\underline{\underline{A}})}$$

$$= \left[\frac{1}{4a'\Delta(o)} \right] \begin{bmatrix} -d(a^{*2} + |a|^2 - |b|^2) - d^*b^2 - 2a^*b\Gamma, & 2(\Gamma|a|^2 + \text{Re}(abd^*)) \\ 2(\Gamma|a|^2 + \text{Re}(abd^*)), & -d^*(a^2 + |a|^2 - |b|^2) - db^{*2} - 2ab^*\Gamma \end{bmatrix}$$

Where:

$$a' \equiv \text{Re}(a) \quad ; \quad \Delta(o) \equiv |a|^2 - |b|^2$$

The above expression is one of general applicability. It is valid for an arbitrary single mode bose operator in the linearised approximation, as any linearised single mode system will be characterised by these parameters a, b, d, Γ . In the situation of the present problem, we have:

$$a = \kappa + 4\chi n \quad ; \quad a' = \kappa' + 4\chi' n$$

$$b=d = 2\chi\alpha_0^2$$

Where $n = |\alpha_0|^2$ is the solution to the deterministic state equation. The expression for the correlation function can now be simplified to give:

$$\underline{\underline{C}} = \left[\frac{1}{2a'\Delta(o)} \right] \begin{bmatrix} -da^*[\Gamma + a'] & , & \Gamma|a|^2 + |d|^2a' \\ \Gamma|a|^2 + |d|^2a' & , & -d^*a[\Gamma + a'] \end{bmatrix}$$

This is then, the general expression for the first order term of the correlation function of the bose system. In operator terms, we would have:

$$\approx C \equiv \begin{bmatrix} \langle \hat{a}^2 \rangle - \langle \hat{a} \rangle^2, & \langle \hat{a}^+ \hat{a} \rangle - |\langle \hat{a} \rangle|^2 \\ \langle \hat{a}^+ \hat{a} \rangle - |\langle \hat{a} \rangle|^2, & \langle \hat{a}^{+2} \rangle - \langle \hat{a}^+ \rangle^2 \end{bmatrix}$$

The total intensity in the cavity (or total photon number) is; to first order in the asymptotic expansion*:

$$\begin{aligned} \bar{n} &= |\alpha_0|^2 + \langle \alpha_0 \alpha_0^+ \rangle \\ &= n + (\Gamma |a|^2 + |d|^2 q') / (2 a' \Delta(0)) \end{aligned}$$

Thus there is a coherent and an incoherent part to the total intensity. We first look at the linear cavity limit, where $\kappa \rightarrow 0$. In this limit the incoherent intensity is due to thermal fluctuations. Provided the driving field is coherent, we obtain:

$$\bar{n} = n + n^{th}$$

That is, the intensities of the coherent field and the thermal background are additive in a linear cavity; this is to be expected as they are uncorrelated.

In the nonlinear situation we obtain:

$$\bar{n} = n + n^{th} \left(\frac{|a|^2}{\Delta(0)} \right) + \left(\frac{|d|^2}{2 \Delta(0)} \right)$$

* We omit terms in \bar{n} due to second order corrections in $\langle \alpha \rangle$.

Thus this analysis would predict an increase in the background fluctuation due to the nonlinearity, with a maximum at $|a|^2 = |d|^2$. This maximum is the critical point divergence, which is the point where the linear analysis breaks down.

Finally, there is an additional term proportional to $|d|^2$. This gives the intensity of quantum fluctuations in the system, and is due to the nonlinearity in the polarisability.

The effect of both quantum fluctuations and thermal fluctuations is to increase the total photon number. However the next order correlation function that is measurable, (the second order correlation function) shows that these are physically different types of process. While thermal fluctuations always increase $g^2(0)$ above the input value of 1 for a coherent driving field, the quantum noise terms can decrease $g^2(0)$ to cause antibunching photon statistics. We show this by calculating the correlation function to first order in the asymptotic expansion:

$$\begin{aligned}
 g^2(0) &= 1 + 2(\langle \alpha_0 \alpha_0^\dagger \rangle + \text{Re}(\alpha_0^* \langle \alpha_0^2 \rangle / \alpha_0)) / n \\
 &= 1 + \left[\frac{\Gamma |a|^2 + |d|^2 a' - 2 \text{Re}(\chi a^* [\Gamma + a'] n)}{a' \Delta(0) n} \right]
 \end{aligned}$$

Here the coefficient of Γ is positive-definite, while the other terms involving quantum fluctuations can be negative. Of course, the total value of $g^2(0)$ must obey the fundamental restriction of : $g^2(0) \geq 1 - \frac{1}{n}$.

A table of the relevant parameters is summarised below, where $a = a' + ia''$

$$|d|^2 = 4(\chi'^2 + \chi''^2)n^2$$

$$a' = \kappa' + 4\chi'n$$

$$a'' = \kappa'' + 4\chi''n = (\omega_1 - \omega_2) + 4\chi''n$$

$$\Delta(0) = a'^2 + a''^2 - |d|^2$$

$$\Gamma = 2\kappa'n_h + \Gamma_2$$

(g) Time dependent correlations close to a stable branch

Just as the one-time correlations have been calculated using the linearised method, so can the spectrum be calculated. This is most simply obtained by Fourier transforming the differential equation to give (Appendix B):

$$\begin{aligned} \rho'(\omega_0 + \omega) &= n\delta(\omega) + \left(\frac{1}{\pi}\right) \text{Re} \left[\left(\frac{A}{\approx} + i\omega \right)^{-1} \frac{C}{\approx} \right]_{21} \\ &= n\delta(\omega) + \left(\frac{1}{2\pi a' \Delta(0)} \right) \text{Re} \left[\frac{|d|^2 a^* (\Gamma + a') + (i\omega + a) (\Gamma |a|^2 + |d|^2 |a'|)}{\Delta(i\omega)} \right] \end{aligned}$$

Where:

$$\Delta(z) = (z + a^*)(z + a) - |d|^2$$

This is the general expression for the linearised spectrum of a coherently driven single mode nonlinear boson system with a finite temperature thermal reservoir. The behaviour of the spectrum is governed by the roots of $\Delta(z)$ which are $-\lambda^\pm$, where:

$$\lambda^\pm = a' \pm \sqrt{|d|^2 - a''^2}$$

Here a', d, a'' are defined as in section 3.1 (f). In general the roots are complex, resulting in a double peaked spectrum with two quasi-Lorentzian lines. The lines coalesce to give a single peaked spectrum when the roots are real, which occurs for:

$$\eta^2(\chi'^2 - 3\chi''^2) - 2\kappa''\chi''\eta - \frac{1}{4}\kappa''^2 \geq 0$$

In addition to the Lorentzian lines, there is a delta function part of the spectrum, which corresponds to radiation transmitted at the input frequency.

In order to understand the effect of the nonlinearity on the spectrum, we first compare this result with the case of a linear interferometer. In this case we have $\chi = d = 0$ so the earlier formula simplifies to give:

$$S(\omega + \omega_i) = \eta \delta(\omega) + \left[\frac{1}{2\pi\kappa' \Delta(0)} \right] \text{Re} \left[\frac{(i\omega + \kappa) \Gamma |\kappa|^2}{\Delta(i\omega)} \right]$$

where:

$$\eta = |E|^2 / [\kappa'^2 + \kappa''^2]$$

$$\Delta(i\omega) = (i\omega + \kappa)(i\omega + \kappa^*)$$

In this case we see that the pole at $-i\omega = \kappa$ vanishes, leaving only a pole at $-i\omega = \kappa^*$. On taking the real part this has a Lorentzian peak at $\omega = \omega_1 - \omega_0$. Hence the final result is obtained (Louisell, 1973):

$$S(\omega) = \left[\frac{|E|^2 \delta(\omega - \omega_0)}{\kappa'^2 + \kappa''^2} \right] + \left(\frac{1}{2\pi} \right) \left[\frac{\Gamma}{\kappa'^2 + (\omega - \omega_1)^2} \right]$$

Thus the overall spectrum is nonsymmetric for $\omega_1 \neq \omega_0$. There is an "elastic" peak at the driving frequency ω_0 , and a Lorentzian peak at the interferometer tuning ω_1 , due to thermal fluctuations. If we compare this result with the nonlinear interferometer, it approaches the linear case at a low enough driving field.

However as $|E|$ is increased, the tuning point varies, as the cavity refractive index is power dependent, when χ'' is non zero. In addition, both symmetrically placed peaks can develop a finite peak height. The frequencies of the quasi Lorentzian peaks are at:

$$\omega = \omega_0 \pm \delta\omega$$

$$\delta\omega = \sqrt{\kappa''^2 + 8n\kappa''\chi'' + 4n^2(3\chi''^2 - \chi'^2)}$$

In the case of thermal fluctuations, the spectrum is nonsymmetric in general, with a peak in the fluctuation spectrum at the effective cavity tuning point. An additional part of the spectrum originates from the quantum fluctuations. This is not proportional to Γ , and is due entirely to the nonlinear polarisability. This spectrum is completely symmetric relative to ω_0 : so that the total

spectrum becomes symmetric in the limit $\Gamma \rightarrow 0$. For $\Gamma > 0$ there will be an additional thermal fluctuation spectrum which is nonsymmetric when the roots of $\Delta(z)$ are complex.

A similar behaviour is noted by Wodkiewicz (1978) in the case of detuned atomic fluorescence with a fluctuating driving field. In this case, there is a symmetric spectrum with a coherent input, that becomes nonsymmetric when fluctuations are included.

The next measurable time dependent correlation function is the second order correlation function:

$$g^2(\tau) = \frac{\langle \hat{a}^\dagger(0) \hat{a}^\dagger(\tau) \hat{a}(\tau) \hat{a}(0) \rangle}{\langle \hat{a}^\dagger(\tau) \hat{a}(\tau) \rangle \langle \hat{a}^\dagger(0) \hat{a}(0) \rangle}$$

$$= 1 + 2 \operatorname{Re} [\mathcal{G}_{21}(\tau) + \mathcal{G}_{11}(\tau) \left(\frac{\alpha_0^*}{\alpha_0} \right)] / n$$

Here \mathcal{G} is the time dependent correlation matrix for α . The Fourier transform is calculable using methods similar to those for the spectrum, with:

$$\tilde{\mathcal{G}}_{\mu\nu}(\omega) = \frac{1}{2\pi} \left[(\underline{A} + i\omega)^{-1} \mathcal{G}(0) + \mathcal{G}(0) (\underline{A}^\top - i\omega)^{-1} \right]_{\mu\nu}$$

We note that $\mathcal{G}(0)$ is symmetric, and the first part of the Fourier transform just gives the familiar spectral terms which are positive-definite. These are the terms (\mathcal{G}_{21}) which correspond to a classical process with thermal fluctuations, and would result in $\tilde{g}^2(\omega) > 0$ everywhere. However the other terms must be negative for some frequencies, to result in antibunching. It can be seen that $\tilde{g}^2(\omega)$ is more interesting from this point of view than $g^2(\tau)$, as any $g^2(\tau)$ for a classical process can have an anti-

correlation with $g^{(2)}(\tau) < 1$; $\tau \neq 0$. It would be sensible to attempt to generalise the idea of antibunching to antibunching at a frequency (ω): on the other hand it is meaningless to talk about antibunching at a time ($\tau \neq 0$), since any classical process could come under this definition, if it were oscillatory. The final result for the laboratory frame transform $\hat{g}^{(2)}(\omega)$ does not involve the rotating frame frequency ω_0 , and is symmetric under $\omega \rightarrow -\omega$:

$$\hat{g}_2(\omega) = \delta(\omega) + [\tilde{g}_{12}(\omega) + \tilde{g}_{21}(\omega) + \tilde{g}_{11}(\omega) \left(\frac{\alpha_0^*}{\alpha_0}\right) + \tilde{g}_{22}(\omega) \left(\frac{\alpha_0}{\alpha_0^*}\right)] / n$$

This can be calculated explicitly to give a result similar to the spectrum (to first order in the asymptotic expansion):

$$\hat{g}_2(\omega) = \delta(\omega) + \left[\frac{1}{2\pi a' \Delta(\omega)} \right] \text{Re} \left\{ \left[\frac{|d|^2 a^* (\Gamma + a') + (i\omega + a)(\Gamma |a|^2 + |d|^2 a')}{n \Delta(i\omega)} + (\omega \rightarrow -\omega) \right] - 2\chi \left[\frac{\Gamma |a|^2 + |d|^2 a' + (i\omega + a^*) a^* (\Gamma + a')}{\Delta(i\omega)} + (\omega \rightarrow -\omega) \right] \right\}$$

The first term in this result gives the part of $\hat{g}^{(2)}(\omega)$ from the spectrum: this is always positive, and therefore would result in $g^{(2)}(\omega) > 0$. In the case of a linear interferometer, only this term is present, so that

$g^{(2)}(0) \gg 1$. On the other hand for a linear interferometer it is possible to have $g^{(2)}(\tau) < 1$ for $\tau \neq 0$ - this is a classical anticorrelation property and should not be confused with antibunching.

The next term in the result has the possibility of either sign, as it is not positive-definite. This is the part of the correlation function that corresponds to quantum

fluctuations, and has a nonclassical behaviour. Thus we see that antibunching in frequency space can be inferred if $\tilde{g}^2(\omega) < 0$: this is the correct generalisation of antibunching at $\tau = 0$.

3.2 MOMENT CALCULATIONS WITH POTENTIAL SOLUTIONS

(a) Existence of potential solutions

In previous sections, the Fokker-Planck equation for a single mode nonlinear system was obtained in the complex P-representation, and quantum corrections were obtained to first order in the fluctuation variance. It is also of some interest to carry out the calculation of moments in the steady-state, in regions where the linearisation technique is not applicable. This is especially valuable when there are large departures from coherent photon statistics, as in the nonlinear absorber or in a bistable system.

The calculations can be carried out by means of an exact solution of the Fokker-Planck equation, known as a potential solution, which exists whenever the following "potential equations" are satisfied (Haken, 1975):

$$\partial_{\mu} v_{\nu} = \partial_{\nu} v_{\mu}$$

Where:

$$v_{\rho}(\underline{x}) \equiv +[D_{\rho\nu}(\underline{x})]^{-1} [2A_{\nu}(\underline{x}) + \partial_{\sigma} D_{\sigma\nu}(\underline{x})]$$

$$\partial_t P(\underline{x}) = [\partial_{\mu} A_{\mu}(\underline{x}) + \frac{1}{2} \partial_{\mu} \partial_{\nu} D_{\mu\nu}(\underline{x})] P(\underline{x})$$

On applying these to the previously obtained Fokker-Planck equation, one obtains straightforward results in the limits of $\Gamma \gg |\chi n|$ or $\Gamma \ll |\chi n|$. These are the "thermal" or "quantum" noise limits respectively. In the "thermal" limit, the Fokker-Planck diffusion is due to thermal type fluctuations in the driving-field or reservoirs. In the "quantum" limit, the fluctuations are quantal in nature, and originate from the commutation properties of boson algebra.

Thus the "thermal" Fokker-Planck equation is similar in many respects to the classical equations of Brownian motion described by a Langevin equation. On the other hand, the "quantum" Fokker-Planck equation has no direct classical counterpart.

We therefore treat these different limiting situations on an individual basis, and find very different behaviour both in the relevant integration manifolds, and in the photon statistics.

(b) The "thermal" limit: Landau-Ginzberg potential

We first deal with the thermal limit where we approximate the diffusion array by:

$$\tilde{D} = \begin{bmatrix} 0 & , & \Gamma \\ \Gamma & , & 0 \end{bmatrix}$$

In this case, we have:

$$\tilde{A} = \begin{bmatrix} \kappa\alpha + 2\chi\alpha^2\alpha^* - E_0 \\ \kappa^*\alpha^* + 2\chi^*\alpha\alpha^{*2} - E_0^* \end{bmatrix}$$

so that the potential equations reduce to:

$$\frac{\partial}{\partial\alpha} [\kappa\alpha + 2\chi\alpha^2\alpha^*] = \frac{\partial}{\partial\alpha^*} [\kappa^*\alpha^* + 2\chi^*\alpha\alpha^{*2}]$$

It is easily seen that a solution is only possible when $\kappa = \kappa^*$, $\chi = \chi^*$; that is for purely absorptive nonlinearity and an input field tuned to the interferometer frequency.

In this case, the solution to the Fokker-Planck equation is:

$$\begin{aligned} P(\underline{\alpha}) &= \exp\left[-\int^{\underline{\alpha}} v_M(\underline{\alpha}') \cdot d\underline{\alpha}'\right] \\ &= \exp\left[\frac{2}{\Gamma} \left(E_0 \cdot \alpha^* + E_0^* \cdot \alpha - \kappa\alpha\alpha^* - \chi(\alpha\alpha^*)^2 \right)\right] \end{aligned}$$

We note that for $E_0 = 0$, this just gives the well known Landau-Ginzberg form of the laser distribution function: that is, the theory reduces to single mode laser theory with $\kappa < 0$ above threshold and $\kappa > 0$ below threshold. In the case of a finite E_0 , the potential is again well known as the potential for a single mode laser with a coherent, tuned

driving field (Haken (1977); Chow, Scully & van Stryland (1975)). It is interesting that the potential of the laser below threshold is the same as that of a two photon absorber with thermal fluctuations; this demonstrates that the cause of laser saturation is similar to two photon absorption.

The potential has the property that it is bounded and integrable on the domain of $\alpha^{\dagger} = \alpha^*$, $\alpha \in \mathbb{C}$. For this reason the Glauber-Sudarshan P-representation is well defined, and the moments can be obtained on integration in the usual way:

$$P(r, \theta) = \exp \left[\frac{2}{\Gamma} (2E_0 \sqrt{R} \cos \theta - \kappa R - \chi R^2) \right]$$

$$\alpha = \sqrt{R} e^{i\theta}$$

Here we suppose the input phase is defined so E_0 is real, and on integration over θ the n'th moment is:

$$I_n = \pi \int_0^{\infty} \left[R^n \exp\left(\frac{-2}{\Gamma}(\kappa R + \chi R^2)\right) \sum_m \left(\frac{4E_0^2 R}{\Gamma^2}\right)^m \frac{1}{(m!)^2} \right] dR$$

The integration over R can be made numerically, or expressed as a parabolic cylinder function (Gradshteyn & Ryzhik, 1965):

$$I_n = \pi \sum_{m=0}^{\infty} (n+m)! \left[\frac{2E_0}{\Gamma} \right]^m \frac{1}{(m!)^2} \left(\frac{4\chi}{\Gamma} \right)^{\frac{-m}{2}} \exp\left[\frac{\kappa^2}{4\Gamma\chi} \right] D_{-m} \left(\frac{\kappa}{\sqrt{\Gamma\chi}} \right)$$

Here $\nu = (n+m+1)$ and D_{-y} is a parabolic cylinder function. This expression reduces to the well known result for the laser in the case of $E_0 = 0$, while giving a series expansion for the corrections due to the external field in the case $E_0 > 0$. In general the moments have increased coherence for $E_0 > 0$ relative to the results for $E_0 = 0$; i.e. the fluctuations are reduced. The expressions for the mean photon number and $g^2(0)$ are as follows:

$$\bar{n} = I_1 / I_0$$

$$g^2(0) = (I_2 I_0) / (I_1)^2$$

These expressions only hold for purely absorptive κ, χ and it is readily seen that there can be no bistability under these circumstances. From earlier work we know that there is no turning point in the state equations for real κ, χ unless $\kappa < 0$. However in this case (the laser above threshold) the lower branch of the state equation is unstable.

In terms of the potential, it is readily seen that the potential function (in terms of phase and amplitude) is of form:

$$V(R, \theta) \propto V(R) - \sqrt{R'} \cdot \cos \theta \quad (E_0 > 0)$$

Thus the global attractor is at $\theta = 0$, as this gives a minimum with respect to θ . There is no local minimum at $\theta = \pi$, which is unstable under phase drift. On investigating the behaviour under variations in R , it can be verified that only one stable positive minimum exists.

In summary there is no bistability for the laser with an injected resonant signal (in this model).

(c) The "quantum" limit: use of a complex manifold

In order to handle problems like dispersive bistability or photon antibunching in a nonlinear absorber, it is necessary to turn to the limit of $\Gamma \rightarrow 0$ to obtain potential solutions. This is physically reasonable as a limit, since there is no incoherent optical pumping (as in the laser) to give a large degree of thermal fluctuations. In these situations, Γ can be expected to be small provided $\kappa T \ll \hbar \omega_0$, and the input driving field is well stabilised.

In the limit of $\Gamma \rightarrow 0$, the diffusion array is:

$$\underline{D} \approx \begin{bmatrix} -2\chi\alpha^2 & , & 0 \\ 0 & , & -2\chi^*\alpha^{+2} \end{bmatrix}$$

$$\underline{A} \approx \begin{bmatrix} \kappa\alpha + 2\chi\alpha^2\alpha^+ - E_0 \\ \kappa^*\alpha^+ + 2\chi^*\alpha\alpha^{+2} - E_0^* \end{bmatrix}$$

The calculation of \underline{V} is straightforward:

$$v_1 = \left(\frac{-1}{\chi}\right) \left(\frac{\bar{K}}{\alpha} + 2\chi\alpha^+ - E_0/\alpha^2\right)$$

$$v_2 = \left(\frac{-1}{\chi^*}\right) \left(\frac{\bar{K}^*}{\alpha^+} + 2\chi^*\alpha - E_0^*/\alpha^{+2}\right)$$

$$\frac{\partial v_1}{\partial \alpha^+} = \frac{\partial v_2}{\partial \alpha} = -2$$

where we have defined $\bar{\kappa} = \kappa - 2\chi$. The calculation of $\bar{\kappa}^*$ is similar, and the equality of crossderivations is then obtained directly.

The next step is to integrate the generalised "force" \tilde{v}_1 to obtain the potential function; once again from Appendix A we obtain:

$$\begin{aligned} P(\underline{\alpha}) &= \exp\left[-\int^{\underline{\alpha}} v_p(\underline{\alpha}') d\alpha'\right] \\ &= \exp\left[\int^{\underline{\alpha}} \frac{1}{\chi}\left(\frac{\bar{\kappa}}{\alpha} + 2\chi\alpha^+ - E_0/\alpha^2\right) d\alpha \right. \\ &\quad \left. + \frac{1}{\chi^*}\left(\frac{\kappa^*}{\alpha^+} + 2\chi^*\alpha - E_0^*/\alpha^{+2}\right) d\alpha^+\right] \\ &= \exp\left[\left(\frac{\bar{\kappa}}{\chi}\right)\ln\alpha + \left(\frac{\bar{\kappa}}{\chi}\right)^*\ln\alpha^+ + \left(\frac{E_0}{\chi\alpha}\right) + \left(\frac{E_0^*}{\chi^*\alpha^+}\right) + 2\alpha\alpha^+\right] \end{aligned}$$

Now this expression is the potential solution for the steady-state distribution function. We simplify this by defining the driving phase so that (E_0/χ) is real. This can always be obtained by redefining the relative phase of α, α^+ , and does not alter the final results. Hence the following expression is obtained:

$$P(\underline{\alpha}) = \alpha^{(\mu-2)} \alpha^{+(\nu-2)} \exp\left[\left(\frac{E_0}{\chi}\right)\left(\frac{1}{\alpha} + \frac{1}{\alpha^+}\right) + 2\alpha\alpha^+\right]$$

Where:

$$\begin{aligned} \mu &\equiv \left[\frac{\kappa}{\chi}\right] \\ \nu &\equiv \left[\frac{\kappa}{\chi}\right]^* \end{aligned}$$

It can be seen immediately that the usual integration domain of the complex plane with $\alpha^+ = \alpha^*$ is not possible: the potential diverges for $|\alpha|^2 \rightarrow \infty$. Instead it is

necessary to choose alternative domains so the distribution function vanishes correctly at the boundary. This means choosing new paths of integration for α, α^+ that are to be line integrals on the individual (α, α^+) complex planes. In other words, the new domain will be a complex manifold embedded in the space C^2 . Firstly a variable change is made to $\beta \equiv 1/\alpha$, $\beta^+ \equiv 1/\alpha^+$. The normalisation integral is then obtained (where \mathcal{C} is the integration path):

$$\begin{aligned} I(\mu, \nu) &= \iint_{\mathcal{C}} \beta^{-\mu} \beta^{+\nu} \exp\left[\frac{E_0}{x}(\beta + \beta^+) + \frac{2}{\beta\beta^+}\right] d\beta d\beta^+ \\ &= \iint_{\mathcal{C}} \sum_{n=0}^{\infty} \left[\frac{2^n}{n!}\right] \beta^{-\mu-n} \beta^{+\nu+n} \exp\left[\frac{E_0}{x}(\beta + \beta^+)\right] d\beta d\beta^+ \end{aligned}$$

The integrand is now in a recognisable form as corresponding to a sum of gamma function integrals. It is therefore appropriate to define each path of integration to be a Hankel path of integration, from $(-\infty)$ on the real axis around the origin in an anticlockwise direction and back to $(-\infty)$. With this definition of the integration domain, the following gamma function identity holds (Abramowitz & Stegun 1964):

$$\frac{1}{\Gamma(\mu+n)} = \left[\frac{e^{1-\mu-n}}{2\pi i}\right] \int_{\mathcal{C}} \alpha^{-\mu-n} \exp(c\alpha) \cdot d\alpha \quad [c > 0]$$

Hence, applying this result to both β and β^+ integrations, one obtains:

$$I(\mu, \nu) = -4\pi^2 \sum_{n=0}^{\infty} \left[\frac{2^n \left[\frac{E_0}{x}\right]^{\mu+\nu+2(n-1)}}{n! \Gamma(\mu+n) \Gamma(\nu+n)} \right] \quad \left[\frac{E_0}{x} > 0\right]$$

The series is a transcendental function which can be written in terms of the generalised Gauss hypergeometric series. That is, there is a hypergeometric series called ${}_0F_2$ which is defined as follows (Gradshteyn & Ryzhik, 1965):

$${}_0F_2(\mu, \nu, z) = \sum_{n=0}^{\infty} \frac{z^n}{(\mu)_n (\nu)_n n!}$$

Where:

$$(\mu)_n \equiv \mu(\mu+1) \dots (\mu+n-1) = \frac{\Gamma(\mu+n)}{\Gamma(\mu)}$$

From now on for simplicity we will write just $F(\mu, \nu, z)$ instead of ${}_0F_2$. Now the normalisation integral can therefore be rewritten in the following form:

$$I(\mu, \nu) = \left[\frac{-4\pi^2 (E_0/\chi)^{\mu+\nu-2}}{\Gamma(\mu) \Gamma(\nu)} \right] F(\mu, \nu, z)$$

Where:

$$z \equiv 2|E_0/\chi|^2$$

The moments of the distribution function divided by the normalisation factor give all the observable one time correlation functions. Luckily the moments have exactly the same functional form as the normalisation factor (with the replacement of (μ, ν) by $(\mu+i, \nu+i)$) so that no new integrals need to be calculated. The i 'th order correlation function is therefore:

$$f^{(i)} \equiv \langle (\hat{a}^\dagger)^i (\hat{a})^i \rangle_\rho$$

$$g^{(i)} = \left[\frac{|E_0|^2 \Gamma(\mu) \Gamma(\nu) F(i+\mu, i+\nu, z)}{\Gamma(\mu+i) \Gamma(\nu+i) F(\mu, \nu, z)} \right]$$

This is the general expression for the i 'th order correlation function of a nonlinear single mode boson system with a coherent driving field and zero temperature heat baths.

Of particular interest are the average intensity (or photon number) and the correlation function $g^2(0)$ (which gives the relative degree of photon bunching or antibunching):

$$\bar{n} = \left[\frac{|E_0|^2 F(1+\mu, 1+\nu, z)}{\mu \nu F(\mu, \nu, z)} \right]$$

$$g^2(0) = \left[\frac{\mu \nu F(\mu, \nu, z) F(\mu+2, \nu+2, z)}{(\mu+1)(\nu+1) [F(\mu+1, \nu+1, z)]^2} \right]$$

These can be obtained either directly from tables of the relevant hypergeometric series, or else by numerical summation of the series which is reasonably efficient (Appendix C). Specific graphs of these functions are given in sections 3.2 - 3.5, where the individual physical situations in absorptive and dispersive cases are discussed.

(d) Discussion of theoretical results

In the previous sections, results were obtained for a theory of the single mode boson system with an externally coherent driving field, and both nonlinear dispersion and absorption. In the case of relatively small fluctuations, results can be obtained using an asymptotic expansion in the fluctuation variance.

For a "thermal" system, with dominant thermal fluctuations, the results are very similar to a classical oscillator with thermal fluctuations, a nonlinear damping, and an anharmonic Hamiltonian. In the general case of finite dispersive terms, the spectrum is asymmetric with a coherent peak at the driving frequency and an incoherent intensity maximum at the effective cavity tuning. The distribution function can be obtained exactly only with zero dispersion (that is, gain or absorption only), in which case it has the Landau-Ginzberg type of dependence, with α as the order parameter.

For a "quantum" system, with dominant quantum fluctuations, the spectrum is completely symmetric relative to the driving frequency: asymmetric spectra can only come from external fluctuations. This type of result, with a symmetric spectrum from quantum fluctuations and an asymmetric spectrum from external fluctuations is also obtained in the case of atomic resonance fluorescence with a detuned driving field (Wodkiewicz 1978, Hassan 1977), thus showing a similarity between these two types of driven quantum systems.

In the case of the driven nonlinear cavity the distribution function can be obtained exactly in the limit of zero thermal noise; but it has a completely different character to the Landau-Ginzberg type result obtained with thermal fluctuations.

In fact the distribution cannot be defined on the same integration domain as the laser distribution, as it would not be normalised. Instead the distribution is defined on an integration domain with $\alpha^\dagger \neq \alpha^*$. As mentioned in Chapter 2, this corresponds to a density matrix with a nondiagonal representation in terms of coherent states.

This shows the utility of the complex P-representation, which can be adapted to provide exact solutions to Fokker-Planck equations that include dispersive bistability and antibunching. No exact distributions for this type of situation were found previously using the Glauber-Sudarshan P-representation.

We now proceed to discuss the results relative to specific physical situations. It is worthwhile to group the results according to the underlying physics involved, so the following cases will be treated individually:

Section 3.3 - The laser with injected signal - $\chi''=0$, $\kappa' < 0$

Section 3.4 - The nonlinear absorber - $\chi''=0$, $\kappa' > 0$

Section 3.5 - Dispersive optical bistability - $\chi' = 0$, $\kappa' > 0$

3.3 THE LASER WITH INJECTED SIGNAL

(a) Introduction: The laser

The single-mode laser is a physical problem that has been studied by many researchers both in theory and in experiments. Good summaries of the theoretical treatments are given in Haken (1970), Louisell (1973). In the notation of this chapter, a laser above threshold has $E \neq 0$, $\kappa'' = \chi'' = 0$, $\kappa' < 0$ and $\chi' > 0$. With this notation, the Fokker-Planck equation is then similar to the well known rotating wave van der Pol oscillator model of a laser: with the addition of quantum noise terms proportional to $\chi \alpha^2$. Exactly the same quantum noise terms are found in a thorough treatment of the laser to lowest order in α^2 (Louisell 1973). However in the laser these terms are normally much less than the "thermal" type terms proportional to Γ ; which are enhanced by the optical pumping of the lasing atoms.

The laser with an injected external signal corresponds to the same situation, but with $E \neq 0$. This is treated by Chow, Scully, van Stryland (1975) and Haken (1977). This situation is of interest because with an injected signal it is possible to entrain the laser oscillations to the same frequency and phase as the input field. As the problem has been treated previously, we shall give a brief description here. One point of interest in the present treatment is that it is possible to use the stochastic equations to describe frequency entrainment when the cavity frequency is

different from the input frequency. This is not possible with the distributions of Chow et al (1975), Haken (1977): these are restricted to the frequency matched case, as shown in section 3.2.

We note that, while in previous sections a potential was derived holding in the limit $\Gamma \rightarrow 0$, this is not applicable in the laser case. In fact the laser always has a finite "thermal" type of background fluctuation due to the pumping mechanism. Thus the presence of this type of fluctuation prevents a potential solution from existing except in the case of zero detuning. We shall see later that this is related to the presence of a hard-mode instability that always exists in the laser case for a finite detuning of the input field. In the vicinity of the hard mode, it is therefore necessary to directly integrate the nonlinear equations of motion by numerical means, as neither linearised perturbation theory nor potential solutions can be utilised.

However other techniques of analysis of limit cycle stability exist, that have been utilised in the study of the van der Pol equations. Deterministic techniques of solution are summarised in Minorsky (1962), Stoker (1950). Methods based on cyclic averaging of stochastic terms are treated in Kolomietz (1972): however this subject has not been treated in detail for the injected signal case.

The methods used in the van der Pol equation were utilised by Tang and Statz (1967) in the earliest theoretical treatment of phase-locking: these authors obtain expressions for the small detuning limit similar to

those in the next section. Phase-locking was first observed by Stover & Steier (1966). However the different types of transition at medium and large detuning do not seem to have been observed in laser systems yet.

We now summarise the relevant formulae from section 3.1 for the case of an absorptive nonlinearity ($\chi''=0$): the same formulae also apply to 3.3 apart from the different sign of κ' :

State equation and turning points:

$$|E|^2 = n[\kappa''^2 + (2\chi n + \kappa')^2]$$

$$n^{\pm} = [-2\kappa' \pm \sqrt{\kappa'^2 - 3\kappa''^2}]/(6\chi)$$

Mean correlation and photon number:

$$\bar{n} = n + \frac{\Gamma'}{2} \left[\frac{\kappa''^2 + (\kappa' + 4\chi n)^2}{(\kappa' + 4\chi n)\Delta(0)} \right] + \left[\frac{2\chi^2 n^2}{\Delta(0)} \right]$$

$$g^2(0) = 1 + 2 \left[\left(\frac{\bar{n}}{n} - 1 \right) - \frac{\chi(\Gamma' + \kappa' + 4\chi n)}{\Delta(0)} \right]$$

$$\Delta(0) = \kappa''^2 + \kappa'^2 + 8\kappa'\chi'n + 12\chi'^2 n^2$$

Spectrum: peaks at frequencies:

$$\omega = \omega_0 \pm \sqrt{(\omega_1 - \omega_0)^2 - 4\chi^2 n^2}$$

$$(|\omega_1 - \omega_0| > 2\chi n)$$

We now discuss these formulae for the laser case.

(b) State equation and turning points

In this case, of an externally driven laser, the stability properties will depend on the detuning relative to the laser linewidth parameter (κ'). We therefore treat different ranges of the detuning parameter (κ'') individually. In the classification of different regions of limit cycle stability, we follow the work of Stoker (1950) on the van der Pol equation.

(i) Zero detuning ($\kappa'' = 0$)

This is the situation treated by Chow et al (1975), where potential solutions exist for the full Fokker-Planck equation. The state equation is:

$$|E|^2 = n(\kappa' + 2\gamma n)^2$$

This is illustrated in fig (3.3.1) where it can be seen that the upper turning point is at $E = 0$, $2\gamma n = -\kappa'$; this is the laser operating point. The lower branch has $\text{Tr}(\underline{A}) > 0$, and is always unstable. In other words, no bistability occurs in this case due to the amplifying nature of the medium: this is a completely different situation to that occurring in optical bistability (Chapter 5).

However it is possible to have a discontinuous transition in an order parameter, even though there is no bistability. This would be achieved by letting the external field reduce to zero and change in sign ($E \rightarrow 0 \rightarrow -|E|$). In this case the internal field amplitude would have a discontinuous transition in the deterministic limit.

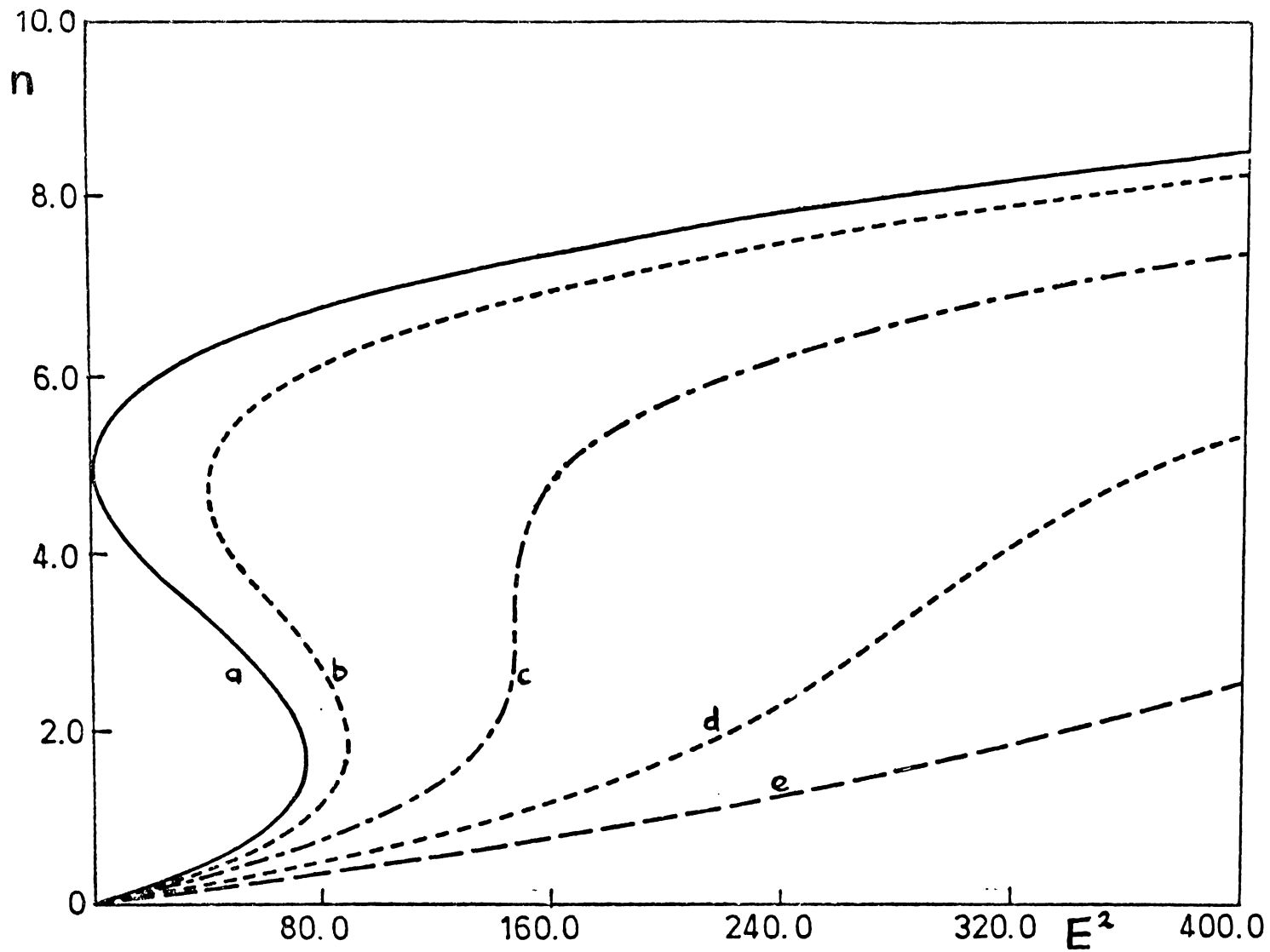


Fig (3.3.1) Laser with an injected signal; state equation of number vs input power ($K' = -10, \chi = 1$):

- | | | |
|-------------------------|-------------------------|-------------------------|
| (a) $K'' = 0$ | (b) $K'' = 5/\sqrt{3}$ | (c) $K'' = 10/\sqrt{3}$ |
| (d) $K'' = 15/\sqrt{3}$ | (e) $K'' = 20/\sqrt{3}$ | |

(ii) Small detuning ($0 < \kappa'' \leq \kappa'/2$)

The graph of the state equation is shown in fig. (3.3.1) relative to the previous situation. Clearly a turning point occurs at $|E^+| > 0$. However the lower branch is unstable with $\text{Tr}(A) > 0$. The physical meaning of this is that with a small driving field, the laser oscillates close to its natural frequency: this appears as a hard-mode relative to the injected signal frame of reference. Entrainment (synchronisation) of the laser occurs at a threshold of (n^+, E^+) where:

$$n^+ \equiv [2|\kappa'| + \sqrt{\kappa'^2 - 3\kappa''^2}] / (6\chi)$$

$$|E^+|^2 = n^+ [\kappa''^2 + (2\chi n^+ + \kappa')^2] \simeq \kappa''^2 n^+$$

Thus the input power for entrainment increases as the square of the detuning in the limit of $|\kappa''| \ll |\kappa'|$.

Above the transition, the state equation correctly predicts the stable points. However below the entrainment threshold, the solution is a stable limit cycle. In this case, the equation of motion can be solved numerically (fig 3.3.2, 3.3.3), showing an increasingly nonlinear behaviour close to the entrainment point, with a longer period. In fig 3.3.4 we investigate the frequency of the cycles as a function of the injected signal. This shows that while the amplitude has a discontinuous (first-order type) transition, the frequency has a continuous (second-order type) transition as a function of the injected coherent signal power.

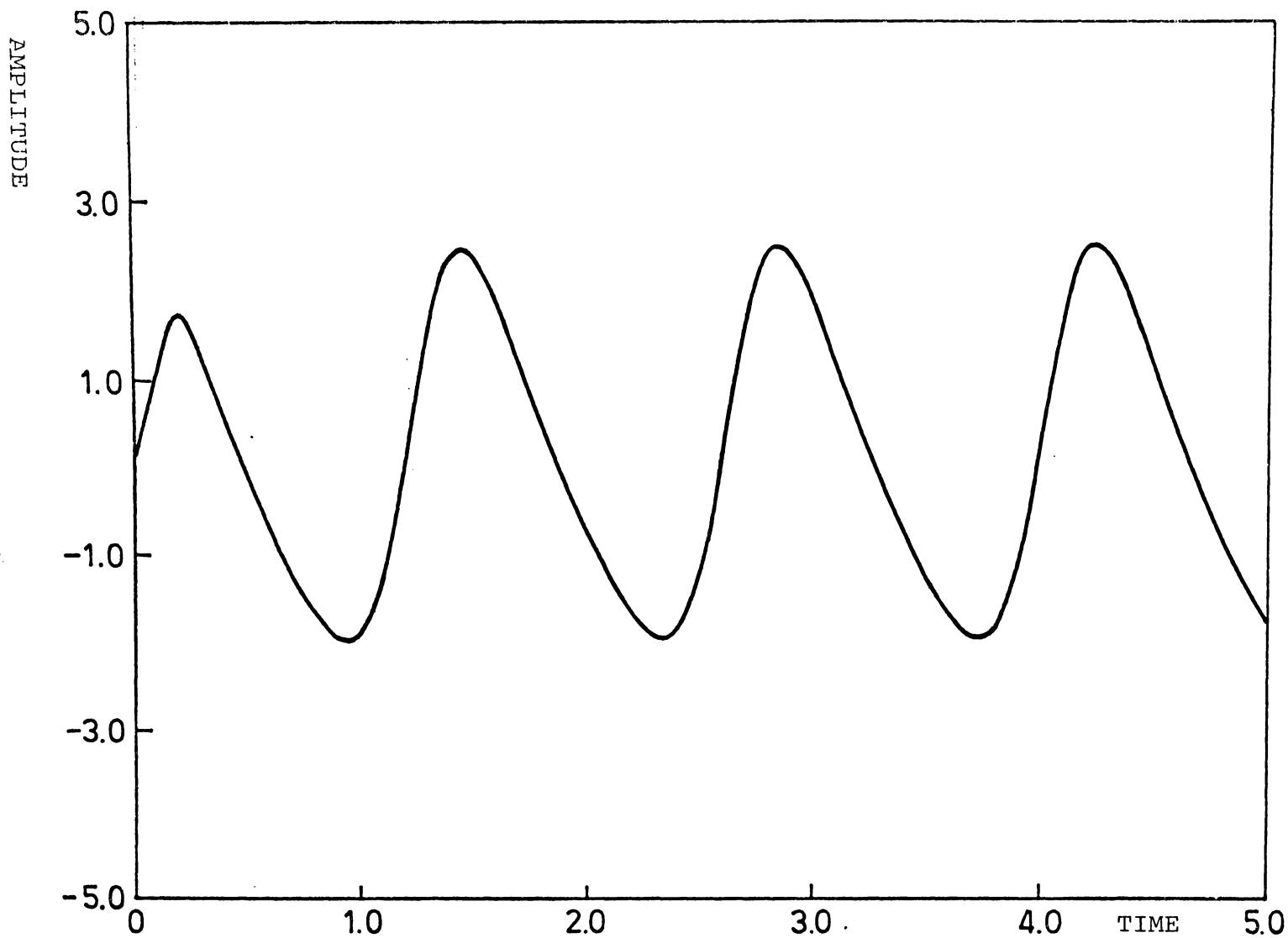


Fig (3.3.2) Laser with an injected signal; limit cycles of amplitude vs time for a low level input ($K = -10 + i5$, $\chi = 1$, $E = 5$).

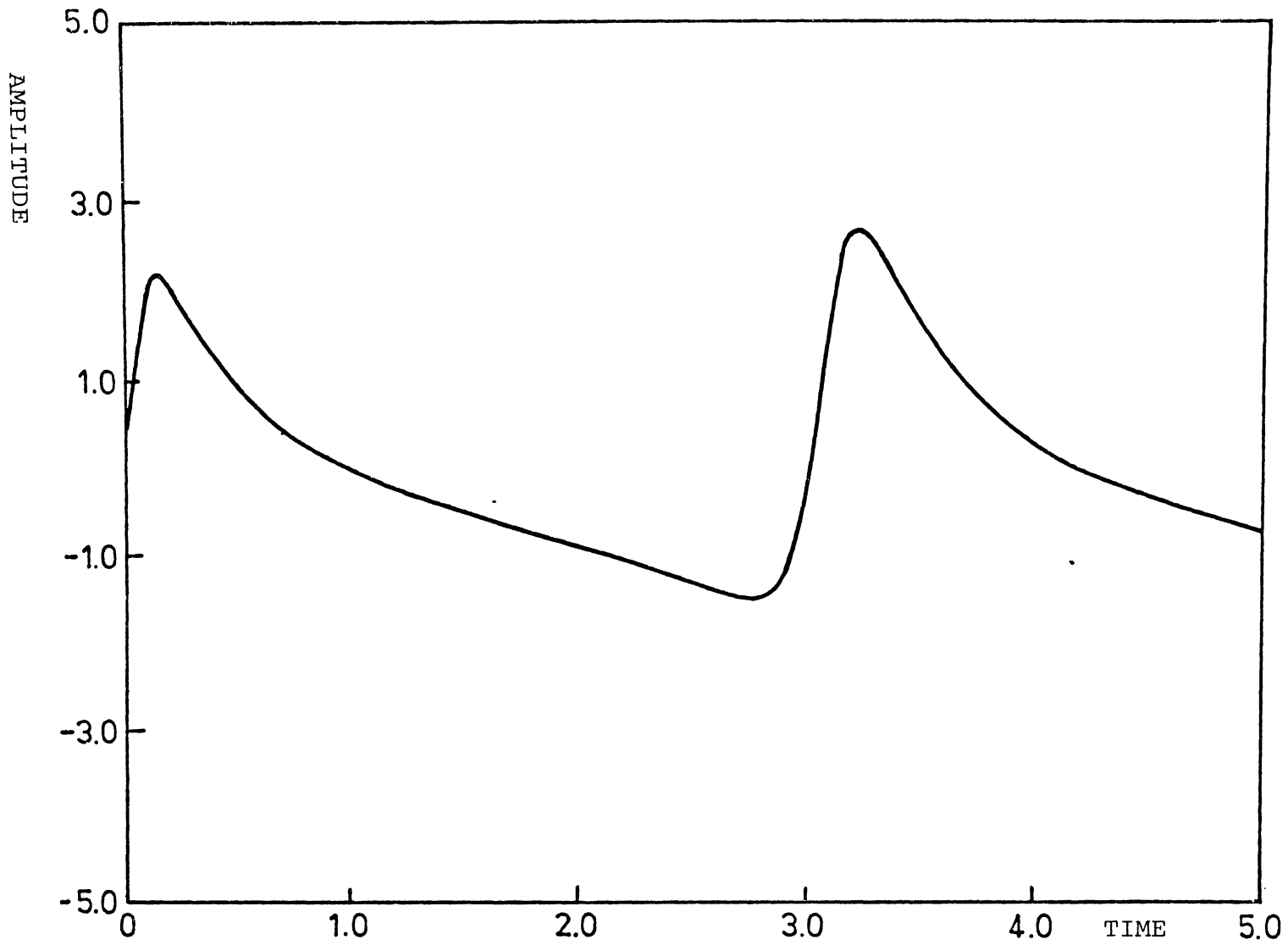


Fig (3.3.3) Laser with an injected signal; limit cycles of amplitude vs time close to threshold ($\kappa = -10 + i5$, $\chi = 1.0$, $E = 10.0$).

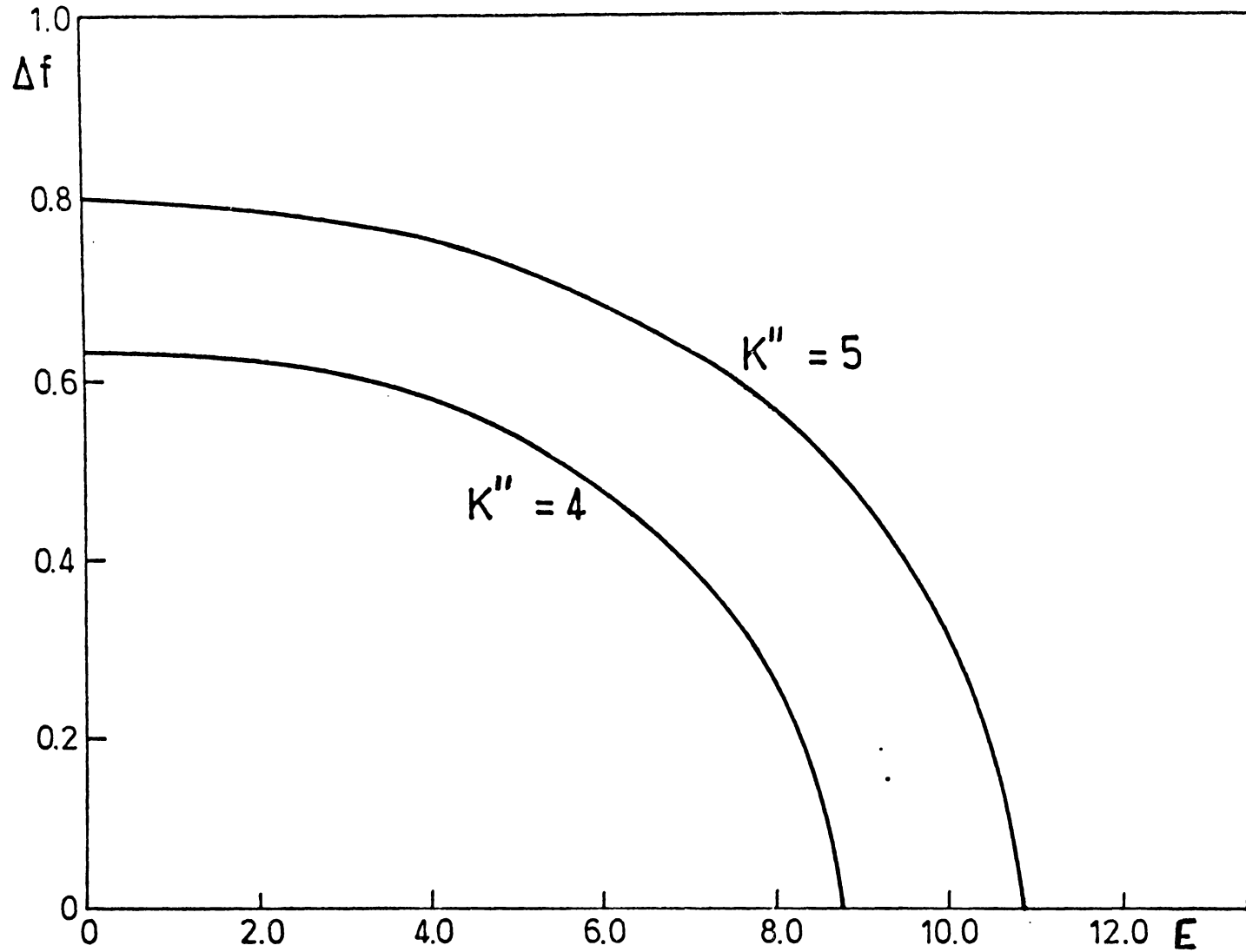


Fig (3.3.4) Laser with an injected signal; limit cycle frequency vs input amplitude for different detuning ($K' = -10$, $\alpha = 1.0$).

(iii) Medium detuning ($\kappa'/2 < \kappa'' < \kappa'/\sqrt{3}$)

In this case the graph of the state equation appears qualitatively similar to the previous situation: that is, there is still a multiple valued region. However the lower branch stability is different in this situation. In fact it is readily verified that in some parts of the lower branch one can obtain $\text{Tr}(A) > 0$, with stable eigenvalues. Thus it is clear that at least part of the lower branch is locally stable, leading to a bistability in the laser intensity. However only part of the lower branch is stable, while for smaller $(|E|)$ the lower branch is in fact unstable. A detailed study of the limit cycle in this case by Stoker (1950) predicts that it is possible to have a bistable region where either a limit cycle or a stable point occur, depending on the initial values of the equations.

The value of $\kappa'' = \kappa'/\sqrt{3}$ in this case is a critical one, that divides a region of bistability from a range of detuning where only continuous (second-order) transitions in the amplitude are possible. This gives a state equation (as shown in fig 3.2.1) which has an inflexion point, but is never multiple-valued.

(iv) Large detuning ($\kappa'' > \kappa'/\sqrt{3}$)

In this case the graph of the state equation is single-valued (fig 3.3.1). However the entrainment threshold still occurs, at:

$$n^{\dagger} = |\kappa'/4\chi|$$

$$|E^{\dagger}|^2 = n^{\dagger} [\kappa''^2 + \frac{1}{4}\kappa'^2]$$

This is a different type of threshold from that obtained with small detuning, even though there is once again no bistability. The frequency of the limit cycles does not vary continuously from zero (relative to the rotating frame). Instead there is a definite non-zero frequency at threshold due to the eigenvalue being complex. However the amplitude does vary continuously: that is, the transition can be thought of as second-order with regard to the field amplitude as an order parameter.

We finally note that for large enough detuning, other modes of the Fabry-Perot will become entrained so that the original lasing mode will be quenched. This offers an alternate form of switching the laser frequency, that necessitates a multimode theory. For reasons of space, we do not treat this problem here. However, the possibility of optical bistability in a multimode laser system is pointed out by Lugovoi (1978), Lamb (1964).

(c) Correlation function and photon number

In the case of the laser above threshold, the correlation function and photon number have been calculated previously and are well known (see Haken 1970 for a review of this field). We therefore shall restrict ourselves to the case of

$|\epsilon| > |\epsilon^*|$, where the laser is entrained by an injected coherent signal. In the laser above threshold, Γ is large: and n^{th} must include the photon number due to the

optical pumping of the atoms. The present theory therefore reduces to an externally driven van der Pol oscillator with thermal fluctuations. In reality higher order terms occur in the exact Fokker-Planck equation for the high intensity laser: these will be mentioned in Chapter 5.

The final expression for the mean correlation and photon number is therefore:

$$\bar{n} = n + \left(\frac{\Gamma}{2}\right) \left[\frac{\kappa''^2 + (\kappa' + 4\chi n)^2}{(\kappa' + 4\chi n) \Delta(0)} \right]$$

$$g^2(0) \simeq 1 + 2\left(\frac{\bar{n}}{n} - 1\right)$$

Clearly there is a singularity at $\Delta(0) = 0$, which corresponds to the entrainment point. However when the input signal increases above the entrainment point, the output becomes increasingly coherent provided the intra cavity laser is operating above the laser threshold. It should be noticed that the singularity at $\Delta(0) = 0$ can only occur for $|\kappa''| < |\kappa'|/\sqrt{3}$, so that the state equation is multiple valued. No corresponding singularity occurs for $|\kappa''| > |\kappa'|/\sqrt{3}$.

(d) Output spectrum

We first calculate the spectral peaks which occur at:

$$\omega = \omega_0 \pm \sqrt{(\omega_1 - \omega_0)^2 - 4\chi^2 n^2}$$

Thus the spectrum is single-peaked for $|\kappa''| < 2\chi n$. At this point we note that for the natural laser operating point, we have $2\chi n = \kappa'$. In the vicinity of the laser operating point, we can say that there is a single peak at the input frequency for $|\kappa''| < |\kappa'|/\sqrt{3}$ provided the input power is above the entrainment threshold.

In the case of large detuning ($\kappa'' > \kappa'/\sqrt{3}$) we have a hard-mode transition at $4\chi n = \kappa'$ followed by a spectral transition from double-peaked to single-peaked at $2\chi n = \kappa''$. Thus a double-peaked spectrum can be observed for $(\kappa'' > \kappa'/\sqrt{3})$ within a certain range of input power. As mentioned in section 3.1, the double-peaked spectrum has the greatest intensity closest to the effective cavity frequency. The appearance of the double-peaked spectrum in the entrainment threshold region for $\kappa'' > \kappa'/\sqrt{3}$ indicates the different nature of the hard-mode transition with a large detuning of the input signal, relative to the small detuning transition.

3.4 THE NONLINEAR (TWO-PHOTON) ABSORBER

(a) Introduction: Photon antibunching

The nonlinear absorber has become of recent interest owing to the photon statistical properties expected in this situation. In an analysis of two-photon absorption in a single-mode interferometer, both fluctuation-reduction in the driving field, and the possibility of photon antibunching are predicted (Chaturvedi, Drummond & Walls, 1977). This model differs from previous classical (Weber 1971) and quantum (Chandra & Prakash 1970, McNeil & Walls 1974, Simaan & London 1975, Every 1975, Paul et al 1976) treatments which have no driving field. A steady-state is obtained in a related model of two-photon absorption within a laser (Bandilla & Ritze, 1976). However experiments to date on nonlinear absorption and fluctuation reduction use an external laser to provide the input to the nonlinear absorber (Krasinski et al, 1977).

Investigation of the coherent driving field case leads to the prediction of antibunching photon statistics for the mode, provided thermal and driving field fluctuations are small. The prediction of photon antibunching is of great interest as this can only be obtained within a quantum theory of the electromagnetic field. A classical theory would always predict $g^2(0) \geq 1$: therefore the observation of antibunching ($g^2(0) < 1$) would be a verification of present Q.E.D. theory.

Now antibunching has been inferred from experiments on resonance fluorescence (Kimble et al 1977,1978). However

in this situation the extent of antibunching is masked by Poissonian fluctuations in the number of illuminated atoms (Jakeman et al 1977, Carmichael, Drummond, Meistre & Walls, 1978). In addition, it has been suggested that in this case, photon antibunching is purely a result of atomic operator properties, rather than due to the quantum nature of the radiation field (Bullough, 1977). For this reason, it is worthwhile to understand in detail the quantum theory of the nonlinear or two-photon absorber for a single-mode interferometer, as in this case quantum field theory is needed to obtain results.

The formulae for the linearised theory are identical with the results given in section 3.2. The chief difference is that in the two-photon absorber we can expect Γ to be small (for a coherent driving field). In addition the one-photon loss term is always absorptive, as no amplification occurs in this case. While the linearised results are valid for large \bar{n} , they cannot predict antibunching to a greater extent than $(1 - 1/\bar{n})$ due to the limitations imposed by quantum theory. Therefore in order to treat the large antibunching obtained for $\bar{n} \leq 1$, it is necessary to utilise the potential solutions of section 3.1 that hold in the limit of $\Gamma \rightarrow 0$.

(b) State equation and correlation function

In the nonlinear absorber, the state equation is always singlevalued, without instabilities. For this reason no nonequilibrium transitions arise. The photon number increases steadily with increasing $|E|$, to reach an asymptotic value of:

$$n = |E_0/2\chi|^{2/3}$$

In this limit, the value of $g^2(\omega)$, \bar{n} can be calculated as an asymptotic series in $(1/n)$. From the formulae of sections 3.1 and 3.2 we obtain:

$$\bar{n} = n + \frac{1}{6} + \left(\frac{\Gamma}{6\chi n}\right) + O\left(\frac{1}{n^2}\right)$$

$$g^2(\omega) = 1 - \frac{1}{3\bar{n}} + \left(\frac{\Gamma}{6\chi n^2}\right) + O\left(\frac{1}{n^2}\right)$$

Thus to leading order in $(1/n)$ it is possible to obtain antibunching. Now this is possible in optical systems when Γ is due to the thermal background. However in typical experiments, the phase and amplitude fluctuations in the input field are appreciable due to the high input intensity necessary for large nonlinear absorption. This situation is discussed by Chaturvedi, Drummond & Walls (1977), where phase and amplitude fluctuations are included in the driving field for a comparison with the results of experiments by Krasinski & Dinev (1976).

The results obtained with the inclusion of phase and amplitude fluctuations are:

$$g_2(0) = 1 - \frac{1}{3\bar{n}} + \left(\frac{\Gamma}{6\chi n^2}\right) + \left[\frac{2a(E_0)}{3\chi n(6\chi n + b(E_0))}\right].$$

Here we have included the terms discussed in section 3.1, as coming from a simple model of fluctuations in a single-mode laser: phase fluctuations do not contribute to this order.

We now suppose that $b(E_0)$ is small, i.e. there are long correlation times in the input amplitude fluctuations. In this case we have:

$$g_2(0) = 1 - \frac{1}{3\bar{n}} + \frac{1}{n^2} \left[\frac{\Gamma}{6\chi} + \frac{a(E_0)}{9\chi^2} \right]$$

It is interesting to note that the term in $a(E_0)$ can also be obtained directly from the state equation, by letting α follow $E(t)$ adiabatically in the limit of a long correlation time.

In order to compare the output of a nonlinear with a linear absorber, we compare this result with the case of a linear interferometer of the same output intensity; that is -

$$n = |E_0/2\chi|^{2/3} \quad (\text{nonlinear}) \quad = |E_0/\kappa|^2 \quad (\text{linear})$$

In order to make a valid comparison we express the correlation function in both cases solely in terms of E_0 and n :

$$g_2(0) = 1 - \frac{1}{3\bar{n}} + \frac{\Gamma}{3E_0\sqrt{\bar{n}}} + \frac{4a(E_0)}{9E_0^2} \quad (\text{nonlinear})$$

$$g_2(0) = 1 + \frac{\Gamma}{E_0\sqrt{\bar{n}}} + \frac{4a(E_0)}{E_0^2} \quad (\text{linear})$$

The difference between a linear and nonlinear absorber is as follows (for the same input and output intensity):

- the nonlinear absorber introduces antibunching for a coherent input field.
- thermal (rapidly correlated) fluctuations are reduced by a factor of 3 (asymptotically).
- amplitude (slowly correlated) fluctuations are reduced by a factor of 9 (asymptotically).
- to first order, phase fluctuations do not alter $g^2(0)$.

(c) Output spectrum

The general expression for the linearised output spectrum is given in section 3.1. For simplicity, we suppose that $\Gamma = \kappa = 0$; this is the asymptotic region where the nonlinear absorption is large. In this limit, the expression for the spectrum simplifies somewhat, and we obtain:

$$S(\omega + \omega_0) = n\delta(\omega) + \left[\frac{16(\chi n)^3}{\pi(\omega^2 + 36\chi^2 n^2)(\omega^2 + 4\chi^2 n^2)} \right]$$

In this limit, therefore, the spectrum is a product of Lorentzian lines, with the spectrum varying as $(1/\omega^4)$ for large detuning. Since an ordinary Lorentzian varies as

(ω^2) for large ω it is very clear that this corresponds to a narrower line than usual (in that it gives a finite second moment after the asymptotic limit has been obtained).

An additional measurable quantity that is of interest is the Fourier transform of the correlation function, $\tilde{g}^2(\omega)$. From section 3.1, this is given by:

$$g^2(\omega) = \delta(\omega) - \left[\frac{2\chi}{\pi(\omega^2 + (\chi n)^2)} \right]$$

Thus in this case, the Fourier transform of the correlation function displays an antibunching behaviour in frequency space while the spectrum is of course positive.

(c) Potential solutions

In the limit of zero temperature and a coherent input, potential solutions are very useful in studying the non-linear absorber. They are able to be extended to all input fields, rather than being restricted to the high field limit as with asymptotic expansions. In this respect the potential solutions are limited only by the restriction to zero external fluctuations. In reality fluctuations from

thermal backgrounds will be significant near the limit of zero driving field, so the present theory only holds in an idealised situation.

No nonequilibrium transitions occur, although there is some unusual behaviour for $E_0 \rightarrow 0$, where there is a rapid change in the mean photon number from zero to one-half for low linear absorption (fig 3.4.1). In fact the case of $\Gamma = E_0 = \kappa = 0$ has been studied previously by Loudon & Simaan (1975). These authors find that there is a steady-state that can occur with $\bar{n} = 1/2$, $g^2(0) = 0$. This is due to the fact that the nonlinear absorber cannot absorb a single photon. The present results generalise the exact results of Loudon & Simaan to a finite driving field and finite linear absorption, which is more physically realistic. In fact we find the following limits for a finite linear absorption:

$$\begin{aligned} \lim_{E_1 \rightarrow 0} \bar{n} &= 0 && (\kappa' > 0) \\ &= 1/2 && (\kappa' = 0) \end{aligned}$$

$$\lim_{E_1 \rightarrow 0} g^2(0) = \left[\frac{\kappa'}{\chi' + \kappa'} \right]^2$$

The above limits are restricted to a coherent driving field at zero temperature.

In practice external fluctuations will always be present. The effect of finite temperature depends on the ratio of \bar{n} to n_{th} . The present results apply for:

$$\chi' \bar{n} \gg \kappa' n_{th}$$

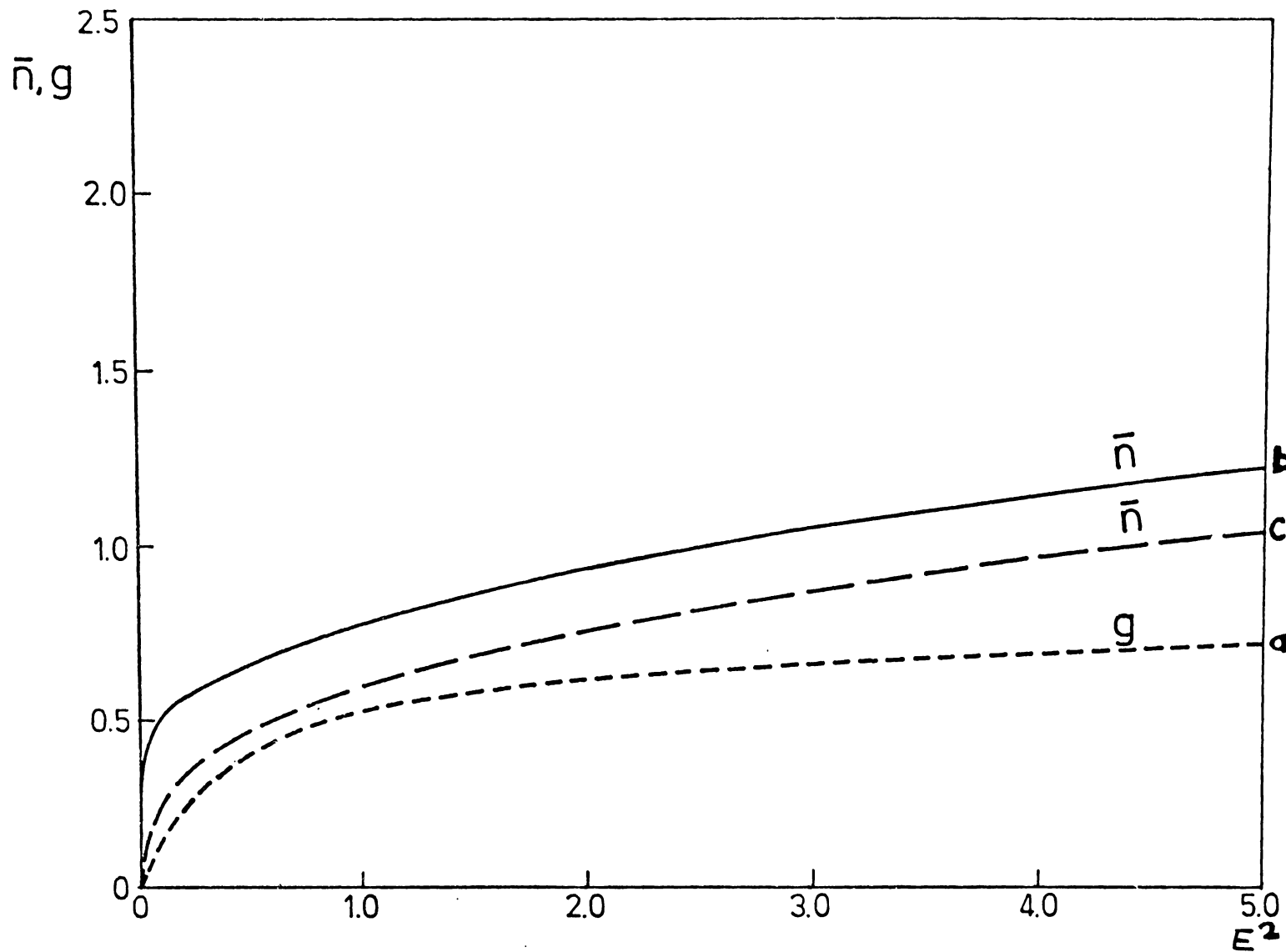


Fig (3.4.1) Nonlinear absorber; correlation and photon number vs input power ($\kappa' = 0.1$, $\chi = 1$, $\Gamma = 0$).

(a) $g^2(0)$ - exact (b) \bar{n} - exact (c) \bar{n} - semiclassical

Thus while in typical optical experiments it is straightforward to obtain $\bar{n} \gg n^{\text{th}}$, we also require a high-quality cavity with a very nonlinear medium (with $\chi' \gg \kappa' \frac{n^{\text{th}}}{n}$) in order to achieve this. In practice, the above results will only hold for $E_0 > 0$, since even low-temperature thermal fluctuations would become significant for $E_0 = 0$. The limiting values are useful in indicating the order of antibunching expected, at low driving field: while it is straightforward to evaluate moments numerically for a finite driving field (Appendix C).

3.5 THE DISPERSIVE CAVITY WITH BISTABILITY

(a) Dispersive bistability

The development of the laser as a coherent light source has encouraged the study of light propagation in nonlinear media. The motivation of much recent study has been that logic or communications devices utilising coherent radiation as a communications medium would be a very useful possible application.

In particular interest has been directed toward optical bistability as the basis for switching or other nonlinear

devices (Venkatesan, 1976). While initially research was directed toward an absorptive nonlinearity, it was found simpler to have a detuned interferometer with a dispersive nonlinearity in practical experiments (Gibbs, McCall, Venkatesan, 1976). The semiclassical theory of a purely dispersive bistability is discussed by Marburger & Felber (1978).

In this section, the origin of the bistability is essentially the same as that of Marburger & Felber; although restricted to a single mode. The semiclassical treatment is then identical to the theory of an anharmonic oscillator, which is well known to have bistability. This single-mode treatment also permits a detailed investigation of the quantum statistical properties of the bistable transition, which cannot be obtained semiclassically.

The relevant formulae from section 3.1 are summarised below, for the case of a dispersive nonlinearity ($\chi' = 0$).

State equation and turning points:

$$|E|^2 = n [\kappa'^2 + (2\chi''n + \kappa'')^2]$$

$$n^{\pm} = [-2\kappa'' \pm \sqrt{\kappa''^2 - 3\kappa'^2}] / (6\chi'')$$

Mean correlation and photon number:

$$\bar{n} = n + n_{th} \left[\frac{\kappa'^2 + (\kappa'' + 4\chi''n)^2}{\Delta(\omega)} \right] + \left[\frac{2\chi''^2 n^2}{\Delta(\omega)} \right]$$

$$g^2(0) = 1 + \left[\frac{2n_{th}}{n} \right] \left[\frac{1\kappa'^2 + 8n^2\chi''^2 + 6n\kappa''\chi''}{\Delta(\omega)} \right] - \left[\frac{4|\chi''|^2 n + 2\chi''\kappa''}{\Delta(\omega)} \right]$$

$$\Delta(\omega) = (\kappa'^2 + \kappa''^2 + 8\kappa''\chi''n + 12\chi''^2 n^2)$$

Spectrum: peaks at frequencies -

$$\omega = \omega_0 \pm \sqrt{\kappa''^2 + 8\kappa''\chi''n + 12\chi''^2 n^2}$$

(Provided $\kappa''^2 + 8\kappa''\chi''n + 12\chi''^2 n^2 > 0$)

We now discuss these formulae for the case of the dispersive cavity with bistability: ($\kappa''\chi'' < 0$), and without bistability: ($\kappa''\chi'' > 0$).

(b) Discussion of results

Just as in the externally driven laser, the stability properties depend on the detuning parameter. However the results are much simpler as there is no hard-mode instability. A bistable behaviour is only obtained for $\kappa''\chi'' < 0$. In

fact the bistable region depends closely on the detuning, which must be greater than a critical value:

$$\kappa''^2 > 3\kappa'^2$$

Once the detuning parameter is large enough, there is a bistable state equation, with upper and lower turning points given by the formulae of section 3.4. However this does not give the steady-state behaviour which is determined by the extent of the quantum fluctuations. In fig 3.5.1 we graph both the semiclassical equation, and the exact result for the photon number with quantum fluctuations (which has no hysteresis). The extent to which bistability is observed in practice will depend on the fluctuations: which in turn determine the time for random switching from one branch to the other.

A sharper transition is obtained at a larger detuning, and with a smaller relative value of nonlinearity (to reduce quantum fluctuations). On the other hand, a larger nonlinearity gives a lower threshold to observe the transition: this is a significant factor in practical applications (Marburger et al 1978). The relative effects of different detuning are shown in figs 3.5.1, 3.5.2. In these figures, the exact results are obtained from the potential solutions of section 3.2.

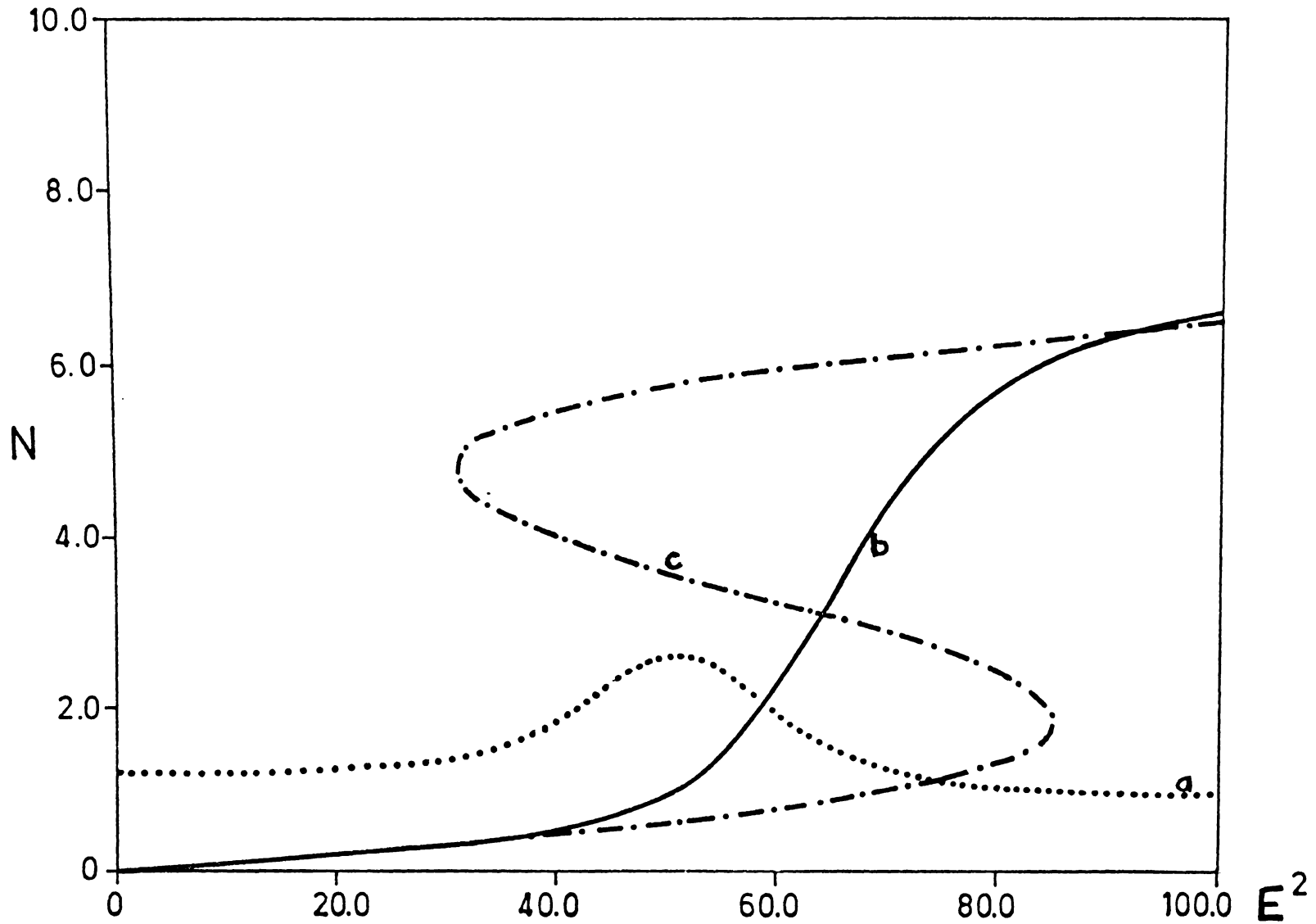


Fig (3.5.1) Dispersive bistability; correlation and photon number vs input power ($\kappa = 2.5 - i10$, $\chi'' = 1.0$, $\Gamma = 0$)
 (a) $g^2(0)$ - exact (b) \bar{n} - exact (c) \bar{n} - semiclassical

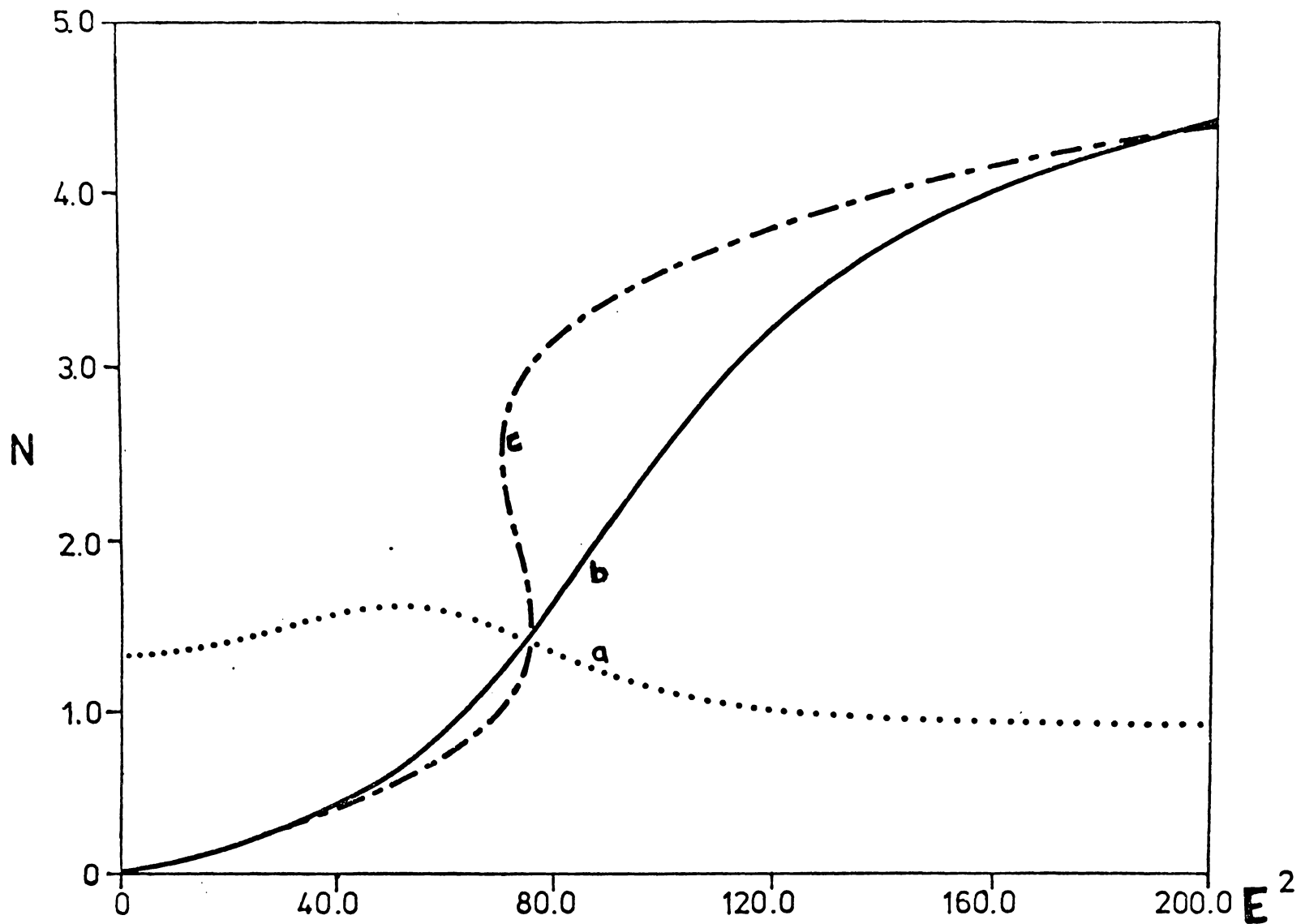


Fig (3.5.2) Dispersive bistability; correlation and photon number vs input power (close to critical point: $\kappa=5-i10$, $\chi=1.0$, $\Gamma=0$).

(a) $g^2(0)$ - exact (b) \bar{n} - exact (c) \bar{n} - semiclassical

(c) Spectrum and photon statistics

We now turn to the transmitted light spectrum, which was obtained in section 3.1. In general the spectrum is double-peaked, although there is a certain range of photon numbers where the lines coalesce to give a single line.

These points are at:

$$n = \left[\frac{1}{3} \pm \frac{1}{6} \right] \left| \frac{\kappa''}{\chi''} \right|$$

Thus, the region of a single line spectrum includes the range of n where bistability is observed. As the threshold point is approached from below, the spectral lines first coalesce then one line diverges at the threshold point. The reverse situation occurs above the threshold. In this case there is a double line above the bistable region. On reducing the driving intensity, the lines coalesce then diverge, as before.

Of special interest is the relative behaviour of the spectrum with and without thermal fluctuations. In the case without fluctuations the spectrum is symmetric relative to the input frequency. When thermal fluctuations are included the line closest to the effective interferometer tuning is enhanced: at low driving intensity this corresponds to the linear result. However when the input intensity is increased, the spectral lines coalesce, and then a crossing-over effect occurs: above the bistable threshold the line farthest away from the original linear tuning becomes relatively enhanced. The physical reason

for this behaviour (shown in figs 3.5.3 - 3.5.5) is that the effective refractive index of the medium is changed by the driving field.

The correlation function is also given (in the limit of $\Gamma \rightarrow 0$) in the figures 3.5.1, 3.5.2. It can be seen that the correlation function displays photon bunching in the bistable region, due to larger fluctuations in this region. In a linearised analysis, one would obtain a similar result, except with divergences at the turning points. This is due to the instability in the state equation, which makes the linearised analysis break down here.

Finally we note that from the linearised result for $g^2(0)$, it can be verified that the thermal fluctuations always result in photon bunching (in a stable region). However while the quantum fluctuations cause photon bunching for a low driving field (if $\chi''\kappa'' < 0$) they also give rise to antibunching at a high enough field. In fact at a very high driving field, the result is:

$$g^2(0) \rightarrow 1 - \frac{1}{3\bar{n}}$$

It is interesting to note that the result in this limit becomes identical to that for the nonlinear absorber. In the monostable detuning direction ($\chi''\kappa'' > 0$), it can be noted that the quantum fluctuations will result in photon antibunching for all driving fields, provided external fluctuations are small. The physical reason for this behaviour is that a fluctuation tending to increase the

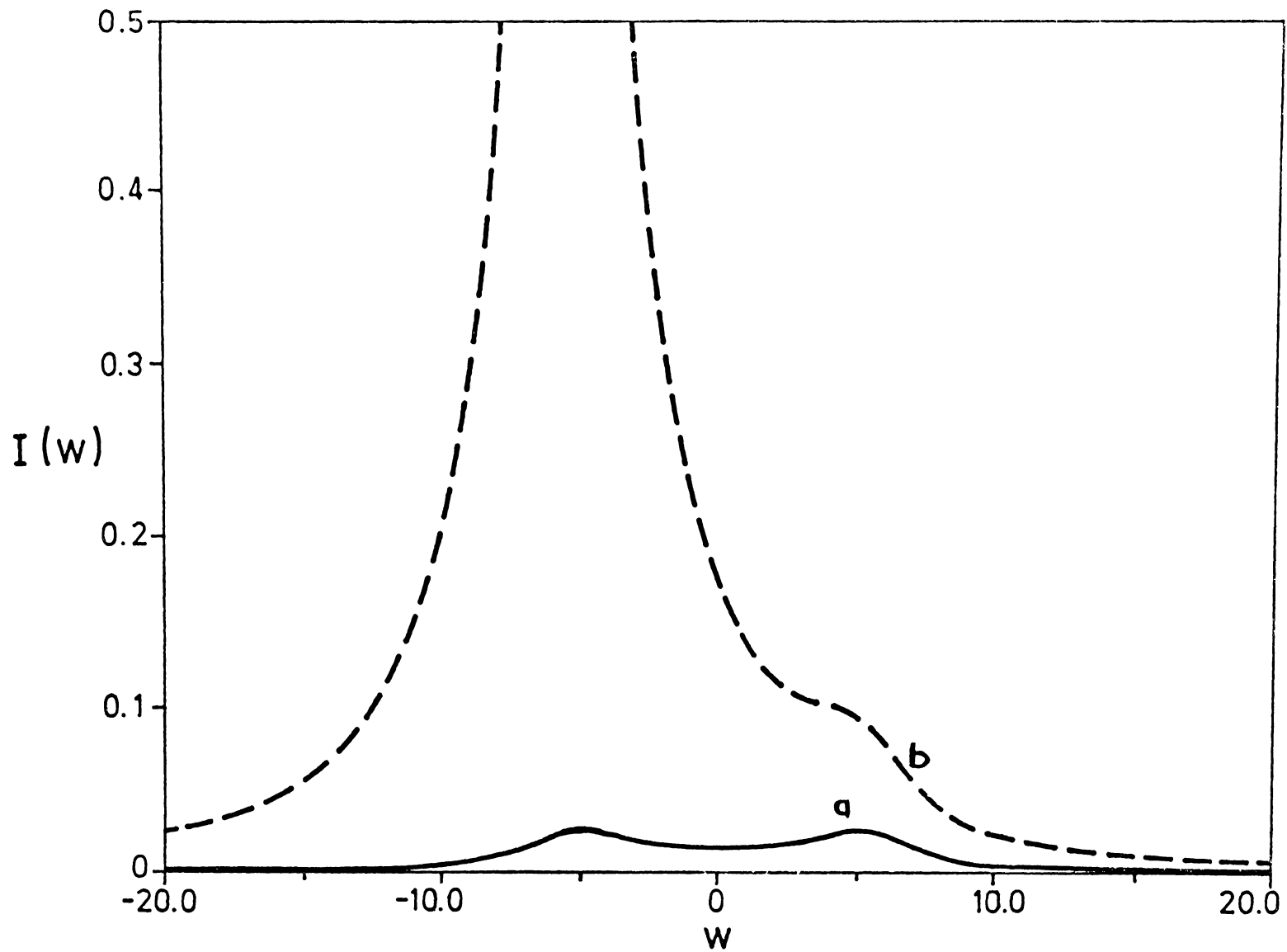


Fig (3.5.3) Dispersive bistability spectrum; quasilinear region (arbitrary units).

(a) zero temperature

(b) finite temperature

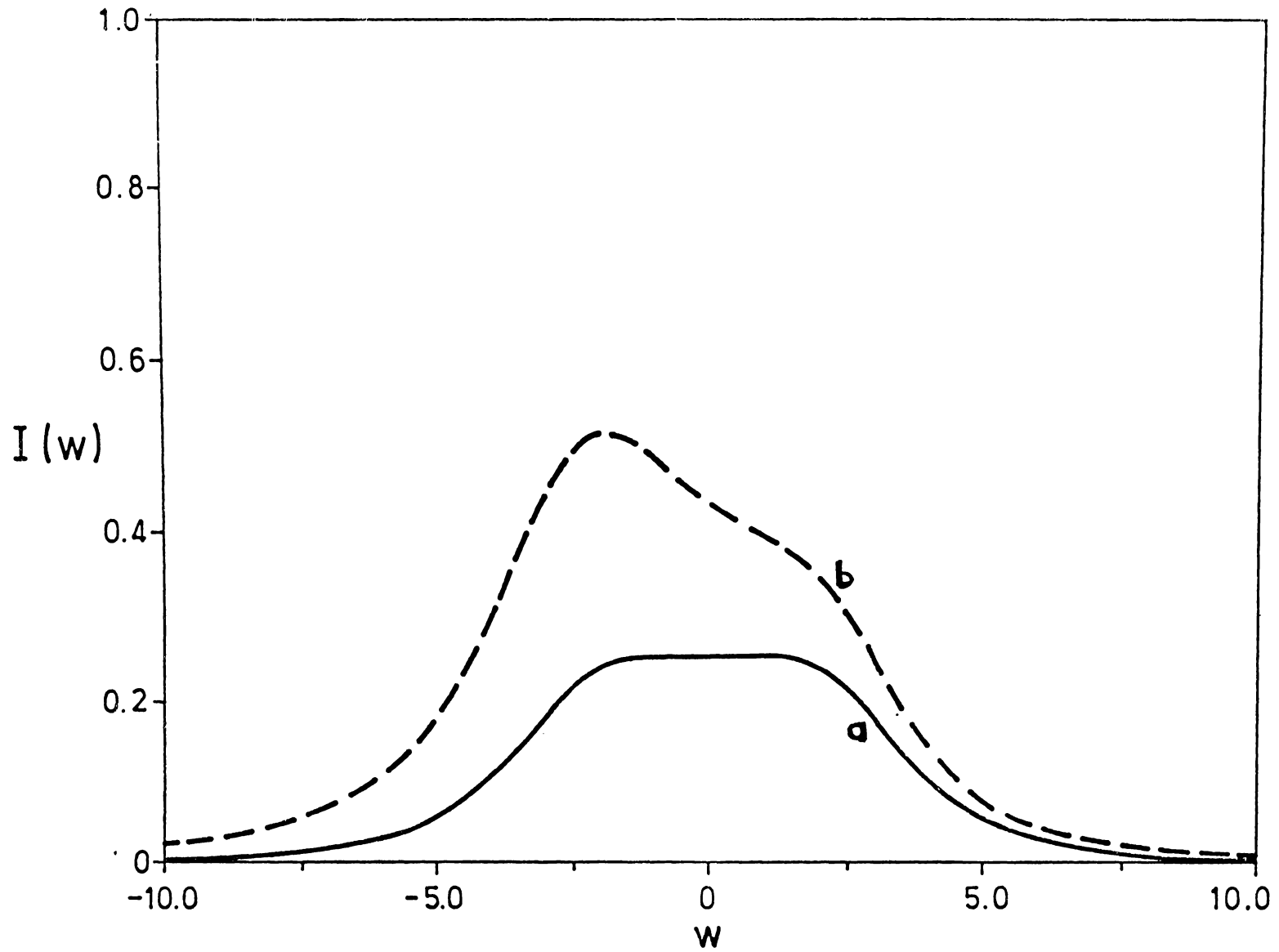


Fig (3.5.4) Dispersive bistability spectrum; subthreshold region (arbitrary units).

(a) zero temperature

(b) finite temperature

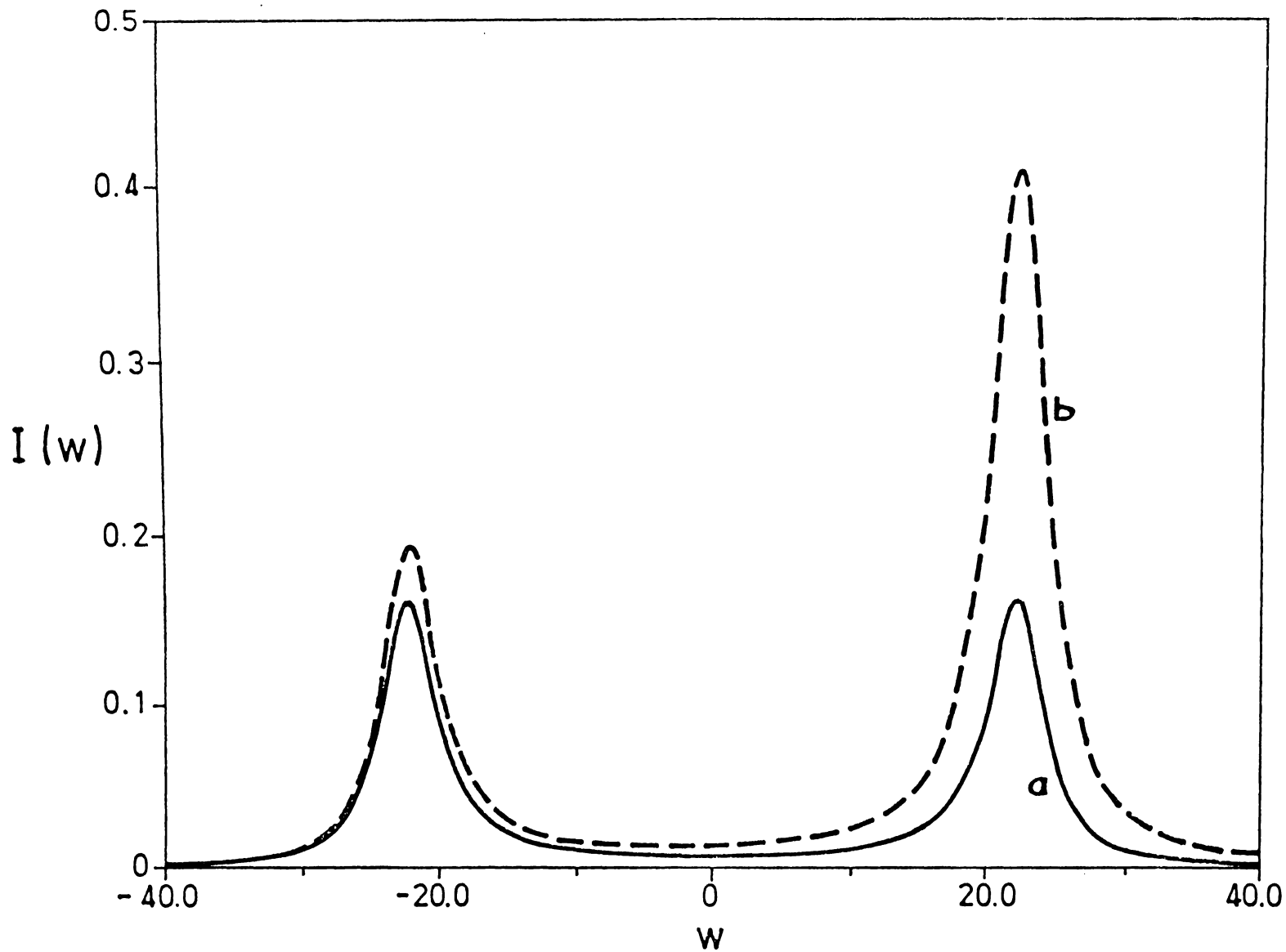


Fig (3.5.5) Dispersive bistability spectrum; upper branch region (arbitrary units).

(a) zero temperature

(b) finite temperature

field intensity also changes the effective refractive index, causing a detuning of the interferometer. For a high enough input intensity, therefore, both the dispersive and the absorptive nonlinearities tend to reduce fluctuations.

CHAPTER 4: COUPLED MODE TRANSITIONS

In Chapter 3, we dealt with a nonlinear medium, in which the cubic polarisability led to various nonequilibrium transitions, including bistable behaviour. We now turn to the quadratic term in the polarisability which leads to a mode-mode coupling between different frequencies, provided there is wavelength matching. In fact the first experiment in modern nonlinear optics was the generation of ultraviolet radiation (.347nm), from a ruby laser (.694 nm) focussed on a quartz crystal (Franken et al, 1961).

In this chapter we include a quadratic polarisability leading to mode-mode coupling, with both modes defined by a Fabry-Perot interferometer. In the theoretical treatment, we take account of depletion in the driving field, quantum fluctuations, and damping. A treatment of this type has not been obtained in earlier work on subharmonic generation and second harmonic generation. A deterministic analysis of stability of the coupled mode equations in second and subharmonic generation was originally given by McNeil et al (1978): some of these results have been included here for completeness. However the chief aim of this chapter is to include quantum fluctuations and to obtain the distribution function in the limit of adiabatic elimination of the second harmonic. This allows a direct comparison with the results for a cubic polarisability in the single mode treatment of Chapter 3, and an exact solution for the complex phase-space p-function in the zero-temperature limit.

A full discussion of classical nonlinear optics is given by Bloembergen (1965). Solutions to the coupled classical equations were given by Armstrong et al (1962). A quantum mechanical treatment of the coupled modes (without a driving field) was given by Walls (1970) and Walls & Tindle (1971, 1972). Further treatments have been given by Crosignani et al (1972), Dewael (1975), Perina (1976), Kosierowski & Tanas (1977), Nayak & Bohanty (1977). Stoler (1974) predicted the possibility of transient antibunching in subharmonic generation. Recently Mostowski & Rzazewski (1978) have pointed out the possibility of transient photon antibunching in second harmonic generation, although this was implicit in the earlier papers of Walls & Tindle (1971, 1972). A system of nonlinear interactions inside a Fabry-Perot cavity including damping and an external driving field was considered by Graham (1968, 1973), who studied subharmonic generation in particular, although without a detailed treatment of the quantum fluctuations.

The new feature in the present treatment is the inclusion of quantum fluctuations and mode-mode coupling between the input frequency and the output frequency. This leads to new features depending on the type of input used. As well as the well known critical point transition in subharmonic generation, there can be limit cycles in second harmonic generation (as pointed out by McNeil et al 1978); and bistability, or antibunching statistics when both modes are excited with different phase relationships. When the second harmonic mode decays rapidly enough to be adiabatically eliminated, there is a great similarity between this

situation and the model of nonlinear dispersion and absorption treated in Chapter 3: with a detuned driving field, dispersive optical bistability occurs.

4.1 THEORY OF THE COUPLED-MODE SYSTEM

(a) Hamiltonian and master equation

In this case, the nonlinear polarisability to order $\chi^{(2)}$ is sufficient to result in a mode-mode coupling. The procedure of deriving an effective Hamiltonian is virtually identical to that presented in section 3.1, so we need not repeat this. Just as previously, the rotating wave approximation is employed to eliminate rapidly varying terms. The chief difference between this and the one-mode problem is that the quadratic polarisability becomes significant, and it is necessary to have wavelength matching between the modes for a significant coupling to occur. We obtain an interaction Hamiltonian (assuming real, plane-polarised mode functions) of:

$$H_I = \left[\frac{i\hbar\eta}{2} \right] (\hat{a}_1^{\dagger 2} \hat{a}_2 - \hat{a}_1^2 \hat{a}_2^{\dagger})$$

Where :

$$\eta \equiv - \left(\frac{\hbar\omega^3}{2\epsilon_0} \right)^{1/2} \int \underline{u}(\underline{r}) \cdot \underline{\chi}^{(2)}(\underline{r}) : \underline{u}(\underline{r}) \underline{u}(\underline{r}) d^3 \underline{r}$$

Here we have assumed that only the modes at frequencies ω_1 and $\omega_2 \approx 2\omega_1$ are significant, with a coupling via the nonlinear crystal polarisability. We now suppose the nonlinear crystal is placed within a Fabry-Perot interferometer. Both modes are driven with external coherent phase-locked driving fields, and damping of the cavity modes is included.

We suppose in general that the input frequencies are at exactly $\omega_j, 2\omega_j$. However, in a realistic situation where there can be frequency dispersion or mistuning, it is possible that the input frequencies are not the same as the interferometer resonances.

The interaction Hamiltonian describing this system is written as:

$$\hat{H} = \sum_{j=1}^5 \hat{H}_j$$

$$\hat{H}_1 = i\hbar [E_1 \hat{a}_1^\dagger e^{-i\omega_1 t} - E_1^* \hat{a}_1 e^{i\omega_1 t}]$$

$$\hat{H}_2 = i\hbar [E_2 \hat{a}_2^\dagger e^{-2i\omega_1 t} - E_2^* \hat{a}_2 e^{2i\omega_1 t}]$$

$$\hat{H}_3 = [\hat{\Gamma}_1 \hat{a}_1^\dagger + \hat{\Gamma}_1^\dagger \hat{a}_1]$$

$$\hat{H}_4 = [\hat{\Gamma}_2 \hat{a}_2^\dagger + \hat{\Gamma}_2^\dagger \hat{a}_2]$$

$$\hat{H}_5 = (i\hbar\eta/2) [\hat{a}_1^{\dagger 2} \hat{a}_2 - \hat{a}_1^2 \hat{a}_2^\dagger]$$

Here \hat{a}_1, \hat{a}_2 are boson operators for the field modes at frequencies ω_1, ω_2 . The input fields at frequencies $\omega_j, 2\omega_j$ are E_1, E_2 , and are assumed to be coherent. The operators $\hat{\Gamma}_{1,2}$ are reservoir operators, with corresponding decay rates of κ'_1, κ'_2 . Finally the nonlinear

medium gives the nonlinear coupling term η , where the phases of $\hat{a}_{1,2}$ are defined so that η is real.

In the case of no losses, the Heisenberg equations of motion would be readily obtained (assuming perfect frequency matching):

$$\partial_t \hat{a}_1 = E_1 + \eta \hat{a}_1^\dagger \hat{a}_2$$

$$\partial_t \hat{a}_2 = E_2 - (\eta/2) \hat{a}_1^2$$

It can be seen that with E_1 as the driving field, second harmonic generation occurs: while with E_2 as the driving field, there is subharmonic generation. In order to study this in detail, it is necessary to include loss terms, giving a master equation in the Markov approximation (Louisell, 1973). For simplicity we include detuning together with damping:

$$\kappa_j \equiv \kappa_j' + i(\omega_j - j\omega_i) \quad [j=1,2]$$

The interaction picture master equation for the reduced density operator $\hat{\rho}$ is:

$$\partial_t \hat{\rho} = \sum_{j=1}^5 \hat{\mathcal{L}}_j[\hat{\rho}]$$

$$\hat{\mathcal{L}}_1[\hat{\rho}] = [E_1 \hat{a}_1^\dagger - E_1^* \hat{a}_1, \hat{\rho}] - i(\omega_1 - \omega_i) [\hat{a}_1^\dagger \hat{a}_1, \hat{\rho}]$$

$$\hat{\mathcal{L}}_2[\hat{\rho}] = [E_2 \hat{a}_2^\dagger - E_2^* \hat{a}_2, \hat{\rho}] - i(\omega_2 - 2\omega_i) [\hat{a}_2^\dagger \hat{a}_2, \hat{\rho}]$$

$$\hat{\mathcal{L}}_3[\hat{\rho}] = \kappa_1' [[\hat{a}_1, \hat{\rho}, \hat{a}_1^\dagger] + [\hat{a}_1, \hat{\rho} \hat{a}_1^\dagger]] + 2\kappa_1' n_1^{th} [[\hat{a}_1, \hat{\rho}], \hat{a}_1^\dagger]$$

$$\hat{\mathcal{L}}_4[\hat{\rho}] = \kappa_2' [[\hat{a}_2, \hat{\rho}, \hat{a}_2^\dagger] + [\hat{a}_2, \hat{\rho} \hat{a}_2^\dagger]] + 2\kappa_2' n_2^{th} [[\hat{a}_2, \hat{\rho}], \hat{a}_2^\dagger]$$

$$\hat{\mathcal{L}}_5[\hat{\rho}] = (\eta/2) [\hat{a}_1^\dagger \hat{a}_2 - \hat{a}_1^2 \hat{a}_2^\dagger, \hat{\rho}]$$

Here κ'_1 , κ'_2 are the cavity half-widths at frequencies ω_1 , ω_2 respectively; while n_1^{th} , n_2^{th} are the thermal photon numbers. As we will be mainly interested in mode (1), which experiences the greatest effect due to thermal fluctuations, we assume that $n_2^{th} \approx 0$ in this chapter. The above master equation is similar to those derived by Graham (1968) for parametric oscillations. We now introduce the Fokker-Planck equation in the complex P-representation following the method of section 2.1. After partial integration the following equation is obtained for the complex P-function:

$$\begin{aligned} \frac{d}{dt} P(\underline{\alpha}) = & \left\{ \partial_{\alpha_1} [\kappa_1 \alpha_1 - E_1 - \eta \alpha_2 \alpha_1^*] + \partial_{\alpha_1^*} [\kappa_1^* \alpha_1^* - E_1^* - \eta \alpha_2^* \alpha_1] \right. \\ & + \partial_{\alpha_2} [\kappa_2 \alpha_2 - E_2 + \eta \alpha_1^2 / 2] + \partial_{\alpha_2^*} [\kappa_2^* \alpha_2^* - E_2^* + \eta \alpha_1^{*2} / 2] \\ & \left. + \frac{1}{2} [\partial_{\alpha_1}^2 (\eta \alpha_2) + \partial_{\alpha_1^*}^2 (\eta \alpha_2^*) + 2 \Gamma \partial_{\alpha_1} \partial_{\alpha_1^*}] \right\} P(\underline{\alpha}) \end{aligned}$$

Where:

$$\Gamma \equiv 2\kappa_1 n_1^{th} \quad ; \quad \underline{\alpha} \equiv [\alpha_1, \alpha_1^*, \alpha_2, \alpha_2^*]$$

In general this Fokker-Planck equation is not soluble by potential methods. We therefore turn to the stochastic equations in order to have a method of solution that is at least valid in an asymptotic limit. In addition, the stochastic equations can be used to adiabatically eliminate the stable mode in a simple way, although this can also be obtained directly from the Fokker-Planck equation (Gordon, 1967).

Following the method of section 2.3, the following stochastic equations are obtained:

$$\partial_t \begin{bmatrix} \alpha_1 \\ \alpha_1^\dagger \end{bmatrix} = \begin{bmatrix} E_1 + \eta \alpha_2 \alpha_1^\dagger - \kappa_1 \alpha_1 \\ E_1^* + \eta \alpha_2^\dagger \alpha_1 - \kappa_1^* \alpha_1^\dagger \end{bmatrix} + \begin{bmatrix} \eta \alpha_2 & \Gamma \\ \Gamma & \eta \alpha_2^\dagger \end{bmatrix}^{1/2} \begin{bmatrix} \eta_1(t) \\ \eta_2(t) \end{bmatrix}$$

$$\partial_t \begin{bmatrix} \alpha_2 \\ \alpha_2^\dagger \end{bmatrix} = \begin{bmatrix} E_2 - (\eta/2) \alpha_1^2 - \kappa_2 \alpha_2 \\ E_2^* - (\eta/2) \alpha_1^{\dagger 2} - \kappa_2^* \alpha_2^\dagger \end{bmatrix}$$

Here $\eta_1(t)$, $\eta_2(t)$ are delta-correlated Gaussian random processes, so that $(\alpha_j, \alpha_j^\dagger)$ are not complex conjugate except in the mean. These equations therefore define a probability distribution in a four-dimensional complex phase-space. If we were to regard each complex variable as a pair of real variables, the underlying space would be an eight-dimensional real space. The extra dimensions, relative to a classical description, allow nonclassical processes like photon antibunching to occur. However any normal ordered moment or correlation function can still be obtained in a straightforward way as a complex phase-space moment or correlation, evaluated relative to a real positive probability distribution.

(b) Deterministic analysis

In the deterministic limit of $\eta \rightarrow 0$ (which can also be regarded as the thermodynamic limit of $V \rightarrow \infty$), the stochastic terms are real and we can put $\alpha_1^* = \alpha_1^+$, $\alpha_2^* = \alpha_2^+$. This simplifies the global analysis of the equations, which now correspond to those of classical non-linear optics. A deterministic analysis is given by McNeil, Drummond & Walls (1978). This analysis is included here, in a more complete form.

It is first necessary to solve for the steady-state behaviour: for simplicity we assume that E_1, E_2 , are real. Hence one obtains (with on-resonance driving fields):

$$\alpha_2^0 = \left(\frac{1}{\kappa_2}\right) [E_2 - \eta \alpha_1^0]^2 / 2]$$

$$\alpha \equiv \alpha_1^0 = \left(\frac{1}{\kappa_1}\right) [E_1 + \eta \alpha_2^0 \alpha_1^0]^*$$

$$\alpha^* \alpha^2 + 2\left(\frac{\kappa_1 \kappa_2}{\eta^2}\right) \alpha - 2\left(\frac{E_2}{\eta}\right) \alpha^* - \left(\frac{2\kappa_2 E_1}{\eta^2}\right) = 0$$

Now, solutions exist either for $\alpha = \alpha^*$ or $\alpha \neq \alpha^*$. We call these in-phase or out-of-phase respectively. In general, therefore, it is necessary to define:

$$\alpha = r e^{i\phi}$$

$$r^3 + 2\left(\frac{\kappa_1 \kappa_2}{\eta^2}\right) r - 2\left(\frac{E_2}{\eta}\right) r \cos 2\phi - \left(\frac{2\kappa_2 E_1}{\eta^2}\right) \cos \phi = 0$$

$$\sin 2\phi + \left(\frac{\kappa_2}{\eta E_2 r}\right) E_1 \sin \phi = 0$$

We first study the in-phase solutions, which correspond to $\phi = 0$, so that:

$$r^3 + \left[\frac{2\kappa_1\kappa_2}{\eta^2} - \frac{2E_2}{\eta} \right] r - \left[\frac{2\kappa_2 E_1}{\eta^2} \right] = 0$$

The number of roots are classified according to the value of Δ , where:

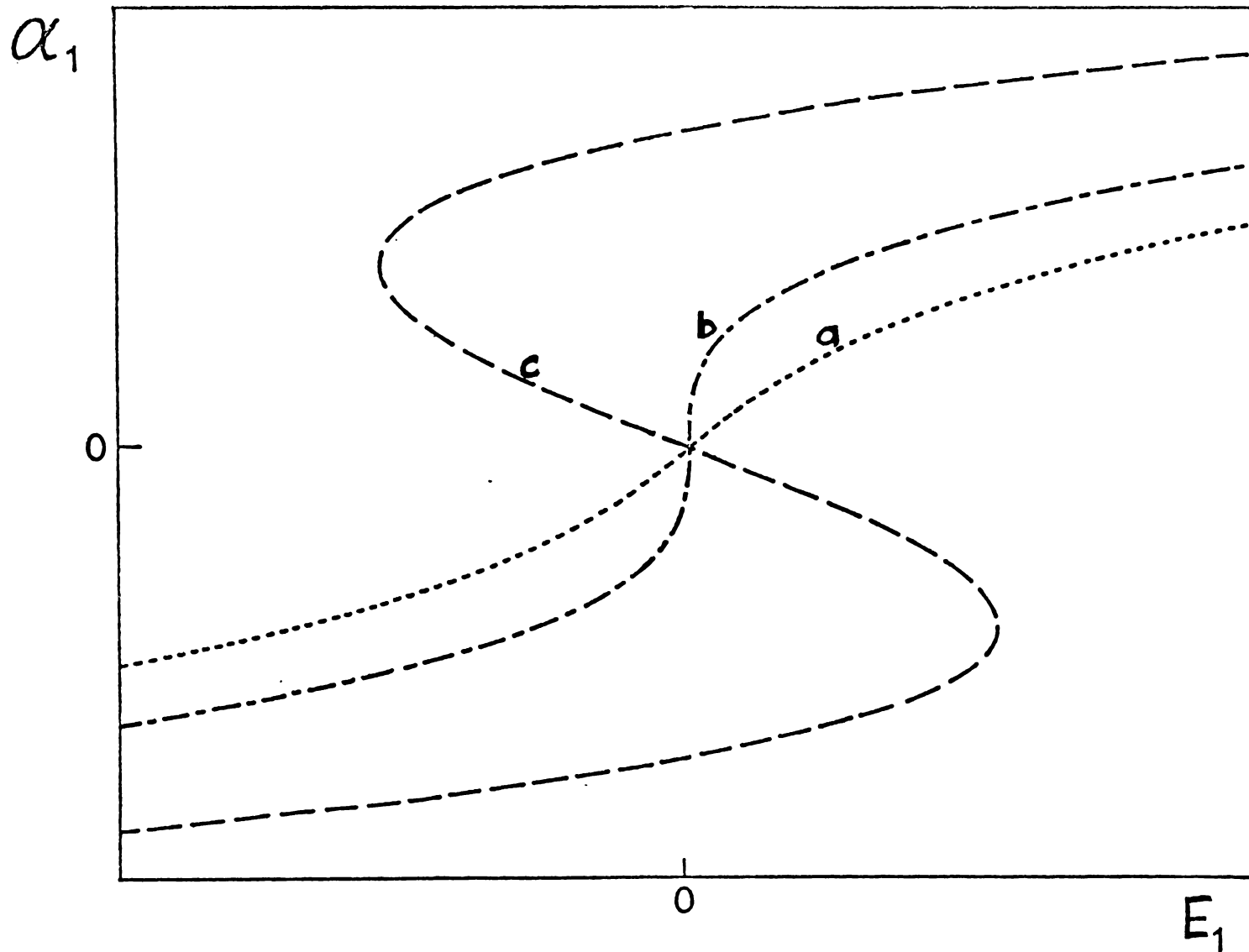
$$\Delta \equiv \left[\frac{\kappa_2 E_1}{\eta^2} \right]^2 + \left[\frac{2}{3\eta^2} (\kappa_1\kappa_2 - \eta E_2) \right]^3$$

Now for $\Delta > 0$, there is one real root, while for $\Delta < 0$, there are three roots giving the possibility of bistability. The bifurcation occurs at $\Delta = 0$. This describes a locus in the (E_1, E_2) plane which gives a boundary of bistability according to:

$$E_2 = \left[\frac{\kappa_1\kappa_2}{\eta} \right] + \left(\frac{3\eta}{2} \right) \left(\frac{\kappa_2 E_1}{\eta^2} \right)^{\frac{2}{3}}$$

In the case of $E_1 = 0$ (which is ordinary subharmonic generation) the locus reduces to a single point which is the critical point of subharmonic generation (Graham, 1973).

In the bistable region, there are three real roots. With a large enough driving field ($E_2 > E_2^c \equiv \kappa_1\kappa_2/\eta$) there is bistable behaviour in the cavity (fig 4.1.1). The stable branches have field amplitudes (α) of different sign, giving a behaviour reminiscent of a magnetic system. That is, there is the following analogy with a magnetic phase transition:



Fig(4.1.1) Sub/second harmonic generation; state equation of interferometer amplitude vs input amplitude.

(a) $E_2 < E_2^c$

(b) $E_2 = E_2^c$

(c) $E_2 > E_2^c$

$$\begin{aligned}
 E_1 &\leftrightarrow H \\
 \alpha &\leftrightarrow B \\
 E_2 &\leftrightarrow T^{-1} \\
 \kappa_1, \kappa_2 / \eta &\leftrightarrow T_c^{-1}
 \end{aligned}$$

The turning points are obtained on differentiating the state equation, and setting $\partial E_i / \partial r = 0$. Hence we obtain:

$$\left(\frac{3}{2}\right) r^2 - (E_2 / \eta) + (\kappa_1, \kappa_2 / \eta^2) = 0$$

We will see later, that this is identical with the boundary of stability. That is, the central branch is unstable and the upper and lower branches are stable.

The previous solutions were obtained with $\phi = 0$ (i.e. in-phase solutions). However in fact it is possible to also obtain solutions with $\phi \neq 0$, in the case of

$E_2 < (-E_2^c)$. This also gives a bistable region, which is closely related to the in-phase region by the symmetry transformation:

$$\begin{aligned}
 E_2 &\rightarrow -E_2 ; & \hat{a}_2 &\rightarrow -\hat{a}_2 \\
 E_1 &\rightarrow iE_1 ; & \hat{a}_1 &\rightarrow +i\hat{a}_1
 \end{aligned}$$

It is readily verified that this leaves the master equation invariant; so that one expects a related bifurcation to occur for $E_2 < (-E_2^c)$ as we shall show.

In this case, the cavity mode has a non-zero relative phase so that:

$$\cos\phi = -\left(\frac{\kappa_2 E_1}{2\eta E_2}\right)/r$$

$$r^2 = \left(\frac{2}{\eta}\right)(-E_2 - E_2^c)$$

Thus we see that the out-of-phase solutions can only exist for:

$$E_2 < -E_2^c$$

There is a clearly symmetric relation between these solutions which give a bifurcation for negative (E_2) and the bistable solutions for positive (E_2). In each case, for a second harmonic driving field of large intensity there is the possibility of multiple steady-states. However, to determine which of the solutions is stable, it is necessary to evaluate the eigenvalues for the decay of fluctuations which we turn to in part (c).

It is also possible to analyse the steady-states for an arbitrary choice of the relative input phases; however we have restricted the analysis here to the case of real input amplitudes, for simplicity.

(c) Stability properties

While the previous analysis gave the steady-states, it does not of itself yield information on stability. We therefore turn to the stability of fluctuations close to the steady-state, following the analysis of McNeil et al (1978). In this case, as before, we suppose the driving fields are on resonance. The linear stability equation is:

$$\frac{\partial}{\partial t} \begin{bmatrix} \delta\alpha_1 \\ \delta\alpha_1^+ \\ \delta\alpha_2 \\ \delta\alpha_2^+ \end{bmatrix} = - \begin{bmatrix} +\kappa_1, -\eta\alpha_2^0, -\eta\alpha_1^{0*}, 0 \\ -\eta\alpha_2^0, +\kappa_1, 0, -\eta\alpha_1^0 \\ +\eta\alpha_1^0, 0, +\kappa_2, 0 \\ 0, +\eta\alpha_1^{0*}, 0, +\kappa_2 \end{bmatrix} \begin{bmatrix} \delta\alpha_1 \\ \delta\alpha_1^+ \\ \delta\alpha_2 \\ \delta\alpha_2^+ \end{bmatrix}$$

This gives an equation for the determinant that factorises to yield the following four eigenvalues:

$$(-\lambda + \kappa_1)(-\lambda + \kappa_2) + |\eta\alpha_1^0|^2 \pm |\eta\alpha_2^0|(-\lambda + \kappa_2) = 0$$

Applying the Hurwitz theorem to these quadratics, gives the following criteria for stability:

$$\kappa_1\kappa_2 + |\eta\alpha_1^0|^2 > \kappa_2 |\eta\alpha_2^0| \quad \dots \quad (A)$$

$$\kappa_1 + \kappa_2 > |\eta\alpha_2^0| \quad \dots \quad (B)$$

The corresponding eigenvalues are as follows:

$$\lambda_1, \lambda_2 = \frac{1}{2} \left[-\eta|\alpha_2^0| + \kappa_1 + \kappa_2 \pm \sqrt{(-\eta|\alpha_2^0| + \kappa_1 - \kappa_2)^2 - 4|\eta\alpha_1^0|^2} \right]$$

$$\lambda_3, \lambda_4 = \frac{1}{2} \left[\eta|\alpha_2^0| + \kappa_1 + \kappa_2 \pm \sqrt{(\eta|\alpha_2^0| + \kappa_1 - \kappa_2)^2 - 4|\eta\alpha_2^0|^2} \right]$$

Stability occurs when both 3(A) and 3(B) are satisfied. As shown in McNeil et al (1978), violation of relation 3(B) leads to limit cycle behaviour. However it is readily seen that the violation of relation 3(A) leads to a bistable region.

This can be seen by substituting for α_1^0 in equation 3(A), giving:

$$K_1 K_2 + |\eta \alpha_1^0|^2 > \eta |E_2 - \eta \alpha_1^0|^2 / 2|$$

If we compare this with the equations in the previous section, it is clear that for $E_2 > 0$, the turning point in the bistable state equation agrees with the boundary of stability. Thus we can identify the middle branch in fig 4.1.1 as the unstable branch.

In the case of $E_2 < 0$ the situation is slightly different, as both out-of-phase and in-phase solutions can potentially occur. We first take the case of a real amplitude ("in-phase") solution. From the Hurwitz criterion, one obtains for stability:

$$E_1^2 > \left(\frac{8\eta}{K_2}\right) E_2 [|E_2| - E_c]$$

This gives a line of critical points in the (E_1, E_2) plane, which reduces to the critical point for subharmonic generation, when the primary driving field is zero.

It is also possible to obtain complex amplitude ("out-of-phase") solutions. In this case one obtains the following relation for stability:

$$E_1^2 < \left[\frac{8\eta}{\kappa_2^2} \right] E_2^2 (|E_2| - E_c)$$

In summary, for $E_2 < -E_c$ there is a line of critical points. This line is a boundary between a stable real amplitude solution, and a pair of (in general complex amplitude) solutions. The different types of solution have an exchange of stability along the critical line. The bifurcation behaviour in this case is analogous to spontaneous symmetry breaking in an equilibrium critical point phase transition.

(d) Adiabatic elimination of the harmonic mode

So far we have treated the stability properties of the coupled mode system, from a classical equation approach. In general it is possible to treat the coupled equations as (4 x 4) matrices and obtain the correlation properties due to thermal and quantum fluctuations. However in order to obtain a comparison with the results of Chapter 3, we shall in the following, work in the limit of $|\kappa_2| \gg |\kappa_1|$. In this case the variables $(\alpha_2, \alpha_2^\dagger)$ can be adiabatically eliminated from the stochastic equations. This leaves a

simpler set of equations to work with, that readily allow a comparison with the single-mode case treated previously.

The equations obtained on adiabatic elimination of $(\alpha_2, \alpha_2^\dagger)$ are as follows:

$$\frac{\partial}{\partial t} \begin{bmatrix} \alpha_1 \\ \alpha_1^\dagger \end{bmatrix} = \begin{bmatrix} E_1 + \eta \frac{\alpha_1^\dagger}{\kappa_2} (E_2 - \eta \frac{\alpha_1^2}{2}) - \kappa_1 \alpha_1 \\ E_1^* + \eta \frac{\alpha_1}{\kappa_2^*} (E_2^* - \eta \frac{\alpha_1^{\dagger 2}}{2}) - \kappa_1^* \alpha_1^\dagger \end{bmatrix} + \begin{bmatrix} \frac{\eta}{\kappa_2} (E_2 - \frac{\eta \alpha_1^2}{2}), \Gamma \\ \Gamma, \frac{\eta}{\kappa_2^*} (E_2^* - \frac{\eta \alpha_1^{\dagger 2}}{2}) \end{bmatrix}^{1/2} \begin{bmatrix} \xi_1(t) \\ \xi_2(t) \end{bmatrix}$$

A new Fokker-Planck equation can also be defined relative to the reduced stochastic equations, which is:

$$\begin{aligned} \frac{\partial}{\partial t} P(\alpha_1) = & \left\{ \frac{\partial}{\partial \alpha} \left(\kappa_1 \alpha_1 - E_1 - \eta \left(\frac{\alpha_1^\dagger}{\kappa_2} \right) \left(E_2 - \eta \frac{\alpha_1^2}{2} \right) \right) \right. \\ & + \frac{\partial}{\partial \alpha^\dagger} \left(\kappa_1^* \alpha_1^\dagger - E_1^* - \eta \left(\frac{\alpha_1}{\kappa_2^*} \right) \left(E_2^* - \eta \frac{\alpha_1^{\dagger 2}}{2} \right) \right) \\ & \left. + \frac{1}{2} \left(\frac{\partial^2}{\partial \alpha^2} \left(\frac{\eta}{\kappa_2} \left[E_2 - \eta \frac{\alpha_1^2}{2} \right] \right) + \frac{\partial^2}{\partial \alpha^{\dagger 2}} \left(\frac{\eta}{\kappa_2^*} \left[E_2^* - \eta \frac{\alpha_1^{\dagger 2}}{2} \right] \right) + \left[\frac{\partial}{\partial \alpha} \frac{\partial}{\partial \alpha^\dagger} \right] \right\} P(\alpha_1) \end{aligned}$$

At this point we can make a direct comparison with the case of nonlinear dispersion and absorption for a single mode. In the case of zero second harmonic driving field (i.e. $E_2 = 0$) we obtain identical equations provided we define:

$$\chi^{(e)} = \left(\frac{\eta^2}{4\kappa_2} \right) = \frac{\eta^2 (\kappa_2' - i\kappa_2'')}{4(\kappa_2'^2 + \kappa_2''^2)}$$

Thus both nonlinear dispersion and absorption occur.

Exactly the same bistable behaviour and antibunching will occur in this case: and the complete analysis of

Chapter 3 can be utilised. The linear dispersion (κ_1'') depends on the detuning of mode (1); while the nonlinear dispersion (χ_2'') depends on the detuning of the second harmonic mode (but with the opposite sign). This therefore provides a technique of obtaining dispersive optical bistability in a medium with a quadratic non-linearity (that is, a medium with no centre of inversion). Clearly, when $E_2 = 0$, the introduction of detuning and arbitrary input phase poses no new problems and steady-state behaviour obtained in section 3.1 will occur. In particular, as noted previously, the system can be bistable when the following relation holds:

$$\chi_1'^2 \kappa_1'^2 + \chi_2''^2 \kappa_2''^2 + 8\chi_1'\chi_2''\kappa_1'\kappa_2'' - 3\kappa_1'^2 \chi_2''^2 - 3\kappa_2''^2 \chi_1'^2 > 0$$

In terms of the detuning parameters, this defines a critical locus in the (κ_1'' , κ_2'') plane which gives a boundary of bistability. When the above relation holds, dispersive bistability will occur for a certain range of input field intensities.

We now proceed (for $E_2 \neq 0$) to analyse the properties of the reduced equations. First of all, we note that the actual steady-states available are identical to those of the full coupled equations. (In the case of a detuning in the input fields, the state equation would involve additional phase parameters relative to those discussed earlier.) The correlations close to a stable branch are obtained by linearising the stochastic equations just as in section 3.1, with the following results:

$$\begin{bmatrix} \alpha_1(t) \\ \alpha_1^*(t) \end{bmatrix} = \begin{bmatrix} \alpha_0 \\ \alpha_0^* \end{bmatrix} + \begin{bmatrix} \delta\alpha(t) \\ \delta\alpha^*(t) \end{bmatrix}$$

$$\frac{\partial}{\partial t} \delta\alpha(t) = -\underline{\underline{A}} \cdot \delta\alpha(t) + \underline{\underline{D}}(\alpha_0)^{1/2} \cdot \xi(t)$$

Here the linearised coefficients $\underline{\underline{D}}$, $\underline{\underline{A}}$ are given by:

$$\underline{\underline{D}} = \begin{bmatrix} -d & \Gamma \\ \Gamma & -d^* \end{bmatrix}$$

$$\underline{\underline{A}} = \begin{bmatrix} a & d \\ d^* & a^* \end{bmatrix}$$

Where:

$$d \equiv \left(\frac{\eta}{\kappa_2}\right) \left(\frac{\eta \alpha_0^2}{2} - E_2\right)$$

$$a \equiv \kappa_1 + \left[\frac{\eta^2 |\alpha_0|^2}{\kappa_2}\right]$$

The interesting point resulting from this is that the nonlinear interferometer with second harmonic generation, obeys virtually the same equations as the single-mode nonlinear interferometer in the limit of $|\kappa_2| \gg |\kappa_1|$. The chief difference is that there is the possibility of an extra driving field, as well as the primary field (E_1). Despite this, all the formulae developed in section 3.1 can be used, when expressed in terms of the parameters (d, a).

In the case where all the parameters are real (i.e., for resonant excitation and in-phase driving fields) the results obtained in section 3.1 can be simplified:

$$\underline{\underline{C}} = \left[\frac{1}{2(a^2-d^2)} \right] \begin{bmatrix} -d(\Gamma+a) & , & \Gamma a + d^2 \\ \Gamma a + d^2 & , & -d(\Gamma+a) \end{bmatrix}$$

$$\bar{n} = n + \left(\frac{\Gamma a + d^2}{2(a^2-d^2)} \right)$$

$$g^2(0) = 1 + \frac{1}{n} \left(\frac{\Gamma - d}{a+d} \right)$$

$$\int (w_{\phi} + w) = n \delta(\omega) + \left(\frac{1}{4\pi} \right) \left[\frac{\Gamma - d}{\omega^2 + (a+d)^2} + \frac{\Gamma + d}{\omega^2 + (a-d)^2} \right]$$

Here n is the deterministic photon number for the in-phase solution, so that:

$$n^{3/2} + 2 \left(\frac{\kappa_1 \kappa_2}{\eta^2} - \frac{E_2}{\eta} \right) n^{1/2} - \left(\frac{2 \kappa_2 E_1}{\eta^2} \right) = 0$$

$$d = 2\chi n - \frac{\eta E_2}{\kappa_2}$$

$$a = \kappa_1 + 4\chi n$$

These results illustrate that in the adiabatic limit, the only difference in the fluctuations between the case presently treated and the case treated in section 3.1 is the presence of an extra quantum fluctuation term due to the driving field (E_2). This term is significant in subharmonic generation, but not in second harmonic generation.

4.2 POTENTIAL SOLUTIONS IN THE ADIABATIC LIMIT

(a) The "thermal" limit for potential solutions

As the previous discussion of potential equations is directly applicable to the coupled mode system in the adiabatic limit, the reader is referred to section 3.2. One obtains straightforward results in the limits of:

$$(a) \quad \Gamma \gg \left| \frac{\eta E_2}{\kappa_2} - 2\chi n \right|$$

$$(b) \quad \Gamma \ll \left| \frac{\eta E_2}{\kappa_2} - 2\chi n \right|$$

The first case is the "thermal" limit, where the Fokker-Planck diffusion is due to thermal type fluctuations in the driving field or reservoirs. In this case, one obtains potential equations in the following form:

$$\begin{aligned} \frac{\partial}{\partial \alpha} \left[\kappa_1 \alpha + 2\chi \alpha^2 \alpha^* - E_1 - \frac{\eta \alpha^*}{\kappa_2} E_2 \right] \\ = \frac{\partial}{\partial \alpha^*} \left[\kappa_1^* \alpha^* + 2\chi^* \alpha^{*2} \alpha - E_1^* - \frac{\eta \alpha}{\kappa_2^*} E_2^* \right] \end{aligned}$$

A solution is possible only if $\kappa_1 = \kappa_1^*$, $\kappa_2 = \kappa_2^*$: that is, for both modes tuned (to ω_j & $2\omega_j$ respectively). In this case, on integrating, the solution to the Fokker-Planck equation is just:

$$\begin{aligned} P(\alpha) = \exp \left\{ -\frac{2}{\Gamma} \left[\kappa_1 |\alpha|^2 + \chi |\alpha|^4 - E_1 \alpha^* - E_1 \alpha \right. \right. \\ \left. \left. - \left(\frac{\eta E_2}{\kappa_2} \right) \alpha^{*2} - \left(\frac{\eta E_2^*}{\kappa_2^*} \right) \alpha^2 \right] \right\} \end{aligned}$$

This is identical to the result obtained by Graham (1973), for subharmonic generation: except that his result only includes the driving field E_2 , without the input term E_1 .

This potential in fact is applicable to the bistable situation, and can be directly compared with the laser potential of section 3.2 (we suppose E_1, E_2 are both real):

$$\text{(Laser): } P(R, \theta) = \exp \left[\frac{-2}{\Gamma} (\kappa_1 R + \chi R^2 - 2E_1 \sqrt{R} \cdot \cos \theta) \right]$$

$$\text{(Coupled modes): } P(R, \theta) = \exp \left[\frac{-2}{\Gamma} (\kappa_1 R + \chi R^2 - 2E_1 \sqrt{R} \cdot \cos \theta - (\frac{2\eta E_2}{\kappa_2}) R \cos 2\theta) \right]$$

In the case of the laser, it was not possible to have bistability (even for $\kappa_1 < 0$) as there was only one local minimum with respect to variation in θ . However in the coupled mode case, it can be seen that more than one local minimum in the θ -variable can occur, due to the extra term describing coupling to the input field. For this reason, it is possible for bistability to occur, with both input fields coherent and phase-locked relative to each other.

(b) The "quantum" limit for potential solutions

In this case, we must take the limit of small thermal fluctuations. The potential is derived as in part (a), with the use of the quantum fluctuation terms only (i.e., $\Gamma = 0$). Hence the following result is obtained:

$$v_1 = -2[\alpha_1 + 2\kappa_2(E_1 - \bar{\kappa}_1 \alpha_1) / (c^2 - \eta^2 \alpha_1^2)]$$

$$v_2 = -2[\alpha_1 + 2\kappa_2^*(E_1^* - \bar{\kappa}_1^* \alpha_1^*) / (c^{*2} - \eta^2 \alpha_1^{*2})]$$

Where:

$$c \equiv \sqrt{2\eta E_2}, \quad \bar{\kappa}_1 \equiv \kappa_1 - 2\chi^{(e)} \equiv \kappa_1 - \frac{\eta^2}{2\kappa_2}$$

The equality of crossderivatives follows immediately, and the potential is therefore obtained on integrating:

$$P(\alpha) = \exp \left\{ 2\alpha\alpha^* + \left(\frac{\bar{\kappa}_1}{2\chi}\right) \ln(c^2 - \eta^2 \alpha^2) + \left(\frac{\bar{\kappa}_1^*}{2\chi^*}\right) \ln(c^{*2} - \eta^2 \alpha^{*2}) + \left(\frac{2\kappa_2 E_1}{c\eta}\right) \ln\left(\frac{c + \eta\alpha}{c - \eta\alpha}\right) + \left(\frac{2\kappa_2 E_1^*}{c^*\eta}\right) \ln\left(\frac{c^* + \eta\alpha^*}{c^* - \eta\alpha^*}\right) \right\}$$

In order to obtain observable moments for this case, it is necessary to integrate on a suitable manifold defined so that the distribution and its derivatives all vanish at the boundary of integration. First of all, for pure second-harmonic generation it can be noted, that the result is identical to that of section 3.2.

Next we suppose that sub-harmonic generation occurs. In this case it can be seen that the distribution has singularities at $\alpha = \pm(\eta/c)$. In order to integrate the distribution function, a similar method can be used to that of section 3.2.

As the exponential factor does not introduce any new singularities, we expand this in a power series.

Hence the expression for the n'th moment is:

$$I_n = \sum_{m=0}^{\infty} 2^m \oint_C \frac{z_1^{j_1-1} z_2^{j_2-j_1-1} \left[\frac{(c\alpha^*)^{m+n}}{m!} \right] (c^*-\eta\alpha^*)^{j_2^*-j_1^*-1} (c+\eta\alpha)^{j_1^*-1}}{e} d\alpha d\alpha^*$$

On making a variable change this reduces to:

$$I_n = \sum_{m=0}^{\infty} \oint_C \frac{z_1^{j_1-1} (1-z_1)^{j_2-j_1-1} [(1-\frac{1}{2}z_1)(1-\frac{1}{2}z_2)]^{m+n} (1-z_2)^{j_2^*-j_1^*-1} z_2^{j_1^*-1}}{e} dz_1 dz_2 \times \left[\left(\frac{2^m}{m!} \right) \left(\frac{4cc^*}{\eta^2} \right)^{m+n+1} (2c)^{j_2-2} (2c^*)^{j_2^*-2} \right]$$

Where:

$$\begin{aligned} j_1 &\equiv \left(\frac{\kappa_1}{2\chi} \right) + \left(\frac{2\kappa_2 E_1}{c\eta} \right) \\ j_2 &\equiv \kappa_1 / \chi = 4\kappa_1 \kappa_2 / \eta^2 \\ j_1 &\equiv \frac{1}{2} (1 + \eta\alpha/c) \\ j_2 &\equiv \frac{1}{2} (1 + \eta\alpha^*/c^*) \end{aligned}$$

It is now necessary to find an integration path for the function. Fortunately, these integrals are identical to the expression defining a Gauss hypergeometric function. The line integrals are defined on a path that encircles each pole and traverses the Riemann sheets so that the initial and final values of the integrand are equal, which allows partial integration operations to be defined. The result is (MacRobert, 1938):

$$I_n = \left[\sum_{m=0}^{\infty} \left(\frac{2^m (4|c|^2/\eta^2)^{m+n+1}}{m!} \right) \left| F_1(-m+n, j_1, j_2, 1/2) B(j_1, j_2-j_1) \right|^2 \right. \\ \left. \times (2c)^{j_2-2} (2c^*)^{j_2^*-2} \times \left| (1 - e^{2\pi i j_1}) (1 - e^{2\pi i (j_2-j_1)}) \right|^2 \right]$$

The above expression is an exact result for the moments in the quantum limit of the coupled mode system. It holds in the limit of a coherent driving field, a zero temperature heat bath and adiabatic elimination of the second harmonic. The special functions can be evaluated either from tables or by direct numerical summation of the relevant series.

A comparison of the present result with the result of section 3.2 shows a very similar series, expressed in terms of gamma-function integrals instead of the present integrals which are related to the beta-function and hypergeometric function. We believe this shows an elegant relation between quantum fluctuations in nonlinear boson systems, and the theory of functions of several variables in the complex plane. As far as we know, the exact solutions of this type have not been obtained in earlier work; and could prove useful in other fields as well as quantum optics, where nonlinear boson interactions occur. In previous treatments of quantum fluctuations in sub-harmonic generation, the nonlinear fluctuation terms were neglected in the steady-state; so that only the thermal type of potential solution for resonant excitation was obtained (Graham, 1973).

4.3 SECOND HARMONIC GENERATION

(a) Stability properties and state equation

In the case of second-harmonic generation, a relatively straightforward state equation is found that is identical to the state equation of section 3.1, for the mode at the input frequency:

$$|E_1|^2 = n |\kappa_1 + 2\chi n|^2$$

Where:

$$\chi \equiv \eta^2 / (4\kappa_2) \quad ; \quad n \equiv \alpha \alpha^*$$

Now given that the above equation is solved for the lower frequency phase and amplitude, the second-harmonic phase and amplitude is then obtained from:

$$\alpha_2^o = \left(\frac{-1}{\kappa_2} \right) (\eta \alpha_1^2 / 2)$$

In the case of a resonant driving field, both fields increase uniformly in amplitude with $|E_1|$. When detuning is included, it is possible to have dispersive bistability in the state equation. Now the detuning of the first mode changes the linear dispersion parameter (κ_1'') while the detuning of the second mode changes the nonlinear dispersion parameter (χ''). It is clear that bistability occurs in this case for a large enough detuning, as obtained in section 3.1. In practice, it would be feasible to alter the detuning of either mode with the use of a medium of frequency-dependent refractive index. It can be noted that the bistability in this case occurs in the output at

both frequencies while previously it was only present at the input frequency (section 3.5).

In order to determine the stability properties relative to a solution for the state equation, it is necessary to satisfy the Hurwitz criterion for the eigenvalues. In the adiabatic limit discussed previously, this is straightforward: exactly the same stability properties hold as in section 3.1, with stable, unstable and stable branches of the state equation.

In the general case, we can find a solution for the eigenvalues most simply with both modes tuned to the input frequencies. In this situation, the Hurwitz criterion is given in section 4.1(c). It is easy to verify that the first relation (3A) is always satisfied. However the relation (3B) is violated at a large driving field:

$$\kappa'_1 + \kappa'_2 > |\eta \alpha_2^0| = |\eta^2 \alpha_1^2 / (2\kappa_2)| \quad . \quad . \quad . \quad (B)$$

This gives a hard-mode instability for a large driving field, as pointed out by McNeil et al (1978). The strength of the input field at this threshold is:

$$E_1^c = \left[\frac{\kappa_2 + 2\kappa_1}{\eta} \right] (2\kappa_2 (\kappa_1 + \kappa_2))^{1/2}$$

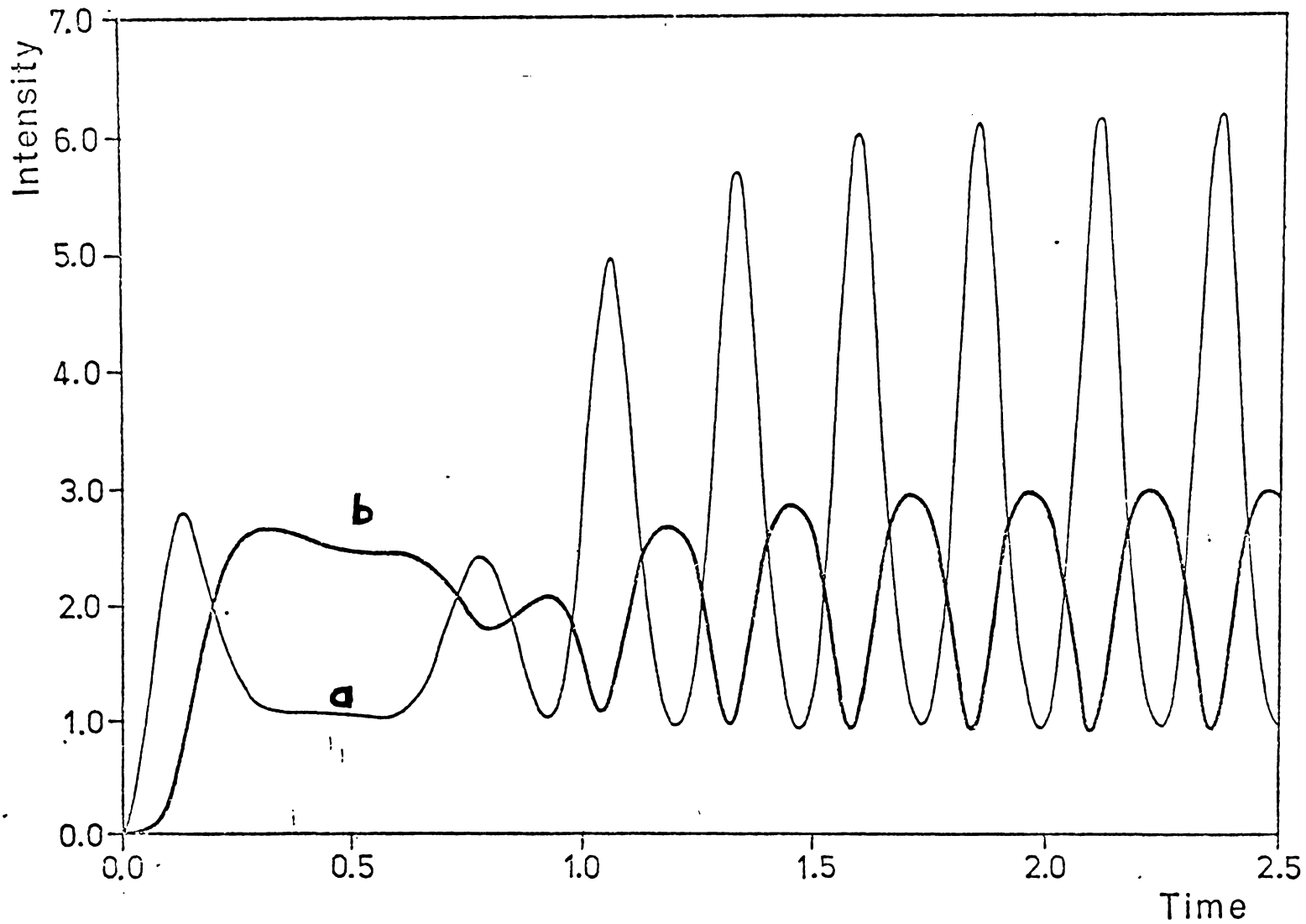
Above the threshold, a limit cycle behaviour occurs. Interestingly, this cyclic behaviour involves coupling of phase as well as of amplitude in the cavity modes. Limit cycles do not occur, for the case of purely real amplitudes. This is different from the spiking behaviour in a strongly pumped laser (Risken & Nummedal (1968);

Haken & Ohno (1976)) which occurs in the real amplitude equations. In fig 4.3.1 we give a numerical integration of the deterministic equations above threshold, showing the limit cycles in both mode intensities. The initial value in this case gives (α_1) a complex part to start the cycles.

It can be noted that the ground state has a neutral stability relative to the limit cycles, owing to the real amplitudes that occur in time-development. It is necessary for an out-of-phase fluctuation to occur (from thermal or quantum noise sources) before limit cycles can develop.

(b) Correlation properties

In the adiabatic limit, the correlation properties and spectrum, for second-harmonic generation are given by the results in section 3.1. In general in this limit, there is a "split" spectrum when any detuning is present, while a single line occurs without detuning. In all cases, photon antibunching results at high driving fields



Fig(4.3.1) Second harmonic generation; limit cycles of intensity vs time above the hard mode threshold.

(a) primary intensity

(b) second harmonic intensity

provided the external fluctuations are small. Physically this is due to enhanced production of the second-harmonic when the primary field increases in intensity. This results in a reduction of fluctuations in the primary field. We note that these calculations apply for the primary field only.

In the general case, it is necessary to diagonalise (4 x 4) arrays to obtain the correlation properties; this can be obtained in a similar way to the single-mode case discussed previously. We note however that in this case a "split" spectrum can occur without any detuning. The eigenvalues in this case are:

$$\lambda_1, \lambda_2 = \frac{1}{2} \left[-\eta |\alpha_2^0| + \kappa_1 + \kappa_2 \pm \sqrt{(-\eta |\alpha_2^0| + \kappa_1 - \kappa_2)^2 - 8\eta \kappa_2 |\alpha_2^0|} \right]$$

$$\lambda_3, \lambda_4 = \frac{1}{2} \left[\eta |\alpha_2^0| + \kappa_1 + \kappa_2 \pm \sqrt{(\eta |\alpha_2^0| + \kappa_1 - \kappa_2)^2 - 8\eta \kappa_2 |\alpha_2^0|} \right]$$

Thus a frequency splitting occurs below the hard-mode instability, at a field amplitude given by:

$$8\eta \kappa_2 |\alpha_2^0| = (\kappa_1 - \kappa_2 \pm \eta |\alpha_2^0|)^2$$

This frequency splitting is the precursor to the limit cycles that occur above the hard-mode transition, and was first predicted by McNeil et al (1978).

4.4 SUBHARMONIC GENERATION

(a) Stability properties and state equations

We now turn to the case of subharmonic generation, which gives the following state equation (we suppose K_1, K_2, E_2 are all real parameters):

$$(i) \quad \alpha_1^0 = 0 \quad ; \quad \alpha_2^0 = E_2 / K_2 \quad (|E_2| < E_2^c)$$

$$(ii) \quad \alpha_1^0 = \pm \left[\frac{2}{\eta} (|E_2| - E_2^c) \right]^{1/2} \quad ; \quad \alpha_2^0 = \frac{K_1}{\eta} \quad (|E_2| > E_2^c)$$

$$E_2^c \equiv \left(\frac{K_1 K_2}{\eta} \right)$$

It can be verified that case (i) is stable for $|E_2| < E_2^c$ while solution (ii) is stable for $|E_2| > E_2^c$. No additional instabilities occur when the full coupled stability equations are used, so that the critical point E_2^c is the only nonequilibrium transition in this case.

The problem of subharmonic generation is analysed using an approximate potential function by Graham (1973). In McNeil et al (1978) it is pointed out that in addition to the critical point transition, there can be spectral transitions in which damped oscillations in the two-time correlation functions appear. These are due to the appearance of imaginary terms in the eigenvalues of the coupled linearised deterministic equations. However, in the adiabatic limit there are no spectral transitions. In the following treatment, we will work in the adiabatic limit to obtain the spectrum and correlation function of subharmonic generation, with the inclusion of nonlinear

quantum fluctuation terms. These terms are omitted in the treatment by Graham (1973).

(b) Correlation properties in the adiabatic limit

In the general case, all correlation properties for the quantum limit are obtainable from the potential function of section 4.2. These solutions, which are exact in the limit of the steady-state and zero temperature reservoirs, give all the one-time correlation functions for arbitrary detuning and driving fields. By comparison, the potential function of Graham (1973) includes only the fluctuations due to the finite width of the distribution for a coherent state in the Wigner representation, neglecting the non-linear quantum fluctuations that are included in the present treatment.

While the potential solutions require numerical or tabular means to obtain the moments, it is possible to obtain approximate results by linearising the stochastic equations. From section 4.1 the linearised equations are (for the resonant case with κ_1, κ_2, E_2 real):

$$\frac{\partial}{\partial t} \begin{bmatrix} \delta\alpha_1 \\ \delta\alpha_1^* \end{bmatrix} = - \begin{bmatrix} a & d \\ d^* & a^* \end{bmatrix} \begin{bmatrix} \delta\alpha_1 \\ \delta\alpha_1^* \end{bmatrix} + \begin{bmatrix} -d & \Gamma \\ \Gamma & -d^* \end{bmatrix} \begin{bmatrix} \xi_1(t) \\ \xi_2(t) \end{bmatrix}$$

Where:

$$d = \left[\frac{\eta^2}{2\kappa_2} \right] d_0^2 - \left[\frac{\eta E_2}{\kappa_2} \right]$$

$$a = \kappa_1 + \left[\frac{\eta^2}{\kappa_2} \right] |d_0|^2$$

Here we suppose the deterministic equations have been solved to give the deterministic values for a stable branch. Using the results obtained in part (a) the values for d , a can be simplified:

(i) ($|E_2| < E_2^c$)

$$\begin{cases} d = -\eta E_2 / \kappa_2 \\ a = \kappa_1 \end{cases}$$

(ii) ($|E_2| > E_2^c$)

$$\begin{cases} d = -\kappa_1 \\ a = \kappa_1 + \eta (|E_2| - E_2^c) / (2\kappa_2) \end{cases}$$

The results obtained in section 3.1 can now be used to obtain the correlation function and spectrum (d , a are both real in this case):

$$\bar{n} = n + \left(\frac{\Gamma a + d^2}{2(a^2 - d^2)} \right)$$

$$g^2(0) = 1 + \frac{1}{\bar{n}} \left(\frac{\Gamma - d}{a + d} \right) \dots \dots (E_2 > E_2^c)$$

$$S(\omega + \omega_j) = n \delta(\omega) + \left(\frac{1}{4\pi} \right) \left[\frac{\Gamma - d}{\omega^2 + (a+d)^2} + \frac{\Gamma + d}{\omega^2 + (a-d)^2} \right]$$

Thus it can be noted that the fluctuations result in a finite mean photon number (even when the deterministic

result is zero, below threshold). Similarly the fluctuations always result in photon bunching relative to the coherent state. This is the complement to the case studied in section 4.3 where the quantum fluctuations resulted in photon antibunching with a coherent driving field on resonance (and zero-temperature reservoirs).

The spectrum is obtained similarly, by substituting the above values of (\mathbf{d}, \mathbf{q}) in the expression derived in section 4.1. Clearly in the on resonance case, the spectrum has a single peak at the input frequency. However it can be noted that in the neighbourhood of the critical point one of the eigenvalues vanishes, giving divergent critical fluctuations. In this vicinity, the linearised analysis is not valid and must be replaced by an exact solution of the relevant Fokker-Planck equation. The one-time correlation functions or moments are in this case obtainable from the potential solutions of section 4.2.

Finally, we point out that for a subcritical driving field (with $|E_2| < E_2^c$) the expression given above for the intensity correlations should be corrected as follows (in a Gaussian approximation for large Γ):

$$\begin{aligned}
 g^2(0) &\approx \frac{2 \langle \alpha, \alpha_1^* \rangle^2 + \langle \alpha_1^2 \rangle \langle \alpha_1^{*2} \rangle}{\langle \alpha, \alpha_1^* \rangle^2} \\
 &\approx 2 + \frac{\langle \alpha_1^2 \rangle \langle \alpha_1^{*2} \rangle}{\langle \alpha, \alpha_1^* \rangle^2} \\
 &\approx 2 + [(\eta \kappa_2 E_2 (\Gamma + \kappa_1)) / (\eta^2 E_2^2 + \Gamma \kappa_1 \kappa_2^2)]
 \end{aligned}$$

This analysis should be replaced by the complete potential solution, for $(\Gamma \rightarrow 0)$ and in the vicinity of the critical point.

4.5 SUB/SECOND HARMONIC GENERATION

(a) Sub/second harmonic bistability

In the case of both modes driven by external coherent phase-locked fields, we note that bistability can occur as pointed out in section 4.1. For simplicity, we treat the case of real, resonant input fields. In this case for a large enough second-harmonic driving field there can be bistability for:

$$|E_2| > E_2^c = \frac{\kappa_1 \kappa_2}{\eta}$$

As pointed out earlier, this can best be regarded using the analogy with a magnetic phase transition. On varying the primary input (E_1) it is possible to obtain a bistable characteristic with turning points at:

$$r^2 = \left(\frac{2}{3\eta}\right)(E_2 - E_2^c)$$

The stable branches have amplitudes of a different sign, so that to detect the bistable output it would be necessary to use a phase-sensitive detector (i.e. the fringe shift could be detected).

While in this case the second harmonic driving field has a minimum value, there is no minimum threshold, as the threshold intensity (for the primary input), tends to zero at the critical point. It is possible that this device could have potential as an optical switching unit, in which the phase is switched rather than the amplitude. Being a solid-state device, this could have advantages over the bistable operation demonstrated by Gibbs et al

(1976) using an atomic vapour with nonlinear refractive index inside a cavity. Electrical circuit switches based on sub/second harmonic bistability have in fact been suggested in computer logic applications (von Neumann).

(b) Correlations and photon antibunching

We note that the linearised results for correlations are identical to those found in section 4.4 except for changes in the deterministic amplitude (d_0) due to the extra input fields. For the real amplitude solutions, the deterministic amplitude is obtained by solving the cubic equation:

$$C = r^3 + r(B-A)$$

Where:

$$A = 2E_2/\eta$$

$$B = 2\kappa_1\kappa_2/\eta^2$$

$$C = 2\kappa_2E_1/\eta^2$$

The mean photon number is then given (in the limit of $\Gamma \rightarrow 0$) by:

$$\bar{n} = n + \frac{1}{2} \left[\frac{(n-A)^2}{(2n+B)^2 + (n-A)^2} \right]$$

Where:

$$n \equiv r^2$$

The boundary of stability is given by the vanishing of the denominator in the above expression for (\bar{n}) . In the vicinity of these regions (which have been analysed in section 4.1) the linearised analysis diverges and can be replaced by the exact solutions derived in section 4.2. Apart from this, the denominator in the above expression is always positive so that the quantum fluctuations increase \bar{n} relative to the deterministic value.

The intensity correlation function can be obtained in a similar way. This gives a result valid for real amplitude solutions, except in the vicinity of $n=0$ solutions and in the vicinity of the critical divergences mentioned previously. The first terms in the expression for $g^2(0)$ as an asymptotic series in $(\frac{1}{\hbar})$ are:

$$g^2(0) = 1 + \frac{1}{\hbar} \left[\left(\frac{2\kappa_2 \Gamma}{\eta^2} \right) + A - n \right] / [3n - A + B]$$

As the denominator is positive in the region of stable real, single-valued solutions, we see that the existence of photon bunching or antibunching is determined by the sign of $(\frac{2\kappa_2 \Gamma}{\eta^2} + A - n)$:

$$n < \frac{2E_2}{\eta} + \frac{2\kappa_2 \Gamma}{\eta^2} \quad \text{—photon bunching}$$

$$n > \frac{2E_2}{\eta} + \frac{2\kappa_2 \Gamma}{\eta^2} \quad \text{—photon antibunching}$$

The boundary for the change in photon statistics is at:

$$C^2 = (\bar{\Gamma} + A)(\bar{\Gamma} + B)^2 \quad \left(\bar{\Gamma} \equiv \frac{2\kappa_2 \Gamma}{\eta^2} \right)$$

$$\therefore E_1^2 = \frac{2}{\eta} \left(E_2 + \frac{\kappa_2 \Gamma}{\eta} \right) (\Gamma + \kappa_1)^2$$

Thus the phase diagram for the system can be thought of as being defined by five lines:

- (a) $E_1^2 = \left(\frac{8\eta}{27\kappa_2^2}\right)(E_2 - E_2^c)^3$ (bistability boundary for $E_2 > 0$)
- (b) $E_1^2 = \left(\frac{8\eta}{\kappa_2^2}\right)E_2^2(-E_2 - E_2^c)$ (bistability boundary for $E_2 < 0$)
- (c) $E_1^2 = \frac{2}{\eta}\left(E_2 + \frac{\kappa_2\Gamma}{\eta}\right)(\Gamma + \kappa_1)^2$ (change in photon statistics boundary)
- (d) $|\eta\alpha_2^0| = \kappa_1 + \kappa_2 \quad (E_1 > 0)$ (hard mode instability for $E_1 > 0$)
- (e) $|\eta\alpha_2^0| = \kappa_1 + \kappa_2 \quad (E_1 < 0)$ (hard mode instability for $E_1 < 0$)

This "Phase diagram" is only a true phase diagram in the limit of zero fluctuations; which corresponds to a coherent driving field, zero temperature reservoirs, and the infinite volume limit. In addition, a complete phase diagram would include complex input amplitudes, resulting in a four-dimensional space of input parameters. This would mean that the boundaries of stability would be three-dimensional manifolds embedded in the four-dimensional space of input amplitudes. However in the present work we have included only real input amplitudes, which gives the main features of the nonequilibrium transitions that occur in the coupled mode equations.

In the case of ($A < n$), as remarked earlier, photon antibunching with ($g^2(0) < 1$) is possible. This effect can be maximised by letting E_2 have negative values. In this case the antibunching is enhanced relative to the result in section 4.3. This requires that the second-harmonic driving field is input (180°) out-of-phase relative to the real phase solutions discussed in part (a). In the case that E_2 has large negative values, it is clear that the intensity correlation function would tend to the quantum limit of ($1 - 1/n$), which corresponds to a pure number state. However this limit is not physically accessible due to the existence of a critical point instability for large negative values of E_2 .

In order to analyse this more exactly, we note the following solution to the state equation in the relevant region:

$$n \approx [C/(B-A)]^2$$

provided:

$$1 \ll n \ll |B-A| \quad ; \quad |B-A|^2 \ll C^2 \ll |B-A|^3$$

Provided $E_2 \approx -E_2^c$, it is clear that stability properties are satisfied, and the result for the intensity correlation function is, (with $\Gamma = 0$):

$$g^2(0) = 1 - \frac{1}{2n}$$

Now normally, when a second harmonic is frequency converted to give a field at half the frequency, one obtains a photon bunching effect, as would occur here at large enough ($|E_2|$). However in this case the field is input in addition to a primary field, and 180° out-of-phase. In this situation the additional field causes induced emission of photons out of the primary mode, thus enhancing the antibunching effect relative to the case of a single primary input. This is a similar mechanism to that proposed by Stoler (1974), for a transient situation. Here we have the possibility of a measurement being made in the steady state.

The interesting feature of the nonclassical correlations obtained in this way, is that they are essentially a property of the interacting radiation modes only. The nonlinear medium has only entered the Hamiltonian via coupling between the field modes, and the type of correlation obtained is a function of the phase and amplitude of the input driving fields. A verification of these correlations would provide evidence that nonclassical correlation properties are inherent in the structure of the radiation field, rather than due to a neoclassical mechanism in which the field is a classical one.

CHAPTER 5: COOPERATIVE FLUORESCENCE

In Chapters 3 and 4 the aim of the theory was to deal with a quantum field, where interactions were all included in the Hamiltonian of the field. This procedure is reasonable in much of nonlinear optics, provided atomic saturation is negligible. In this chapter we turn to a specific model of the nonlinear interaction, a dipole interaction with N two-level atoms within an interferometer. In this case, some new types of nonequilibrium transitions can occur that are due specifically to the atomic transition properties.

In sections 5.1 and 5.2 we give an introduction to cooperative fluorescence theory, and to the atomic operator algebra resulting in the Maxwell-Bloch equations. In sections 5.3 to 5.6 we treat the case of adiabatically eliminating the atomic variables. We first treat the nonequilibrium transitions and bistable region for homogeneous broadening, including detuning of the atoms and the interferometer. In section 5.4 the inhomogeneous broadening of the atomic line is included. In section 5.5 the theory is extended to include quantum fluctuations by adapting the well known laser Fokker-Planck equation (Haken, 1970). In section 5.6 a Gaussian input field is treated, in which case augmented photon bunching occurs instead of bistability.

In sections 5.7 to 5.9 we treat the case of adiabatically eliminating the field variables, giving a

collective decay mode. Within the cooperation lifetime, the collective atomic "spin" is invariant (J^2 -invariance) allowing the use of atomic coherent states in treating this problem. This allows us to solve the semiclassical (Maxwell-Bloch) equations exactly in the adiabatic, J^2 -invariant limit, as shown in section 5.7. In section 5.8 this is used to solve for the exact semiclassical spectrum, demonstrating the existence of multiple sidebands in this approximation above threshold (although the extra sidebands vanish in the strong field limit). In section 5.9 we turn to the quantum fluctuations in this case, and obtain the exact distribution function in the thermodynamic limit. This shows the existence of a non-equilibrium critical point, with a distribution over a family of "Lotka-Volterra" cycles above the critical point.

5.1 INTRODUCTION: COOPERATIVE FLUORESCENCE AND OPTICAL BISTABILITY

The term "cooperative fluorescence" is a lengthy title for a simple process. It is well known that when an atom is irradiated by a near-resonant field, fluorescent radiation is emitted close to the transition frequency. When a collection of atoms is similarly irradiated the fluorescence is modified by cooperative effects that depend in a nonlinear way on the number of atoms present. There is a corresponding nonlinear modification of the propagating field. In this chapter, effects that arise in this way are termed "cooperative fluorescence", to distinguish them from the well known behaviour of one atom fluorescence.

In order to give some background to this topic, we recall that early perturbation theory treatments of resonance fluorescence of one atom were given not long after the introduction of nonrelativistic quantum mechanics, by Weisskopf and Wigner (1930, 1931). These treatments were restricted to low intensity radiation: for monochromatic excitation at low intensities the fluorescent light is monochromatic, and at the same frequency. Earlier results were obtained using the correspondence principle by Kramers and Heisenberg, who calculated the scattering cross-section of atomic electrons. At long wavelengths the elastic scattering cross-section varies as ω^4 (Rayleigh's law). At short wavelengths a classical analysis predicts a constant cross-section given by the free electrons (Thomson

scattering). When the final atomic state is different from the initial, the scattered light will have a different frequency (Raman effect): this leads to the Stokes line in atomic absorption spectra, which is a red-shifted line.

The achievement of Weisskopf & Wigner was to introduce radiation damping into the theory of Kramers & Heisenberg, which would have predicted an infinite cross-section on resonance. The Wigner-Weisskopf theory on the other hand, gave a finite Lorentzian absorption line. Other line-broadening effects occur in practice, including collision-broadening, and inhomogeneous broadening due to Doppler effects and spatial inhomogeneity.

Nonlinear effects were initially neglected in the study of resonance fluorescence, possibly because of the lack of high intensity sources prior to the development of the laser. The spectrum of fluorescent light at high input intensity was calculated by Mollow (1969) who analysed a coherent light source interacting with a two-level atom, and predicted a three-peak spectrum. Experiments by Walther et al (1975) and by Wu, Grove & Ezekiel (1975) verified this calculation. Other calculations were made by Oliver, Resayne & Tallet (1971), Hassan & Bullough (1975), Swain (1975), Smithers & Freedhoff (1975), Cohen-Tannoudji (1975). The next topic of interest was the intensity correlation function, which was first calculated by Carmichael & Walls (1975,1976). These workers predicted photon antibunching in the fluorescent radiation, which was observed by Kimble et al (1977,1978).

While the above work was for one-atom interactions, there was also great interest in nonlinear cooperative atomic interactions. In an excellent early work, Dicke (1954) showed the possibility of cooperative super-radiant effects, which were first observed by Skribanowitz et al (1973). While superradiance is a transient phenomenon, of greater interest to workers at this time was the observation of laser oscillations, predicted by Schawlow & Townes (1958). The similar phenomenon of the maser, in the microwave region, was first proposed by Weber (1953). A good summary of the early theoretical work on the laser, and corresponding experiments, is given by Haken (1970).

More recently, interest has arisen in cooperative nonlinear atomic fluorescence with an external coherent driving field, because of the possible applications as nonlinear quantum optical devices in the fields of optical communications and computer logic (Venkatesan, 1977). The interaction of identical two-level atomic systems with a coherent driving field, and a collective reservoir of radiation modes, was discussed by Senitzky (1972) who obtained approximate results valid for very strong and very weak fields, showing the existence of a threshold for oscillations. Exact results valid for all input intensities in the thermodynamic limit were obtained by Drummond & Carmichael (1978), showing the existence of a critical point phase transition for this Hamiltonian, in the thermodynamic limit and rotating wave approximation. These results are discussed in detail and extended, in the

present thesis. The problem discussed by Senitzky represents a highly cooperative situation with a J^2 -invariant (collective) decay mechanism similar to the decay mechanism in super-fluorescence: for this reason the results obtained in this case would apply within a "cooperation lifetime" from the onset of interaction. The relationship between J^2 -invariant and J^2 -breaking decay is discussed by Walls et al (1978).

A lot of the current interest in cooperative fluorescence was stimulated by the idea that optical bistability could occur in a nonlinear medium enclosed within a high-Q Fabry-Perot interferometer (Seidel; Szoke et al (1969); Austin & De Shazer (1971); Spiller (1971, 1972); McCall (1974)).

Optical bistability was first observed by Gibbs et al (1976). However, while a great deal of theoretical work was directed toward the problem of absorptive (resonant) bistability (Bonifacio & Lugiato (1976, 1978), Meystre (1978), Narducci et al (1978), Carmichael & Walls (1977), Willis (1977)), it was found in practice that it was simpler to observe optical bistability in a dispersive experiment, with detuning of the laser relative to the atomic transition and Fabry-Perot interferometer (Gibbs et al, 1976). More recently, the dispersive nonlinearity in a Kerr medium was proposed as a source of bistability (Felber & Marburger (1976); Marburger & Felber (1978)). This has been already discussed in a Hamiltonian model including quantum fluctuations, in section 3.5 of this thesis. One of the objectives of this chapter is to unify the work on a Kerr medium with cooperative fluorescence

models of optical bistability, by obtaining exact expressions in various cases for the anharmonicity parameter. We are able to show that with a high-Q interferometer, in the dispersive limit (of large detuning of the atomic transition), the nonlinear polarisability results - including quantum fluctuations - are obtained exactly. This gives a microscopic justification of the Hamiltonian model used in Chapter 3.

When both dispersion and partial atomic saturation occur, the problem of the region of bistability is more difficult. This was discussed by Bonifacio and Lugiato (1978), Willis & Day (1978), who did not however derive the complete bistability region. The bistability region for a running wave and homogeneous broadening was obtained originally by Hassan, Drummond & Walls (1978), and also by Agrawal & Carmichael (1978 a,b). These results are extended in this thesis, as we include an arbitrary mode function (which is more realistic than a running wave) and also investigate inhomogeneous broadening.

Both inhomogeneous broadening and transverse mode structures were included in the work of McCall (1974), who obtained expressions for the differential gain without calculating the bistable state equation in these cases. Effects due to a Lorentzian inhomogeneous broadening are mentioned by Bonifacio & Lugiato (1978), while Doppler broadening is mentioned by Willis & Day (1978). However these authors do not give details of the bistability regions in these cases. Work in this direction (including numerical results) has been obtained by Sandle (1978). In the present thesis we give general expressions for the

single-mode state equation including inhomogeneous broadening and an arbitrary mode structure. Exact numerical results are obtained for the case of Gaussian broadening and a running wave. In this situation, the effect of inhomogeneous broadening is very significant. The numerical studies show that dispersive bistability can be achieved with lower atomic densities and lower threshold intensities than in the inhomogeneously broadened absorptive case. This is in general agreement with the observations of Gibbs et al (1976), Venkatesan (1977).

5.2 ATOMIC OPERATORS AND BLOCH EQUATIONS

(a) Atomic operators

In the quantum theory for an n-level atom, an n-vector of complex numbers represents any pure state. The statistical properties of a mixture of states is represented by a density operator defined as:

$$\hat{\rho} = \sum_k \rho_{kk} |k\rangle\langle k|, \quad \sum_k \rho_{kk} = 1$$

Any observable property is obtained on taking the trace with the corresponding operator.

The interaction of the atom with the electromagnetic field is obtained from the interaction Hamiltonian that takes account of individual particle-field interactions (Sakurai, 1967). To lowest order the interactions are dominated by electric dipole terms in optical regions. However not all transitions are dominated by electric dipole terms, which can be forbidden when there are parity or angular momentum selection rules. In these cases, other transitions become significant, like the magnetic dipole (M1) or electric quadrupole (E2) transitions. These have typically longer lifetimes (10^{-3} s) compared with lifetimes of order (10^{-8} s) for the electric dipole transitions.

In the dipole approximation, the electric dipole operator ($\hat{\mu}$) is expanded in a basis of eigenvectors of the atomic Hamiltonian. This gives a total Hamiltonian that includes interactions with an external field:

$$\hat{\underline{M}} = \sum_{k \in \Lambda} \underline{M}_{k e} |k\rangle\langle e|$$

$$\hat{H}_a = \sum_i \hbar \omega_i |i\rangle\langle i|$$

$$\hat{H} = \hat{H}_a - \hat{\underline{M}} \cdot \hat{\underline{E}}$$

For two-level atoms, atomic raising and lowering operators are defined as follows:

$$\hat{\sigma}^+ \equiv |1\rangle\langle 0|$$

$$\hat{\sigma}^- \equiv |0\rangle\langle 1|$$

Where $|0\rangle$ is the ground state, and $|1\rangle$ is the atomic excited state. These can be used to define operators with spin- $\frac{1}{2}$ commutation relations, which are proportional to Pauli matrices:

$$\hat{\sigma}^\pm = \hat{\sigma}^1 \pm i \hat{\sigma}^2$$

$$\hat{\sigma}^3 \equiv \frac{1}{2} \{ |1\rangle\langle 1| - |0\rangle\langle 0| \}$$

$$[\hat{\sigma}^i, \hat{\sigma}^j] = i \epsilon_{ijk} \hat{\sigma}^k$$

Other useful operator relations can be found in Agarwal (1974). In this case the dipole operator is expressed as follows, where \underline{R} is a vector with complex components that specifies the polarisation transition properties:

$$\hat{\underline{M}} = \underline{R} \hat{\sigma}^+ + \underline{R}^* \hat{\sigma}^-$$

Hence the total Hamiltonian in the dipole and rotating wave approximations is as follows, for interacting atoms:

$$\begin{aligned}\hat{H} &= \hat{H}_A + \hat{H}_F + \hat{H}_{AF} \\ \hat{H}_A &= \sum_{M=1}^N \hbar \omega_M \hat{\sigma}_M^z \\ \hat{H}_F &= \sum_{\lambda} \hbar \omega_{\lambda} \hat{a}_{\lambda}^{\dagger} \hat{a}_{\lambda} \\ \hat{H}_{AF} &= \hbar \sum_{\lambda} \sum_M [g_{\lambda M} \hat{a}_{\lambda}^{\dagger} \hat{\sigma}_M^{-} + g_{\lambda M}^* \hat{a}_{\lambda} \hat{\sigma}_M^{+}] \\ g_{\lambda M} &= \mathbf{p}^* \cdot i \mathbf{u}_{\lambda}^*(\mathbf{r}_M) \left[\frac{\omega_{\lambda}}{2 \hbar \epsilon_0} \right]^{1/2} = g_{\lambda} \cdot \mathbf{u}_{\lambda}^*(\mathbf{r}_M)\end{aligned}$$

Here \mathbf{r}_M , ω_M are the position and transition frequency of the M 'th atom. Atomic velocity can be included by a change in the effective transition frequency (Haken, 1970), or by allowing for time-dependent positions.

In some cases, it is useful to deal with collective spin operators. These are especially useful when the atoms are in a volume small compared to a wavelength, or if interactions with a single travelling wave mode are included. For this purpose, we define:

$$\begin{aligned}\hat{J}^{\pm} &= \sum_M \hat{\sigma}_M^{\pm} e^{\pm i \mathbf{k}_{\lambda} \cdot \mathbf{r}_M} \\ \hat{J}^z &= \sum_M \hat{\sigma}_M^z\end{aligned}$$

Where \underline{k}_λ is the single-mode wave-vector. These operators are useful as they correspond to field mode operators in the adiabatic limit of rapid field decay. In this limit, as shown by Bonifacio et al (1971), the field correlations are:

$$\langle \hat{a}_\lambda^{+n} \hat{a}_\lambda^n \rangle \propto \langle \hat{J}^{+n} \hat{J}^{-n} \rangle$$

(b) Maxwell-Bloch equations

The Maxwell-Bloch equations are semiclassical equations that include field-atom coupling and damping. Reviews are given by Haken (1970), Kryukov & Ketokhov (1970), Lamb (1971). Here we derive the equations from a Hamiltonian method following Louisell (1973). In fact the equations treated are similar to those of a single-mode laser, and a Fokker-Planck equation can be derived also (see Haken, 1970, and the references mentioned there).

We suppose the atoms have a pencil-shaped distribution in the z -direction; so that the field modes in the (x, y) directions are treated as reservoirs, for atomic decay. The total Hamiltonian is therefore:

$$\hat{H} = \sum_{j=1}^5 \hat{H}_j$$

$$\hat{H}_1 = \hbar \left[\sum_{\lambda} \omega_{\lambda} \hat{a}_{\lambda}^{+} \hat{a}_{\lambda} + \sum_{M=1}^N \omega_M \sigma_M^z \right]$$

$$\hat{H}_2 = \hbar \sum_{\lambda} \sum_{\mu} \left[g_{\lambda\mu} \hat{a}_{\lambda}^{\dagger} \hat{\sigma}_{\mu}^{-} + g_{\lambda\mu}^{*} \hat{a}_{\lambda} \hat{\sigma}_{\mu}^{+} \right]$$

$$\hat{H}_3 = i\hbar \sum_{\lambda} \left[\hat{a}_{\lambda}^{\dagger} E(t) e^{-i\omega_{\lambda} t} - \hat{a}_{\lambda} E^{*}(t) e^{i\omega_{\lambda} t} \right]$$

$$\hat{H}_4 = \sum_{\lambda} \left[\hat{\Gamma}_{\lambda} \hat{a}_{\lambda}^{\dagger} + \hat{\Gamma}_{\lambda}^{\dagger} \hat{a}_{\lambda} \right]$$

$$\hat{H}_5 = \sum_{\mu} \left[\hat{\Gamma}_{\mu} \hat{\sigma}_{\mu}^{+} + \hat{\Gamma}_{\mu}^{\dagger} \hat{\sigma}_{\mu}^{-} + \hat{\Gamma}_{\mu}^{\mathcal{Z}} \hat{\sigma}_{\mu}^{\mathcal{Z}} \right]$$

Here $\omega_{\lambda}, \omega_{\mu}$ are as defined previously, while $E(t)$ is an external driving field of frequency ω_j . The reservoirs for energy dissipation are $\hat{\Gamma}_{\lambda}, \hat{\Gamma}_{\lambda}^{\dagger}$ for the field mode λ , and $\hat{\Gamma}_{\mu}, \hat{\Gamma}_{\mu}^{\dagger}, \hat{\Gamma}_{\mu}^{\mathcal{Z}}$ for the individual atoms. In this treatment each reservoir describes an individual decay process, without coupling or correlations between reservoirs. The above Hamiltonian does not explicitly include collision processes, which can be significant in some situations. These have been treated from a master equation approach also. However collisional broadening generally results in a Lorentzian line-shape of a similar type to that of this model (Louisell, 1973).

The master equation for this process is obtained as in Chapter 1, with the following result:

$$\begin{aligned} \frac{\partial}{\partial t} \hat{\rho} &= \left(\frac{1}{i\hbar} \right) \left[H_1 + H_2 + H_3, \hat{\rho} \right] + \hat{\mathcal{L}}_4[\hat{\rho}] + \hat{\mathcal{L}}_5[\hat{\rho}] \\ \hat{\mathcal{L}}_4[\hat{\rho}] &= \sum_{\lambda} \kappa_{\lambda} \left\{ \left[\hat{a}_{\lambda} \hat{\rho}, \hat{a}_{\lambda}^{\dagger} \right] + \left[\hat{a}_{\lambda}, \hat{\rho} \hat{a}_{\lambda}^{\dagger} \right] + 2n_{\lambda}^{\text{th}} \left[\left[\hat{a}_{\lambda}, \hat{\rho} \right], \hat{a}_{\lambda}^{\dagger} \right] \right\} \\ \hat{\mathcal{L}}_5[\hat{\rho}] &= \sum_{\mu} \left\{ \left(\frac{\gamma_{\mu}}{2} \right) \left\{ (1+n_{\mu}^{\text{th}}) \left[\left[\hat{\sigma}_{\mu}^{-} \hat{\rho}, \hat{\sigma}_{\mu}^{+} \right] + \left[\hat{\sigma}_{\mu}^{-}, \hat{\rho} \hat{\sigma}_{\mu}^{+} \right] \right] + \right. \right. \\ &\quad \left. \left. + n_{\mu}^{\text{th}} \left[\left[\hat{\sigma}_{\mu}^{+} \hat{\rho}, \hat{\sigma}_{\mu}^{-} \right] + \left[\hat{\sigma}_{\mu}^{+}, \hat{\rho} \hat{\sigma}_{\mu}^{-} \right] \right] \right\} + \right. \\ &\quad \left. + \gamma_{\mu} \left\{ \left[\hat{\sigma}_{\mu}^{\mathcal{Z}} \hat{\rho}, \hat{\sigma}_{\mu}^{\mathcal{Z}} \right] + \left[\hat{\sigma}_{\mu}^{\mathcal{Z}}, \hat{\rho} \hat{\sigma}_{\mu}^{\mathcal{Z}} \right] \right\} \right\} \end{aligned}$$

Here κ_λ , n_λ^{th} are the decay rate and thermal occupation number of mode (λ). Similarly, γ_0 is the Einstein A-coefficient for the atoms, n^{th} the thermal occupation number of the atomic decay reservoirs, and γ_p is the coefficient of any extra phase decay processes. The equilibrium atom inversion depends on n^{th} as follows:

$$\langle \hat{\sigma}_M^z \rangle = d^0 = -\frac{1}{2} \left[\frac{1}{1+2n^{\text{th}}} \right]$$

$$n^{\text{th}} = \left[\exp(\hbar\omega / kT) - 1 \right]^{-1}$$

The above description applies to an arbitrary group of N distinguishable atoms. The combined Maxwell-Bloch equations are obtained on utilising a semiclassical decorrelation. In fact these are similar to the Heisenberg equations of motion, with the addition of decay rates arising from the energy dissipation into thermal reservoirs:

$$\frac{\partial}{\partial t} \langle \hat{a}_\lambda \rangle = -\kappa_\lambda \langle \hat{a}_\lambda \rangle - i \sum_M g_{\lambda M} \langle \hat{\sigma}_M^- \rangle + E(t) \quad (\& \text{c.c.})$$

$$\frac{\partial}{\partial t} \langle \hat{\sigma}_M^- \rangle = -\gamma_M \langle \hat{\sigma}_M^- \rangle + 2i \sum_\lambda g_{\lambda M}^* \langle \hat{a}_\lambda \rangle \langle \hat{\sigma}_M^z \rangle \quad (\& \text{c.c.})$$

$$\frac{\partial}{\partial t} \langle \hat{\sigma}_M^z \rangle = -\gamma_M^{\text{eff}} [\langle \hat{\sigma}_M^z \rangle - d^0] + i \sum_\lambda \left\{ g_{\lambda M} \langle \hat{a}_\lambda^+ \rangle \langle \hat{\sigma}_M^- \rangle - g_{\lambda M}^* \langle \hat{a}_\lambda \rangle \langle \hat{\sigma}_M^+ \rangle \right\}$$

The above equations are the semiclassical Maxwell-Bloch equations, which form the basis for much current theoretical work on optical bistability, as well as describing superradiance, atomic fluorescence and the semiclassical behaviour of a laser. The equations have been written in the rotating frame relative to the input frequency ω_0 . The definition of symbols is as follows:

$$\kappa_\lambda \equiv \kappa'_\lambda + i(\omega_\lambda - \omega_j)$$

$$\gamma_M \equiv \gamma_P + \gamma_0(n^{th} + 1/2) + i(\omega_M - \omega_j)$$

$$\gamma_{11} \equiv \gamma_0(1 + 2n^{th})$$

These equations clearly reduce to the Einstein rate equations when there is no longitudinal coherent field (i.e. $\langle \hat{a}_\lambda \rangle = 0$). However in much of the following work it will be useful to work with a single coherent field mode, thus neglecting spatial fluctuations. This approximation is related to the spatial mean field theory approximations used in statistical mechanics. The validity of the single-mode method is investigated by Meystre (1978) using a numerical method. In his work it was found that the single-mode method is valid for low mirror transmission and low absorption, when used to study optical bistability. A similar result was also obtained by Bonifacio & Lugiato (1978).

A particularly simple equation results when the single-mode is a travelling wave, so that all the coupling parameters are equal. Here it is useful to set:

$$\bar{g} = g_\lambda / \sqrt{V}$$

In this case one obtains:

$$\frac{\partial}{\partial t} \langle \hat{a} \rangle = -\kappa \langle \hat{a} \rangle - i \sum_M \bar{g} \langle \hat{\sigma}_M^- \rangle + [(\dagger)] \quad (\& \text{c})$$

$$\frac{\partial}{\partial t} \langle \hat{\sigma}_M^- \rangle = -\gamma_M \langle \hat{\sigma}_M^- \rangle + 2i \bar{g}^* \langle \hat{a} \rangle \langle \hat{\sigma}_M^z \rangle \quad (\& \text{c})$$

$$\frac{\partial}{\partial t} \langle \hat{\sigma}_M^z \rangle = -\gamma_{11}^M [\langle \hat{\sigma}_M^z \rangle - d_0] + i \{ \bar{g} \langle \hat{a}^\dagger \rangle \langle \hat{\sigma}_M^- \rangle - \bar{g}^* \langle \hat{a} \rangle \langle \hat{\sigma}_M^+ \rangle \}$$

In the above equations, the atomic operators have been redefined by a phase factor to remove the spatial phase-dependence of the travelling-wave mode function. In this case, the only difference between different atoms arises from inhomogeneous broadening. This can be described by an inhomogeneous atomic frequency distribution. One of the most common types of inhomogeneous broadening is the Gaussian line-shape (either due to Doppler broadening, or in the solid-state, due to inhomogeneity in the medium). Here the equations can be written in terms of a line-shape function, and we will treat this case in section 5.4. We will suppose that there are N atoms distributed over an active volume V_0 , with density ρ_0 . In cases where the active volume is different from the mode quantisation volume, it will be useful to define an effective atomic density by setting:

$$\begin{aligned}\rho &= \sum_{\mu} |u(\underline{r}_{\mu})|^2 \\ &= \rho_0 \int_{V_0} |u(\underline{r})|^2 d^3r\end{aligned}$$

We note that this coincides with the usual definition of the density in the case that the active volume is the same as the total volume. The integration relative to V_0 means integration over the active volume V_0 , which is less than or equal to the total interferometer volume V_r . The effective density of atoms (ρ) is less than or equal to the actual density (ρ_0) within the active volume.

5.3 DISPERSIVE BISTABILITY IN A HIGH-Q INTERFEROMETER

(a) Adiabatic elimination of atomic variables

In the case of a high-Q cavity, the atomic variables can be adiabatically eliminated provided $\kappa' \ll \gamma_{\perp}$; that is, provided the atomic variables relax on a much faster time-scale than the interferometer modes. Thus we will analyse the problem of a high-Q interferometer with an external coherent driving field, and an internal medium of two-level atoms, with the atoms decaying independently by spontaneous emission. We suppose that the atoms are driven off resonance, so that dispersive nonlinearity dominates over absorptive nonlinearity. It is in this case that optical bistability has been most easily observed (Gibbs et al, 1976).

Effects that can be significant due to spatial propagation (Saunders et al 1976, McGillivray & Feld 1976, Saunders & Bullough 1977) and self-focussing (Marburger & Felber 1978) are neglected. We expect that ignoring spatial propagation is a good approximation in the present situation for these reasons:

- (i) In a high-Q interferometer, the nonresonant modes are damped rapidly: we suppose that mode spacings exceed the nonlinear frequency shifts.
- (ii) The spatial mean field approach has been shown to be valid for low transmission and absorption.
- (iii) In dispersive operation, the atomic absorption is indeed low.

- (iv) In a solid state medium, the mode structure can be included directly in the state equation.
- (v) In a Doppler broadened medium, atomic velocity can be included by direct integration. This is shown in detail in section 5.4.

The model treated here is similar in its treatment of atomic variables to that of McCall (1974): however, by utilising single mode approximations it is possible to obtain state equations which enable a direct calculation of the bistable region. The state equation for a travelling wave on resonance is identical to that of Bonifacio & Lugiato (1976). Here we generalise these results to dispersive bistability, and include the effects of the standing wave mode functions. While most experiments take place in a standing wave interferometer, we emphasise also the results for a travelling wave (ring cavity). These give the simplest equations, and the critical region can be obtained in detail.

We also give a derivation of the equivalent anharmonicity parameter in the limit of large atomic detuning (dispersive limit), for comparison with the results of Chapter 3.

From section 5.2, the general result for the steady-state of the atomic variables is (in the case of no Doppler broadening):

$$j_M^- \equiv \langle \hat{\sigma}_M^- \rangle = [2ig_M^* d_M \alpha] / \gamma_M$$

$$d_M \equiv \langle \hat{\sigma}_M^z \rangle = d^0 / \Pi_M$$

Where:

$$\alpha \equiv \langle \hat{a} \rangle$$

$$\Pi_M \equiv [1 + 2|g_M \alpha|^2 [\gamma_M^{-1} + \gamma_M^{*-1}] / \gamma_M'']$$

Hence the result for the field variables is as follows, when the atomic variables have been adiabatically eliminated:

$$\frac{\partial}{\partial t} \alpha = -\kappa \alpha + E(t) + 2\alpha \sum_M \frac{d^0 |g_M|^2}{\gamma_M \Pi_M}$$

This result can include both inhomogeneous broadening and an arbitrary mode function. As we shall treat inhomogeneous broadening in section 5.4, the following results will assume homogeneous broadening only. In this case, one obtains, for a mode function $u(\underline{r})$, the following equation (where $g_M \equiv g u^*(\underline{r}_M)$):

$$\frac{\partial}{\partial t} \alpha = -\kappa \alpha + E(t) + 2\alpha d^0 (\rho_0 |g|^2 / \gamma) \int_{V_0} \left[\frac{|u(\underline{r})|^2 d^3 \underline{r}}{\Pi(\underline{r})} \right]$$

$$\Pi(\underline{r}) \equiv [1 + 4|g \alpha|^2 |u(\underline{r})|^2 \gamma^\perp / [\gamma_{||} |\gamma|^2]]$$

It is useful to analyse the equations resulting with reduced variables, defined in terms of the threshold photon number (n_0), as follows:

$$V = [V_0 \rho_0 / \rho]$$

$$C = [-|g|^2 \rho d_0 / (\kappa' \gamma_{\perp})]$$

$$n_0 = [\gamma_{\perp} \gamma_{\parallel} V / (4|g|^2)]$$

$$y = E_0 / [\kappa' \sqrt{n_0}] \quad ; \quad x = \alpha / \sqrt{n_0}$$

$$\gamma = \gamma^M = \gamma^{\perp} (1 + i\delta) = \gamma^{\perp} + i(\omega_0 - \omega_i)$$

$$\kappa = \kappa' (1 + i\lambda) = \kappa' + i(\omega_1 - \omega_i)$$

Here (ω_0) is the atomic frequency, (ω_1) the interferometer frequency, E_0 is the driving amplitude for a coherent driving field without fluctuations, V is the effective volume, and ρ the effective atomic density.

The expression for the steady-state values of (x) is as follows:

$$|y|^2 = |x|^2 \left| (1 + i\lambda) + 2C [1 - i\delta] \int_{V_0} \left[\frac{|u(\underline{r})|^2 \left(\frac{\rho_0}{\rho}\right) d^3 \underline{r}}{1 + \delta^2 + \sqrt{|u(\underline{r})|^2 \rho_0^2}} \right] \right|^2$$

This is the general expression for the state equation of the field amplitude, given an arbitrary mode function $u(\underline{r})$, which is normalised so that:

$$\int_{V_r} |u(\underline{r})|^2 d^3 \underline{r} = 1 \quad ; \quad \int_{V_0} |u(\underline{r})|^2 \left(\frac{\rho_0}{\rho}\right) d^3 \underline{r} = 1$$

It can be seen that the stability properties largely depend on \mathcal{C} , λ , δ , γ . These four parameters are the system cooperativity (\mathcal{C}), the interferometer detuning (λ), the atomic detuning (δ), and the input field (γ). In section 5.4 we will introduce a fifth parameter, the inhomogeneous broadening (σ). In the remainder of the present section, we determine the stability properties of the high-Q interferometer, for various mode functions.

(b) Stability properties of the deterministic equations

We now analyse the stability properties of the deterministic equations after adiabatic elimination of the atomic variables. It is possible to use the analysis of section 3.1, relative to a general "state function" $f(n)$:

$$\frac{\partial}{\partial t} \begin{bmatrix} \alpha \\ \alpha^* \end{bmatrix} = \begin{bmatrix} E_0 - \alpha f(n) \\ E_0^* - \alpha^* f^*(n) \end{bmatrix}$$

Here the "state function" can be defined to include both a mode function and inhomogeneous broadening, by including a different coupling (g_μ) for each atom, as well as a different atomic detuning (δ_μ). The state function (from 5.3a) is:

$$f(n) \equiv \kappa - 2d^0 \sum_M \left[\frac{|g_M|^2 \gamma_M^*}{|\gamma_M|^2 + 4n|g_M|^2 \gamma_L / \gamma_{II}} \right]$$

As demonstrated in section 3.1, the Hurwitz criterion for stable eigenvalues is obtained to be:

$$(A) \quad 2 \operatorname{Re} \left[f(n) + n \frac{\partial f}{\partial n} \right] > 0$$

$$(B) \quad |f(n)|^2 + n \left[f^*(n) \frac{\partial f}{\partial n} + f(n) \frac{\partial f^*}{\partial n} \right] > 0$$

The first criterion for stability usually corresponds to the onset of a hard mode. Stability occurs in this case provided:

$$\kappa' - 2d^0 \sum_M \left[\frac{|g_M|^2 |\gamma_M|^2 \gamma_L}{(|\gamma_M|^2 + 4n|g_M|^2 \gamma_L / \gamma_{II})^2} \right] > 0$$

Now for optical bistability, the atoms are not inverted and $d^0 < 0$ at all (positive) temperatures. Hence there is no hard-mode instability in optical bistability, in the high-Q limit. It is worth pointing out that instabilities can occur in the full coupled atom field system. This is shown by an analysis of the full coupled equations including spatial fluctuations, by Bonifacio & Lugiato (1978).

In the case of $d^0 > 0$, there is a totally different type of stability property. This is the situation that evolves when the atoms are optically pumped (i.e. the

atomic reservoirs are at negative absolute temperatures). In this case, the present set of equations is identical to the simplest model of a laser with an injected external signal (Haken, 1970,1977). Clearly there can be a violation of the Hurwitz criterion for positive d^0 : this is just the situation of laser oscillation. In section 3.3 this was treated with the use of a gain coefficient: i.e. ($\kappa' < 0$). In the present situation we see that oscillation can occur at threshold for:

$$(\kappa^e)' \equiv \kappa' - 2d^0 \sum_M |g_M|^2 \gamma_{\perp} / |\gamma_M|^2 < 0$$

Here κ^e is the effective cavity decay rate (which is negative for laser action). If the input frequency is different from the natural laser frequency, then as shown in section 3.3, a hard-mode instability can occur due to free oscillations that are not entrained to the injected signal. Thus we have shown that the stability properties of optical bistability are different from those of the single-mode laser. For optical bistability, the first Hurwitz criterion is always stable. In this respect our results differ from those of Gilmore & Narducci (1978), who suggested that additional terms had to be added to the Hamiltonian to obtain phase stability in this problem. However, the results from the Hurwitz criterion demonstrate that this is not necessary, as the optical bistability equations already have local stability relative to phase drift, in the adiabatic limit of a high-Q interferometer.

We next turn to the second criterion. As shown in section 3.1, the unstable regions in this case are

determined by the turning-points of the state equation. These are therefore determined in detail (for a travelling wave mode) in the following calculation.

(c) Bistability with a travelling wave mode

The simplest treatment of stability properties is obtained in the case of a travelling wave or ring cavity, with $|u|^2 = \frac{1}{2}$. The steady state equation is obtained to be in this case:

$$|y| = |x| \left| 1 + i\lambda + \frac{2C[1 - i\delta]}{1 + \delta^2 + |x|^2} \right|$$

This state equation was obtained by Hassan, Drummond & Walls (1978) and by Bonifacio & Lugiato (1978).

Now the simplest possible situation is obtained for $\delta = \lambda = 0$ where purely absorptive bistability can occur for $C > 4$ (Bonifacio & Lugiato, 1976). The state equation in this case is:

$$y = x \left[1 + \frac{2C}{1 + |x|^2} \right]$$

This is shown in fig 5.3.1. In fact for homogeneous broadening the value $C=4$ is a crucial one: no bistability occurs for $C < 4$ even including detuning. Of more interest is the region of bistability as a function of (δ, λ) for

$c > 4$. We note that on resonance, the lower threshold is at $|\alpha|^2 = n_0$ for $c \gg 4$: so n_0 is indeed the threshold photon number.

In order to find the limits under which bistability may be observed we find the turning points of the state equation, and hence the equation for a point of inflexion. In the case of a ring cavity this defines a boundary of bistability given by:

$$\left(\frac{27}{4}\right) c (1 + \delta^2)(1 + \lambda^2) = (\delta\lambda + c - 1)^3 \quad \dots\dots (A)$$

It is possible to discuss the ring cavity problem in some detail as it is analytically tractable relative to the standing wave problem, which we shall return to later. We therefore calculate the region of bistability in the following cases, for a ring cavity:

- (i) $\delta = \lambda = 0$. In this case we obtain absorptive bistability for $c > 4$ for a certain range of driving field. This result was first obtained by Bonifacio & Lugiato (1976); see fig 5.3.1.
- (ii) $\lambda = 0, \delta \neq 0$. In this case the atoms are detuned and the cavity response is less cooperative. For $c \gg 1$ bistability occurs for $c^2 > \frac{27\delta^2}{4}$ (fig 5.3.2).
- (iii) $\delta = 0, \lambda \neq 0$. In this case the cavity is detuned relative to the driving field but the atoms are on resonance. The transmitted field X is reduced relative to case (ii) by the detuning of the cavity, and bistability occurs for $c^2 > \frac{27\lambda^2}{4}$.

(iv) $\lambda\delta < 0$. In this case both the atoms and the cavity are detuned in opposite directions. For $C, |\lambda|, |\delta| \gg 1$ one finds that bistability occurs for $C > 4|\delta\lambda|$. In this case a large driving field is required to reach the critical point, with:

$$y_c^2 = \left(\frac{27}{16}\right) C^2 \quad , \quad x_c^2 = \frac{3C}{4} |\delta/\lambda|^2$$

(v) $\lambda\delta > 0$. In this case, the atoms and cavity are detuned in the same direction. One finds that bistability occurs for $C > \frac{1}{2} |\delta\lambda|$; thus lower values of C than in case (iv) are needed, for the same value of $|\delta\lambda|$. In this situation the input field at threshold for a given value of C is lower than in the previous examples. Overall, the minimum critical driving field occurs with: (Fig 5.3.3)

$$\delta = \lambda = \sqrt{2C} \left[1 - \sqrt{3/2C} \right]$$

$$y_c^2(\min) = (64/3) \sqrt{2C/3}$$

$$x_c^2(\min) = 4 \sqrt{2C/3}$$

The overall region of bistability for a given value of C as a function of (δ, λ) can be obtained on solving equation (5.3c.A) numerically. However in the limit of large C , the region is given almost entirely by the cases (iv) and (v). This is shown in a sketch of the bistability region in fig 5.3.4.

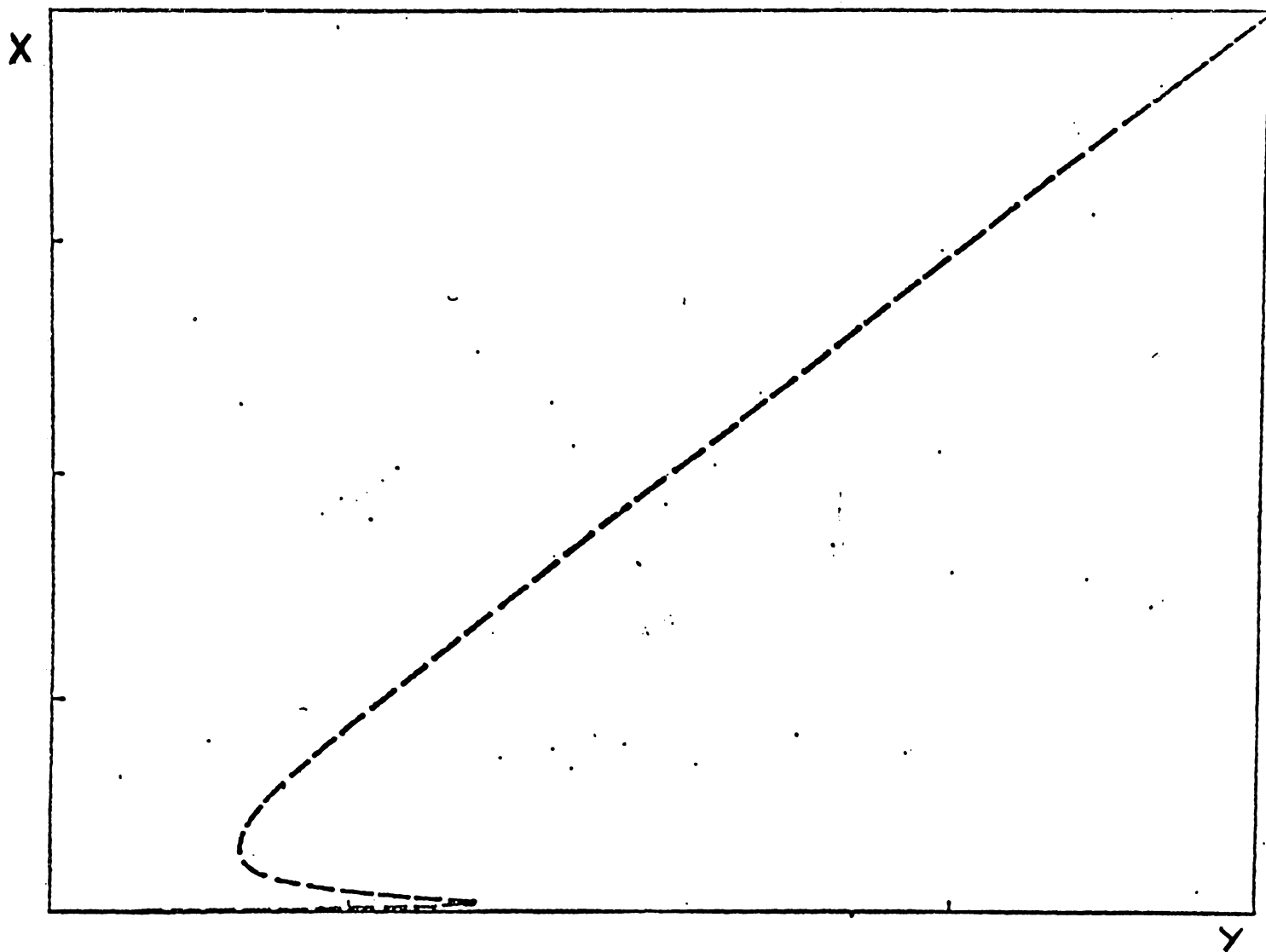


Fig (5.3.1) Absorptive bistability; state equation of interferometer amplitude vs input amplitude ($c = 40$).

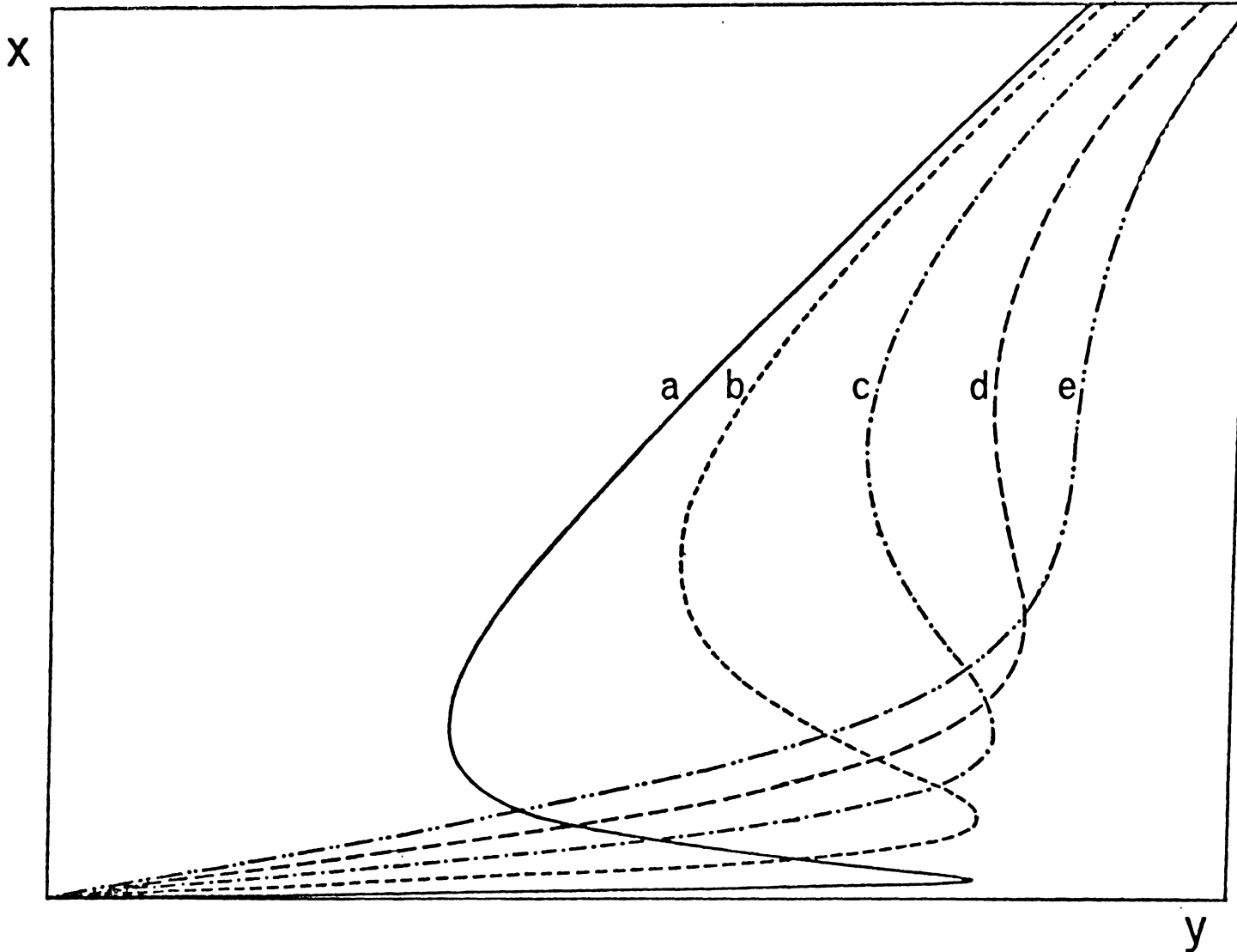


Fig (5.3.2) Detuned atoms bistability; state equation of interferometer amplitude vs input amplitude ($c = 40$).

- | | | |
|-------------------|-------------------|------------------|
| (a) $\delta = 0$ | (b) $\delta = 4$ | (c) $\delta = 8$ |
| (d) $\delta = 12$ | (e) $\delta = 16$ | (critical point) |

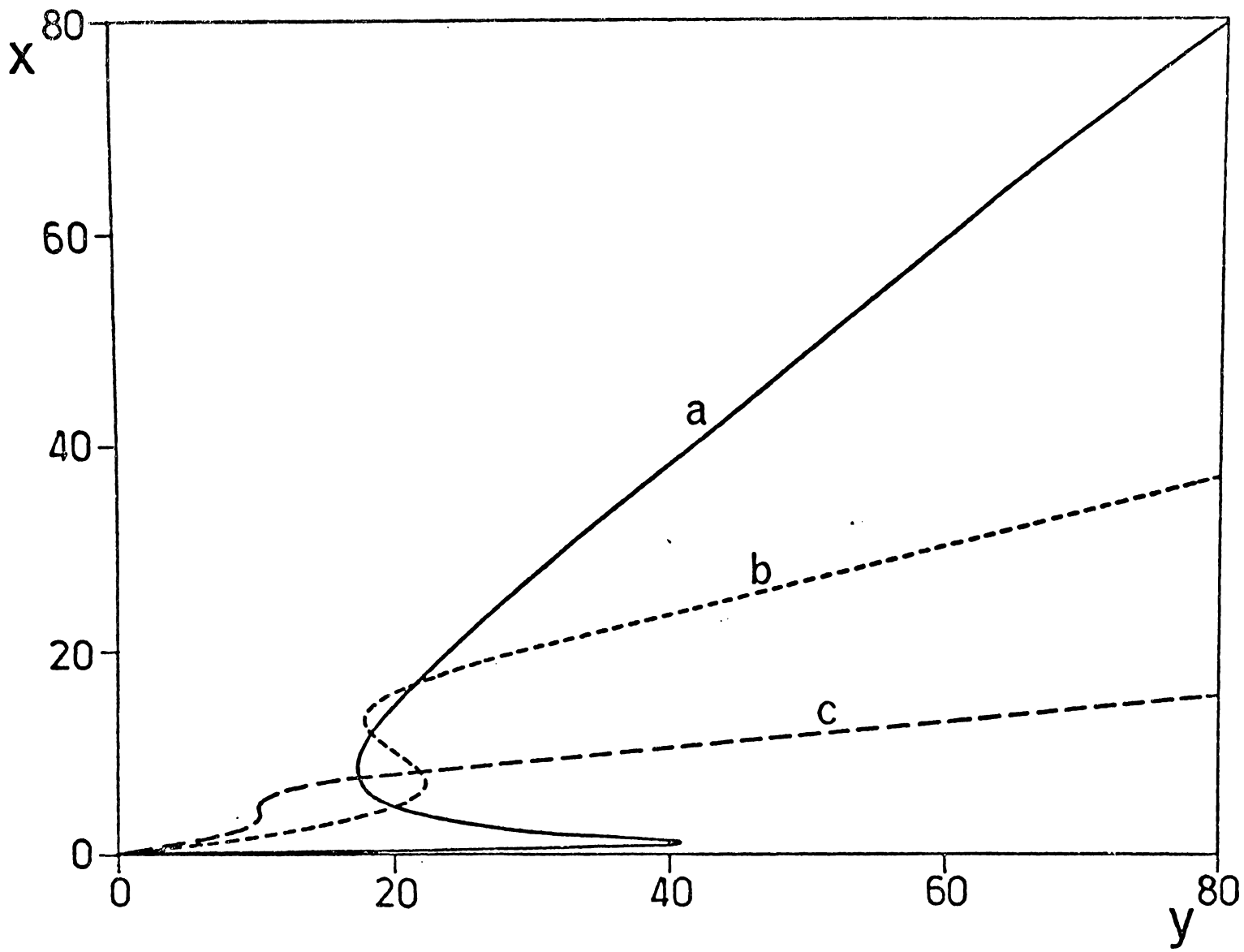


Fig (5.3.3) Detuned atoms and interferometer bistability; state equation of interferometer amplitude vs input amplitude ($c = 40$).

(a) $\delta = \lambda = 0$ (b) $\delta = 10, \lambda = 2.5$
(c) $\delta = \lambda = 7$ (critical point)

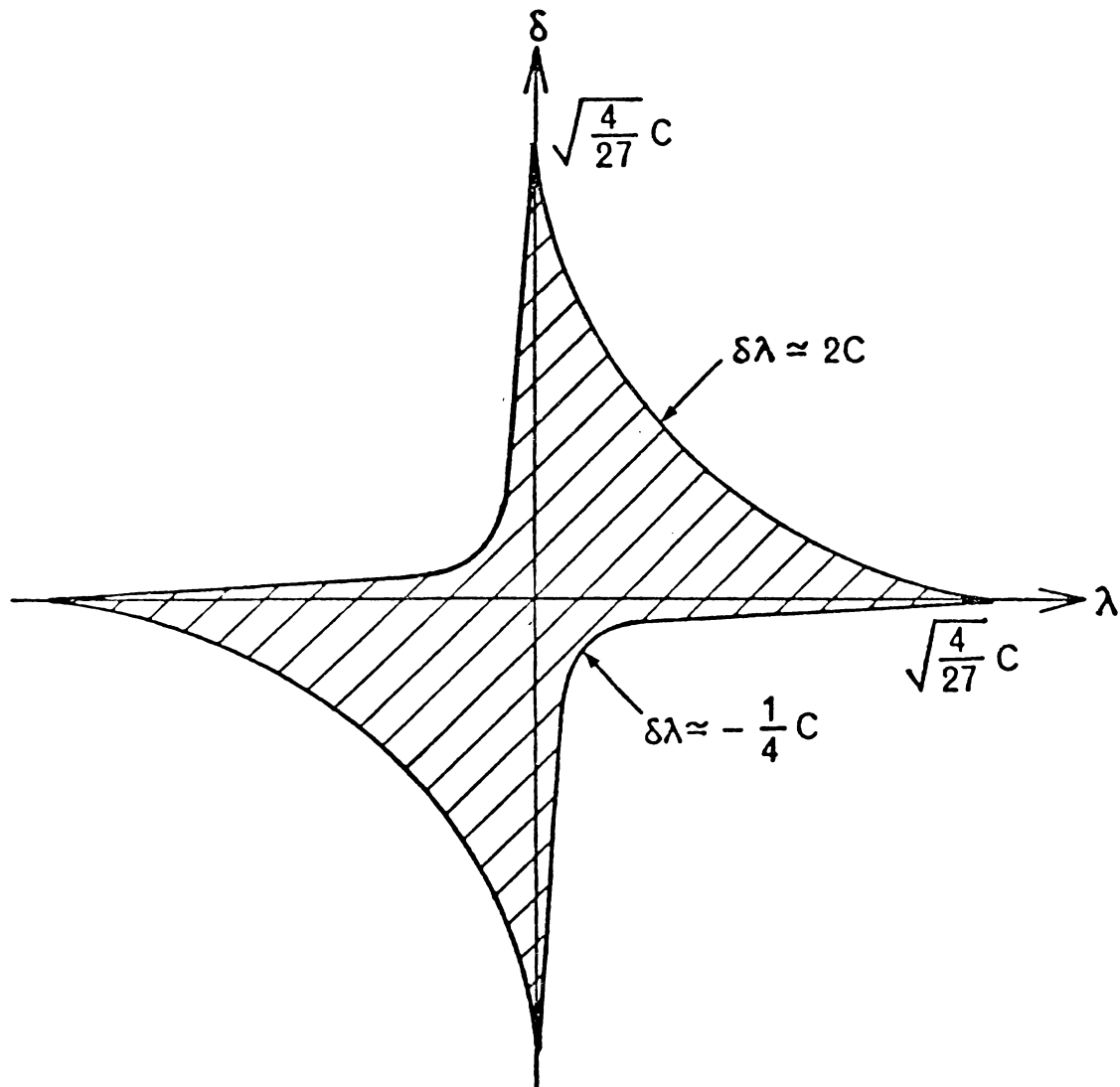


Fig (5.3.4) Schematic diagram of the bistability region as a function of δ, λ for $C \gg 4$.

(d) Bistability with a standing wave mode

In the following, we will suppose that the mode function corresponds to the simplest standing wave case, with:

$$u(\underline{r}) = \sqrt{\frac{2}{V_r}} \cdot \sin \underline{k} \cdot \underline{r}$$

In this case the state equation is as follows:

$$|y| = |\chi| \left| (1+i\lambda) + 4c [1-i\delta] \int_0^{2\pi} \frac{\sin^2 \phi \cdot d\phi / 2\pi}{1+\delta^2 + 2\chi^2 \sin^2 \phi} \right|$$

Here the volume integral has been replaced by an integral over the standing wave phase. The integrations can be calculated to give the following final result:

$$|y| = |\chi| \left| (1+i\lambda) + \frac{2c [1-i\delta]}{|\chi|^2} \left[1 - \sqrt{1 + 2|\chi|^2 / (1+\delta^2)} \right] \right|$$

It can be shown readily that the above result gives very similar behaviour to the travelling wave case for resonant atoms and interferometer. In this case, the equation reduces to:

$$|y| = |\chi| \left[1 + \frac{2c}{|\chi|^2} \left[1 - \sqrt{1 + 2|\chi|^2} \right] \right]$$

A similar equation is obtained for the single-mode laser with a standing wave mode by Haken (1970), without an external input field, and with the opposite atomic inversion.

A similar type of threshold behaviour and bistability occurs as in the travelling wave case of optical bistability. In addition, the limiting behaviour at both very large and very small driving fields, is

identical to the case discussed previously. The threshold behaviour is also similar on resonance. The chief difference between the different field modes occurs for dispersive optical bistability. In this case, an approximate treatment is available even for a general field mode, so this will be discussed in relation to the case of an arbitrary mode function.

(e) The dispersive limit: general field modes

In the case of large atomic detuning, the dispersive effects dominate over absorptive effects. In this case, dispersive optical bistability can occur through a change in the refractive index of the medium due to nonlinear polarisability. This provides an exact, microscopic derivation for the anharmonicity parameter of the model described in section 3.5. We expand the state equation as an asymptotic series in $|\alpha/\delta|^2$ where δ is proportional to the atomic detuning:

$$\frac{\partial}{\partial t} \alpha = E_0 - \kappa^e \alpha - 2\chi^e \alpha |\alpha|^2 + O(\frac{1}{\delta^5})$$

where:

$$\kappa^e \equiv \kappa - 2d^0 \sum_M \frac{|g_M|^2}{\gamma_M} = \kappa + \left(\frac{2c\kappa'}{1+i\delta} \right)$$

$$\chi^e \equiv \text{Im} \left[4d^0 \sum_M \frac{|g_M|^4 \gamma_{\perp}}{\gamma_M \gamma_{\parallel} |\gamma_M|^2} \right] i \equiv \chi(\delta) \cdot I^u$$

$$I^u \equiv \left[\frac{V^2}{V_0} \right] \int_{V_0} |u(r)|^4 d^3r \quad ; \quad \chi(\delta) \equiv \frac{c\kappa'\delta^i}{n_0(1+\delta^2)^2}$$

All the deterministic results on bistability from Chapter 3 can be now utilised with the above parameters $\kappa^{(e)}$, $\chi^{(e)}$, describing the effective decay rate and anharmonicity. The effects of different transverse and longitudinal field modes in the active region are all described by the quartic mode integral I^u . This integral was also obtained in the calculation in Chapter 3 of the anharmonicity parameter. We note that the above expansion is only used provided: $|\alpha|^2/[\eta_0(1+\delta^2)] \ll 1$. In this limit, from Chapter 3, the boundary of bistability is obtained by:

$$(\lambda - 2\delta c/(1+\delta^2))^2 = 3(1 + 2c/(1+\delta^2))^2$$

For large λ, δ, c this reduces to:

$$c = \frac{1}{2}(\delta\lambda) \quad , \quad \delta\lambda > 0$$

Thus in the dispersive limit, the same boundary of bistability is found for a general field mode and active region as for the travelling wave case (with the cooperativity parameter defined appropriately).

However the details of the behaviour of the system for a given input intensity depend on the anharmonicity parameter, which in turn is defined by the quartic integral I^u . In particular, one obtains:

$$\text{(Travelling wave): } I^u = 1$$

$$\text{(Standing wave) : } I^u = 3/2$$

Other cases can similarly be calculated, and the quartic

integral is further modified when the active volume (V_o) is different from the interferometer volume (V_r). We note that the input intensity at threshold is proportional to $(\chi^e)^{-1}$. Thus a reduction in the threshold input intensity of about 33% can be expected for a standing wave mode, relative to a travelling wave mode.

The main point of this section, is therefore that in the dispersive limit one recovers the straightforward theory of Chapter 3. In fact we will show later that this similarity can also be extended to include quantum fluctuations.

5.4 INHOMOGENEOUS BROADENING IN A HIGH-Q INTERFEROMETER

(a) State equations

In the case of inhomogeneous broadening, there is a distribution over the transition frequencies of the individual atoms, which we write as $N(\omega)$. This can be either due to Doppler broadening (where the frequency shift is from a velocity distribution) or due to spatial heterogeneity in a solid-state medium. The actual frequency distribution depends closely on the details of the medium involved: however a generally applicable distribution is the Gaussian distribution. This is certainly applicable for Doppler broadening, where one obtains:

$$N(\omega) = N \cdot \frac{1}{\sqrt{2\pi\sigma^2\gamma_L^2}} \cdot \exp\left[-\frac{1}{2}\left(\frac{\omega-\omega_0}{\gamma_L\sigma}\right)^2\right]$$

$$\sigma\gamma_L = \sqrt{\frac{kT}{Mc^2}} \cdot \omega_0$$

Here $N = \int N(\omega) \cdot d\omega$ is the total number of atoms, ω_0 is the central frequency of the inhomogeneously broadened atoms, and σ is the relative width parameter, defined to be dimensionless. The same distribution can also be used for some cases of a solid-state medium (with a redefinition of σ).

If both inhomogeneous broadening and a standing wave mode function are included, one can obtain a set of Maxwell-Bloch equations, to involve integration over space and frequency simultaneously. This means that the atoms are assumed to be fixed during an interaction lifetime. However for the case of large velocity

components in the propagation direction of the field, this assumption would not be valid. In these cases of large Doppler broadening, an alternative treatment is necessary where one assumes that the atomic velocity is constant (i.e. there are no collisions) on a time-scale long relative to the atomic decay rate. This case will be treated in section 5.4(d). Apart from this, the results from a fixed-atom approximation are applicable to the solid-state case, and to the Doppler broadened case with a travelling wave.

The "fixed-atom" approximation results in the following Maxwell-Bloch equations:

$$\frac{\partial}{\partial t} \bar{j}(\underline{r}, \omega) = -\gamma(\omega) \bar{j}(\underline{r}, \omega) + 2ig^* \alpha d(\underline{r}, \omega) u(\underline{r}) \quad (\& \text{c.c.})$$

$$\frac{\partial}{\partial t} d(\underline{r}, \omega) = -\gamma_{11} [d(\underline{r}, \omega) - d^0] + i[g\alpha^* \bar{j}(\underline{r}, \omega) u^*(\underline{r}) - \text{c.c.}]$$

$$\frac{\partial}{\partial t} \alpha = -\kappa\alpha - ig \int \int_{V_0} N(\omega) u^*(\underline{r}) \bar{j}(\underline{r}, \omega) d\underline{r} d\omega \quad (\& \text{c.c.})$$

With adiabatic elimination of the atomic variables one then obtains:

$$\bar{j}(\underline{r}, \omega) = 2ig^* \alpha d(\underline{r}, \omega) \cdot \alpha / \gamma(\omega)$$

$$d(\underline{r}, \omega) = d^0 / \Pi(\underline{r}, \omega)$$

Where:

$$\Pi(\underline{r}, \omega) = \left[1 + \frac{n |u(\underline{r})|^2 V}{n_0 (1 + \delta^2)} \right] \quad (n \equiv \alpha \alpha^*)$$

$$\gamma(\omega) = \gamma_{\perp} + i(\omega - \omega_i) = \gamma_{\perp} (1 + i\delta)$$

Hence the final state equation after adiabatic elimination of the atomic variables is:

$$\frac{\partial}{\partial t} \alpha = -\kappa \alpha + E(t) + 2\alpha d^0 |g|^2 \left\{ \int \frac{N(\omega) |u(\underline{r})|^2 d^3 r d\omega}{\gamma(\omega) \Pi(\underline{r}, \omega)} \right\}$$

The state equation with reduced variables is then obtained on defining a new inhomogeneous broadening function $g(\delta)$:-

$$|\dot{\alpha}| = |\alpha| \left| 1 + i\lambda + 2c \left\{ \int \frac{g(\delta - \delta_0) (1 - i\delta) |u(\underline{r})|^2 \left(\frac{\rho_0}{\rho}\right) d^3 \underline{r} d^3 \delta}{1 + \delta^2 + |x u(\underline{r})|^2 V} \right\} \right|$$

$$g(\delta - \delta_0) = \frac{\gamma_{\perp}}{N} \cdot N(\delta \gamma_{\perp} + \omega_i)$$

For the case of Gaussian broadening treated in this chapter, the distribution function is given by:

$$g(\delta - \delta_0) = \frac{1}{\sqrt{2\pi\sigma^2}} \cdot \exp \left[-\frac{1}{2} \left(\frac{\delta - \delta_0}{\sigma} \right)^2 \right]$$

$$\delta_0 = (\omega_0 - \omega_i) / \gamma_{\perp}$$

A similar state equation was obtained by Bonifacio & Lugiato (1978), although these authors neglect the mode function, and calculate the state equation only for Lorentzian broadening. In the remainder of this section we treat the case of Gaussian inhomogeneous broadening. This is applicable for Doppler broadening, and holds for some other types of inhomogeneous broadening as well.

(b) Travelling wave case

In the case of a travelling wave, the equation for the steady state is:

$$|y|^2 = |x|^2 \left[\left(1 + \frac{2c}{1+|x|^2} \cdot U_0(u^0, t) \right)^2 + \left(\lambda - \frac{2c}{\sqrt{1+x^2}} V_0(u^0, t) \right)^2 \right]$$

Here the integrals in frequency are specifically obtained in terms of Voigt functions (Sandle 1978, Reichel 1968):

$$U_0(u^0, t) = \frac{1}{\sqrt{4\pi t}} \int_{-\infty}^{\infty} \exp\left(-\frac{(u^0 - u)^2}{4t}\right) \cdot \frac{du}{1+u^2}$$

$$V_0(u^0, t) = \frac{1}{\sqrt{4\pi t}} \int_{-\infty}^{\infty} \exp\left(-\frac{(u^0 - u)^2}{4t}\right) \cdot \frac{u du}{1+u^2}$$

where we have made the following variable change:

$$u = s / \sqrt{1+x^2}$$

$$2t = \sigma^2 / (1+x^2)$$

$$u^0 = s^0 / \sqrt{1+x^2}$$

The state equation above is easily evaluated by numerical integration of the Voigt functions. An approximate result, valid for large σ^2 , can be found on utilising the asymptotic expansion described by Reichel (1968). This leads to the following critical point:

$$c = \sigma^2 / 2$$

$$y^c = \sigma \sqrt{\frac{\pi}{2}}$$

This is the critical point in the large σ limit, for zero detuning of the atoms and interferometer ($\lambda = \delta^o = 0$). It should be noted that a much larger cooperativity parameter is required now, since with homogeneous broadening bistable behaviour was obtained with $C \geq 4$.

This implies that for the absorptive case, a much greater cooperativity parameter is required to observe optical bistability with inhomogeneous broadening, relative to the homogeneous broadening situation. This prediction is verified by numerical results (fig 5.4.1). In this figure, we graph the critical case with large inhomogeneous broadening, on resonance. This is compared with the homogeneous case, and the dispersive bistability case. It can be clearly seen that dispersive operation allows observation of bistability even when this would not be observable in the absorptive case. This theoretical result also agrees in general with the experiments of Gibbs et al (1976), Venkatesan (1977).

Further numerical investigations were made of the effect of varying C with fixed detuning parameters (fig 5.4.2). The largest value of C was chosen to correspond to the absorptive critical point, where there was no bistability. By including a detuning of the atoms and interferometer of a similar order of magnitude to the inhomogeneous broadening, bistability was regained (in experiments of course, the laser and interferometer would have to be detuned). The effect of varying C , the cooperativity parameter, was then investigated. It was found that with decreasing values of C , the threshold

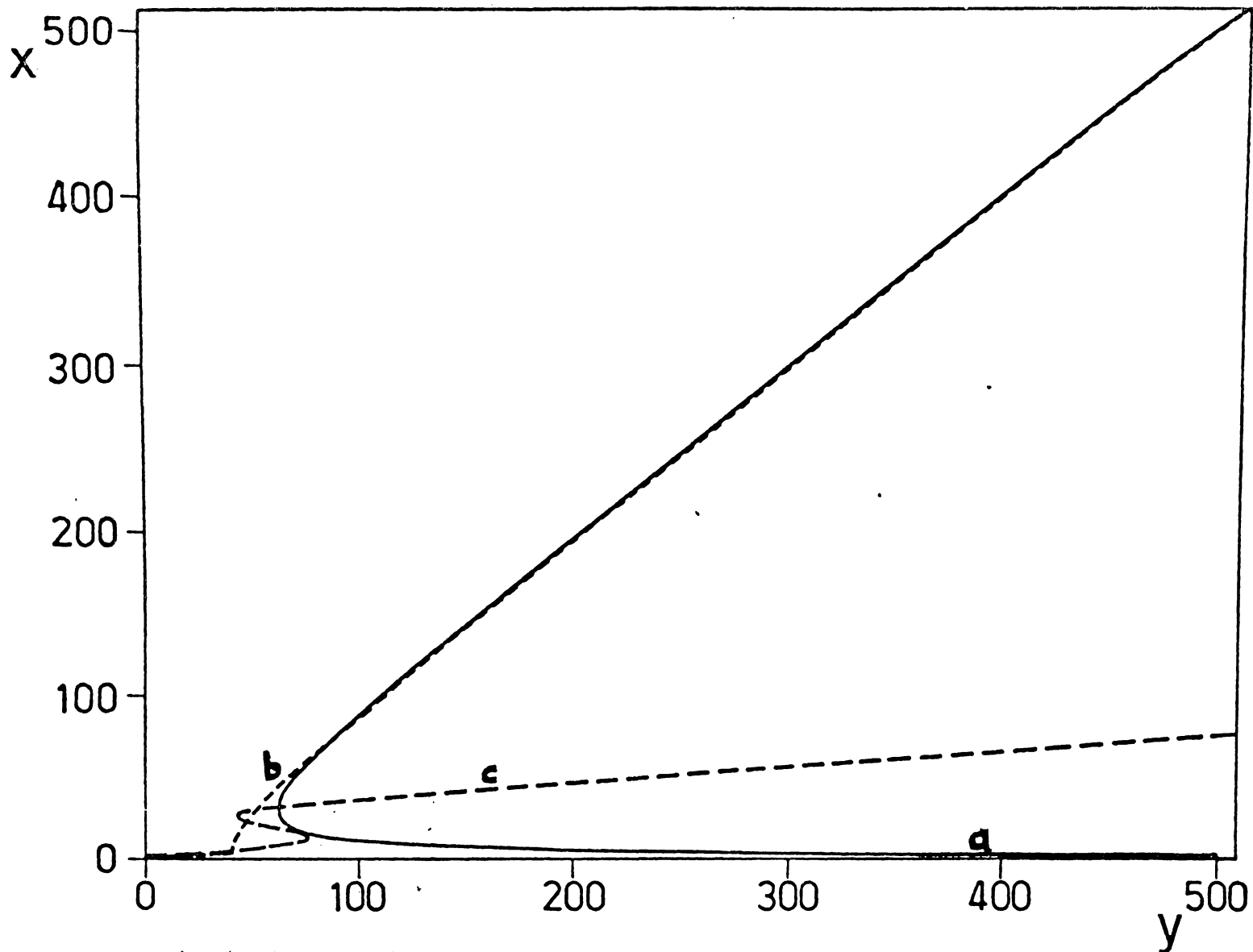


Fig (5.4.1)

Bistability with inhomogeneous broadening; state equation of interferometer amplitude vs input amplitude ($c = 500$).

(a) $\delta = \lambda = \sigma = 0$ (resonant, homogeneous case)

(b) $\delta = \lambda = 0, \sigma = 31$ (resonant, critical point)

(c) $\delta = \sigma = 31, \lambda = 10$ (nonresonant, bistable region)

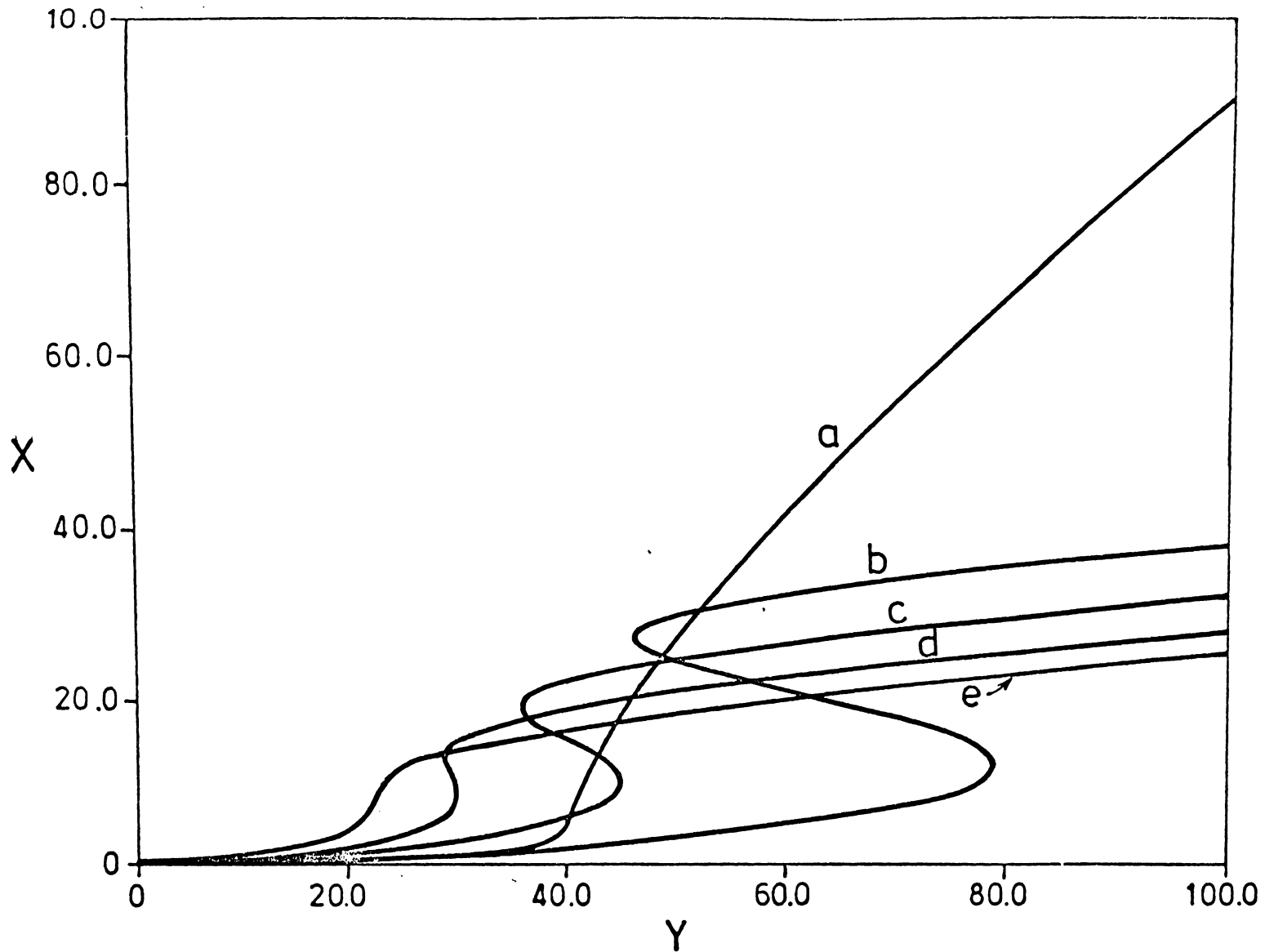


Fig (5.4.2) Bistability with inhomogeneous broadening; state equation of interferometer amplitude vs input amplitude for different values of c ($\sigma = 31$):

- | | | | |
|----------------|-----------------------------|----------------|-----------------------------|
| (a) $c = 500,$ | $\delta = \lambda = 0$ | (b) $c = 500,$ | $\lambda = 10, \delta = 31$ |
| (c) $c = 400,$ | $\lambda = 10, \delta = 31$ | (d) $c = 340,$ | $\lambda = 10, \delta = 31$ |
| (e) $c = 300,$ | $\lambda = 10, \delta = 31$ | | |

input field intensity steadily decreased, although bistability was retained. Finally a new critical point was reached at lower values of ζ and γ_c than with the resonance case. This demonstrates clearly that dispersive operation in the inhomogeneous broadening case has advantages in requiring both a lower atomic density and a lower input amplitude at threshold, to observe bistable behaviour.

(c) The dispersive limit: solid-state case

The previous results give a general picture of the influence of inhomogeneous broadening on the state equation for optical bistability. However these results all apply to the case of a travelling wave mode. In many experiments, the use of a Fabry-Perot interferometer results in a standing wave mode. We therefore wish to investigate the effects of different interferometer geometries: in the simplest case, we treat a solid-state medium so that the fixed-atom approximation is applicable. In the case of a mode function of $\sin \underline{k} \cdot \underline{r}$, one obtains the following state equation:

$$|y| = |x| \left| (1+i\lambda) + \frac{2\zeta}{|x|^2} \int \left[1 - \sqrt{1 + 2|x|^2 / (1+\delta^2)} \right] g(\delta - \delta_0) (1-i\delta) d\delta \right|$$

In general this type of integral can only be evaluated numerically. We therefore, turn to the case of the dispersive limit for a general mode function. In this case the nonlinear polarisability equation of Chapter 3 is recovered:

$$\frac{\partial}{\partial t} \alpha = E(t) - \kappa \alpha - 2\chi^e \alpha |\alpha|^2$$

Here the linear term is given by:

$$\kappa^e = \kappa + 2c\kappa' \int \frac{g(\delta - \delta_0) d\delta}{1 + i\delta}$$

This term is in fact the same for any mode function, whether standing or travelling wave, provided the overall volume of the cavity is fixed. The reason for this is the overall normalisation of the mode function, which means that the linear term only depends on the effective atomic density. The physical effect of the atomic density is to alter the (complex) refractive index of the intra-cavity medium, in the linear limit. The integrals over the inhomogeneous broadening can be expressed in terms of Voigt functions, as before.

The nonlinear term is obtained to be:

$$\chi^e = I^u \cdot \int g(\delta - \delta_0) \cdot \chi(\delta) \cdot d\delta ; \quad \chi(\delta) = \frac{ic\kappa'\delta}{n_0(1+\delta^2)^2}$$

where $\chi(\delta)$ is defined as in section 5.3. Here the effect of the different mode functions factorises out of the equations, while the integral over the inhomogeneous broadening is related to the Voigt functions utilised previously. These integrals are best evaluated either

numerically or with the use of tables, for a given detuning (δ_0) and inhomogeneous line-width (σ). Finally it is worthy of note, that in the dispersive limit obtained above the theory of optical bistability has a strong resemblance to the theory of a single-mode laser. The chief differences arise in the sign of d^0 (which is positive for a laser, negative for optical bistability) and in the external injected signal $E(\dagger)$. These equations can therefore be regarded as a microscopic basis for the theory of Chapter 3, where the laser and the dispersive absorber were treated on a unified basis.

(d) The dispersive limit: Doppler broadened case

We now wish to analyse the effects of different mode functions in the case of a standing wave and large Doppler broadening. This case is interesting simply because it was in a situation of this type that optical bistability was first observed (Gibbs et al 1976, Venkatesan 1977). Further experiments are also taking place (Sandle, 1978) showing that this is a realistic situation to investigate.

In fact laser action on a steady-state basis was first observed in this type of situation, and the theory for the laser case was discussed by Haken & Sauermann (1963), Lamb (1964). In the dispersive limit, an approach

can be used that is similar to the laser theory, with the changes mentioned previously.

We suppose that the mode function is a standing wave, described by an overall envelope function (that could represent a Gaussian quasi-mode in a spherical Fabry-Perot interferometer):

$$U(\underline{r}) = \bar{u}(\underline{r}) \times \sqrt{2} (\cos \underline{k} \cdot \underline{r})$$

The normalisation is chosen so that to a good approximation (with a "slowly varying envelope") one has:

$$\int_{V_r} |\bar{u}(\underline{r})|^2 d^3 \underline{r} = 1$$

Here the notation \int_{V_r} means integration over the volume of the interferometer, which can be different from the volume of active atoms. In order to describe Doppler broadening, each atom is treated on an individual basis with a fixed velocity (that is, the velocity is changed by collisions on a time-scale much longer than the free decay time). This imposes a limitation on the atomic density that can be described by this theory. We also assume a fixed orientation of the atomic dipole moments relative to the vector of polarisation of the light mode, for simplicity.

In this case, the interaction parameter g_{μ} for the μ 'th atom at position \underline{r}_{μ} , and velocity \underline{v}_{μ} has the form (Haken, 1970):

$$g_M = -i \bar{u}(r_M) \cdot \frac{g}{\sqrt{2}} [e(t) + e^*(t)]$$

$$e(t) \equiv \exp(i \underline{k} \cdot (\underline{r}_M + \underline{v}_M t))$$

The equations for the atomic polarisation and inversion from section 5.2 become:

$$[\partial_t + \gamma] j_M = -\sqrt{2} g \alpha d_M \bar{u}(r_M) [e(t) + e^*(t)]$$

$$[\partial_t + \gamma_{11}] d_M = \gamma_{11} d_0 + \left(\frac{g}{\sqrt{2}}\right) \bar{u}(r_M) [j_M \alpha^* + j_M^* \alpha] [e(t) + e^*(t)]$$

We assume that the envelope function is slowly varying so that the time dependence of $\bar{u}(r_M)$ due to the atomic velocity can be neglected (this is not always the case in practical experiments - see Venkatesan (1977)). In the dispersive limit, the above equations can be solved iteratively as the steady-state inversion remains close to its thermal value. Therefore the first approximation to the time dependent polarisation of the atoms is:

$$j_M^{(1)}(t) = -\sqrt{2} g \alpha d^0 \bar{u}(r_M) \left[\frac{e(t)}{\gamma + i\gamma_{\perp} \delta_M} + \frac{e^*(t)}{\gamma - i\gamma_{\perp} \delta_M} \right]$$

$$\delta_M \equiv \frac{1}{\gamma_{\perp}} \underline{k} \cdot \underline{v}_M \quad ; \quad e(t) = \exp(i \underline{k} \cdot \underline{r}_M + i\gamma_{\perp} \delta_M t)$$

Here $\gamma_{\perp} \delta_M$ represents the Doppler frequency shift, and it is significant that there are Doppler shifts both to positive and negative frequencies relative to the original atomic transition frequency. Similarly, a first order correction to the atomic inversion can be calculated:

$$d_M^{(1)}(t) = -|\bar{u}(r_M) \cdot g_\alpha|^2 d^0 \left[\frac{e(t)^2}{(\gamma + i\gamma_\perp \delta_M)(\gamma_{||} + 2i\gamma_\perp \delta_M)} + \frac{1}{(\gamma + i\gamma_\perp \delta_M)\gamma_{||}} + (\delta_M \rightarrow -\delta_M) \right] + c.c.$$

There are a total of eight terms in this expression, which is abbreviated with the use of the symmetry in $(\delta_M \rightarrow -\delta_M)$ and $(\gamma \rightarrow \gamma^*)$.

Finally, this first order correction in d_M is used to generate a second order correction in j_M . In the following expression, rapidly varying components that disappear on phase averaging, are omitted:

$$j_M^{(2)}(t) = \sqrt{2} g^3 \alpha |\alpha|^2 |\bar{u}(r_M)|^3 d^0 \left[\frac{e(t)}{\gamma + i\gamma_\perp \delta_M} \left\{ \frac{1}{(\gamma + i\gamma_\perp \delta_M)(\gamma_{||} + 2i\gamma_\perp \delta_M)} + \frac{2}{\gamma_{||}\gamma_\perp(1 + (\delta_M + \delta_0)^*)} + (\gamma \leftrightarrow \gamma^*) \right\} + (\delta_M \leftrightarrow -\delta_M) \right]$$

These expressions for the polarisation are then used to generate an equation for the field amplitude (α). We note that the assumption that the field amplitude varies slowly relative to the atomic decay time corresponds to the high-Q assumption that has been used before, to adiabatically eliminate the atomic variables. The final expression, for the field amplitude, is:

$$\frac{\partial}{\partial t} \alpha = -\kappa^e \alpha + E(t) - 2\chi^e \alpha |\alpha|^2$$

Here the equivalent linear and nonlinear polarisability terms (κ^e, χ^e) are obtained by summing up the individual induced polarisations of atoms, and noting that any rapid time variation will disappear on averaging

over the relative phases of a large number of active atoms. The linear term is obtained from $j_M^{(1)}$. Due to the symmetry of the Maxwell-Boltzmann distribution (under $V_M \rightarrow -V_M$) this is the same as that obtained previously:

$$K^{(e)} = \kappa + 2c\kappa' \int \frac{g(\delta - \delta_0) d\delta}{1 + i\delta}$$

$$g(\delta) \equiv \frac{1}{\sqrt{2\pi\sigma^2}} \exp\left(-\frac{\delta^2}{2\sigma^2}\right)$$

The nonlinear term is obtained from $j_M^{(2)}$, and this is as follows:*

$$\begin{aligned} \chi^{(e)} &= \frac{i}{2} I_m |g^+| d^0 \sum_M |\bar{u}(r_M)|^4 \left\{ \frac{1}{\gamma + i\gamma_{\perp} \delta_M} \left[\frac{1}{(\gamma + i\gamma_{\perp} \delta_M)(\gamma_{\parallel} + 2i\gamma_{\perp} \delta_M)} \right. \right. \\ &\quad \left. \left. + \frac{2\gamma_{\perp}}{\gamma_{\parallel}(\gamma_{\perp}^2 + \gamma_{\perp}^2(\delta_M + \delta_0)^2) + (\gamma \rightarrow \gamma^*)} \right] + (\delta_M \rightarrow -\delta_M) \right\} \\ &= i I_m \left[\frac{c\kappa' I^q}{8 n_0} \right] \left\{ \int \frac{g(\delta) d\delta}{1 + i(\delta + \delta_0)} \left[\frac{1}{(1 + i(\delta + \delta_0))(1 + i\delta)} + \frac{2}{(1 + (\delta + \delta_0)^2)} \right. \right. \\ &\quad \left. \left. + (\delta_0 \rightarrow -\delta_0) \right] + (\delta \rightarrow -\delta) \right\} \end{aligned}$$

It is interesting to notice that the first term in the integrand is due to the time-dependent response of the atoms, and the second term is due to the same type of inhomogeneous broadening as obtained previously. However the terms with the opposite sign in (δ_0) are new terms that originate from the interaction of the standing wave with the atoms at a finite velocity. These give a different behaviour to the terms in a fixed-atom

* We assume in these equations that $\gamma_{\parallel} = 2\gamma_{\perp}$, and include only dispersive nonlinearity which dominates in the dispersive case.

approximation, and give rise to the "Lamb dip" tuning response in the case of a single-mode laser.

Once again, the significant point of this development is that in the dispersive limit the equations for optical bistability with Doppler broadening and standing wave modes, reduce to the nonlinear equations treated already in Chapter 3. This gives a microscopic basis for the Hamiltonian treatment given in that chapter. The value of the nonlinear polarisability term $\chi^{(e)}$ depends on the degree of atomic detuning, and can be found numerically from the above integral expression, which holds for large values of detuning and all values of the inhomogeneous line-width (provided the expansion parameter is not too large).

5.5 QUANTUM FLUCTUATIONS IN A HIGH-Q INTERFEROMETER

(a) Introduction

In this section, the problem of quantum fluctuations in optical bistability is treated. The significance of the quantum fluctuations in this problem, as mentioned earlier, is that these fluctuations provide a limitation to the operational possibilities of a nonlinear device based on optical bistability. The fluctuations will cause phase and amplitude fluctuations in the device output, and also can result in spontaneous switching between the locally stable branches of the state equation.

Earlier treatments of this problem have been given by Bonifacio, Gronchi & Lugiato (1978), and by Willis (1977,1978), Willis & Day (1978). These authors have derived Fokker-Planck equations describing the quantum fluctuations, in the Glauber-Sudarshan P-representation. Their methods involve the adiabatic elimination of the atomic variables from the master equation itself (Lugiato, 1975 , and Picard & Willis,1978). However while these authors have mainly been interested in the absorptive case, their results are somewhat different (despite starting from similar Hamiltonians). In the present treatment, we will instead use a c-number representation of the complete interacting atom-field system, before adiabatically eliminating the atoms. This method is well known, and has been used in the case of the single-mode laser. The results obtained for optical bistability differ from the single-mode laser, due to the absence of any optical pumping in the present problem.

The advantage of using the full Fokker-Planck equations, is that it is simpler to determine the type of approximations that have been used. The method also has limitations, as it is necessary to truncate a differential equation of infinite order to obtain results. This truncation may not be accurate for a high intensity laser, as pointed out by Mandel (1974). However, truncations or other approximations have also been used in previous work on optical bistability. The truncation should be a good approximation in the dispersive limit, where the distribution of atomic variables is relatively well-behaved.

We are therefore mainly interested in the dispersive limit of this problem, in order to obtain a microscopic justification for the results obtained using a nonlinear (quartic) Hamiltonian in Chapter 3. Some degree of comparison will also be obtained with the results of previous authors.

The Fokker-Planck equation is obtained from the normal ordered representation of atomic and field operators. We will use the complex P-representation of Chapter 2, as in general the resulting Fokker-Planck equation would not have positive-definite diffusion in the usual ("diagonal") representation. The quantum-classical correspondence then has the following form:

$$\int_{\mathcal{D}} P(\underline{\alpha}) X(\underline{\lambda}, \underline{\alpha}) d^2\alpha_1 d^2\alpha_2 d^2\alpha_3 d^2\alpha_4 d^2\alpha_5$$

$$= \text{Tr}[\hat{\rho} \hat{X}(\underline{\lambda})]$$

Where:

$$\underline{\alpha} \equiv [J^+, D, J^-, \alpha^+, \alpha]$$

$$X(\underline{\lambda}, \underline{\alpha}) = \exp[i \underline{\lambda} \cdot \underline{\alpha}]$$

$$\hat{\chi}(\underline{\lambda}) = e^{i\lambda_1 \hat{J}^+} \cdot e^{i\lambda_2 \hat{J}^z} \cdot e^{i\lambda_3 \hat{J}^-} \cdot e^{i\lambda_4 \hat{a}^+} \cdot e^{i\lambda_5 \hat{a}}$$

We have written the equations in this way in order to make it clear, that (J^+, J) are not complex-conjugate, while D can be complex and (α^+, α) are not complex-conjugate. Thus the distribution is defined on \mathbb{C}^5 (not \mathbb{R}^5 as usually defined).

The derivation of the Fokker-Planck equation proceeds exactly as in the case of a single-mode laser. However we have explicitly used the complex P-representation, as this provides a better foundation for equations that can result in "complex noise" processes.

The result for the single-mode laser can be referred to in the work of several researchers including Haken, Risken & Weidlich (1967), Gordon (1967), Lax (1968), Haken (1970), Louisell (1973). These authors treat two and three level systems with optical pumping; while for optical bistability the underlying Fokker-Planck equations can be simplified by treating two-level systems without optical pumping.

Here we follow the notation of Haken (1970). The result for a single running mode, homogeneously broadened line, without extra phase-destroying processes ($\gamma_p = 0$) and with the atomic reservoirs at zero temperature is:

$$\begin{aligned}
\frac{\partial}{\partial t} P(\underline{\alpha}) = & \left\{ \chi_{\perp} \left[N(e^{\frac{\partial}{\partial D}} - 1) + \frac{\partial}{\partial J^-} J^- + \frac{\partial}{\partial J^+} J^+ + 2(e^{\frac{\partial}{\partial D}} - 1) D \right] \right. \\
& - i\bar{g} \left\{ \left[e^{-\frac{\partial}{\partial D}} J^+ - \frac{\partial^2}{\partial J^2} J^- + 2 \frac{\partial}{\partial J} D \right] \alpha - \right. \\
& \quad \left. \left. - \left[e^{-\frac{\partial}{\partial D}} J^- - \frac{\partial^2}{\partial J^2} J^+ + 2 \frac{\partial}{\partial J} D \right] \alpha^+ + \right. \right. \\
& \quad \left. \left. + \left[-\frac{\partial}{\partial \alpha} + \alpha^+ \right] J^- - \left[-\frac{\partial}{\partial \alpha^+} + \alpha \right] J^+ \right\} + \right. \\
& \left. + \kappa' \left[\frac{\partial}{\partial \alpha} \cdot \alpha + \frac{\partial}{\partial \alpha^+} \cdot \alpha^+ + 2n_{th} \frac{\partial^2}{\partial \alpha \partial \alpha^+} \right] \right\} P(\underline{\alpha})
\end{aligned}$$

This equation is essentially the Fokker-Planck equation of a laser without optical pumping. It is easily verified, that while the above equations omit detuning and an external driving field, the inclusion of these factors only alters the first order differential terms in the above equations. Hence the final Fokker-Planck equation after truncation is as follows:

$$\begin{aligned}
\frac{\partial}{\partial t} P(\underline{\alpha}) = & \left\{ \left[\chi \frac{\partial}{\partial J^-} \cdot J^- + \chi^* \frac{\partial}{\partial J^+} \cdot J^+ - 2i\bar{g} \left(\frac{\partial}{\partial J} \cdot D \alpha - \frac{\partial}{\partial J^+} \cdot D \alpha^+ \right) \right. \right. \\
& \quad \left. \left. + i\bar{g} \left(\frac{\partial^2}{\partial J^2} \cdot J \alpha - \frac{\partial^2}{\partial J^2} \cdot J \alpha^+ \right) \right] - \left[\frac{\partial}{\partial \alpha} E_0 + \frac{\partial}{\partial \alpha^+} E_0^* \right] \right. \\
& \quad \left. + \left[\chi_{\parallel} \frac{\partial}{\partial D} \left(D + \frac{N}{2} \right) + i\bar{g} \frac{\partial}{\partial D} \left(J^+ \alpha - J^- \alpha^+ \right) + \right. \right. \\
& \quad \left. \left. + \frac{1}{2} \chi_{\parallel} \frac{\partial^2}{\partial D^2} \left(D + \frac{N}{2} \right) - \frac{1}{2} i\bar{g} \frac{\partial^2}{\partial D^2} \left(J^+ \alpha - J^- \alpha^+ \right) \right] \right. \\
& \quad \left. + \left[\kappa \frac{\partial}{\partial \alpha} \cdot \alpha + \kappa^* \frac{\partial}{\partial \alpha^+} \cdot \alpha^+ + i\bar{g} \left(\frac{\partial}{\partial \alpha} \cdot J^+ - \frac{\partial}{\partial \alpha^+} \cdot J^- \right) + 2\kappa' n_{th} \frac{\partial^2}{\partial \alpha \partial \alpha^+} \right] \right\} P(\underline{\alpha})
\end{aligned}$$

Even though the diffusion array in this problem is not positive-definite, we recognise from the results of Chapter 2 that it is possible to define an equivalent Fokker-Planck equation with positive-semidefinite diffusion. Hence a stochastic differential equation can be then defined with complex noise terms. This is on a

rigorous basis, as long as it is recognised that (J^-, J^+) and (α, α^+) are not complex-conjugate while D also has values that can be complex. The resulting equations are as follows:

$$\frac{\partial}{\partial t} J^- = -\gamma J^- + 2i\bar{g} D \alpha + \Gamma_J$$

$$\frac{\partial}{\partial t} J^+ = -\gamma^* J^+ - 2i\bar{g} D \alpha^+ + \Gamma_{J^+}$$

$$\frac{\partial}{\partial t} D = -\gamma_{||} [D + N/2] - i\bar{g} (J^+ \alpha - J^- \alpha^+) + \Gamma_D$$

$$\frac{\partial}{\partial t} \alpha = -\kappa \alpha - i\bar{g} J^- + \Gamma_\alpha$$

$$\frac{\partial}{\partial t} \alpha^+ = -\kappa^* \alpha^+ + i\bar{g} J^+ + \Gamma_{\alpha^*}$$

In the absence of the stochastic terms, these equations simply reproduce the semiclassical results of section 5.2. The present set of equations includes stochastic terms, and in addition is defined on a larger dimensional space than the semiclassical equations. The relationship between the classical phase-space and the complex phase-space that includes quantum fluctuations, has already been discussed in Chapters 2 and 3. Finally, it is worth pointing out that the only approximation in these equations is the truncation of the higher order derivatives in $(\partial/\partial D)$. While in the present thesis, we will be interested in the adiabatic limit of a high- Q cavity, it should be recognised that this set of stochastic differential equations in five complex variables can also be utilised to investigate situations where the atoms are not adiabatically eliminated. The non-zero correlations for the stochastic terms, are as follows:

$$\langle \Gamma_J(t) \Gamma_J(t') \rangle = 2i\bar{g} J^-_{\alpha} \delta(t-t')$$

$$\langle \Gamma_{J^+}(t) \Gamma_{J^+}(t') \rangle = -2i\bar{g} J^+_{\alpha} \delta(t-t')$$

$$\langle \Gamma_D(t) \Gamma_D(t') \rangle = [i\bar{g} (J^+_{\alpha} - J^-_{\alpha}) + \gamma_{11} (D + N/2)] \delta(t-t')$$

$$\langle \Gamma_{\alpha}(t) \Gamma_{\alpha}^*(t') \rangle = 2\kappa' n_{th} \delta(t-t')$$

Thus it is clear that while the field equations by themselves have the usual character of a damped harmonic oscillator with "classical" noise terms (Louisell, 1973), it is the stochastic behaviour of quantum fluctuations in the atomic variables that make it necessary to use a complex phase-space. The physical origin of this non-classical behaviour is related to spontaneous emission and atomic resonance fluorescence, which are known to have a nonclassical statistical behaviour (Carmichael & Walls, 1976; Kimble et al, 1977). The statistical behaviour in this case is greatly different from the laser case; where the incoherent optical pumping provides the dominant source of fluctuations, which are similar to those from a classical noise source (Haken, 1970).

(b) Adiabatic elimination of the atomic variables

In the limit of $\gamma_{\perp} \gg \kappa'$, the atoms decay on a much faster time scale than the field variables, and can be adiabatically eliminated. This procedure is really an asymptotic one, that results in an asymptotic series in (κ'/γ_{\perp}) . However we shall be only interested in the leading terms of this series. Discussion of the adiabatic elimination method with stochastic variables or Fokker-Planck equations is given by Gordon (1967), Haken (1970, 1975, 1977), Louisell (1973). The elimination technique involves setting \dot{J}^+ , \dot{J}^- , \dot{D} equal to zero, and then solving for the atomic variables. The resulting values of J^+ , J^- , including stochastic terms, are a function of (α, α^*) and can be used in the field equations to give results that only involve the field variables.

As the first step we set \dot{J}^- , \dot{D} equal to zero (results for J^+ follow from the symmetry properties of the equations):

$$J^- = [2i\bar{g}D\alpha + \Gamma_J] / \gamma$$

$$\begin{aligned} D &= -N/2 + (i\bar{g}(J^-\alpha^* - J^+\alpha) + \Gamma_D) / \gamma_{\parallel} \\ &= -N/2 + \frac{\Gamma_D}{\gamma_{\parallel}} + \frac{i\bar{g}}{\gamma_{\parallel}} \left[\frac{(2i\bar{g}D\alpha + \Gamma_J)\alpha^*}{\gamma} + \frac{(2i\bar{g}D\alpha^* - \Gamma_{J^+})\alpha}{\gamma^*} \right] \end{aligned}$$

Solving for the inversion (D) gives:

$$D = \left\{ -\frac{N}{2} + \frac{\Gamma_D}{\gamma_{11}} + \frac{i\bar{g}}{\gamma_{11}} \left[\frac{\Gamma_J \alpha^\dagger}{\gamma} - \frac{\Gamma_{J+\alpha}}{\gamma^*} \right] \right\} \Pi^{-1}(\delta)$$

$$\Pi(\delta) = \left[1 + \frac{2 |g|^2 \alpha \alpha^\dagger}{\gamma^2} \right] = \left[1 + \frac{\alpha \alpha^\dagger}{(1+\delta^2) n_0} \right]$$

$$J^- = \frac{1}{\gamma} \left\{ \Gamma_{J^-} + \left[\frac{2i\bar{g}\alpha}{\Pi(\delta)} \right] \left[-\frac{N}{2} + \frac{1}{\gamma_{11}} \left(\Gamma_D + \frac{i\bar{g}\alpha^\dagger \Gamma_J}{\gamma} - \frac{i\bar{g}\alpha \Gamma_{J^\dagger}}{\gamma^*} \right) \right] \right\}$$

These results give the adiabatic values of the atomic variables in terms of the field variables (α, α^\dagger) and the stochastic functions ($\Gamma_J, \Gamma_{J^\dagger}, \Gamma_D$). We will use the notation of ($\alpha \alpha^\dagger \equiv n$) in the following equations.

We note that the correlation properties of the stochastic terms, themselves depend on (J^+, J^-, D). The next step is to therefore approximate these correlations with the use of the semiclassical values of (J^+, J^-, D). In other words, we use the zero'th order approximation for the atomic variables to evaluate the correlation coefficients. This is an asymptotic procedure that depends on having relatively small stochastic fluctuations compared to the semiclassical values. This can be regarded as the first term in an asymptotic series in ($1/N$), for N atoms. With this approximation, the correlation properties are:

$$\langle \Gamma_J(t) \Gamma_J(t') \rangle = [2|\bar{g}|^2 \alpha^2 N / (\gamma \Pi(\delta))] \delta(t-t')$$

$$\langle \Gamma_{J^+}(t) \Gamma_{J^+}(t') \rangle = [2|\bar{g}|^2 \alpha^{+2} N / (\gamma^* \Pi(\delta))] \delta(t-t')$$

$$\langle \Gamma_D(t) \Gamma_D(t') \rangle = [4\gamma_L |\bar{g}|^2 \alpha \alpha^+ N / (1\gamma_L^2 \Pi(\delta))] \delta(t-t')$$

We can now write down the complete stochastic equations, for the field variables. (We only give the results for α , as those for α^+ follow from the usual symmetries):

$$\frac{\partial \alpha}{\partial t} = E(t) - \kappa \alpha - \frac{\bar{g}^2 \alpha N}{\gamma \Pi(\delta)} + \Gamma(t)$$

Here the full stochastic term $\Gamma(t)$ is as follows:

$$\Gamma(t) \equiv \bar{g} \left[\frac{i\bar{g}}{\gamma} \right] \left[\Gamma_J + \left[\frac{i\bar{g}\alpha}{\gamma_L \Pi(\delta)} \right] \left(\Gamma_D + \frac{i\bar{g}\alpha^+ \Gamma_J}{\gamma} - \frac{i\bar{g}\alpha \Gamma_{J^+}}{\gamma^*} \right) \right]$$

A stochastic term corresponding to α^+ is similarly defined to be $\Gamma^+(t)$, where:

$$\Gamma^+(t) = \Gamma_{\alpha^+} + \left[\frac{i\bar{g}}{\gamma^*} \right] \left[\Gamma_{J^+} + \left[\frac{i\bar{g}\alpha^+}{\gamma_L \Pi(\delta)} \right] \left(\Gamma_D - \frac{i\bar{g}\alpha \Gamma_{J^+}}{\gamma^*} + \frac{i\bar{g}\alpha^+ \Gamma_J}{\gamma} \right) \right]$$

The correlation properties of $\Gamma(t), \Gamma^+(t)$ are then obtained from the atomic variable correlation properties:

$$\begin{aligned} \langle \Gamma(t) \Gamma(t') \rangle &= \langle \Gamma_J(t) \Gamma_J(t') \rangle \left(\frac{-\bar{g}^2}{\gamma^2} \right) \left(1 - \frac{\bar{g}^2 n}{\gamma \gamma_{\perp} \Pi(\delta)} \right)^2 \\ &+ \langle \Gamma_{J^+}(t) \Gamma_{J^+}(t') \rangle \left(\frac{-\bar{g}^2}{\gamma^2} \right) \left(\frac{\bar{g}^2 \alpha^2}{\gamma^* \gamma_{\perp} \Pi(\delta)} \right)^2 \\ &+ \langle \Gamma_D(t) \Gamma_D(t') \rangle \left(\frac{\bar{g}^2 \alpha}{\gamma \gamma_{\perp} \Pi(\delta)} \right)^2 \end{aligned}$$

$$\therefore -d = D_{11}(\underline{\alpha}) = \left[\frac{-2c\kappa' \alpha^2}{(1+\delta^2 + \alpha\alpha^*)^3} \right] \left[(1-i\delta)^3 + \frac{1}{2}(\alpha\alpha^*)^2 \right]$$

$$\begin{aligned} \langle \Gamma(t) \Gamma^*(t') \rangle &= \langle \Gamma_J(t) \Gamma_J(t') \rangle \left(\frac{\bar{g}^2}{|\gamma|^2} \right) \left(1 - \frac{\bar{g}^2 n}{\gamma \gamma_{\perp} \Pi(\delta)} \right) \left(\frac{\bar{g}^2 \alpha^2}{\gamma \gamma_{\perp} \Pi(\delta)} \right) \\ &+ \langle \Gamma_{J^+}(t) \Gamma_{J^+}(t') \rangle \left(\frac{\bar{g}^2}{|\gamma|^2} \right) \left(1 - \frac{\bar{g}^2 n}{\gamma^* \gamma_{\perp} \Pi(\delta)} \right) \left(\frac{\bar{g}^2 \alpha^2}{\gamma^* \gamma_{\perp} \Pi(\delta)} \right) \\ &+ \langle \Gamma_D(t) \Gamma_D(t') \rangle \left(\frac{\bar{g}^4 n}{|\gamma|^2 \gamma_{\perp}^2 \Pi^2(\delta)} \right) \\ &+ \langle \Gamma_{\alpha}(t) \Gamma_{\alpha}^*(t') \rangle \end{aligned}$$

$$\therefore \Gamma_d = D_{21}(\underline{\alpha}) = 2\kappa' n_{th} + \left[\frac{4c\kappa'(\alpha\alpha^*)^2}{(1+\delta^2 + \alpha\alpha^*)^3} \right] \left[1 + \frac{1}{4}(\alpha\alpha^*) \right]$$

Using the functions defined above, the complete Fokker-Planck equation would then be:

$$\frac{\partial}{\partial t} P(\underline{\alpha}) = \partial_M \left[A_M(\underline{\alpha}) + \frac{1}{2} \partial_{\nu} D_{M\nu}(\underline{\alpha}) \right] P(\underline{\alpha}) \quad \{ \underline{\alpha} \equiv [\alpha, \alpha^*] \}$$

$$A_1(\underline{\alpha}) = \left\{ \kappa + \frac{2c\kappa'}{(1+i\delta)\Pi(\delta)} \right\} \alpha - E(t)$$

$$A_2(\underline{\alpha}) = \left\{ \kappa^* + \frac{2c\kappa'}{(1-i\delta)\Pi(\delta)} \right\} \alpha^* - E^*(t)$$

Here A_M is the usual semiclassical term involved in optical bistability, and the other terms D_{12}, D_{22} are defined by:

$$D_{12}(\underline{\alpha}) = \Gamma_0 = D_{21}(\underline{\alpha})$$

$$D_{22}(\underline{\alpha}) = -d^+ \equiv D_{11}^*(\alpha^+, \alpha)$$

The chief difference between these results, and the results of Willis, and of Bonifacio & Lugiato (loc. cit), is that in our equations there are additional terms that are diagonal in the diffusion array, while previous authors have only obtained off-diagonal terms. We note that these diagonal terms are present both for large and small field amplitudes. In fact in the dispersive limit, they are the dominant terms. As this is the physical region of interest to us, it will be significant to compare the dispersive limit results obtained here, with results obtained earlier (in Chapter 3) using the nonlinear polarisability model.

By comparison, the result of Willis and Day is as follows:

$$D_{11} = 0$$

$$D_{21} = \frac{2CK'}{(1+s^2)} \left[\frac{|X|^2}{1+s^2+|X|^2} \right]$$

These authors have used approximations in deriving the Fokker-Planck equation that are valid for large photon number: in fact the technique of adiabatic elimination via the master equation seems to have been first used to treat the high intensity laser. For this reason, their

approach may be regarded as complementary to the present one, which holds in a different physical region (especially in the dispersive limit). We note that our D_{MV} approaches a constant at saturation, which is similar in this respect to the result of Willis & Day (1978), Willis (1978). However the coefficient is numerically different in the present result, which may be due to the approximations used by Willis & Day in deriving their Fokker-Planck equation.

We now turn to the dispersive limit of the present result, where the atoms are not saturated, so any error introduced by truncation of the Fokker-Planck equation would be expected to be minimised. In this case the leading terms in an expansion in $|\alpha/\delta|$ are:

$$D_{11} = -\frac{i \cdot 2c\kappa' \alpha^2}{\delta^3 n_0} + O[|\alpha/\delta|^4]$$

$$D_{22} = \frac{i \cdot 2c\kappa' \alpha^{*2}}{\delta^3 n_0} + O[|\alpha/\delta|^4]$$

$$D_{12} = D_{21} = 2\kappa' n_{th} + O[|\alpha/\delta|^4]$$

This can be compared with the result for the dispersive limit obtained in section 5.3(e) and the results of Chapter 3. We note that in the dispersive limit, the deterministic equations become:

$$\frac{\partial}{\partial t} \alpha = E(t) - \kappa^e \alpha - 2\chi^e \alpha |\alpha|^2$$

$$\frac{\partial}{\partial t} \alpha^* = E^*(t) - \kappa^{e*} \alpha^* - 2\chi^{e*} \alpha^* |\alpha|^2$$

where:

$$\kappa^e \equiv \kappa + \left(\frac{2c\kappa'}{1+i\delta} \right)$$

$$\chi^e = \frac{ic\kappa'}{\delta^3 n_0}$$

Hence the full stochastic equations in the dispersive (lossless) limit are:

$$\frac{\partial}{\partial t} \begin{bmatrix} \alpha \\ \alpha^\dagger \end{bmatrix} = \begin{bmatrix} E(t) - \kappa^e \alpha - 2\chi^e \alpha^2 \alpha^\dagger \\ E^*(t) - \kappa^{e*} \alpha^\dagger - 2\chi^{e*} \alpha^\dagger^2 \alpha \end{bmatrix} + \begin{bmatrix} -2\chi^e \alpha^2 & 2\kappa' n_{th} \\ 2\kappa' n_{th} & -2\chi^{e*} \alpha^\dagger^2 \end{bmatrix}^{1/2} \begin{bmatrix} \xi_1(t) \\ \xi_2(t) \end{bmatrix}$$

These are the stochastic equations that are equivalent to the Fokker-Planck equation obtained above, in the dispersive limit. We note that these equations are exactly identical to the equations derived in Chapter 3 from a nonlinear polarisability model.

Thus in the dispersive limit, the problem of dispersive optical bistability in a fluorescent atomic system, reduces to the equations treated in Chapter 3 for the case of a nonlinear polarisability. This can be regarded as a justification for the Hamiltonian model of dispersive optical bistability obtained previously. Both the nonlinear polarisability model and the present model of a fluorescent atomic system, reduce to exactly the same Fokker-Planck equation and stochastic differential equation (including quantum fluctuations in the field), once we have taken the limits of large atomic detuning and a high-Q interferometer.

Another limit of interest, is the case of purely absorptive nonlinearity. In this case, the equations reduce to:

$$\begin{aligned} \frac{\partial}{\partial t} P(\underline{y}) = & \left\{ \frac{\partial}{\partial x} \left[x \left(1 + \frac{2c}{1+|x|^2} \right) - y \right] \right. \\ & + \frac{\partial}{\partial x^+} \left[x^+ \left(1 + \frac{2c}{1+|x|^2} \right) - y^+ \right] \\ & + \frac{1}{n_0} \left[\frac{\partial^2}{\partial x^2} \left[\frac{-cx^2}{(1+|x|^2)^3} \left(1 + \frac{1}{2}|x|^4 \right) \right] + (x \leftrightarrow x^+) \right. \\ & \left. \left. + \frac{\partial^2}{\partial x \partial x^+} \left[2n_h + \frac{4c|x|^4}{(1+|x|^2)^3} \left(1 + \frac{1}{4}|x|^2 \right) \right] \right] \right\} P(\underline{z}) \end{aligned}$$

Here, as previously, we have defined:

$$\begin{aligned} c &= N \bar{g}^2 / (2\kappa \gamma_{\perp}) \\ n_0 &= \gamma_{\perp}^2 / (2 \bar{g}^2) \\ x &= \alpha / \sqrt{n_0} \\ x^+ &= \alpha^+ / \sqrt{n_0} \\ y &= E_0 / (\kappa \sqrt{n_0}) \end{aligned}$$

We note that the relative size of the fluctuations in the reduced variables, scales as: c/n_0 . Therefore this increases with an increased number of atoms, but is decreased with large γ_{\perp} (i.e. in the adiabatic limit). We finally remark that in the limit of large atomic saturation, the effect of atomic correlations is small and the results obtained above reduce to the same equation that would be obtained from the master equation adiabatic elimination method of Mandel (1974). This is demonstrated explicitly in Appendix D.

(c) Correlations and spectrum

We can obtain the correlations and spectrum for small fluctuations close to a stable branch, on following the method of Chapter 3. Let α_0 be the solution to the deterministic state equation so that:

$$A_M(\alpha_0, \alpha_0^*) = 0$$

On linearising the stochastic differential equation obtained previously, one has:

$$\frac{d}{dt} \begin{bmatrix} \delta\alpha \\ \delta\alpha^* \end{bmatrix} = - \underset{\approx}{A} \begin{bmatrix} \delta\alpha \\ \delta\alpha^* \end{bmatrix} + \underset{\approx}{D}[\alpha_0] \begin{bmatrix} f_1(t) \\ f_2(t) \end{bmatrix}$$

Here $\underset{\approx}{D}$, $\underset{\approx}{A}$ are as defined in Chapter 3. These have the general form:

$$\underset{\approx}{D} = \begin{bmatrix} -d & \Gamma_d \\ \Gamma_d & -d \end{bmatrix}$$

$$\underset{\approx}{A} = \begin{bmatrix} a & b \\ b^* & a^* \end{bmatrix}$$

Where:

$$d = -D_{11}(\alpha_0, \alpha_0^*) = \left[\frac{2c\kappa'x^2}{(1+\delta^2+xx)^3} \right] \left((1-i\delta)^3 + \frac{1}{2}(xx)^2 \right)$$

$$\Gamma_d = D_{12}(\alpha_0, \alpha_0^*) = \left[\frac{4c\kappa'(xx)^2}{(1+\delta^2+xx)^3} \right] \left(1 + \frac{1}{4}(xx) \right)$$

$$a = \kappa + \frac{2c\kappa'}{(1+i\delta)\pi(\delta)^2}$$

$$b = \frac{-\alpha_0^2}{(1+\delta^2)n_0} \left[\frac{2c\kappa'}{(1+i\delta)\pi(\delta)^2} \right]$$

$$\pi(\delta) \equiv \left[1 + \frac{|\alpha_0|^2}{n_0(1+\delta^2)} \right]$$

Here c, x, x^+, δ, n_0 are as in section 5.5(b)

The expressions for the correlation function and spectrum then follow from the equations given in Chapter 3. In particular, in the dispersive limit, one has $d=b$, so the results from the nonlinear polarisability model follow directly. Outside the dispersive limit, the more general expression obtained in Chapter 3 must be used:

$$S(\omega+\omega_i) = n\delta(\omega) + \left[\frac{1}{4\pi a' \Delta(\omega)} \right] \operatorname{Re} \left[\frac{1}{\Delta(i\omega)} \left\{ b^* d (a^2 + |a|^2 - |b|^2) + \right. \right. \\ \left. \left. + b d^* |b|^2 + 2a^+ |b|^2 \Gamma_{+2}(i\omega+a) (\Gamma_{+1}|a|^2 + \operatorname{Re}(abd^*)) \right\} \right]$$

where:

$$\Delta(i\omega) \equiv (i\omega + a)(i\omega + a^*) - |b|^2$$

In the absorptive case, the spectrum becomes:

$$S(\omega+\omega_i) = n\delta(\omega) + \frac{1}{4\pi} \left[\frac{\Gamma_d - d}{\omega^2 + (a+b)^2} + \frac{\Gamma_d + d}{\omega^2 + (a-b)^2} \right] \\ = n\delta(\omega) + \frac{\zeta K' X^2}{(2\pi)(1+X^2)} \left[\frac{2X^2 - 1}{(1+X^2)^2} \times \left(\frac{1}{\omega^2 + (a+b)^2} \right) + \frac{1}{\omega^2 + (a-b)^2} \right]$$

The spectrum in the absorptive limit is identical to the result of Lugiato (1979; Nuovo Cimento; preprint) obtained from a different but essentially equivalent calculation for the absorptive case only.

5.6 COOPERATIVE FLUORESCENCE WITH A GAUSSIAN INPUT

(a) Introduction

In the previous sections, the emphasis has been on the statistical properties and nonequilibrium transitions found, with a completely coherent input. However in some cases (as with a multi-mode laser input) there can be large fluctuations in the driving field. It has been shown by Chrostowski & Krasinski (1978), that the interaction of a Gaussian field with a saturable dye cell, leads to large values of the normalised intensity correlation (photon bunching) in the transmitted field. It is therefore of interest to calculate the response of the high-Q interferometer with a cooperative fluorescent medium, and Gaussian fluctuations in the input field.

We therefore analyse a model in which the input field is a mixture of a resonant coherent part, with a part having "thermal" (delta-correlated) statistics relative to the interferometer response time. It is still possible for the input to be reasonably monochromatic, even with a band width greater than the interferometer bandwidth; so a single-mode calculation is reasonable provided the interferometer resonances are sufficiently broadly spaced relative to the input bandwidth. In the limit of completely Gaussian input statistics, this can represent a model of a multi-mode laser input to the non-linear interferometer.

We assume that because of the large fluctuations in the input field, the effect of quantum fluctuations (due

to the nonlinear medium) is negligible. Thus the analysis is rather similar to that of sections 3.2 and 4.2 for the case of a large thermal background. The case of a combination of coherent and thermal photon statistics is presented here, to give a comparison with the potential solutions obtained earlier. In fact, as far as we know, this may be the only case in which a true potential is available in absorptive bistability (the case of dispersive bistability has already been treated in sections 3.2, 3.5). The reason for this, is that the quantum fluctuations derived earlier (either in our approximation, or in the approximations of Bonifacio & Lugiato (1978), Willis (1978)) do not readily allow the use of potential solutions. It is possible that some exact solution will be found: in the meantime the case of dominant Gaussian fluctuations in the input provides a useful first step towards the study of the distribution function in absorptive bistability.

The main point of interest in this section, is therefore the response of the nonlinear system to a fluctuation in the input field where:

$$E(t) = E_0 + E_1(t)$$

$$\langle E_1(t) E_1^*(t') \rangle = \Gamma \delta(t-t')$$

$$\langle E_1(t) E_1(t') \rangle = 0$$

In general with this type of input, a distribution is obtainable even including arbitrary mode-structures and

(solid-state) inhomogeneous broadening: provided the broadening is symmetric relative to the input frequency. However the simplest case will prove to be for a travelling wave, without inhomogeneous broadening. We give a detailed treatment of this case for $E_0 = 0$, and derive asymptotic correlation functions to all orders, showing the existence of enhanced photon bunching.

We also show that the threshold for enhancement depends on the order of the correlation function: this suggests that the device is a correlation filter that can change the photon statistics by enhancing the n'th order correlations relative to lower order correlations. This could have possible applications in multi-photon spectroscopy, where enhanced higher order correlation functions would augment higher order multi-photon processes relative to lower order ones.

(b) Distribution function

In the case where both mode structure and symmetric inhomogeneous broadening are present, one obtains after adiabatic elimination of atomic variables:

$$\frac{d}{dt}\alpha = E_0 - \kappa\alpha + 2\alpha d_0 \sum_{\mu} \frac{\gamma_{\perp} |g_{\mu}|^2}{\gamma_{\mu} \Pi_{\mu}} + E_1(t)$$

This can be regarded as an Ito stochastic differential equation, with E_1 as the random function. It therefore corresponds to the following Fokker-Planck equations for the Glauber-Sudarshan P-function:

$$\frac{\partial}{\partial t} P(\underline{\alpha}) = \left[\frac{\partial}{\partial \alpha} \left(\kappa \alpha - E_0 - 2\alpha d^0 \sum_M \frac{\gamma_{\perp} |g_M|^2}{|\gamma_M|^2 \Gamma_M} \right) + \frac{1}{2} \left[\frac{\partial^2}{\partial \alpha \partial \alpha^*} + c.c. \right] \right] P(\underline{\alpha})$$

Following the standard potential methods of section 3.2, one can integrate to obtain:

$$P(\underline{\alpha}) = \exp \left[\frac{2}{\Gamma} \left(-\kappa |\alpha|^2 + E_0 \alpha^* + E_0^* \alpha + \frac{\gamma_{\parallel} d^0}{2} \sum_M \ln \left(|\gamma_M|^2 + \frac{4|g_M \alpha|^2 \gamma_{\perp}}{\gamma_{\parallel}} \right) \right) \right]$$

The above equation is the general expression for the distribution function in purely absorptive optical bistability, and can include both the field mode structure and symmetric inhomogeneous broadening via the coupling terms (g^M) for each atom. This applies when the input laser and the interferometer are tuned to the atomic frequency, with Gaussian fluctuations in the input radiation and only one mode interacting with the input field.

In the case of homogeneous broadening and a travelling wave (uniform) mode function, this simplifies to:

$$P(\underline{\alpha}) \propto \exp \left[\frac{2}{\Gamma} \left(-\kappa |\alpha|^2 + E_0 \alpha^* + E_0^* \alpha - 2(\kappa \eta_0 \ln(|\alpha|^2 + \eta_0)) \right) \right]$$

Here ζ, η_0 are as defined previously: they are the cooperativity parameter and threshold photon number respectively.

It is straightforward to graph this numerically, versus the real and imaginary part of α . The result is, as expected, a distribution with twin maxima in the bistable region, with each maximum being locally stable. This is completely different from the pseudo-potential suggested by Gilmore & Narducci (1978), which had a "sombbrero" shape with no bistability. The "sombbrero" distribution is correct for the laser with an injected signal, but not for the physically different situation embodied in optical bistability. We finally note that in the case of the homogeneously broadened travelling wave, our result is similar to the thermodynamic potential mentioned by Bonifacio & Lugiato (1978) who derived it from a different point of view.

(c) Correlation functions

We now wish to calculate the correlation functions, in the case of a purely Gaussian input with a travelling wave and no inhomogeneous broadening. This gives the following distribution function:

$$P(\alpha) \propto (|\alpha|^2 + n_0)^{-\epsilon} \exp\left[-\frac{|\alpha|^2}{\bar{n}}\right]$$

where:

$$\bar{n} \equiv \Gamma/2\kappa$$

$$\epsilon \equiv 2\langle n_0 \rangle / \bar{n}$$

On integration, the j 'th moment of the distribution is obtained to be:

$$\begin{aligned} I_j &= \pi \int_0^{\infty} R^j (R+n_0)^{-\epsilon} \exp\left(-\frac{R}{\bar{n}}\right) .dR \\ &= \pi (\bar{n} n_0)^{\frac{(j-\epsilon)}{2}} \bar{n} e^{\left(\frac{n_0}{2\bar{n}}\right)} j! W_{-\frac{j-\epsilon}{2}, \frac{j+1-\epsilon}{2}}\left(\frac{n_0}{\bar{n}}\right) \end{aligned}$$

Here the moment integrals have been expressed as Whittaker functions (Gradshteyn & Ryzik, 1965).

In order to demonstrate that photon bunching can occur, we will turn to the behaviour in the limit of $\bar{n} \rightarrow \infty$ of this equation. In this limit of a large number of atoms, ϵ becomes a very critical parameter, and the behaviour of the moments depends on the size of $(j+1)$ relative to ϵ . The limiting values are as follows:

(i) $(j+1) < \epsilon$:

$$\begin{aligned} I_j &\simeq \pi \int_0^{\infty} \frac{R^j dR}{[R+n_0]^{\epsilon}} = \pi B(j+1, \epsilon-j-1) \times n_0^{(j+1-\epsilon)} \\ &= \pi n_0^{(j+1-\epsilon)} \frac{\Gamma(j+1) \Gamma(\epsilon-j-1)}{\Gamma(\epsilon)} \end{aligned}$$

(ii) $(j+1) > \epsilon$:

$$\begin{aligned} I_j &\simeq \pi \int_0^{\infty} R^{j-\epsilon} e^{-\frac{R}{\bar{n}}} .dR \\ &= \pi \bar{n}^{(j+1-\epsilon)} \Gamma(j+1-\epsilon) \end{aligned}$$

The above results are true asymptotically, for $\bar{n} \rightarrow \infty$ with ϵ finite. We now examine the behaviour of the n 'th order intensity correlation function:

$$g^{(n)} = I_n [I_0^{-1}]$$

In this case, there are three distinct regions.

$$(i) \quad \epsilon > (j+1)$$

$$g^{(j)} = n_0^j \times j! \Gamma(\epsilon - j - 1) / \Gamma(\epsilon - 1)$$

$$(ii) \quad (j+1) > \epsilon > 1$$

$$g^{(j)} = \bar{n}^{(j+1-\epsilon)} n_0^{(\epsilon-1)} \Gamma(j+1-\epsilon) \cdot (\epsilon-1)$$

$$(iii) \quad 1 > \epsilon$$

$$g^{(j)} = \bar{n}^j \Gamma(j+1-\epsilon) / \Gamma(1-\epsilon)$$

We note here that with decreasing (ϵ) which corresponds to increasing Γ , each correlation function is uniformly increasing. However there is a much greater rate of increase in the middle range, for large values of C (because $\bar{n} \gg n_0$). Therefore this region can be regarded as the threshold. For the j 'th correlation function the threshold point is at:

$$\bar{n}_{thr} \equiv \left[\frac{\Gamma_{thr}}{2\kappa} \right] = 2(n_0) / (j+1)$$

For all the correlation functions, the region (iii) gives a saturation behaviour, in which none of the correlations increase very rapidly. Instead the effective nonlinearity of the medium is reduced (as 50% of the atomic populations are approaching inversion). The saturation point is at:

$$\bar{n}_{sat} = \left[\frac{\Gamma_{sat}}{2\kappa} \right] = 2(n_0) > \bar{n}_{thr}$$

We can illustrate this more clearly in the case of $g^{(j)}(0)$, by calculating $g^{(j)}(0)$ to leading order. In this case due to the normalisation factor it is necessary to deal with four individual regions. These correspond to sub-threshold; increasing $g^{(j)}(0)$; decreasing $g^{(j)}(0)$; and saturated behaviour respectively.

- (i) Subthreshold: ($\epsilon > j+1$) $\ln g^{(j)}(0) \simeq 0$
- (ii) Increasing: ($j+1 > \epsilon > 2$) $\ln g^{(j)}(0) \simeq (j+1-\epsilon) \ln(\frac{\bar{n}}{n_0})$
- (iii) Decreasing: ($2 > \epsilon > 1$) $\ln g^{(j)}(0) \simeq (\epsilon-1)(j-1) \ln(\frac{\bar{n}}{n_0})$
- (iv) Saturated: ($\epsilon < 1$) $\ln g^{(j)}(0) \simeq 0$

In the asymptotic limit, we therefore have all correlation functions with a maximum at:

$$\bar{n} = C n_0$$

The input field and value of the correlation function at maximum will be approximately:

$$\Gamma_{\max} \approx 2CKn_0$$

$$\ln g^{(j)}_{\max} \approx (j-1) \ln C$$

Thus there is a very close relationship between the cooperativity parameter as defined earlier, and the degree of intensity correlation with a Gaussian input field (in the large C limit).

We finally point out that the present analysis predicts that there will be a different threshold for correlation functions of different orders. In fact this means that for low input intensities, there can be an enhancement of $g^{(j)}$ relative to $g^{(j-1)}$ (and other lower order correlations as well). This could have some use as a correlation filter in practical applications, for augmenting higher order multi-photon processes in the output of the interferometer relative to lower order multi-photon and single-photon processes. One limitation however is clearly the reduction in intensity due to dissipation in the nonlinear medium.

Preliminary numerical work has verified the results obtained above for the lower order correlation functions, and the results of this work will be reported elsewhere. However the results obtained analytically have some value in showing that dramatic changes in correlation functions can be obtained in cooperative systems of this type: it is possible that one could regard the correlation functions themselves as "order parameters" in this type of situation.

5.7 VOLTERRA CYCLES AND THE COOPERATIVE FLUORESCENT CRITICAL POINT

(a) Introduction

Cooperative fluorescence in its most nonlinear form involves a quantum state evolving like an "angular momentum oscillator" of a fixed cooperation number J . In this situation the atoms have a definite phase relationship and are described completely by the collective operators \hat{J}^{\pm} , \hat{J}_z . Now this is the driven version of a superfluorescent collective system (Bonifacio & Lugiato, 1975), and is characterised by an extremely fast response time below threshold, as the atoms follow a collective behaviour and emit radiation broadened by a factor of N (for N atoms) relative to the one-atom case.

In fact true cooperative behaviour in an atomic system is difficult to achieve, being limited by factors known as the "coherence length" l_c and the "cooperation lifetime" τ_c . However super-radiance has been observed in practice: this is the cooperative spontaneous emission from an excited collective atomic system (Dicke, 1954) which was first observed by Skribanowitz et al (1973). The observations actually give somewhat different behaviour to that originally predicted by Dicke, with more than one pulse being produced (Dicke's original work gave one directed pulse of $(sech)^2$ intensity). The reason for this behaviour is the propagation effects in an extended dielectric rod (Saunders, Hassan & Bullough, 1976).

The Dicke theory is strictly correct only for atoms without dipole-dipole interactions in the small volume limit (i.e., a point system). In the case of a driven system, similar limitations hold: a simplified theory is obtained by ignoring spatial propagation effects. Now it can be asked if this will give a realistic model for an experiment. In fact there is no doubt that spatial propagation effects will be relevant in practice in observing "driven super-fluorescence". However even the single-mode model has not been solved for this case, so it is worthwhile to obtain solutions for the simple case as a first step toward understanding this situation.

The quantum mechanical master equation we work with simply has a driving field and a reservoir coupled to the collective operators (Agarwal, 1974). Therefore, it has the following form in the rotating frame:

$$\frac{\partial \hat{\rho}}{\partial t} = \left(\frac{-i\Omega}{2} \right) [\hat{J}_+ + \hat{J}_-, \hat{\rho}] + \frac{\gamma}{2} [2\hat{J}_- \hat{\rho} \hat{J}_+ - \hat{J}_+ \hat{J}_- \hat{\rho} - \hat{\rho} \hat{J}_+ \hat{J}_-]$$

We emphasise that the same master equation (at least, in the collective damping) was obtained by Glauber & Haake (1974) for an extended system with the single-mode method. This is simply the generalisation to spin-J operators of spin- $\frac{1}{2}$ resonance fluorescence.

Similar but more general master equations are treated approximately by Bonifacio & Lugiato (1978), Agarwal et al (1978), Walls et al (1978). These treatments have all involved various factorisation assumptions: and

it is the advantage of the present equation that it can be treated using the atomic coherent state representation without factorisation assumptions. An early treatment of this problem is given by Senitzky (1972) who however did not solve the classical equations of motion or give the quantum corrections except for approximations only valid for very large and very small driving fields.

By the use of the ACS representation, it is possible to solve the semiclassical equations exactly, and obtain the quantum corrections to the distribution function in an asymptotic expansion valid for large J , and for all driving fields. This is the region where we shall see behaviour analogous to a critical point phase transition, with the development of Volterra-Lotka like limit-cycles above the threshold.

Below threshold the system has a "super-fluorescent" behaviour with fluorescent intensity proportional to J . This cooperative branch is stable until a critical driving field is reached, when an ordered dissipative structure is created like a family of Lotka-Volterra cycles (Glansdorff & Prigogine, 1971, Lotka, 1920, Volterra, 1931). Critical slowing down occurs close to the threshold point which is identified as a nonequilibrium critical point in the thermodynamic limit. Above threshold the polarisation average decreases with increasing driving field, and the average inversion is zero above threshold in the limit $J \rightarrow \infty$.

Using the large J limit, and a semiclassical factorisation, the correlation functions and spectrum can

also be calculated. Below threshold, the spectrum is a coherent delta-function, at the input frequency. Above threshold, the spectrum splits into multiple sidebands.

With the inclusion of quantum fluctuations, it is shown in section 5.9, that the semiclassical factorisation is correct to leading order (on a time scale of less than γ^{-1}) with quantum corrections being of order $1/J$. These results therefore do not contradict the calculations for $J = 1, 3/2$ of Agarwal et al (1976) where quantum fluctuations are large. However the full spectrum in the large- J limit, including finite line-widths due to quantum fluctuations, remains an open question.

(b) Semiclassical results

The semiclassical (Maxwell-Bloch) equations are as follows (no inhomogeneous broadening, on resonance):

$$\langle \dot{a} \rangle = -i\bar{g} \langle J^- \rangle + E - \kappa \langle a \rangle$$

$$\langle \dot{J}^- \rangle = -\gamma_{\perp} \langle J^- \rangle + 2i\bar{g} \langle J^{\pm} \rangle \langle a \rangle$$

$$\langle \dot{J}_z \rangle = -\gamma_{\parallel} [\langle J_z \rangle + J] + i\bar{g} [\langle J^- \rangle \langle a^+ \rangle - \langle J^+ \rangle \langle a \rangle]$$

We now eliminate the cavity field adiabatically by setting $\kappa \gg \gamma_{\perp}, \gamma_{\parallel}$:

Hence (for E with a real phase):

$$\langle a \rangle = \frac{1}{\kappa} [E - i\bar{g} \langle \hat{J}_- \rangle]$$

$$\frac{d}{dt} \langle \hat{J}_- \rangle = -\gamma_{\perp} \langle \hat{J}_- \rangle + \frac{2i\bar{g}}{\kappa} [E - i\bar{g} \langle \hat{J}_- \rangle] \langle \hat{J}_z \rangle$$

$$\frac{d}{dt} \langle \hat{J}_z \rangle = -\gamma_{\parallel} [\langle \hat{J}_z \rangle + J] + \frac{i\bar{g}}{\kappa} [E(\langle \hat{J}_- \rangle - \langle \hat{J}_+ \rangle) + 2i\bar{g} \langle \hat{J}_+ \rangle \langle \hat{J}_- \rangle]$$

In the time less than the individual atom decay times ($\gamma_{\parallel}^{-1}, \gamma_{\perp}^{-1}$) we have the possibility of super-radiant behaviour, described by the following semi-classical equations:

$$\frac{d}{dt} \langle \hat{J}_+ \rangle = \left(\frac{-2i\bar{g}E}{\kappa} \right) \langle \hat{J}_z \rangle + \frac{2\bar{g}^2}{\kappa} \langle \hat{J}_+ \rangle \langle \hat{J}_z \rangle$$

$$\frac{d}{dt} \langle \hat{J}_z \rangle = \left(\frac{i\bar{g}E}{\kappa} \right) \{ \langle \hat{J}_- \rangle - \langle \hat{J}_+ \rangle \} - \frac{2\bar{g}^2}{\kappa} \langle \hat{J}_+ \rangle \langle \hat{J}_- \rangle$$

This result which is derived for an extended system can be compared now with the corresponding point system equation, derived from the master equation. (Note that all atomic variables are in the interaction picture.)

In this case we obtain:

$$\frac{d}{dt} \langle \hat{J}_+ \rangle = -i\Omega \langle \hat{J}_z \rangle + \gamma \langle \hat{J}_+ \hat{J}_z \rangle$$

$$\frac{d}{dt} \langle \hat{J}_z \rangle = -\left(\frac{i\Omega}{2}\right) \langle \hat{J}_+ - \hat{J}_- \rangle - \gamma \langle \hat{J}_+ \hat{J}_- \rangle$$

This leads to the identification:

$$\Omega = 2\bar{g}E/\kappa \quad ; \quad \gamma = 2\bar{g}^2/\kappa$$

Thus we see that the operator equations of motion (and in fact also the master equation) are the same for either the cavity model of Glauber & Haake or the point system (without dipole-dipole coupling). Other terms also occur in the full equations of motion, like dipole-dipole coupling (Friedberg et al, 1972) or individual atomic decays, that can break the J^2 -invariance symmetry on a long time scale. However we wish to analyse the behaviour during the cooperation lifetime, so these terms are therefore omitted.

In the semiclassical method, the operators are factorised using the direct factorisation $\langle \hat{J}^\alpha \hat{J}^\beta \rangle = \langle \hat{J}^\alpha \rangle \langle \hat{J}^\beta \rangle$. We will show this to be justified (below threshold) in section 5.9, at least in the limit of large J . This leads to a system of nonlinear coupled differential equations that are J^2 -invariant, that is:

$$\begin{aligned}
 \frac{\partial}{\partial t} \langle \hat{J}_z^2 \rangle &= \frac{\partial}{\partial t} \langle \hat{J}_x^2 + \hat{J}_y^2 + \hat{J}_z^2 \rangle \\
 &\approx \frac{\partial}{\partial t} [\langle \hat{J}_z \rangle^2 + \langle \hat{J}^+ \rangle \langle \hat{J}^- \rangle] \\
 &= \langle \hat{J}_z \rangle \{ -i\Omega \langle \hat{J}^+ - \hat{J}^- \rangle - 2\gamma_c \langle \hat{J}^+ \rangle \langle \hat{J}^- \rangle \} \\
 &\quad + [\langle \hat{J}^+ \rangle \{ i\Omega \langle \hat{J}_z \rangle + \gamma_c \langle \hat{J}^- \rangle \langle \hat{J}_z \rangle \} + \text{cc.}] \\
 &= 0
 \end{aligned}$$

The property of J^2 -invariance allows the use of the atomic coherent state representation. In fact the original master equation was J^2 -invariant in the quantum-

mechanical sense of operator invariance. However at this stage it is possible to take advantage of the "semi-classical" \hat{J}^2 -invariance of the factorised equations, and eliminate one variable in the process. We therefore define:

$$\langle \hat{J}^+ \rangle = 2Jz / (1 + z z^*) ; \quad \langle \hat{J}^- \rangle = 2Jz^* / (1 + z z^*)$$

$$\langle \hat{J}^2 \rangle = J(1 - z z^*) / (1 + z z^*)$$

It is trivial that in fact one obtains the invariance properties required, i.e.:

$$\langle \hat{J}^2 \rangle = \langle \hat{J}^2 \rangle + \langle \hat{J}^+ \rangle \langle \hat{J}^- \rangle = J^2$$

We note here that quantum-mechanically one has

$$\langle \hat{J}^2 \rangle = J(J+1) ; \quad \text{thus the approximation breaks}$$

down for small J -values as one would expect. Of course the use of the full quantum atomic coherent state representation does give correct commutation relations, as discussed in section 5.9.

The dynamical equations now transform to the following very simple form:

$$\frac{\partial}{\partial t} z = \left(\frac{i\Omega}{2} \right) (z^2 - 1) + \gamma J z$$

$$\frac{\partial}{\partial t} z^* = \left(\frac{-i\Omega}{2} \right) (z^{*2} - 1) + \gamma J z^*$$

It is simple to verify that this will reproduce the semi-classical equations of motion, and is clearly a much more elegant system to work with. In fact we will use similar

equations (with stochastic terms) for the fully quantum-mechanical problem in section 5.9.

Since this equivalence leads to a solution of the semiclassical equations which have not been solved previously, it is worthwhile to prove it directly.

We prove this in detail as follows:

$$\frac{\partial}{\partial t} \left[\frac{2Jz}{1+zz^*} \right] = \frac{2J(\dot{z} - z^2 \dot{z}^*)}{(1+zz^*)^2}$$

Using the equations for \dot{z}, \dot{z}^* we obtain:

$$\begin{aligned} \frac{\partial}{\partial t} \langle \hat{J}_+ \rangle &= \left[\frac{2J}{(1+zz^*)^2} \right] \left[\frac{1}{2} i\Omega(z^2-1) + \gamma J_3 + \frac{1}{2} i\Omega z^2(z^{*2}-1) - \gamma J_3^2 z^* \right] \\ &= \left[\frac{1}{1+zz^*} \right] \left[-J i\Omega(1-3z^*) \right] + 2J\gamma z(1-3z^*) \left[\frac{1}{(1+3z^*)^2} \right] \\ &= -i\Omega \langle \hat{J}_z \rangle + \gamma \langle \hat{J}_z \rangle \langle \hat{J}_+ \rangle \end{aligned}$$

Similarly the equation for $\frac{\partial}{\partial t} \langle \hat{J}_z \rangle$ is:

$$\begin{aligned} \frac{\partial}{\partial t} \langle \hat{J}_z \rangle &= \left[\frac{-J}{(1+3z^*)^2} \right] \left[(1+3z^*)(3\dot{z}^* + \dot{3}z^*) + (1-3z^*)(3\dot{z}^* + \dot{3}z^*) \right] \\ &= \left[\frac{-2J}{(1+3z^*)^2} \right] \left[3^*(i\Omega(z^2-1) + \gamma J_3) + 3(-i\Omega(z^{*2}-1) + \gamma J_3^*) \right] \\ &= \frac{-i\Omega J(z-3^*)}{(1+3z^*)} - \frac{4J^2\gamma 33^*}{(1+3z^*)^2} \\ &= -\left[\frac{1}{2} \right] i\Omega \langle \hat{J}_+ - \hat{J}_- \rangle - \gamma \langle \hat{J}_+ \rangle \langle \hat{J}_- \rangle \end{aligned}$$

Thus we have shown the equivalence between the original set of semiclassical equations, and the dynamical equations in the atomic coherent state representation.

The great advantage of this representation is that the dynamical equations are completely soluble; one obtains:

$$(t-t_0) = \int_{z_0}^z \frac{2 dz}{i\Omega(z-r^+)(z-r^-)} = \int_{z_0^*}^{z^*} \frac{2 dz^*}{-i\Omega(z^*+r^+)(z^*+r^-)}$$

Here r^\pm are defined as the stationary points of the deterministic equations:

$$\begin{aligned} r^\pm &= \left(\frac{1}{i\Omega}\right) \left\{ -\gamma J \pm \sqrt{(\gamma J)^2 - \Omega^2} \right\} \\ &= i\gamma \pm \chi \end{aligned}$$

Where χ, γ are defined as follows:

$$\gamma = \frac{\Omega_0}{\Omega} \quad ; \quad \Omega_0 \equiv \gamma J$$

$$\chi = \sqrt{1-\gamma^2} \quad (\Omega > \Omega_0) \quad ; \quad = \sqrt{\gamma^2-1} / i \quad (\Omega < \Omega_0)$$

On integrating, the results are:

$$(t-t_0) = \int_{z_0}^z \frac{2}{i\Omega(r^+-r^-)} \ln\left(\frac{z-r^+}{z-r^-}\right) = \int_{z_0^*}^{z^*} \frac{-2}{i\Omega(r^++r^-)} \ln\left(\frac{z^*+r^-}{z^*+r^+}\right)$$

Hence, we obtain:

$$\left[\frac{z-r^+}{z-r^-}\right] = \sqrt{c_0} \cdot \exp(i\Omega\chi t - i\Omega\chi t_0) = \alpha(t)$$

Here c_0, t_0 are real parameters describing the initial values. We note that there is a very different behaviour depending on the amplitude of the driving field relative to the threshold at $\Omega = \Omega_0$. For $\Omega < \Omega_0$, there is a

global attractor at $z = r^-$, with decay time-constant $\tau = (|\Omega_0^2 - \Omega^2|)^{-1/2}$. In fact for $\Omega = 0$ this corresponds to the (sech^2) result of single-pulse super-fluorescence.

Above threshold the solutions are a family of cycles, characterised by c_0 , the initial cycle parameter. We find that c_0 is in the range $0 \leq c_0 \leq \infty$. The solutions all have the same period $2\pi\tau$. Now the cycle parameter is a Hamiltonian-like invariant of the deterministic equations, similar to that of Lotka-Volterra cycles that are found in chemical and ecological systems (Nicolis & Prigogine, 1977). For this reason we have used the term "Lotka-Volterra" cycles to describe these solutions, to distinguish them from the isolated limit cycles that are found in some other nonequilibrium systems (see Chapters 3 and 4). The general behaviour of the system, with a thermodynamic branch below threshold and a dissipative structure when the driving field is increased beyond threshold is typical of many nonequilibrium phase transitions.

In the complex plane the cycles are in fact circular, with solution paths satisfying:

$$c_0 = \left| \frac{z - r^+}{z - r^-} \right|^2$$

On simplifying this expression, one obtains:

$$z z^* (1 - c_0) - z^* (r^+ - c r^-) - z (r^+ - c r^-)^* = c_0 - 1$$

$$\therefore |z - \delta|^2 = \rho^2$$

That is, the cycles are circular with centre at $z = \delta$ and radius ρ where we define:

$$\delta = \left[\frac{r^+ - cr^-}{1 - c} \right] = i\gamma + \chi \left(\frac{1+c}{1-c} \right)$$

$$\rho^2 = \delta\delta^* - 1$$

In summary we have completely solved the deterministic equations for arbitrary initial values, described by real parameters J, c, t_0 .

It is worth pointing out that the point $\Omega = \Omega_0$ is analogous to the critical point of a phase transition, as both the cycle period above threshold and the decay time below threshold have a critical slowing down near $\Omega = \Omega_0$. Furthermore, we will see later that in the thermodynamic limit of $J \rightarrow \infty$, the derivatives of the observables relative to Ω (but not the observables themselves) have a discontinuity at $\Omega = \Omega_0$. This gives a close similarity to the definition of an equilibrium critical point transition, and is the reason why we describe this as a new critical point transition in non-equilibrium statistical physics.

5.8 MULTIPLE SIDEBANDS IN COOPERATIVE FLUORESCENCE

In the previous section we have obtained the solutions to the equations of motion for arbitrary initial values. We now turn to the problem of evaluating observables, in particular the mean values of the polarisation and inversion, as well as the semiclassical spectrum. New results are obtained for an arbitrary driving field above threshold. The results for the steady-state semiclassical mean values below threshold agree with those obtained by Senitzky (1972). Above threshold results were only obtained approximately by Senitzky in the strong field limit: in this limit, the polarisation and inversion are both zero. Approximate results for the spectrum in the strong field limit were obtained by Senitzky (1978), giving extra sidebands compared to the three peaks found by Mollow (1969) for one-atom resonance fluorescence. Unfortunately the extra sidebands in fact vanish in the strong field limit. Therefore it is of much greater interest to calculate the spectrum for a finite driving field, and this is the main objective of this section. The results are of greatest interest in the region of a driving amplitude slightly greater than the threshold point, where the extra sidebands have a maximum fluorescent intensity. The optimum driving field for observation of a five-peak spectrum is predicted to be $\Omega = \sqrt{\frac{4}{3}} \Omega_0$: it seems that this observation would be of great value in confirming present theories of cooperative fluorescence.

We first evaluate the semiclassical behaviour below threshold (noting that this factorisation is expected to be valid for large J values); and obtain the following steady-state results:

$$\text{Inversion: } \langle J_3 / J_0 \rangle = -\sqrt{(1 - \Omega^2 / \Omega_0^2)}$$

$$\text{Polarisation: } \langle J_y / J_0 \rangle = \Omega / \Omega_0$$

$$\text{Dispersion: } \langle J_x / J_0 \rangle = 0$$

$$\text{Spectrum: } \rho(\omega) = \delta(\omega - \omega_0) J^2 (\Omega / \Omega_0)^2$$

$$\text{Correlation function: } g^2(0) = 1$$

These results are only valid relative to the semiclassical factorisation, and within a time-scale where the J^2 operator is invariant. In fact in section 5.9 we will include the quantum fluctuations that are relevant here: we will prove that the results quoted above are the leading terms in an asymptotic expansion in $(1/J)$, and the semiclassical factorisation is correct including terms to order $(1/J)$, below threshold.

In physical terms, the system behaves as a classical oscillator below threshold, with all atoms in phase. However the fluorescent radiation from a real extended system would not be all in phase: it should be recognised that for an extended system the adiabatic elimination of the radiation field means that only the high intensity fluorescence of the "end-fire" mode has been included.

The perpendicular, low-intensity fluorescence from the medium is also present, but is neglected in the approximations leading to the J^2 -invariant equations.

We next turn to the observables above threshold. An integral over a Volterra cycle is necessary to calculate the polarisation. As these integrals are similar for the calculation of any observable above threshold, we shall look at this calculation in detail. Any observable will be a function $O(z, z^*)$, which can be computed as follows, for a cycle distribution function $f(c)$:

$$\langle\langle O \rangle\rangle = \int_0^\infty dc \cdot f(c) \oint_c O(z, z^*) d\tau_c(z)$$

$$d\tau_c(z) \equiv \lambda dz / [\pi i (z - r^+)(z - r^-)]$$

Although this function is nonanalytic (being a function of z and z^*), we can utilise the cycle equation to define z^* in terms of z , and thus obtain a meromorphic function which can be integrated by residues. The cycle equation is simply obtained, for cycles of radius ρ , centre δ :

$$z^* = \delta^* + \rho^2 / (z - \delta)$$

Hence we write the Volterra cycle integral in the following form:

$$\langle O \rangle_c = \oint_c \frac{O(z, \delta^* + \rho^2 / (z - \delta)) \lambda dz}{\pi i (z - r^+)(z - r^-)}$$

This clearly has poles at $z = r_{\pm}^{\pm}$, and it is straightforward to verify that cycles with $c < 1$ enclose r_+ , while cycles with $c > 1$ enclose r_- . In fact it is only necessary to make the calculation for $0 < c < 1$, as the results for $c > 1$ are obtained using the symmetry transformation $[c \rightarrow c^{-1}, z \rightarrow -z^*]$.

The function O will usually have a pole structure, which we now determine. In general, the denominator of O has a factor of form:

$$\begin{aligned} [1+3z^*] &= [(z-\delta)(1+3\delta^*z) + 3\rho^2] / [z-\delta] \\ &= \delta^* (z^2 - \varepsilon^2) / (z-\delta) \end{aligned}$$

Here we define $\varepsilon = \delta/|\delta|$ and utilise the following identity:

$$\rho^2 = \delta\delta^* - 1$$

It is now necessary to determine which if any of the poles $\pm\varepsilon$ are included in the residue theorem. This is straightforward, as the cycle is a circle of radius ρ around the centrepoint δ . Thus we merely have to determine the distance $|\pm\varepsilon - \delta|$:

$$|\pm\varepsilon - \delta| = |\delta| \mp 1$$

Noting that $|\delta| = \sqrt{1+\rho^2}$ the following relation holds:

$$(|\delta|+1)^2 > \rho^2 > (|\delta|-1)^2$$

It therefore follows that the cycle encloses the pole at ξ only: the cycles never enclose the $-\xi$ pole.

The calculation for the polarisation is obtained on using Cauchy's integral theorem:

$$\begin{aligned} \langle J^+ \rangle_c &= \left[\frac{X}{\pi i} \right] \oint_c \frac{2z(z-\delta)J dz}{\delta^*(z^2-\xi^2)(z-r^+)(z-r^-)} \\ &= 2JX \sum_{\text{Res}} \frac{2z(z-\delta)}{\delta^*(z^2-\xi^2)(z-r^+)(z-r^-)} \end{aligned}$$

The residue at $z=r^+$ is evaluated at first; with the following identities:

$$(r^+-\delta) = -2cX/(1-c)$$

$$\begin{aligned} (r^+-\xi^2) &= \frac{1}{\delta^*(1-c)} \left[r_+^2 (c r_+ - r_-) - (r_+ - r_-) \right] \\ &= \frac{c r_+}{\delta^*(1-c)} \left[r_+^2 - r_-^2 \right] \\ &= \frac{4icX\gamma r_+}{\delta^*(1-c)} \end{aligned}$$

Hence the residue reduces to the following simple result:

$$\text{Res}_{(r^+)} = \frac{i}{2X\gamma}$$

The residue at $z=\xi$ is evaluated in a similar way with the following identities:

$$\langle \xi - \delta \rangle = \frac{\delta}{|\delta|} (1 - |\delta|)$$

$$\delta^* (\xi - r^+) (\xi - r^-) = \delta^* (\delta / \delta^* - 2i\gamma \xi - 1)$$

$$= 2i\gamma (1 - |\delta|)$$

Hence once again there is a simple result:

$$\text{Re } s(\xi) = \frac{\xi}{2i\gamma}$$

The overall result is therefore:

$$\langle J^+ \rangle_c = J \times \left[\frac{i}{x\gamma} + \frac{(1-c) + (1+c)(x/i\gamma)}{\sqrt{1+c^2 + 2c(x^2 - \gamma^2)}} \right]$$

Now the "pendulum" result is the situation where the inversion goes through both the north and south poles of the Bloch sphere. In this case we obtain ($\xi = c = 1$):

$$\langle J^+ \rangle = J i \left[\Omega / \Omega_0 - \sqrt{\Omega^2 / \Omega_0^2 - 1} \right]$$

This solution displays a lot of the character expected above threshold, with a gradually decreasing polarisation as the driving field increases and the system is close to the poles of the Bloch sphere for longer times on the average.

We next calculate the mean inversion for the cycle:

$$\begin{aligned} \langle \hat{j}_3 \rangle_c &= 2JX \sum_{\text{Res}} \frac{(z-s) - z(\rho^2 + s^*(z-s))}{s^*(z^2 - \epsilon^2)(z-r^+)(z-r^-)} \\ &= 2JX \sum_{\text{Res}} \frac{2z - s - z^2 s^*}{s^*(z^2 - \epsilon^2)(z-r^+)(z-r^-)} \end{aligned}$$

$$\text{Res}(r^+) = \left[\frac{1-c}{2x} \right] \left[\frac{2r^+ - s - r^{+2} s^*}{4icx\gamma r^+} \right]$$

Now we can simplify the numerator as follows:

$$\begin{aligned} (2r^+)(1-c) + r^+ - cr^- - r^{+2}(cr^+ - r^-) \\ &= -cr^+(r_+ - r_-)^2 \quad (r^- = -1/r_+) \\ &= -4cx^2 r^+ \end{aligned}$$

$$\therefore \text{Res}(r^+) = \frac{i}{2\gamma}$$

$$\begin{aligned} \text{Res}(\epsilon) &= \left[\frac{2\epsilon - s - \epsilon^2 s^*}{4\epsilon i \gamma (1 - |\delta|)} \right] \\ &= \left[\frac{2\epsilon (1 - |\delta|)}{4\epsilon i \gamma (1 - |\delta|)} \right] \\ &= \left(\frac{-i}{2\gamma} \right) \end{aligned}$$

Hence:

$$\langle \hat{j}_3 \rangle_c = 0$$

This result implies that the cycle-average inversion is zero for any cycle above threshold. One expects naturally that this should be true for $\Omega \rightarrow \infty$, but the

result that $\langle \hat{J}_3 \rangle_c = 0$ for all $\Omega > \Omega_0$ is rather unexpected. In particular, it is not true for $J = \frac{1}{2}$. The reason for this discrepancy is the use of the semi-classical factorisation, which is only asymptotically correct, in the large- J limit.

In order to summarise the results obtained above threshold, it is useful to define an auxiliary function as follows:

$$v(c) = \frac{1}{|r^+ - cr^-|}$$

$$= \frac{1}{\sqrt{(1-c)^2 + 4cX^2}}$$

The time average results can be summarised using this function:

$$\text{Inversion:} \quad \langle \hat{J}_3 / J \rangle = 0$$

$$\text{Polarisation:} \quad \langle \hat{J}_y / J \rangle = \frac{\Omega}{\Omega_0} [1 - v(c)X^2(1+c)]$$

$$\text{Dispersion:} \quad \langle \hat{J}_x / J \rangle = v(c)X(1-c)$$

All these results were obtained with a cycle parameter $c < 1$. However the results are invariant under the transformation $c \rightarrow 1/c$, $X \rightarrow -X$ and therefore hold equally for $c > 1$.

In the limit of $\Omega \rightarrow \infty$, it is interesting to note that for the central cycle ($c = 1$) both the mean polarisation and dispersion vanish. However for the cycles with $c \neq 1$, the dispersive term tends to a finite

value, of $(1-c)/(1+c)$, whose sign depends on the cycle parameter. It will be shown later that this implies the existence of a central spectral peak for those cycles with $c \neq 1$ in the limit of a large driving field.

The correlation function above threshold is of interest as it determines the fluorescent spectrum. A general expression for the spectrum is:

$$S(\omega+\omega_0) = \lim_{t \rightarrow \infty} \left(\frac{1}{2\pi t} \right) \iint_0^t dt_1 dt_2 e^{i\omega(t_1-t_2)} \langle \hat{J}^+(t_2) \hat{J}^-(t_1) \rangle$$

This will first be calculated semiclassically to give a simple expression for the peak areas and frequencies while neglecting quantum noise effects. The system is cyclic of period $2\pi T$, so the spectrum will be a sum of delta functions in the semiclassical decorrelation; where $\omega = \tau^{-1} = \Omega X$:

$$S(\omega+\omega_0) = \sum_n \delta(\omega - \omega_n) \left[\frac{1}{4\pi^2 T^2} \right] \iint_0^{2\pi T} e^{i\omega_n(t_1-t_2)} \langle \hat{J}^+(t_2) \rangle \langle \hat{J}^-(t_1) \rangle dt_1 dt_2$$

Here the mean values cannot be steady-state values, but must be defined relative to a specified initial state in order to determine a spectrum. In particular it will be of interest to determine the spectrum relative to the initial state $J = N/2$, $c = 1$. This corresponds to all the atoms initially in the ground state which is likely to be the simplest possible experiment. From previous results, we know that -

$$e^{i\omega(t-t_0)} = \left[\frac{z - r^+}{\sqrt{c}(z - r^-)} \right]^{\omega T}$$

$$= \left[\frac{z^* + r^-}{\sqrt{c}(z^* + r^+)} \right]^{-\omega T}$$

Thus the spectrum corresponding to initial values of c_0, J, t_0 can be obtained on transforming to integration over z :

$$S(\omega + \omega_0) = \sum_n \delta(\omega - \omega_n) \left| \oint_c \frac{2Jz}{(1+zz^*)} \left[\frac{\sqrt{c}(z - r^-)}{(z - r^+)} \right]^n d\tau_c(z) \right|^2$$

This integral is another Cauchy theorem application. The path of integration is a Volterra cycle path in the complex z -plane. Therefore on integrating we have a term corresponding to each pole inside the path of integration. Define the relevant integral as follows:

$$J(c, m) = \oint_c \frac{2JXz(z-\delta)}{\delta^* (z^2 - \varepsilon^2)} \left[\frac{\sqrt{c}(z - r^-)}{(z - r^+)} \right]^m \frac{dz}{(\pi i)(z - r^+)(z - r^-)}$$

$$= \left[\frac{4JXc^{m/2}}{\delta^*} \right] \sum_{\text{Res}} \left[\frac{z(z-\delta)}{(z-r^+)(z-r^-)(z^2-\varepsilon^2)} \right] \left[\frac{z-r^-}{z-r^+} \right]^m$$

Now for $c \ll 1$ the poles inside the path of integration are at $z = \varepsilon, z = r^+$. Hence the result depends on the value of m as follows:

- (i) $m < 0$ In this case only the pole at $z = \varepsilon$ is to be included, so one obtains:

$$J(\zeta, m) = \left[\frac{J \varepsilon X}{i \gamma} \right] \left[\frac{(\varepsilon - r_-) \sqrt{\zeta}}{(\varepsilon - r_+)} \right]^m$$

(ii) $m = 0$: This case reduces to the previous result for the polarisation:

$$J(\zeta, 0) = \left[\frac{iJ}{\gamma} \right] (1 - \varepsilon X)$$

(iii) $m > 0$ In this integration we take advantage of a theorem of integral calculus that states that if a uniform function has a finite number of singularities then the sum of the residues (including the one at infinity) is zero. In this case the residue at infinity is zero, so the result is (minus the residue at $z = -\varepsilon$); because as stated previously this residue is always outside the cycle path:

$$\begin{aligned} J(\zeta, m) &= \left[\frac{-4J X \zeta^{m/2} \varepsilon (\varepsilon + \delta)}{\delta^4 (\varepsilon + r_+) (\varepsilon + r_-) (-2\varepsilon)} \right] \left[\frac{\varepsilon + r_-}{\varepsilon + r_+} \right]^m \\ &= \left[\frac{J \varepsilon X}{i \gamma} \right] \left[\frac{(\varepsilon + r_-) \sqrt{\zeta}}{(\varepsilon + r_+)} \right]^m \end{aligned}$$

In order to simplify the results, it is useful to have the following identities:

$$|\xi \pm r|^2 = 2[1 \mp v(c)(2x^2 + c - 1)]$$

$$|\xi \pm r|^2 = 2[1 \pm v(c)(1 - c + 2cx^2)]$$

Hence we obtain:

($m < 0$):

$$|J(c, m)|^2 = \left[\frac{J^2 X^2 c^{m/2}}{Y^2} \right] \left[\frac{1 + v(c)(2x^2 + c - 1)}{1 - v(c)(1 - c + 2cx^2)} \right]^m$$

($m > 0$)

$$|J(c, m)|^2 = \left[\frac{J^2 X^2 c^{m/2}}{Y^2} \right] \left[\frac{1 - v(c)(2x^2 + c - 1)}{1 + v(c)(1 - c + 2cx^2)} \right]^m$$

In summary the spectrum is as follows, for $c < 1$:

$$\rho_c^{\downarrow}(\omega + \omega_0) = \frac{J^2}{Y^2} \left[\delta(\omega) |1 - v(c)X(r^+ - cr^-)|^2 + \sum_{n=\pm 1, \pm 2, \dots} \delta(\omega - \omega_n) X^2 c^{n/2} \left[\frac{1 \mp v(c)(2x^2 + c - 1)}{1 \pm v(c)(1 - c + 2cx^2)} \right]^n \right]$$

where the uppermost sign of (\pm) refers to $n > 0$.

The spectrum for $c > 1$ is related to the one for $c < 1$ by the symmetry relation referred to previously. That is the spectrum for $c' = 1/c$ is obtained as follows:

$$\rho_{c'}^{\downarrow}(\omega + \omega_0) = \rho_c^{\downarrow}(-\omega + \omega_0)$$

Both spectra are geometric progressions, with one the mirror image of the other when reflected about the central peak at ω_0 . In general it is also clear that the fluorescence is asymmetric given a value of $c \neq 1$. We will see in the next section, that this is essentially a transient feature due to the particular initial value chosen. In the true (quantum) steady-state, there is a distribution over the cycle parameter which produces a spectrum with both wings.

Of greatest interest is the semiclassical result for $c=1$, which corresponds to an initial ground state. In this case the following completely symmetric result is obtained:

$$P_1(\omega+\omega_0) = \left[\frac{J^2}{\gamma^2} \right] \left\{ \delta(\omega)(1-x)^2 + \sum_{n \neq 0} \delta(\omega - \omega_n) x^2 \left[\frac{1-x}{1+x} \right]^{|n|} \right\}$$

The total power radiated is proportional to the sum of the geometric series:

$$\begin{aligned} P_{\text{tot}} &= \left(\frac{J^2}{\gamma^2} \right) (1-x) \\ &= \left(\frac{J\Omega}{\Omega_0} \right)^2 \left(1 - \sqrt{1 - (\Omega_0/\Omega)^2} \right) \end{aligned}$$

In the strong field limit, we obtain the following result:

$$\lim_{\Omega \rightarrow \infty} (1-x) = \frac{1}{2} \left(\frac{\Omega_0}{\Omega} \right)^2$$

Hence the spectrum to order $(\frac{1}{\Omega})^2$ is of form:

$$\lim_{\Omega \rightarrow \infty} \int_1(\omega + \omega_0) = J^2 \left\{ \delta(\omega) \left[\frac{\Omega_0}{2\Omega} \right]^2 + \frac{1}{4} \sum_{n \neq 0} \delta(\omega - n\Omega) \left[\frac{\Omega_0}{2\Omega} \right]^{2(|n|-1)} \right\}$$

This agrees with the asymptotic result for $n = \pm 1, \pm 2$ obtained by Senitzky (1978) noting that our $\epsilon = 1$ corresponds to his $\alpha = 1$.

The interesting feature of this limit is the vanishing central peak and vanishing sidebands for $|n| > 1$. In reality we will see later that the vanishing central peak is due to neglect of quantum fluctuations: even for an initial ground state, the distribution in ϵ will broaden on a time-scale of γ^{-1} due to spontaneous emission, resulting in a final steady-state with a non-vanishing central peak in the strong field limit. In fact the above result corresponds to a classical sinusoidal oscillator in the rotating frame, with frequency Ω , in the strong field limit.

The vanishing sidebands are a different problem altogether. Senitzky (1978) suggests that this could make the extra sidebands too weak to detect. However in the present result which is valid for all Ω , it is clear that while the extra sidebands vanish in the strong field limit, they have a maximal fluorescent intensity at a much lower driving field. The optimal driving field can be calculated as follows: Suppose we wish to obtain a maximum in the first pair of extra sidebands (giving at

least five peaks that can be detected). Then we have:

$$P = \left(\frac{J^2 X^2}{1-X^2} \right) \left(\frac{1-X}{1+X} \right)^2$$

$$\frac{\partial P}{\partial X} = \left(\frac{2J^2 X(1-2X)}{(1+X)^4} \right)$$

The maximum sideband intensity occurs at $\frac{\partial P}{\partial X} = 0$. This corresponds to: $X = 1/2$. The driving field is therefore $\Omega = \sqrt{4/3} \Omega_0$. At this point we have:

$$\begin{aligned} \sum_i P_i(\omega + \omega_0) = & J^2 \left\{ \delta(\omega) / 3 + \right. \\ & \left. + \sum_{n \neq 0} \delta\left(\omega - \frac{\Omega n}{2}\right) \left[\frac{1}{3} \right]^{|n|+1} \right\} \end{aligned}$$

Hence this would give a ratio of peak areas of

$$1 : 1/3 : 1/9 : 1/27 \quad , \quad \text{and a spacing of } (\Omega/2) \text{ in frequency.}$$

As a finite total of $(1/18)$ of the total fluorescent power is radiated into each of the first extra pair of sidebands, this should be strong enough to be detected (provided Doppler broadening problems do not interfere). A graph of the relative power of each sideband is given in fig 5.8.1.

We finally wish to make some comment about previous work on this subject. As already pointed out, our results verify the asymptotic approximations of Senitzky (1972, 1978), who obtained results valid in the limit of a large

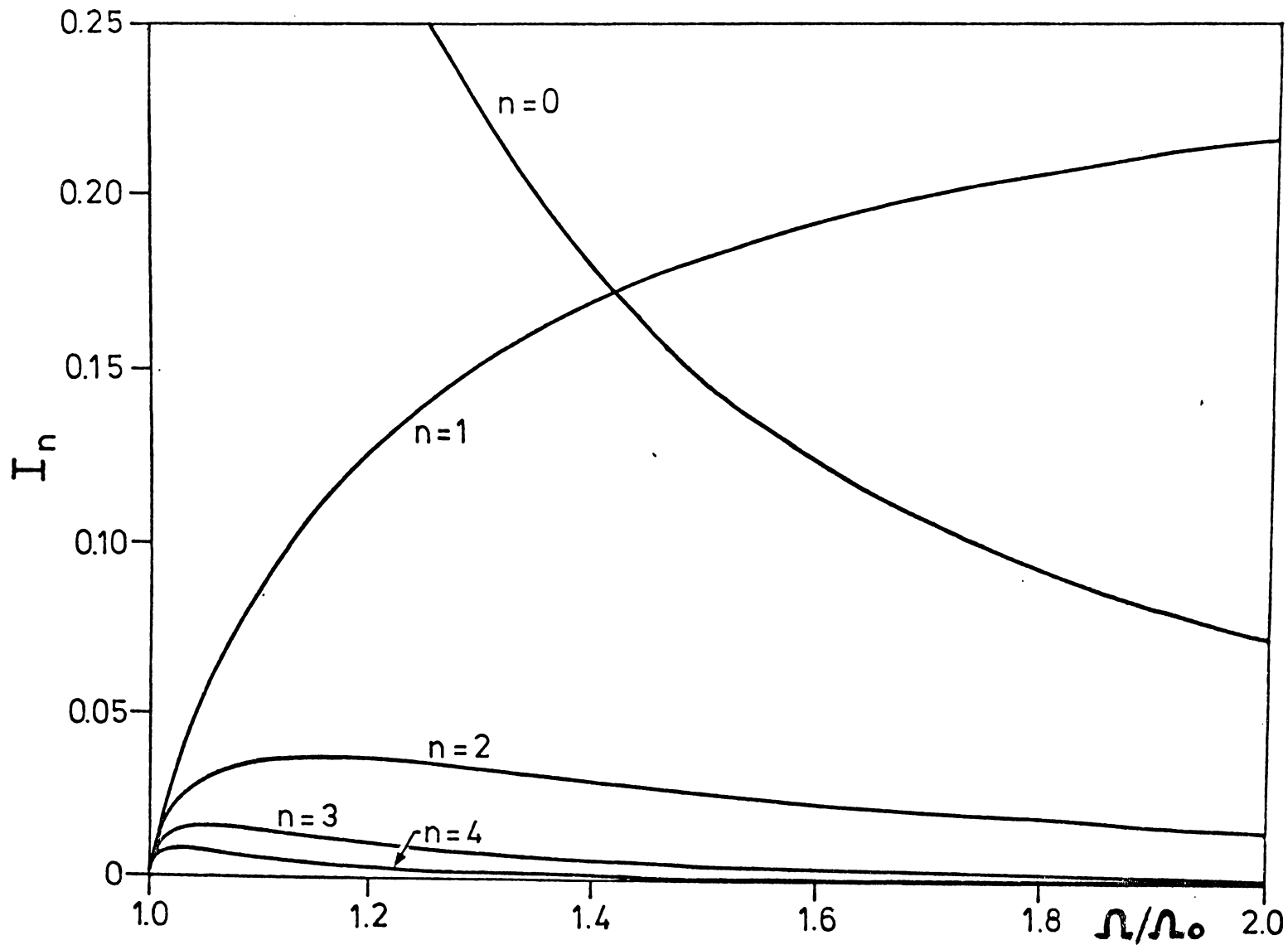


Fig (5.8.1) J^2 -invariant cooperative fluorescence; relative semiclassical peak areas (for multiple sidebands) vs input amplitude ($J \rightarrow \infty$).

driving field only. By comparison, our results use the same factorisation, and give exact results for all driving fields relative to the semiclassical factorisation. The validity of the factorisation will be discussed in section 5.9. Essentially quantum fluctuations are expected to change the cycle phase and amplitude on a time-scale of order γ^{-1} . As each cycle has the same period, this should not change the peak positions in the spectrum: but it can alter the relative peak heights and widths. In particular with a broadening of order γ , it is likely that the less intense sidebands will disappear in the full quantum treatment. Thus while the full quantum spectrum is an open question, we have obtained an exact semiclassical result which is expected to have some of the features of the full quantum spectrum in the limit of a large number of atoms ($J \rightarrow \infty$).

Other previous work includes the work of Agarwal et al (1976), Carmichael & Walls (1977). In the former work, numerical results were obtained for two and three atoms. These authors found no multiple sidebands up to a maximum value of $J = 3/2$: as this is an extremely small value of J , the question of multiple sidebands for much larger values of J still remains open. In the work of Carmichael & Walls (1977), a J^2 -breaking factorisation was used in the calculation of the spectrum, to give a three-peaked (Mollow) spectrum. This therefore applies in a different physical region to our results, which use a J^2 -invariant method. In particular, the J^2 -breaking factorisation is only expected to be valid on time-scales

much longer than the atomic cooperation lifetime.

In summary, the results obtained here are calculations for a J^2 -invariant decay, with a large number of atoms and a finite driving field above threshold. It is in this region that our semiclassical calculation predicts multiple sidebands. It would therefore be desirable to direct research toward this region of interest (either in experiment or theory) as the optimal region for observation of multiple sidebands.

5.9 QUANTUM DISTRIBUTION FUNCTION IN THE COOPERATIVE THERMODYNAMIC LIMIT

(a) Introduction to the Fokker-Planck equation method

In the previous sections on the collective decay Maxwell-Bloch equations, we have utilised a semiclassical factorisation to solve the master equation without as yet discussing the question of quantum fluctuations. In fact this master equation is a special case of a more general master equation that includes J^2 -breaking decays as well as collective decays. This general master equation is discussed by Agarwal et al (1977,1978); Carmichael & Walls (1977); Bonifacio & Lugiato (1977); Willis (1977). These authors have used various factorisations to treat the problem, with adiabatic elimination of the field variables, giving results comparable to the semiclassical theory (including bistability).

The factorisation approximations call for reassessment when used with a J^2 -invariant master equation as we wish to deal with here. A master equation of this type would arise under similar restraints that hold for super-fluorescence and super-radiance (Skribanowitz et al 1973, Dicke 1954). The system would have to initially be in an eigenstate of J^2 (like the ground state), with the decay time for J^2 being longer than the observation time-scale. It is clear that in a physical atomic system, J^2 -relaxation processes would occur on a long enough time-scale, and our results are only valid within a cooperation lifetime. The theory can be regarded as describing N two-level atoms; either in a small volume relative to a wavelength of the coherent field and

without dipole-dipole coupling (Agarwal,1973); or in a large volume and interacting with a single field mode (Glauber & Haake,1974). We emphasise that corresponding results in super-radiance are known to be modified by spatial geometry (Bonifacio & Lugiato,1975; Saunders et al, 1976; MacGillivray & Feld, 1976) and by dipole-dipole interactions (Friedberg et al, 1972).

The interest in investigating a system of this type is that the highly cooperative decay mechanism causes atomic correlations, that can produce new physical effects (Willis, 1977). We have already seen that there is a critical driving field in the semiclassical equations, and that the semiclassical spectrum has multiple sidebands. We therefore focus in this section on deriving a rigorous foundation for our treatment of operators in this problem. The theory developed in this section does not require any factorisations, for the correlations of operators are all included in an exact Fokker-Planck equation representation of the master equation. This is possible because the special case of J^2 -invariant collective damping treated here, allows the use of the atomic coherent state (A.C.S.) representation. Unlike the equations of section 5.5, the present results do not need truncation to yield an equation of the Fokker-Planck form. However it is necessary to utilise the complex phase-space method of Chapter 2, as the distributions resulting would be singular on the usual phase-space. The resulting Fokker-Planck equation describes the cooperative fluorescence of an "angular momentum oscillator" of cooperation number J , illuminated by a coherent field and without any J^2 -relaxation processes, although including a collective decay mechanism.

The Fokker-Planck equation is solved in the limit of $J \rightarrow \infty$, using a stochastic method, with the inclusion of quantum fluctuation terms of order $(1/J)$. At the end of the calculation the limit $J \rightarrow \infty$ can be utilised: however terms of order $(1/J)$ are included during calculation of the distribution function. We mention this point as the order of taking the limit of $J \rightarrow \infty$ is important. As different factorisations only differ in terms of order $(1/J)$ it is necessary to retain these terms throughout the calculation, and take the limit of $J \rightarrow \infty$ when the final distribution is obtained.

Below threshold, the distribution is Gaussian in the thermodynamic limit, with a negative variance in the ϕ -variable. This can be treated using a complex phase space distribution. The fluorescent intensity is proportional to J^2 , similar to that in super-fluorescence.* Critical slowing down occurs near threshold, which is identified as a nonequilibrium critical point for cooperative fluorescence (within the cooperation lifetime). Above threshold, the distribution is obtained using a cycle averaging procedure. A variable change is made to "rotating-frame" variables corresponding to the cycle phase and amplitude. A new cycle-averaged Fokker-Planck equation is then derived, which is solved exactly to give the asymptotic distribution function above threshold.

* The term "super-fluorescence" was first used to describe transient cooperative spontaneous emission from an inverted collective atomic system by Bonifacio & Lugiato (1975). Here we adapt their term to describe a driven collective system, with fluorescence proportional to J^2 .

Our results are different from those obtained with the uncorrelated atom factorisation of Carmichael & Walls (1976). This factorisation approximation gives, instead, a bistable transition at a lower driving field. This is due to the fact that the uncorrelated atom factorisation neglects atomic correlations and breaks the J^2 -invariance symmetry. The difference between the uncorrelated atom results, and the exact results, shows that the inclusion of atomic fluctuation correlations can change the order of a transition, which supports a prediction of Willis (1977).

However the uncorrelated atom factorisation should not be discounted: instead it can be regarded as simulating the J^2 -breaking effects that can physically occur on a long enough time-scale (Walls et al, 1978). Thus this factorisation would have greatest applicability on time-scales long compared to the cooperation lifetime, and for large driving fields, to reduce the relative size of the inter-atomic interactions. In the present section we will be more interested in events occurring within the cooperation lifetime, so processes that are J^2 -invariant will dominate the time-evolution of the atomic system.

In an earlier work of Senitzky (1972), a similar Hamiltonian was proposed, with a J^2 -invariant interaction. This author obtained results valid for ($\Omega \rightarrow 0$; $\Omega \rightarrow \infty$) and recognised the existence of a threshold. The new results obtained here are the exact solution of the semi-classical equations, with the inclusion of quantum corrections (to order $1/J$) for all driving fields, so that the existence of a critical point is proved.

Within the limitations of the J^2 -invariant Hamiltonian

with single-mode interactions between the atoms and the field, the following interaction picture master equation is obtained (Agarwal 1974, Glauber & Haake 1974):

$$\frac{\partial \hat{\rho}}{\partial t} = -\frac{i\Omega}{2} [\hat{J}^+ + \hat{J}^-, \hat{\rho}] + \frac{\gamma}{2} [2\hat{J}^- \hat{\rho} \hat{J}^+ - \hat{J}^+ \hat{J}^- \hat{\rho} - \hat{\rho} \hat{J}^+ \hat{J}^-]$$

Here \hat{J}^\pm are collective atomic raising and lowering operators, Ω is the Rabi frequency, and γ the Einstein A-coefficient. The thermal reservoirs are assumed to be at zero temperature, the field modes have been adiabatically eliminated, and the coherent driving field is assumed to be tuned to the atomic transition frequency. Using the atomic coherent state representation (Arecchi et al, 1972), the following Fokker-Planck equation is obtained in the variables of Glauber & Haake (1974):

$$\begin{aligned} \frac{\partial}{\partial t} P(\underline{z}) = & \left[-\frac{\partial}{\partial z_1} (i\Omega(z_1^2-1)/2 + \gamma(J+1)z_1) \right. \\ & \left. -\frac{\partial}{\partial z_2} (-i\Omega(z_2^2-1)/2 + \gamma(J+1)z_2) \right. \\ & \left. + \frac{\gamma}{2} \left(\frac{\partial^2}{\partial z_1^2} \cdot z_1^2 + 2 \frac{\partial}{\partial z_1} \frac{\partial}{\partial z_2} + \frac{\partial^2}{\partial z_2^2} \cdot z_2^2 \right) \right] P(\underline{z}) \end{aligned}$$

Here J is the cooperation number (that is, $\langle \hat{J}^2 \rangle = J(J+1)$). For N atoms initially in the ground state, we have $J = N/2$. The diffusion matrix is non-positive definite, so that solutions to the Fokker-Planck equation would only exist in a generalised function space, using the standard (diagonal) ACS representation of the density operator.

For this reason, it is desirable to use the complex ACS representation of Chapter 2, so that (z_1, z_2) are not complex-conjugate. This will generate an equivalent

Fokker-Planck equation with positive-definite diffusion, on a four-dimensional phase-space. This is therefore equivalent to an Ito stochastic differential equation (section 2.3):

$$d \begin{bmatrix} z_1 \\ z_2 \end{bmatrix} = \begin{bmatrix} i\Omega(z_1^2 - 1)/2 + \gamma(J+1)z_1 \\ -i\Omega(z_2^2 - 1)/2 + \gamma(J+1)z_2 \end{bmatrix} + \sqrt{\gamma} \begin{bmatrix} z_1 & 1 \\ 1 & z_2 \end{bmatrix} \begin{bmatrix} \xi_1(t) \\ \xi_2(t) \end{bmatrix}$$

Now ξ_1, ξ_2 are delta correlated independent Gaussian random functions, so that z_1, z_2 are not complex-conjugate. In this section, the distribution will be obtained to order $(1/J)$, by expanding in $(1/J)$ and assuming that Ω, γ are both large. We note that the variables Ω, γ can be related to the interferometer properties (from section 5.7), and the effective field - $\langle \alpha \rangle$ which is proportional to the interferometer transmitted field - is given by:

$$\langle \alpha \rangle = \frac{\gamma \bar{g}}{\kappa} \left[\frac{\Omega}{\gamma J} - \frac{J_y}{J} \right]$$

(b) Deterministic solutions

As a first step toward obtaining transient and stability behaviour, we neglect the stochastic terms of order $(1/J)$. This gives the zero'th order term in an asymptotic system size expansion. The solutions obtained are then identical to the semiclassical results obtained previously, with the replacement of (J) by $(1 + J)$. Thus the deterministic solutions and the semiclassical results are identical apart from terms of order $(1/J)$ in the limit of $J \rightarrow \infty$.

The solution behaviour depends on the size of Ω relative to the threshold $\Omega_0 = \gamma(J+1)$. Below threshold there is a characteristic decay time τ , and a global attractor r_- . While above threshold, there is a family of cyclic solutions of period $2\pi\tau$; where:

$$\gamma = \Omega_0 / \Omega$$

$$\chi = \sqrt{\gamma^2 - 1} / i \quad (\Omega < \Omega_0); \quad = \sqrt{1 - \gamma^2} \quad (\Omega > \Omega_0)$$

$$r_{\pm} = i\gamma \pm \chi$$

$$\tau = |\Omega^2 - \Omega_0^2|^{-1/2}$$

The solution paths have already been obtained in previous sections. However, we recollect that there is a critical point analogy at threshold* with Ω analogous to

* This is a different critical point from that found in optical bistability, which occurs at small N values (not large N values).

the temperature: both the decay time below and the cycle period above threshold, have critical slowing down near Ω_0 . The cycles above threshold are like the Lotka-Volterra cycles found in ecological and chemical systems, because the cycle parameter (c) is a Hamiltonian-like invariant of the deterministic equations. One difference however is that the cyclic solutions have the same period in this case; which is not true for Lotka-Volterra cycles. The cycles enclose either r_+ ($c < 1$) or r_- ($c > 1$), with the symmetry of ($c \rightarrow 1/c$, $z \rightarrow -z^*$), where we define the cycle parameter as:

$$c \equiv \left[\frac{z_1 - r_+}{z_1 - r_-} \right] \left[\frac{z_2 + r_-}{z_2 + r_+} \right]$$

We recall from the previous section, the solution path:

$$z(t) = (\alpha(t)r_- - r_+)(\alpha(t) - 1)^{-1}$$

$$\alpha(t) = \sqrt{c} \exp[i\Omega_X t - i|\Omega_X|t_0]$$

This decays rapidly below threshold, to:

$$r_- = i(\gamma + \sqrt{\gamma^2 - 1})$$

Above threshold there are circular paths with centre and radius (δ, ρ):

$$\delta(c) = (r_+ - cr_-)/(1-c)$$

$$\rho(c) = \sqrt{c}(r_+ - r_-)/(1-c)$$

We note that in the (θ, ϕ) variables of the Bloch sphere, we would have:

$$r_- = e^{i\phi_0} dg\left(\frac{\theta_0}{2}\right)$$

$$\phi_0 = \pi/2$$

$$\theta_0 = \sin^{-1}\left(\frac{\Omega}{\Omega_0}\right) \quad (\Omega < \Omega_0)$$

Thus the paths obtained in the Glauber-Haake variables can be readily transformed to the familiar Bloch sphere variables.

(c) Solutions below threshold

The inclusion of diffusion terms allows the distribution to be calculated in the limit of $J, \Omega \rightarrow \infty$. Below threshold it is useful to make a variable change to the (θ, ϕ) variables which are coordinates on the Bloch sphere:

$$z_1 = e^{i\phi} dg\left(\frac{\theta}{2}\right) \quad ; \quad z_2 = e^{-i\phi} dg\left(\frac{\theta}{2}\right)$$

Hence, one obtains the following stochastic differential equation:

$$\frac{d}{dt} \begin{bmatrix} \theta \\ \phi \end{bmatrix} = \begin{bmatrix} -\Omega \sin \phi - \frac{\gamma}{2} \left(\frac{1 - \cos \theta}{\sin \theta} \right) - \gamma J \sin \theta \\ -\Omega \cos \phi \cot \theta \end{bmatrix} + \sqrt{\gamma} \begin{bmatrix} \sqrt{\frac{1 - \cos \theta}{1 + \cos \theta}} \cdot \xi_1(t) \\ \sqrt{\frac{-\cos \theta}{1 + \cos \theta}} \cdot \xi_2(t) \end{bmatrix}$$

The global attractor is now at (θ_0, ϕ_0) where:

$$\phi_0 = \pi/2 \quad ; \quad \theta_0 = \sin^{-1}\left(\frac{\Omega}{\gamma J}\right) + o\left(\frac{1}{J}\right)$$

On linearising, the solution is a Gaussian (asymptotically): except in a neighbourhood of $\Omega = 0$ or $\Omega = \Omega_0$. The variance in ϕ is negative, so the distribution can be expressed as a Gaussian for imaginary values of $(\phi - \phi_0)$. If we define a Gaussian with mean \bar{x} and variance σ^2 as $\mathcal{G}(x - \bar{x} | \sigma^2)$, then this can be written as:

$$\lim_{J \rightarrow \infty} D(\theta, \phi) = \mathcal{G}(\theta - \theta_0 | \frac{1 - \cos \theta_0}{2J \cos \theta_0}) \cdot \mathcal{G}(i(\phi - \phi_0) | \frac{\gamma \sin \theta_0}{2\Omega(1 + \cos \theta_0)})$$

This is approximately a delta function in the limit $J, \Omega \rightarrow \infty$. In particular, the following results are obtained asymptotically:

$$\left. \begin{aligned} \text{Inversion: } \langle \hat{J}_z \rangle / J &= -(1 - \Omega^2 / \Omega_0^2)^{1/2} \\ \text{Polarisation: } \langle \hat{J}_y \rangle / J &= \Omega / \Omega_0 \end{aligned} \right\} \Omega < \Omega_0$$

$$\langle \hat{J}_x \rangle / J = 0$$

It is now of some interest to evaluate the product $\langle \hat{J}_+ \hat{J}_- \rangle$, in order to determine how the operators will factorise. We specifically include terms of order $(1/J)$. Operator products are determined from the atomic coherent state identities:

$$\langle \hat{J}^+ \hat{J}^- \rangle = \int_D D(\theta, \phi) [J - J \cos \theta + J(J-1/2) \sin^2 \theta] d\theta d\phi$$

We note incidentally that if $D(\theta, \phi)$ was a true delta function, one would obtain:

$$\langle \hat{J}^+ \hat{J}^- \rangle = J + \langle \hat{J}_z \rangle + (1 - 1/N) \langle \hat{J}^+ \rangle \langle \hat{J}^- \rangle$$

This is also the result corresponding to an "uncorrelated atom factorisation" as it holds for N uncorrelated atoms.

However when terms of order $(1/J)$ are included, it is necessary to include the finite width of the Gaussian in the (θ, ϕ) space. One obtains asymptotically the following result; for an observable $A(\theta, \phi)$:

$$\langle \hat{A} \rangle \approx A(\theta_0) + \frac{1}{2} \sigma_\theta^2 \left[\frac{\partial^2}{\partial \theta^2} A(\theta_0) \right] + \frac{1}{2} \sigma_\phi^2 \left[\frac{\partial^2}{\partial \phi^2} A(\theta_0) \right]$$

Hence:

$$\begin{aligned} \langle \hat{J}^+ \hat{J}^- \rangle &= (J - J \cos \theta_0 + J(J-1/2) \sin^2 \theta_0) \\ &\quad + \frac{1}{2} \sigma_\theta^2 (J \cos \theta_0 + J(J-1/2) \cdot 2 \cos 2\theta_0) + O(1/J^2) \\ \langle \hat{J}^+ \rangle &= J \sin \theta_0 (1 - \frac{1}{2} \sigma_\theta^2 - \frac{1}{2} \sigma_\phi^2) e^{i\phi_0} \end{aligned}$$

Here we have defined the variances in the (θ, ϕ) directions to be:

$$\sigma_{\theta}^2 = \left[\frac{1 - \cos \theta_0}{2J \cos \theta_0} \right]$$

$$\sigma_{\phi}^2 = \left[\frac{-1}{2J(1 + \cos \theta_0)} \right]$$

On inserting these values into the above expressions, it is easily verified that:

$$\langle \hat{J}^+ \hat{J}^- \rangle = \langle J^+ \rangle \langle J^- \rangle + O(1/J^2)$$

In other words, below threshold the semiclassical factorisation is an improved factorisation relative to the uncorrelated atom factorisation. This is a very significant difference: even though the terms involved are of order $(1/J)$ they are of vital importance in determining the mean values. When the uncorrelated atom factorisation is used, a totally different behaviour is obtained with bistable behaviour instead of a critical point (Carmichael & Walls, 1977).

Thus the inclusion of atomic correlations has indeed changed the order of the nonequilibrium transition. This is a possibility that is mentioned by Willis (1977) and shows that the use of factorisations in interacting atomic systems of this type does merit a very careful study. The above results have been also verified by computer simulations of the stochastic equations for $J = 20$, showing a similar behaviour, with no sign of the bistability inherent in the uncorrelated atom factorisation (although

transition rounding at finite J values does of course occur). Finally, some recent computer studies of H.J. Carmichael (private communication) have also been in general agreement with these results, although obtained with a different technique involving differential-difference equations in the number state representation.

(d) Distribution above threshold

We now wish to calculate the distribution above threshold, and once again it is useful to make a variable change. Noting that each deterministic solution has the same period T , it is clearly reasonable to use a rotating frame method, following a cycle averaging procedure similar to that of Kolomietz (1972).

We therefore scale the time variable and the driving field by γ , to obtain:

$$\frac{d}{dt} \begin{bmatrix} z_1 \\ z_2 \end{bmatrix} = \begin{bmatrix} i\Omega(z_1^2 - 1)/2 & +(J+1)z_1 \\ i\Omega(1 - z_2^2)/2 & +(J+1)z_2 \end{bmatrix} + \begin{bmatrix} z_1^2 & 1 \\ 1 & z_2^2 \end{bmatrix}^{1/2} \begin{bmatrix} \xi_1(t) \\ \xi_2(t) \end{bmatrix}$$

Above threshold ($\Omega > J+1$), there are limit cycles in the deterministic equations, with:

$$\begin{aligned}
t &= \int_0^t \frac{2 dz_1}{i\Omega(z_1 - r^+)(z_1 - r^-)} = \frac{2}{i\Omega(r^+ - r^-)} \ln \left[\frac{z_1 - r^+}{z_1 - r^-} \right] + \omega t \\
&= \int_0^t \frac{2 dz_2}{-i\Omega(z_2 + r^+)(z_2 + r^-)} = \frac{2}{i\Omega(r^- - r^+)} \ln \left[\frac{z_2 + r^-}{z_2 + r^+} \right] + \omega t
\end{aligned}$$

The above deterministic equations are not exact however, in the presence of the stochastic terms. We therefore define new variables as:

$$\begin{aligned}
\alpha_1 &= \left[\frac{z_1 - r^+}{z_1 - r^-} \right] e^{-it/T} \\
\alpha_2 &= \left[\frac{z_2 + r^-}{z_2 + r^+} \right] e^{it/T}
\end{aligned}$$

Here the factor $e^{\pm it/T}$ gives a transformation to a rotating frame, as desired. We note that $\sin\left(\frac{it}{T}\right)$ changes sign under time reversal, while $\cos\left(\frac{it}{T}\right)$ does not. We now can obtain exact equations in $\underline{\alpha}$, by utilising the Ito theorem. We note that the deterministic part of the equation in $\underline{\alpha}$ is only due to the Ito variable change terms, which arise from the diffusion part of the Fokker-Planck equation (Appendix A; Arnold, 1974):

$$\frac{\partial \alpha_M}{\partial t} = \frac{1}{2} \left[\frac{\partial^2 \alpha_M}{\partial z_i \partial z_j} \right] D_{ij}(\underline{z}) + \left[\frac{\partial \alpha_M}{\partial z_i} \frac{\partial \alpha_N}{\partial z_j} D_{ij}(\underline{z}) \right]^{1/2} \xi_N(t)$$

where:

$$D_{ij} = \begin{bmatrix} z_1^2 & 1 \\ 1 & z_2^2 \end{bmatrix}$$

This equation is an exact equation in the rotating frame variables. That is, (α_1, α_2) have been defined to transform away the rapidly varying cycle behaviour of (β_1, β_2) . The next step is to therefore average over a cycle, to obtain equations solely in terms of the values (cycle-averaged in time) of (α_1, α_2) . This is possible only in the limit of $(\Omega, J) \rightarrow \infty$, where the relative fluctuations of (α_1, α_2) within each cycle tend to zero because the cycle period tends to zero. However, the above equations are all expressed in terms of both α and β . We wish therefore to re-express β in terms of α as follows:

$$\alpha'_1 = \left[\frac{\beta_1 - r^+}{\beta_1 - r^-} \right] = \alpha_1 e^{it/\tau}$$

$$\alpha'_2 = \left[\frac{\beta_2 + r^-}{\beta_2 + r^+} \right] = \alpha_2 e^{-it/\tau}$$

$$\beta_1 = \left[\frac{r^- \alpha'_1 - r^+}{\alpha'_1 - 1} \right]$$

$$\beta_2 = \left[\frac{r^- - r^+ \alpha'_2}{-1 + \alpha'_2} \right]$$

With these variables, we find that the above equations can be expressed in terms of slowly varying coefficients, plus rapidly varying coefficients with factors of $\exp(\pm it/\tau)$ that all average to zero. In the limit of $(\Omega, J) \rightarrow \infty$, these rapidly varying coefficients can be neglected in the calculation of the asymptotic distribution function.

The final, cycle-averaged, equation is:

$$\frac{d}{dt} \begin{bmatrix} \alpha_1 \\ \alpha_2 \end{bmatrix} = \begin{bmatrix} \frac{\alpha_1}{4\chi^2} (r_+^2 - 2) \\ \frac{\alpha_2}{4\chi^2} (r_-^2 - 2) \end{bmatrix} + \left(\frac{1}{2\chi} \right) \begin{bmatrix} \alpha_1^2 (r_+^2 + r_-^2 - 4), (\alpha_1^2 \alpha_2^2 + 4\alpha_1 \alpha_2 + 1) \\ (\alpha_1^2 \alpha_2^2 + 4\alpha_1 \alpha_2 + 1), \alpha_2^2 (r_+^2 + r_-^2 - 4) \end{bmatrix}^{\frac{1}{2}} \begin{bmatrix} \xi_1(t) \\ \xi_2(t) \end{bmatrix}$$

This equation now describes a gradual diffusive behaviour in the cycle phase and amplitude, on a time-scale of order χ^{-1} . Thus all the rapidly varying cyclic behaviour has been averaged out, and only a relatively gradual diffusion in the cycle phase and amplitude remains. In order to determine the final distribution, it is necessary to solve the above equation for the distribution in α , and then transform back to the original variables.

We know from the work of Haken (1975), that it is necessary to include the time-reversal behaviour of the variables in determining potential solutions of the above equation expressed in Fokker-Planck form. In fact, while $\text{Re} \left[\frac{d\alpha}{dt} / \alpha \right]$ is time-reversal invariant, we know that $\text{Im} \left[\frac{d\alpha}{dt} / \alpha \right]$ changes sign under time-reversal. We therefore define new drift terms as follows:

$$A_M = A'_M + R_M$$

$$A'_M = \left[\frac{\alpha_M}{4\chi^2} \right] \text{Re} (r_+^2 - 2)$$

$$R_M = \left[\frac{\alpha_M}{4\chi^2} \right] \text{Im} (r_+^2 - 2) \cdot (-1)^{M+1}$$

Here the reversible part R_M can be omitted on calculating the potential. It is straightforward to show that in fact, potential equations are satisfied, and the steady-state distribution is, therefore (from Appendix A):

$$P_{\sim}^{\infty}(\alpha) = \exp \left[- \int^{\alpha} D_{\mu\nu}^{-1}(\alpha') \left[2A'_{\nu}(\alpha') + \partial_{\rho} D'_{\rho\nu}(\alpha') \right] d\alpha'_{\mu} \right]$$

The final distribution can be calculated to be:

$$P^{\infty}(\alpha) = \left[1 + (2-4\gamma^2) \alpha_1 \alpha_2 + (\alpha_1 \alpha_2)^2 \right]^{-1}$$

So far, we have not specified the manifold of integration: however it is readily verified in this case, that the choice $\beta_2 = \beta_1^*$ will result in a normalisable distribution function. In fact the distribution only depends on (α_1, α_2) which is just the cycle parameter mentioned earlier. It is also true that we can write this distribution in terms of (z, \bar{z}) . We readily obtain:

$$P^{\infty}(z) = \left[|z-r_+|^4 + (2-4\gamma^2) |z-r_+|^2 |z-r_-|^2 + |z-r_-|^4 \right]$$

All the above results were obtained without including the time-reversible parts of the Fokker-Planck equation. However it can be verified that the inclusion of the terms (R_M) do not alter the steady-state distribution function.

As the cycle parameter only depends on (α, α_2) or (α, α_1') , this provides a useful way to calculate observables analytically. Given an operator representation $O(z, z^*)$, one obtains the following formula:

$$\langle O \rangle = \int_0^\infty f(c) \oint_c O(z, s^*(c) + \rho^2(c)/[z - s(c)]) \cdot dc \cdot d\tau_c(z)$$

Here $f(c)$ is the distribution function relative to the cycle parameter :

$$f(c) = \left[\frac{XY}{\tan^{-1}(Y/X)} \right] ((1+c)^2 - 4Y^2c)^{-1}$$

The notation \oint_c means integration on a Volterra cycle path, with integration measure:

$$d\tau_c(z) = X dz / [\pi i (z - r^+) (z - r^-)]$$

Some of these integrals have already been calculated in the work of sections 5.7 and 5.8. The new result obtained here is simply the distribution in the cycle parameter to be found in the thermodynamic limit (in the steady-state). The following results are obtained for the inversion and polarisation:

$$\left. \begin{aligned} \langle J_z \rangle / J &= 0 \\ \langle J_y \rangle / J &= \left[\frac{\Omega}{\Omega_0} - \frac{\sqrt{1 - (\Omega_0/\Omega)^2}}{\sin^{-1}(\Omega_0/\Omega)} \right] \end{aligned} \right\} \Omega > \Omega_0$$

These results are graphed versus the input field in fig 5.9.1, which gives the limit $\Omega, J \rightarrow \infty$; Ω/J finite. Similarly, in fig 5.9.2, we have graphed the effective (or transmitted) field given by $(\frac{\Omega}{\Omega_0} - \frac{\langle J^2 \rangle}{J})$. In this case both the exact results (showing a critical behaviour) and the approximate results obtained with the uncorrelated atom factorisation (showing bistable behaviour) are given. It can be seen that the uncorrelated atom factorisation gives a very different picture from the exact result, and that the effect of the atomic correlations is to change the order of the nonequilibrium transition (Willis, 1977). However, the uncorrelated atom approximation can be regarded as simulating the J^2 -breaking decays that would occur on a time-scale much longer than the cooperation lifetime (Walls et al, 1978).

Turning to the time-dependent results, there is a very different behaviour below and above threshold. There is a very rapid approach to the static distribution well below threshold, with a critical slowing-down near threshold in a time of order τ . Above threshold the approach to a static distribution has a fast time-scale of order τ , and a slow time-scale of order γ^{-1} . Clearly the semiclassical equations provide an excellent description for events occurring within the fast time-scale, when J is large (so that the quantum fluctuation terms of order $1/J$ are relatively small). Thus these equations can be used to derive approximate expressions for the transient spectrum observed on a time-scale less than γ^{-1} . In practical experiments, the transient spectrum may be the simplest to

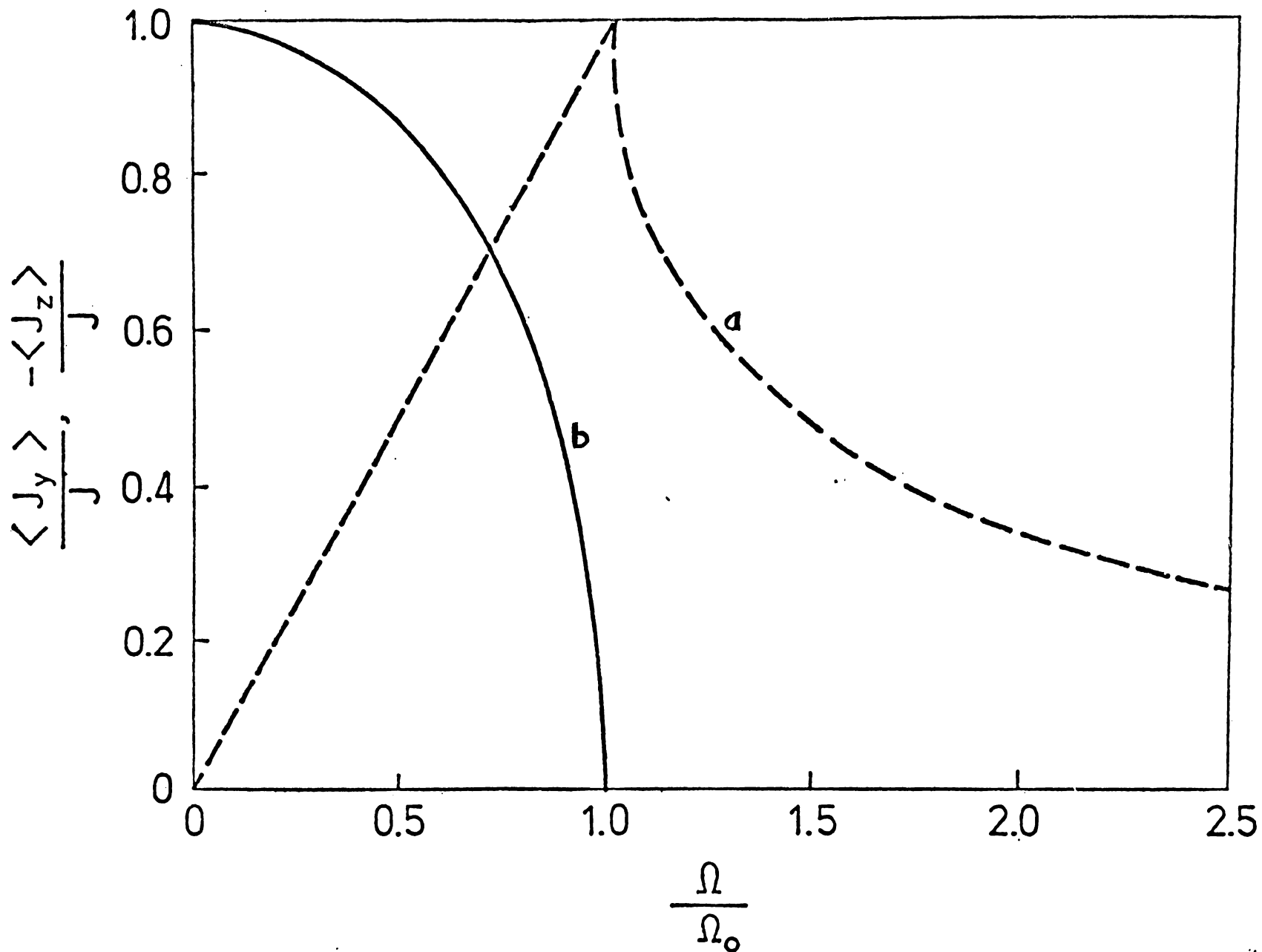


Fig (5.9.1) J^2 -invariant cooperative fluorescence; polarisation (a) and inversion (b) vs input amplitude ($J \rightarrow \infty$).

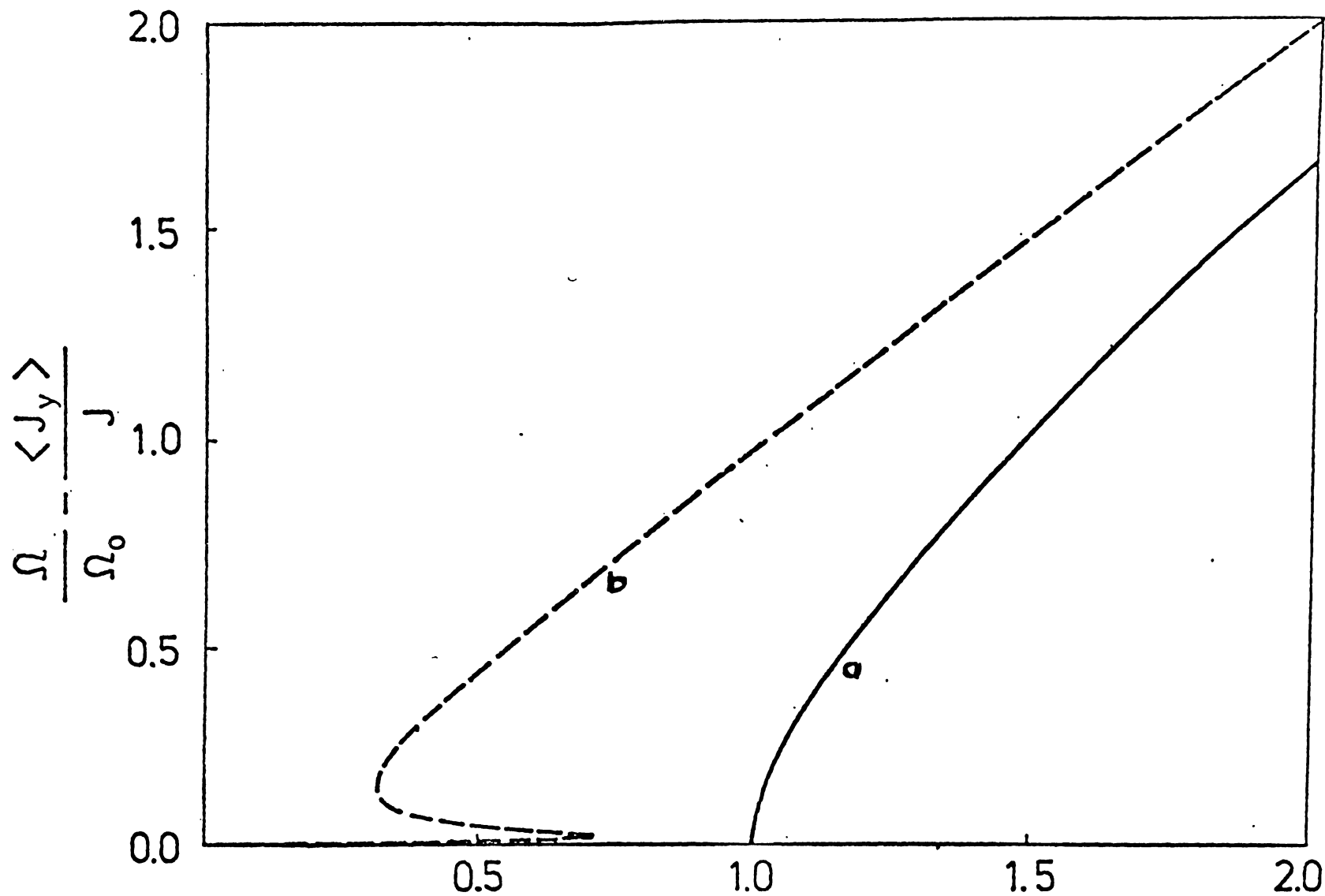


Fig (5.9.2) J^2 -invariant cooperative fluorescence; interferometer amplitude vs input amplitude.

$$\frac{\Omega}{\Omega_0}$$

(a) exact ($J \rightarrow \infty$)

(b) uncorrelated atom factorisation ($J = 40$)

observe. However in theoretical terms, the full quantum spectrum in the steady-state is still an open question, and further work is in progress.

Nevertheless, it is worthy of note, that the full spectrum must average terms corresponding to each individual cycle. As each cycle has the same period, this would alter the weight of each peak, while leaving the frequency of the sidebands unchanged. In addition, terms corresponding to phase and amplitude diffusion would result in a broadening of the sidebands. We would expect only a finite number of sidebands to occur with widths of order γ , in the true quantum spectrum.

(e) Discussion of results

Rigorous results have been obtained for observables, that do not depend on any operator factorisation assumptions. We have shown that the master equation of this section describes a nonequilibrium phase transition, when the system evolves from a state of definite J value. The appropriate thermodynamic limit where the phase transition occurs, is for $\Omega, J \rightarrow \infty$; with (Ω/J) finite. This can be regarded as the cooperative fluorescence critical point, as it generalises one-atom fluorescence to the case of

spin-J collective operators. The results involve a number of approximations (including the dipole and rotating-wave approximations) in the derivation of the master equation: while these have not been discussed in detail, the dipole and R.W. approximations are usually accurate for optical transitions.

It would clearly be interesting to observe this new critical point transition in an experiment; and it seems that techniques developed in the study of super-fluorescence or optical bistability could be adapted for this purpose. One point of particular interest is the rapid response of the interferometer in the region below threshold, relative to the one-atom decay rate. This could possibly find use as a nonlinear device in logic or communications applications. In any case, the observation of this critical behaviour would improve our understanding of nonequilibrium transitions in quantum optics. Further work, both in theory and in experiment, would be of value, in particular toward understanding the full coupled field-matter equations; as J^2 -changing processes and spatial fluctuations provide a limitation to the treatment presented here.

APPENDIX A: FOKKER-PLANCK AND STOCHASTIC DIFFERENTIAL EQUATIONS

(a) Fokker-Planck Equations

By a Fokker-Planck equation, we mean a linear partial differential equation defined on a manifold, that obeys the following equation:

$$\frac{d}{dt} P(\underline{\alpha}, t) = \sum_{\mu=1}^n \left[\frac{d}{d\alpha_{\mu}} \cdot A_{\mu}(\underline{\alpha}, t) + \sum_{\nu=1}^n \frac{d}{d\alpha_{\mu}} \frac{d}{d\alpha_{\nu}} \cdot D_{\mu\nu}(\underline{\alpha}, t) \right] P(\underline{\alpha}, t)$$

Here the complex function $P(\underline{\alpha}, t)$ is defined on an $(n+1)$ dimensional space of $\mathbb{R} \otimes \mathcal{D}$ where \mathcal{D} is the manifold of "phase-space"; so that $\underline{\alpha} \in \mathcal{D}$. In general, t is a real variable while the α are complex. We usually write the above equation without the summation, as this is implied by repeated indices.

When \underline{D} , \underline{A} are invariant in time, it is possible to obtain stationary solutions in some cases, for the limit $t \rightarrow \infty$. Potential equations that result in solutions are obtained by splitting the drift term (\underline{A}) into dissipative and reversible parts; and defining a "force" function -

$$A_{\mu} = A'_{\mu} + R_{\mu}$$

$$v_{\mu} = D_{\mu\rho}^{-1} \left[2A'_{\rho} + \frac{d}{d\alpha_{\sigma}} \cdot D_{\rho\sigma} \right]$$

The potential equations (which allow integration of the potential) and final distribution are:

$$\frac{d}{d\alpha_{\mu}} \cdot v_{\nu} = \frac{d}{d\alpha_{\nu}} \cdot v_{\mu}$$

$$P(\underline{\alpha}) = \exp \left[- \int^{\underline{\alpha}} v_{\mu}(\underline{\alpha}') \cdot d\alpha'_{\mu} \right]$$

In addition, the following equation in R_{μ} must be satisfied:

$$\frac{d}{d\alpha_{\mu}} [R_{\mu}(\alpha) \cdot P^{\infty}(\alpha)] = 0$$

In order to obtain normalisable solutions, we usually require that the distribution be normalisable, and that $(P(\alpha), \frac{d}{d\alpha}P(\alpha))$ vanish at the boundaries of integration. This gives additional restraints on the manifold that the distribution is defined on.

A simple example of the above, is the one-dimensional Gaussian distribution:

$$\frac{d}{dt} P(x,t) = \left[\frac{\partial}{\partial x} \cdot ax + \frac{1}{2} \frac{\partial^2}{\partial x^2} \cdot d \right] P(x,t)$$

$$\therefore P^{\infty}(x) = \exp\left[-\int \left(\frac{2ax'}{d}\right) dx'\right] = C \cdot \exp\left[-\frac{ax^2}{d}\right]$$

The variance of x in this case, is clearly $(d/2a)$.

The above remarks can also be generalised to hold for the case that D_{MV} is singular. In this situation, the potential is defined without using the inverse of D_{MV} . This is true in many cases for Hamiltonian systems; where the following Fokker-Planck equation is found:

$$\begin{aligned} \frac{d}{dt} P[\underline{p}, \underline{x}, t] = & \left[-\frac{\partial}{\partial x_{\alpha}} \cdot \left(\frac{\partial H}{\partial p_{\alpha}} \right) + \frac{\partial}{\partial p_{\alpha}} \cdot \left(\frac{\partial H}{\partial x_{\alpha}} + \left[\alpha \frac{\partial H}{\partial p_{\alpha}} \right] \right) \right. \\ & \left. + D_{\alpha} \frac{\partial^2}{(\partial p_{\alpha})^2} \right] P[\underline{p}, \underline{x}, t] \end{aligned}$$

In this case, the solution is:

$$P^{\infty}[\underline{p}, \underline{x}] = \exp\left[-H(\underline{p}, \underline{x})/kT\right]$$

The reversible part of the drift terms is:

$$\frac{d}{d\alpha_M} [R^M P^\infty] = \left[\left[-\frac{\partial^2 H}{\partial x_\alpha \partial p_\alpha} + \frac{\partial^2 H}{\partial p_\alpha \partial x_\alpha} \right] + \frac{1}{kT} \left[\frac{\partial H}{\partial x_\alpha} \frac{\partial H}{\partial p_\alpha} - \frac{\partial H}{\partial p_\alpha} \frac{\partial H}{\partial x_\alpha} \right] \right] P^\infty = 0$$

Similarly, the "generalised force" (which is only defined relative to momentum variables) is:

$$V_\alpha = +D_\alpha^{-1} \cdot \Gamma_\alpha \frac{\partial H}{\partial p_\alpha}$$

Hence for the solution to exist, we must satisfy the Einstein relation:

$$D_\alpha = kT \Gamma_\alpha$$

The above equations are the equations and potential solutions of Hamiltonian systems in thermal equilibrium. Nevertheless, the Fokker-Planck method is readily adapted to the study of other open systems, in this thesis.

(b) Stochastic differential equations

In the case that the Fokker-Planck equation is defined on a real manifold with $D_{\mu\nu}$ a positive semi-definite matrix, the propagation of probability is equivalent to a stochastic differential equation. This equation can be defined using either Ito or Stratonovic calculus (Arnold 1974), which result in different stochastic equations. The Stratonovic term is in fact equal to the result obtained on taking the limit of a sequence of finite band-width noise terms, and obeys standard calculus. On the other hand, the Ito term, which has advantages in analytic work, needs to have extra terms included on making a variable change.

In this thesis, we have used only the Ito equations. A discussion of these is given by Chaturvedi (1977) in relation to the Stratonovic method. The Ito equation corresponding to the standard Fokker-Planck equation of part (a) is:

$$\frac{d}{dt} \cdot q_{\mu} = -A_{\mu}(q, t) + \sum_{\nu=1}^n B_{\mu\nu}(q, t) \cdot f_{\nu}(t)$$

Here $B_{\mu\nu}(q, t)$, $f_{\nu}(t)$ are defined to satisfy the following equations -

$$D_{\mu\nu}(q, t) = \sum_{\sigma=1}^n B_{\mu\sigma}(q, t) B_{\nu\sigma}(q, t)$$

$$\langle f_{\nu}(t) f_{\mu}(t') \rangle = \delta_{\mu\nu} \delta(t-t')$$

$$\langle f_{\nu}(t) \rangle = 0$$

Thus $\{\xi_M(t)\}$ are delta-correlated, independent, Gaussian random functions: in the Ito calculus they are also uncorrelated with the dependent variables at the same time. The variable-change formula for Ito calculus is as follows, where we wish to define equations in a new set of variables $\beta_M(\underline{\alpha}, t)$:

$$\frac{d}{dt}\beta_M = \left[\frac{\partial \beta_M}{\partial \alpha_\nu} \right] \left[\frac{d}{dt} \alpha_\nu \right] + \frac{\partial \beta_M}{\partial t} + \frac{1}{2} \left[\frac{\partial^2 \beta_M}{\partial \alpha_\nu \partial \alpha_\rho} \right] D_{\nu\rho}(\underline{\alpha}, t)$$

The above equations are also discussed for more general Fokker-Planck equations in section 2.3 of this thesis, giving similar results for variables that are complex.

In solving stochastic differential equations (i.e., if the potential equations of part (a) do not apply) it is useful to obtain asymptotic results by expanding in terms of the variance. To do this, we follow the method of Chaturvedi (1977), and introduce a formal expansion parameter (σ):

$$\frac{d}{dt} \alpha_M = -A_M(\underline{\alpha}, t) + \sigma \sum_{\nu=1}^n B_{M\nu}(\underline{\alpha}, t) \xi_\nu(t)$$

The calculation proceeds by expanding $\underline{\alpha}(t)$ in powers of σ :

$$\underline{\alpha}(t) = \sum_{n=0}^{\infty} \sigma^n \underline{\alpha}^{(n)}(t)$$

The calculation relies on having relatively small stochastic terms ($B_{M\nu}$), so that at the end of the calculation we take $\sigma = 1$. In the linearised results of this thesis, only the first order terms are obtained; although higher order calculations are possible.

The zero'th order result is clearly just the deterministic steady-state:*

$$A_M(\underline{\alpha}) = 0$$

In order for this to be stable, it is necessary to determine the eigenvalues of the drift matrix which must have positive real parts. This is determined as usual by the Hurwitz criterion (Fuchs & Levin, 1961; Haken, 1977).

The first order result is then just the linearised equation:

$$\partial_t \alpha_M^{(1)} = -[\partial_\nu A_M(\underline{\alpha}^{(0)})] \cdot \alpha_M^{(1)} + B_{M\nu}(\underline{\alpha}^{(0)}) f_\nu(t)$$

This is now a linear diffusion equation, which is discussed in Appendix B.

* Except for the cyclic case discussed in section 5.9, where the zero'th order result is transformed to a rotating frame of reference.

APPENDIX B: CORRELATIONS AND SPECTRUM OF A LINEAR
DIFFUSING SYSTEM

We frequently wish to solve for the correlations arising from the following Fokker-Planck equation:

$$\frac{\partial}{\partial t} P(\underline{\alpha}, t) = \sum_{\nu=1}^n \frac{\partial}{\partial \alpha_{\mu}} \left[A_{\mu\nu} \cdot \alpha_{\nu} + \frac{1}{2} \frac{\partial}{\partial \alpha_{\nu}} D_{\mu\nu} \right] P(\underline{\alpha}, t)$$

Where P is a function of the variables $\underline{\alpha}$, and \underline{D} , \underline{A} are (in general) complex matrices. That is we wish to determine:

$$\lim_{t_1, t_2 \rightarrow \infty} \langle \alpha_{\mu}(t_1) \alpha_{\nu}(t_2) \rangle \equiv \mathcal{G}_{\mu\nu}(t_1 - t_2) \equiv \mathcal{G}_{\nu\mu}(t_2 - t_1)$$

We also are interested in the spectrum, or Fourier transform of the correlation function:

$$\tilde{\mathcal{G}}_{\mu\nu}(\omega) = \frac{1}{2\pi} \int_{-\infty}^{\infty} e^{-i\omega t} \mathcal{G}_{\mu\nu}(t) dt$$

In the case of quantum optical systems in the coherent state representation, the usual measurable spectrum is:

$$I(\omega) = \tilde{\mathcal{G}}_{21}(\omega) = \frac{1}{\pi} \text{Re} \int_0^{\infty} e^{-i\omega t} \mathcal{G}_{21}(t) dt$$

Corresponding to this Fokker-Planck equation one finds the following linear stochastic differential equation, which is the same in either Ito or Stratonovic calculus:

$$\frac{\partial}{\partial t} \alpha_{\mu} = -A_{\mu\nu} \cdot \alpha_{\nu} + B_{\mu\nu} \mathcal{F}_{\nu}(t)$$

(We use the Einstein summation method for repeated indices.)

The B-matrix is defined by the following equation:

$$D_{\mu\nu} = B_{\mu\sigma} B_{\nu\sigma}$$

$$\langle \xi_\nu(t) \xi_\mu(t') \rangle = \delta_{\mu\nu} \delta(t-t')$$

That is, the noise terms are delta correlated independent Gaussian processes. Hence we can easily obtain the following result:

$$b_\nu(t) \equiv B_{\nu\mu} \cdot \xi_\mu(t)$$

$$\langle b_\nu(t) b_\mu(t') \rangle = D_{\mu\nu} \cdot \delta(t-t')$$

We can now solve the differential equation for \underline{a} in a straightforward way:

$$a_\mu(t) = \exp[-A_{\mu\nu} \cdot t] a_\nu(0) + \int_0^t dt' \exp[-A_{\mu\nu}(t-t')] b_\nu(t')$$

Now provided the real parts of the eigenvalues of \underline{A} are positive, the initial value term vanishes exponentially for large t giving the following result:

$$\rho_{\mu\nu}(t_2-t_1) = \lim_{t_j \rightarrow \infty} \int_0^{t_1} \int_0^{t_2} \left[e^{\underline{A}(t_1-t)} \underline{D} e^{-\underline{A}^T(t_2-t')} \right]_{\mu\nu} \delta(t-t') dt dt'$$

In fact these equations are still valid, when the diffusion matrix can be nonpositive-definite so the noise is essentially complex. In this case the steady-state distribution would be

a Gaussian in the complex phase-space of section 2.3.

On simplifying by integrating the delta function, one then obtains the correlation functions in terms of the equal time correlation array $\underline{\underline{f}}(0)$:

$$\begin{aligned} \underline{\underline{f}}(0) &\equiv \lim_{t \rightarrow \infty} \int_0^t dt' \left[e^{-\underline{\underline{A}}(t-t')} \underline{\underline{D}} e^{-\underline{\underline{A}}^T(t-t')} \right] \equiv \underline{\underline{C}} \\ \underline{\underline{f}}_{MV}(\omega) &= \frac{1}{2\pi} \left\{ [i\omega + \underline{\underline{A}}]^{-1} \underline{\underline{f}}(0) + \underline{\underline{f}}(0) [-i\omega + \underline{\underline{A}}^T]^{-1} \right\}_{MV} \\ \underline{\underline{f}}_{MV}(t) &= \left\{ e^{-\underline{\underline{A}}t} \underline{\underline{f}}(0) \cdot \Theta(t) + \underline{\underline{f}}(0) e^{\underline{\underline{A}}^T t} \Theta(-t) \right\}_{MV}^* \end{aligned}$$

In the work of Chaturvedi, Matheson, Gardiner & Walls (1977), this is analysed for the case of a (2 x 2) matrix, giving:

$$\underline{\underline{f}}(0) = \frac{[\det \underline{\underline{A}}] \underline{\underline{D}} + [\underline{\underline{A}} - \text{Tr} \underline{\underline{A}}] \underline{\underline{D}} [\underline{\underline{A}} - \text{Tr} \underline{\underline{A}}]^T}{2(\text{Tr} \underline{\underline{A}})(\det \underline{\underline{A}})}$$

And hence, for the spectrum, one obtains:

$$I(\omega) = \frac{1}{\pi} \text{Re} \left[(i\omega + \underline{\underline{A}})^{-1} \underline{\underline{f}}(0) \right]_{21}$$

For more general cases, it becomes necessary to diagonalise $\underline{\underline{A}}$, giving a diagonal array of eigenvalues :

$$\underline{\underline{\lambda}} = \underline{\underline{U}}^{-1} \underline{\underline{A}} \underline{\underline{U}}$$

* We define the Θ -function as:

$$(t > 0): \quad \Theta(t) = 1 \quad ; \quad \Theta(0) = \frac{1}{2} \quad ; \quad \Theta(-t) = 0$$

Hence the correlation matrix can be written in terms of the transformed diffusion array -

$$\underline{\tilde{d}} = U^{-1}(\underline{D})U^{T-1}$$

$$\underline{\tilde{g}}_{\mu\nu}^{(0)} = U_{\mu\rho} \left[\frac{d_{\rho\rho'}}{\lambda_{\rho} + \lambda_{\rho'}} \right] U_{\rho'\nu}^T$$

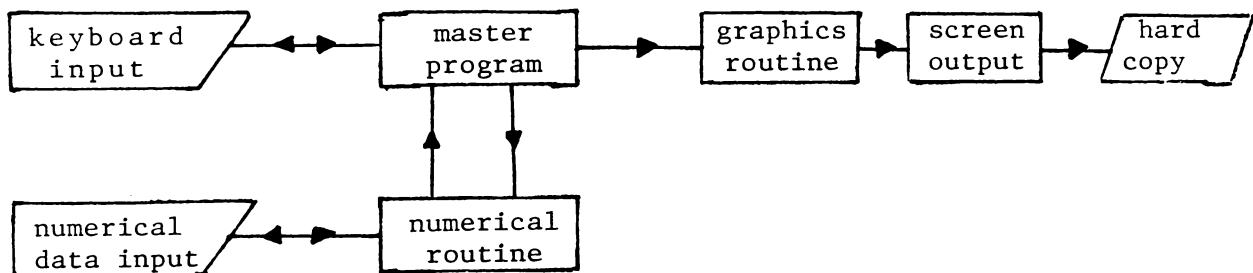
$$\underline{\tilde{g}}_{\mu\nu}^{(\omega)} = \left(\frac{1}{2\pi}\right) U_{\mu\rho} \left[\frac{d_{\rho\rho'}}{(i\omega + \lambda_{\rho})(-i\omega + \lambda_{\rho'})} \right] U_{\rho'\nu}^T$$

These formulae provide techniques for obtaining the linearised spectrum in all cases of quantum systems with stable branches, that are represented by a normal-ordering operator correspondence.

APPENDIX C: NUMERICAL METHODS

As many of the results obtained in this thesis were illustrated by numerical graphic plots, a sample of one of the computer programs utilised is included. The logic of the graphics programs is simple. A routine was written for curve-plotting that was linked to the standard graphics routines of the computer being utilised. This was an interactive master program, that received input data about the type of graph required, from the operator via a C.R.T. screen and keyboard. The master program in turn was linked to the numerical routine required. This was called (as a sub-routine) for each graphic point that was output to the graphics terminal.

A simplified flow-chart is as follows:



The program following is a numerical (Fortran) routine, that was used to generate the data for the correlations from potential solutions in section 3.2. The program has attached to it, a subsidiary routine, that evaluates the hypergeometric functions used in calculating moments from the potential solutions. For simplicity the graphics master

program has been omitted (as this is rather lengthy).

A brief summary of the function of the master program is as follows:

- (1) The master program accepts input through the keyboard specifying the number of dimensions of the graphics output, the size and scale of the graph to be displayed, the range of the independent variable (T), the resolution or stepsize of the independent variable (ΔT), and the number of iterations.
- (2) The subroutine $F()$ is called to initialise the numerical input data array. The integer variable J is set equal to zero to indicate that the subroutine call is for initialisation purposes.
- (3) The subroutine $F()$ accepts input through the keyboard specifying all necessary input parameters, which are placed in the vector array $PA()$, to be used during numerical computation.
- (4) The master program outputs initial graphic data and prints the parameter list $PA()$ for reference purposes. The subroutine $F()$ is then called with the variable J set equal to 1 for the first iteration. During each iteration, the independent variable (T) is initialised at its lowest value, then incremented by (ΔT) for each call until the highest value is reached. Each iteration results in a line output to the graphics screen. Successive iterations are indicated by incrementing J by 1 each time.

- (5) The subroutine F() or numerical routine, returns a coordinate point (X,Y) or (X,Y,Z) for each value of the independent variable T. Different values of J are used to indicate different types of calculation or data that are required for successive iterations. In three dimensional operation, hidden lines are removed for true perspective output.

```

SUBROUTINE F(J,X,Y,Z1,T,PA)
C*****
C    MOMENT PROGRAM FOR THE
C    CALCULATION OF INTENSITY AND G2
C    IN A NONLINEAR BOSE SYSTEM
C*****
    DIMENSION PA(10)
    COMMON A,B,C,OM,G,D,E1,E2
           COMPLEX F2,A,B,C,A0,B0,A1,B1,A2,B2
    IF (J.GT.0) GO TO 100
    TYPE 1
1   FORMAT (' PLEASE INPUT DRIVINGFIELD,DECAY RATE,',
1'DETUNING, '/' ABSORPTIVE AND DISPERSIVE NONLINEARITY')
    ACCEPT 10,OM,G,D,E1,E2
    PA(1)=OM
    PA(2)=G
    PA(3)=D
    PA(4)=E1
    PA(5)=E2
10  FORMAT (5F9.5)
    C=G+(0.0,1.0)*D
    A=E1+(0.0,1.0)*E2
    B=C/A
    C=(CABS(A)**2)/2.0
    A=(B)
    B=REAL(A)+(0.0,-1.0)*AIMAG(A)
    RETURN
100  X=T
     Z=X/C
     A0=A
     B0=B
     A1=A+1.0
     B1=B+1.0
     A2=A+2.0
     B2=B+2.0
     IF (J.GT.1) GO TO 200
     Y=Z*F2(A1,B1,Z)/(2.0*A*B*F2(A0,B0,Z))
    RETURN
200  IF (J.GT.2) GO TO 300
     Y=A*B/(A1*B1)
     Y=ALOG(Y)+ALOG(F2(A0,B0,Z))+ALOG(F2(A2,B2,Z))
     Y=EXP(Y-2.*ALOG(F2(A1,B1,Z)))
    RETURN
300  Y=T
     X=(CABS(A+2.0*T))**2
     X=T*X*C*2.0
     RETURN
END

```

```
FUNCTION F2(A,B,Z)
  COMPLEX F2,A,B,AT,BT,FT,AN,BN,FN,D
  C*****
  C   COMPUTES THE HYPERGEOMETRIC
  C   SERIES CALLED OF2(A,B,Z)
  C   CALLED BY MOMENT PROGRAM
  C*****
  F2=1.
  D=1.0
  AN=A
  BN=B
  FN=1.
  DO 100 N=1,1000
    D=(Z/FN)*D/(AN*BN)
    AN=AN+1.0
    BN=BN+1.0
    FN=FN+1.0
    IF (CABS(D).LT.0.0001) GO TO 200
100  F2=F2+D
    TYPE 1
  1   FORMAT (' NONCONVERGENCE ERROR FROM PROGRAM F2')
200  RETURN
    END
```

APPENDIX D: QUANTUM FLUCTUATIONS OF THE HIGH-Q CAVITY
IN THE LARGE INTENSITY LIMIT

We wish to obtain results for absorptive fluorescence in a high-Q cavity; in the case of large input intensity. In this case, it is possible to approximate the fluorescent atoms as being uncorrelated, and the master equation technique of Mandel (1974) can be utilised. This was originally developed to deal with the high-intensity single mode laser. Starting from the laser equations (as obtained by Mandel, 1974), and including an external field, one would obtain:

$$\begin{aligned} \frac{\partial}{\partial t} P(\alpha) = & \left\{ \frac{\partial}{\partial \alpha} \left[-E + \kappa(1+2C)\alpha \right] \right. \\ & + \frac{\partial}{\partial \alpha^*} \left[-E^* + \kappa(1+2C)\alpha^* \right] \\ & \left. + 2C\kappa \left[\frac{\partial^2}{\partial \alpha \partial \alpha^*} - \frac{\partial}{\partial \alpha} \cdot \alpha - \frac{\partial}{\partial \alpha^*} \cdot \alpha^* \right] \left[1 + \frac{|\alpha|^2}{n_0} - \frac{1}{4n_0} \left(\alpha \frac{\partial}{\partial \alpha} + \alpha^* \frac{\partial}{\partial \alpha^*} \right) \right]^{-1} \right\} P(\alpha) \end{aligned}$$

The above equation is identical to that of Mandel (1974) with the inversion (d_0) at thermal equilibrium, equal to the ground-state, and with the addition of an external coherent field (E).

We now wish to expand the above equation to include only diffusion terms like $(\partial^2/\partial \alpha^2)$, while truncating terms of higher order. This can be accomplished with the use of $(1/n_0)$ as a formal expansion parameter; let:

$$\Pi \equiv 1 + |\alpha|^2 = 1 + |\alpha|^2/n_0$$

$$A \equiv \frac{1}{4} \left[\alpha \frac{\partial}{\partial \alpha} + \alpha^* \frac{\partial}{\partial \alpha^*} \right]$$

$$[\Pi - A/n_0]^{-1} = \Pi^{-1} + \frac{1}{n_0} \Pi^{-1} A \Pi^{-1} + O\left(\frac{1}{n_0^2}\right)$$

We will only include the leading terms of order $(1/n_0)$ in this expansion. The terms of $(1/n_0^2)$ or greater, will be neglected: as they involve either higher order derivatives (which will be truncated) or terms due to commutation of differential operators, which can be neglected for large n_0 .

The overall result, after truncation (and neglect of terms of order $1/n_0^2$) is:

$$\begin{aligned} \frac{\partial}{\partial t} P(\underline{\alpha}) = & \left\{ \frac{\partial}{\partial \alpha} \left[-E + \kappa \alpha \left(1 + \frac{2c}{\Pi(\underline{\alpha})} \right) + O\left(\frac{1}{n_0}\right) \right] \right. \\ & + \frac{\partial}{\partial \alpha^*} \left[-E^* + \kappa \alpha^* \left(1 + \frac{2c}{\Pi(\underline{\alpha})} \right) + O\left(\frac{1}{n_0}\right) \right] \\ & \left. + 2c\kappa \left[\frac{\partial^2}{\partial \alpha \partial \alpha^*} \left(\frac{|\alpha|^2}{\Pi n_0} - \frac{1}{2\Pi^2 n_0^2} \right) - \frac{\partial^2}{\partial \alpha^2} \frac{\alpha^2 |\alpha|^2}{4\Pi^2 n_0^2} - \frac{\partial^2}{\partial \alpha^*{}^2} \frac{\alpha^{*2} |\alpha|^2}{4\Pi^2 n_0^2} \right] \right\} P(\underline{\alpha}) \end{aligned}$$

This equation describes resonance fluorescence in a high-Q cavity, provided the atoms are uncorrelated. In particular, this would be expected to have validity for large atomic saturation ($\alpha \rightarrow \infty$). In this limit, the equation becomes:

$$\frac{\partial}{\partial t} P(\underline{\alpha}) = \left\{ \left[\frac{\partial}{\partial \alpha} (\kappa \alpha - E) + \frac{\partial}{\partial \alpha^*} (\kappa \alpha^* - E^*) \right] + \frac{c\kappa}{2} \left[2 \frac{\partial^2}{\partial \alpha \partial \alpha^*} - \frac{\partial^2}{\partial \alpha^2} \left(\frac{\alpha}{\alpha^*} \right) - \frac{\partial^2}{\partial \alpha^{*2}} \left(\frac{\alpha^*}{\alpha} \right) \right] \right\} P(\underline{\alpha})$$

The deterministic equations can be seen to asymptotically correspond to a linear cavity, with additional fluctuations due to the interaction with the fluorescent atoms. These fluctuation terms are due to the random (quantised) nature of the spontaneous emission from inverted atoms interacting with the radiation mode in the cavity. We note that in this asymptotic limit, the equation resulting is identical to that of section 5.5. Both equations however incorporate a truncation approximation, which would alter the exact distribution in the high-intensity limit (Mandel, 1974).

We wish to emphasise that in the limit treated in this appendix, both the methods of Mandel et al and the method obtained with the equations of Haken et al, result in identical Fokker-Planck equations, after truncation. These theoretical treatments only differ in the terms that include atomic correlations (which are negligible in the limit of large atomic saturation).

The correlations and spectrum are readily obtained from formulae derived in section 3.1, with the substitution:

$$d = \Gamma = c\kappa \quad ; \quad \kappa = a$$

Hence one directly obtains; on linearisation:

$$\zeta \approx \langle \alpha_M \alpha_V \rangle = \left(\frac{\zeta}{2} \right) \begin{bmatrix} -1 & 1 \\ 1 & -1 \end{bmatrix}$$

$$S(\omega + \omega_0) = n \delta(\omega) + \frac{\zeta \kappa}{2\pi(\omega^2 + \kappa^2)}$$

$$g^2(0) = 1$$

This spectrum is equivalent to the spectrum of a linear interferometer with a large amount of "thermal noise", as treated in section 3.1. The corresponding linear interferometer would have $n_{th} = \zeta/2$. That is, the effect of the fluorescent atoms on the spectrum is equivalent to a thermal noise source of occupation number ($\zeta/2$). These fluctuations are intrinsic (quantum) fluctuations which cannot be removed by using a stabilised input, or by reducing the reservoir temperature. Finally, we note that the linearising procedure would require that the quantum fluctuations are small relative to the deterministic photon number (i.e. $\zeta \ll \bar{n}$).

REFERENCES

- M. Abramowitz & I.A. Stegun (1964): "Handbook of Mathematical Functions". (Dover: New York.)
- G.S. Agarwal (1974): in "Springer Tracts in Modern Physics", Vol. 70, edited by G. Hohler. (Springer-Verlag, New York.)
- G.S. Agarwal, A.C. Brown, L.M. Narducci & G. Vetri (1977): Phys. Rev. A15, 1613.
- G.S. Agarwal, L.M. Narducci, D.H. Feng & R. Gilmore (1977): in "Proceedings of the Fourth Rochester Conference on Coherence and Quantum Optics", edited by L. Mandel & E. Wolf. (Preprint.)
- G.S. Agarwal, L.M. Narducci, R. Gilmore & D.H. Feng (1978): Phys. Rev. A18, 620.
- G.S. Agarwal & E. Wolf (1968): Phys. Rev. Lett. 21, 180.
- G.S. Agarwal & E. Wolf (1970): Phys. Rev. D2, 2161; D2, 2187; D2, 2206.
- G.P. Agrawal & H.J. Carmichael (1978): (Preprint.)
- J.A. Armstrong, N. Bloembergen, J. Ducuing & P.S. Pershan (1962): Phys. Rev. 127, 1918.
- L. Arnold (1974): "Stochastic Differential Equations". (Wiley, New York.)
- F.T. Arecchi (1974): "Cooperative Effects" edited by H. Haken. (North Holland, Amsterdam.)
- F.T. Arecchi, E. Courtens, R. Gilmore & H. Thomas (1972): Phys. Rev. A6, 2211.
- J.W. Austin & L.G. De Shazer (1971): J.O.S.A. 61, 650.
- A. Bandilla & H.H. Ritze (1976): Opt. Comm. 19, 169.
- V. Bargmann (1961): Comm. Pure & App. Math. 14, 187.
- J.D. Bjorken & S.D. Drell (1965): "Relativistic Quantum Fields". (McGraw - Hill, New York.)
- R. Bonifacio, P. Schwendimann & F. Haake (1971): Phys. Rev. A4, 302.
- R. Bonifacio, M. Gronchi & L.A. Lugiato (1978): (Preprint).

- R. Bonifacio & L.A. Lugiato (1975): Phys. Rev. A11, 1507.
- R. Bonifacio & L.A. Lugiato (1976): Opt. Comm. 19, 172.
- R. Bonifacio & L.A. Lugiato (1977): (Preprint).
- R. Bonifacio & L.A. Lugiato (1978): Phys. Rev. Lett. 40, 1023; Lett. Nuov. Cim. 21; 505, 510, 517.
- N. Bloembergen (1965): "Nonlinear Optics". (Benjamin, New York.)
- N. Bloembergen (1975): Opt. Comm. 15, 416.
- R.K. Bullough (1977): Royal Society Meeting Discussion (to be published).
- K.E. Cahill & R.J. Glauber (1969): Phys. Rev. 177, 1857, 1882.
- H.J. Carmichael (1975): D. Phil. Thesis (University of Waikato, unpublished).
- H.J. Carmichael, P.D. Drummond, P. Meystre & D.F. Walls (1978): J. Phys. A11, L 121.
- H.J. Carmichael, P.D. Drummond, S.S. Hassan & D.F. Walls (1978): Proc. of Xth International Quantum Electronics Conference (to be published - IEEE J. Quant. Electronics).
- H.J. Carmichael & D.F. Walls (1976): J. Phys. B9, 1199; L 43.
- H.J. Carmichael & D.F. Walls (1977): J. Phys. B10, L 685.
- H.J. Carmichael & G.P. Agrawal (1978): (Preprint).
- Cohen - Tannoudji (1976): in "Proc. 2nd Laser Spectroscopy Conference Megeve" (Springer Verlag, Berlin).
- S. Chaturvedi (1977): D. Phil. Thesis (University of Waikato, unpublished).
- S. Chaturvedi, P.D. Drummond & D.F. Walls (1977): J. Phys. A10, L 187.
- S. Chaturvedi, C.W. Gardiner, I. Matheson & D.F. Walls (1977): J. Stat. Phys. 17, 469.
- S. Chaturvedi, C.W. Gardiner & D.F. Walls (1976): Phys. Lett. 57A, 404.
- N. Chandra & H. Prakash (1970): Phys. Rev. A1, 1696.

- W.W. Chow, M.O. Scully & E.W. van Stryland (1975): Opt. Comm. 15, 6.
- J. Chrostowski & J. Krasinski (1978): Phys. Lett. 65A, 326.
- B. Crosignani, P.D. Porto & S. Solimeno (1972): J. Phys 5A, L 119.
- P. Dewael (1975): J. Phys. A8, 1614.
- R.H. Dicke (1957): Phys. Rev. 93, 99.
- P.D. Drummond & H.J. Carmichael (1978): Opt. Comm. 27, 160.
- P.D. Drummond & S.S. Hassan (1978): (Preprint).
- P.D. Drummond, K.J. McNeil & D.F. Walls (1978): Optics Communications (to appear).
- A. Einstein (1905): Ann der Physik 17, 549.
- I.M. Every (1975): J. Phys. A8, L 69.
- F.S. Felber & J.H. Marburger (1976): App. Phys. Lett. 28, 732.
- P.A. Franken, A.E. Hill, C.W. Peters & G. Weinrich (1961): Phys. Rev. Lett. 7, 118.
- R. Friedberg, S.R. Hartmann & J.T. Manassah (1972): Phys. Lett. 40A, 365.
- B.A. Fuchs & V.I. Levin (1961): "Functions of a Complex Variable" (transl. Pergamon Press, Oxford).
- C.W. Gardiner & S. Chaturvedi (1977): J. Stat. Phys. 17, 429.
- H.M. Gibbs, S.L. McCall & T.N.C. Venkatesan (1976): Phys. Rev. Lett. 36, 1135.
- I.I. Gikhman & A.V. Skorokhod (1971): "Stochastic Differential Equations" (Springer, Berlin).
- P. Glansdorff & I. Prigogine (1971): "Thermodynamic Theory of Structure, Stability & Fluctuations" (Wiley, New York).
- R.J. Glauber (1963a): Phys. Rev. 130, 2529.
- R.J. Glauber (1963b): Phys. Rev. 131, 2766.
- R.J. Glauber (1970): in "Quantum Optics", editors S.M. Kaye and A. Maitland (Academic Press, New York).

- R.J. Glauber & F. Haake (1974): in "Cooperative Effects", edited by H. Haken (North Holland, Amsterdam).
- J.P. Gordon (1967): Phys. Rev. 161, 367.
- I.S. Gradshteyn & I.M. Ryzhik (1965): "Table of Integrals, Series & Products" (Academic Press, New York).
- R. Graham (1968): Z. Physik 211, 469.
- R. Graham (1973): in "Quantum Statistics in Optics and Solid State Physics" (Springer, Berlin).
- F. Haake (1973): in "Quantum Statistics in Optics and Solid State Physics" (Springer, Berlin).
- H. Haken (1970): "Handbuch der Physik", Vol. XXV/2c (Springer, Berlin).
- H. Haken (1974): (editor) "Cooperative Effects" (North Holland, Amsterdam).
- H. Haken (1975): Rev. Mod. Phys. 47, 67.
- H. Haken (1977): "Synergetics" (Springer, Berlin).
- H. Haken & H. Ohno (1976): Opt. Comm. 16, 205.
- H. Haken, H. Risken & W. Weidlich (1967): Z. Physik 206, 355.
- H. Haken & H. Sauermann (1963): Z. Physik 176, 47.
- S.S. Hassan & R.K. Bullough (1975): J. Phys. 8B, L 147.
- S.S. Hassan (1976): Ph.D. Thesis (University of Manchester, unpublished).
- S.S. Hassan, P.D. Drummond & D.F. Walls (1978): Optics Communications (to appear).
- E. Jakeman, E.R. Pike, P.N. Pusey & J.M. Vaughan (1977): J. Phys. A10, L 257.
- H.J. Kimble, M. Dagenais, L. Mandel (1978): (Preprint).
- H.J. Kimble, M. Dagenais, L. Mandel (1977): Phys. Rev. Lett. 39, 691.
- V.G. Kolomietz (1972): in "Stability of Stochastic Dynamical Systems" (Springer, Berlin).
- M. Kozierowski & R. Tanas (1977): Opt. Comm. 21, 229.

- J. Krasinski & S. Dinev (1976): Opt. Comm. 18, 424.
- P. Kryukov & V.S. Letokhov (1970): Sov. Phys. 12, 641.
- W.E. Lamb, Jr. (1964): Phys. Rev. 134, 1429.
- W.E. Lamb, Jr. (1971): Rev. Mod. Phys., 43, 99.
- M. Lax (1968): Phys. Rev. 172, 350.
- A. Lonke (1978): J. Math. Phys. 19, 1110.
- A.J. Lotka (1920): J. Amer. Chem. Soc. 42, 1595.
- W.H. Louisell (1973): "Quantum Statistical Properties of Radiation" (Wiley, New York).
- L.A. Lugiato (1975): Physica 82A, 1.
- V.N. Lugovoi (1978): Soviet Quantum Electronics 5, 344.
- S.K. Ma (1976): "Modern Theory of Critical Phenomena" (Benjamin, Mass.).
- P. Mandel (1974): Physica 77, 174.
- J.H. Marburger & F.S. Felber (1978): Phys. Rev. A17, 335.
- J.H. Marburger & W.H. Louisell (1968): Phys. Rev. 186, 174.
- S.L. McCall (1974): Phys. Rev. A9, 1515.
- J. McGillivray & M. Feld (1976): Phys. Rev. A 14, 1169.
- K.J. McNeil (1976): D. Phil. Thesis (University of Waikato, unpublished).
- K.J. McNeil, P.D. Drummond & D.F. Walls (1978): Optics Communications (to appear).
- K.J. McNeil & D.F. Walls (1974): J. Phys. A7, 617.
- T.M. MacRobert (1938): "Functions of a Complex Variable" (MacMillan, London).
- P. Meystre (1978): Opt. Comm. 27, 277.
- M. Minorsky (1962): "Nonlinear Oscillations" (van Nostrand, New York).
- B.R. Mollow (1969): Phys. Rev. 188, 1969.
- J. Mostowski & K. Rzazewski (1978): Phys. Lett. 66A, 275.

- S. Nakajima (1958): Prog. Theor. Phys. 20, 948.
- L.M. Narducci (1974): in "Cooperative Effects" edited by H. Haken (North Holland, Amsterdam).
- L.M. Narducci, S.S. Mitra, R.A. Shatas & C.A. Coulter (1978): (Preprint).
- N. Nayak & B.K. Bohanty (1977): Phys. Rev. A15, 1173.
- J. von Neumann: U.S. Patent 2, 815, 488.
- G. Nicolis & I. Prigogine (1977): "Self-Organisation in Nonequilibrium Systems" (Wiley, New York).
- G. Oliver, E. Ressayne & A. Tallet (1971): Lett. Nuov. Cim.2, 777.
- H. Paul, U. Mohr & W. Brunner (1976): Opt. Comm. 17, 145.
- J. Perina (1976): J. Phys. B26, 140.
- R.H. Picard & C.R. Willis (1977): Phys. Rev. A16, 1625.
- Y. Pomeau & P. Resibois (1975): Physics Reports 19C, 65.
- I. Prigogine (1945): These de doctorat (University Libre de Bruxelles, unpublished).
- I. Prigogine & P. Glansdorff (1973): Bull. Acad. Roy. Belg. Cl. Sc. 59, 672.
- I. Prigogine & P. Resibois (1961): Physica 27, 629.
- A. Reichel (1968): J. Quant. Spect. Rad. Transfer 8, 1601.
- H. Risken & K. Nummedal (1968): J. App. Phys. 39, 4662.
- J.J. Sakurai (1967): "Advanced Quantum Mechanics" (Addison-Wesley, Reading, Mass.).
- W. Sandle (1978): (private communication).
- R. Saunders, S.S. Hassan & R.K. Bullough (1976): J. Phys. A9, 1725.
- M. Sargent III, M.O. Scully & W.E. Lamb (1974): "Laser Physics" (Addison-Wesley, Reading, Mass.).
- A.L. Schawlow & C.H. Townes (1958): Phys. Rev. 112, 1940.
- H. Seidel (1971): U.S. Patent 3, 610, 731.
- I.R. Senitzky (1972): Phys. Rev. A6, 1171, 1175.

- I.R. Senitzky (1978): Phys. Rev. Lett. 40, 1334.
- Y.R. Shen (1966): Phys. Rev. 155, 921.
- H.D. Simaan & R. Loudon (1975): J. Phys. A8, 539.
- M.E. Smithers & H.S. Freedhoff (1975): J. Phys. B7, L 432.
- E. Spiller (1971): J.O.S.A. 61, 699.
- E. Spiller (1972): J. App. Phys. 43, 1673.
- N. Skribanowitz, I.P. Hermann, J.C. MacGillivray & M.S. Feld (1973): Phys. Rev. Lett. 30, 309.
- M. Steyn-Ross (1979): M. Sc. Thesis (University of Waikato, unpublished).
- J.J. Stoker (1950): "Nonlinear Vibrations in Mechanical & Electrical Systems" (Interscience, New York).
- D. Stoler (1974): Phys. Rev. Lett. 33, 1397.
- H.L. Stover & H.W. Steier (1966): App. Phys. Lett. 8, 91.
- E.C.G. Sudarshan (1963): Phys. Rev. Lett. 10, 277.
- S. Swain (1975): J. Phys. 8B, L 437.
- A. Szoke, V. Daneu, J. Goldhar & N.A. Kurnit (1969): App. Phys. Lett. 15, 376.
- C.L. Tang & H. Statz (1967): J. App. Phys. 38, 323.
- R. Thom (1975): "Structural Stability & Morphogenesis" (Benjamin, Reading, Mass.).
- T.N.C. Venkatesan (1977): Ph.D. Thesis (City University of New York, unpublished).
- V. Volterra (1931): "Theorie Mathematique de la Lutte pour la Vie" (Gouthier-Villars, Paris).
- D.F. Walls (1970): Phys. Letts. 32A, 476.
- D.F. Walls, P.D. Drummond, S.S. Hassan & H.J. Carmichael (1978): Prog. Theor. Phys. (to appear).
- D.F. Walls & C.T. Tindle (1971): Nuov. Cim. Lett. 2, 915.
- D.F. Walls & C.T. Tindle (1972): J. Phys. 5A, 534.
- H. Walther (1975): in "Laser Spectroscopy" edited by S. Haroche et al (Springer, Berlin).

- H.P. Weber (1971): IEEE. J. Quant. Electron. 7, 187.
- J. Weber (1953): Trans. IRE, PGED - 3.
- V.G. Weiskopff & E. Wigner (1930): Z. Phys. 63, 54.
- V.G. Weiskopff & E. Wigner (1931): Z. Phys. 65, 18.
- C.R. Willis (1977): Opt. Comm. 23, 151.
- C.R. Willis (1978): Opt. Comm. 26, 62.
- C.R. Willis & J. Day (1978): (Preprint).
- K. Wodkiewicz (1978): Phys. Lett. 66A, 369.
- F.Y. Wu, R.E. Grove & S. Ezekiel (1975): Phys. Rev. Lett.
35, 1426.
- R. Zwanzig (1964): Physica 30, 1109.